Evaluation de la stabilité et de l'effet dépigmentant de la cystéamine encapsulée dans des liposomes en suspension et lyophilisés

Carla Atallah

N°d'ordre NNT : xxx

THESE de DOCTORAT DE L'UNIVERSITE DE LYON
Opérée au sein de
L'Université Claude Bernard Lyon 1

Ecole Doctorale 206
(Ecole Doctorale de Chimie de Lyon)

Spécialité de doctorat : Génie pharmacotechnique
Discipline : Biochimie/Biotechnologie

Soutenue publiquement le 16/12/2020, par :

Carla ATALLAH

Evaluation de la stabilité et de l'effet dépigmentant de la cystéamine encapsulée dans des liposomes en suspension et lyophilisés

Devant le jury composé de :

M. Fessi Hatem, Pr, Université Lyon 1	Président de jury
Mme. Fourmentin Sophie, Pr, Université du Littoral Côte D'Opale	Rapporteur
Mme. Rosilio Véronique, Pr, Université Paris-Saclay	Rapporteur
M. Legrand François-Xavier, MdC, Université Paris-Saclay	Examinateur
Mme. Robin Sophie, DR, Bioexigence	Examinatrice
M. Since Marc, MdC, Université de Caen Normandie	Examinateur
Mme. CHARCOSSET Catherine, DR CNRS, Université Lyon 1	Directrice de thèse
Mme. GREIGE-Gerges Hélène, Pr, Université Libanaise	Directrice de thèse

Université Claude Bernard – LYON 1

Administrateur provisoire de l'Université	M. Frédéric FLEURY
Président du Conseil Académique	M. Hamda BEN HADID
Vice-Président du Conseil d'Administration	M. Didier REVEL
Vice-Président du Conseil des Etudes et de la Vie Universitaire	M. Philippe CHEVALLIER
Vice-Président de la Commission de Recherche	M. Jean-François MORNEX
Directeur Général des Services	M. Pierre ROLLAND

COMPOSANTES SANTE

Département de Formation et Centre de Recherche en Biologie Humaine	Directrice : Mme Anne-Marie SCHOTT
Faculté d'Odontologie	Doyenne : Mme Dominique SEUX
Faculté de Médecine et Maïeutique Lyon Sud - Charles Mérieux	Doyenne : Mme Carole BURILLON
Faculté de Médecine Lyon-Est	Doyen : M. Gilles RODE
Institut des Sciences et Techniques de la Réadaptation (ISTR)	Directeur : M. Xavier PERROT
Institut des Sciences Pharmaceutiques et Biologiques (ISBP)	Directrice : Mme Christine VINCIGUERRA

COMPOSANTES & DEPARTEMENTS DE SCIENCES & TECHNOLOGIE

Département Génie Electrique et des Procédés (GEP)	Directrice : Mme Rosaria FERRIGNO
Département Informatique	Directeur : M. Behzad SHARIAT
Département Mécanique	Directeur M. Marc BUFFAT
Ecole Supérieure de Chimie, Physique, Electronique (CPE Lyon)	Directeur : Gérard PIGNAULT
Institut de Science Financière et d'Assurances (ISFA)	Directeur : M. Nicolas LEBOISNE
Institut National du Professorat et de l'Education	Administrateur Provisoire : M. Pierre CHAREYRON
Institut Universitaire de Technologie de Lyon 1	Directeur : M. Christophe VITON
Observatoire de Lyon	Directrice : Mme Isabelle DANIEL
Polytechnique Lyon	Directeur : Emmanuel PERRIN
UFR Biosciences	Administratrice provisoire : Mme Kathrin GIESELER
UFR des Sciences et Techniques des Activités Physiques et Sportives (STAPS)	Directeur : M. Yannick VANPOULLE
UFR Faculté des Sciences	Directeur : M. Bruno ANDRIOLETTI

Remerciements

La thèse est un long chemin plein d'obstacles où tu croises des gens qui vont t'aider à arriver au bout du chemin.

J'aimerais tout d'abord remercier Pr. Hélène Greige pour le temps que vous m'avez consacré, pour les connaissances que vous m'avez transmises afin d'évoluer dans le monde de la recherche. Vous êtes mon idole en science et vous m'avez traité comme une de vos filles.

Je tiens également à remercier Dr. Catherine CHARCOSSET d'avoir accepté d'encadrer cette thèse, pour votre présence quotidienne à mes côtés, pour vos qualités scientifiques ainsi que pour votre soutien continu. Vous m'avez toujours encouragé et poussé à faire de mon mieux. Le travail avec vous était un plaisir.

Je remercie également Céline Viennet (Laboratory of Engineering and Cutaneous Biology, UMR 1098, Bourgogne Franche-Comté University), Sophie Robin et Sami Ibazizen (Bioexigence) pour leur aide dans l'application cutanée.

Toute ma reconnaissance envers Pr. Sophie Fourmentin et Pr. Véronique Rosilio pour accepter d'être rapporteuses de ce manuscrit de thèse et à Pr. Hatem Fessi, Dr. François-Xavier LEGRAND, Dr. Sophie Robin et Dr. Marc Since pour m'avoir fait l'honneur d'être examinateurs.

Je souhaite exprimer mes remerciements à Géraldine Augusti pour sa présence au laboratoire et son aide à la réalisation des imageries par TEM au Centre Technologique des Microstructures, Université de Lyon 1. Je remercie aussi Sébastien Urbaniak pour son aide et pour m'avoir formé sur le lyophilisateur.

J’aimerais dire aussi merci à tous mes collègues au Laboratoire des Molécules Bioactives au Liban et au LAGEPP (Lyon) et particulièrement à Maria Espina Benitez pour ses conseils avec la HPLC.

Si je ne me sentais pas trop loin de mon pays et de ma famille, c’est grâce à ma deuxième famille en France. Elissa Ephrem, tu étais là durant ma première année de thèse à m’encourager et me consoler même si tu n’aimais pas trop donner des câlins, tu m’en as donné quand même… Jad Eid, on était perdu à Lyon ensemble à notre arrivée et on l’est toujours à présent… Greta Magnano, ma folle dès la première minute, tu étais toujours là même quand on a failli mourir à cause d’un match de foot, j’ai découvert l’Italie grâce à la meilleure des italiennes… Maroua Rouabah, même si t’étais pas dans mon bureau, en réalité tu étais dans mon bureau, tu étais toujours à mes côtés, à me soutenir et à me remonter le moral et partager des moments de folie… Noëlle Sarkis, ma colloque végétarienne, autre que le composte et le recyclage, tu m’as appris plein de choses, heureusement qu’on s’est confinée ensemble ou bien j’aurai pu devenir folle… Maya Khellaf, my partner in crime, on était toujours ensemble l’une à côté de l’autre si ce n’est pas au bureau, à la maison et même à la salle de sport, des heures et heures qui passaient comme des minutes, tu étais toujours là pour me consoler et tu m’as appris plein de choses surtout les expressions françaises dont je ne connaissais aucune …

Si je consacre tout ce manuscrit pour juste dire merci à Joyce Azzi ça ne serait pas suffisant. Tu étais loin physiquement mais tu étais présente pendant chaque seconde de cette thèse et si j’ai pu surmonter tous les obstacles que j’ai vécu c’était grâce à toi…

Un grand merci à ma famille, mon père Youssef, ma mère Wafaa, mon frère Assaad, ma sœur Grace, son époux Jack et mon neveu Elie. J’espère que vous serez toujours fière de moi.

Enfin, je remercie mon pays le Liban et surtout sa capitale Beyrouth. Tu m’as appris qu’après chaque bas il y a des hauts, tu es vraiment le pays du Phénix et je suis sûre que tu le seras

toujours… Je dédie ce manuscrit de thèse à Beyrouth dans l'espoir qu'elle se relève de sous les décombres

Sommaire

Résumé

La cystéamine, un aminothiol synthétisé par les cellules du corps humain, possède plusieurs activités biologiques notamment un effet radioprotectif et anticancéreux. Elle est connue pour son utilisation dans le traitement de la cystinose, des maladies de Parkinson et de Huntington. Cette molécule a aussi un effet dépigmentant et existe sous différentes formes comme le chlorhydrate de cystéamine. Malgré ses nombreux effets bénéfiques, la cystéamine est hygroscopique, présente des propriétés organoleptiques et un profil pharmacocinétique défavorables. C'est une molécule instable en solution car elle s'oxyde pour former la cystamine. Pour surmonter ces limites, nous avons choisi de développer des formulations de liposomes encapsulant respectivement les deux formes de la molécule (cystéamine et chlorhydrate de cystéamine) dans le but de l'appliquer sur la peau en tant qu'agent dépigmentant. Les suspensions liposomales ont été caractérisées par la distribution en taille des liposomes et le taux d'encapsulation des deux formes de cystéamine pour différentes compositions. Le dosage simultané de la cystéamine et la cystamine par la méthode de chromatographie par paires d'ions a été mis au point. La stabilité de la cystéamine et du chlorhydrate de cystéamine dans les suspensions liposomiales a été ensuite étudiée pour différentes conditions de stockage. Nous avons aussi eu recours à la lyophilisation des suspensions liposomiales pour augmenter la stabilité des formulations au cours de stockage. La caractérisation de la forme lyophilisée après stockage a été évaluée. Les liposomes blancs et encapsulant la cystéamine et le chlorhydrate de cystéamine étaient de taille nanométriques et monodisperses. Des faible taux d'encapsulation ont été obtenus en raison du caractère hydrophile des deux formes de la molécule. La stabilité des deux formes de la cystéamine a augmenté après encapsulation et d'autant plus après lyophilisation des échantillons. Le test de cytotoxicité par MTT, le dosage de la mélanine, l'activité de la tyrosinase ainsi que la pénétration cutanée par cellule de Franz ont été appliqués pour le chlorhydrate de cystéamine

libre et encapsulé. Ces tests ont montré que les formulations choisies ne présentaient pas de cytotoxicité vis-à-vis de la lignée cellulaire de mélanome de souris B16. Le chlorhydrate de cystéamine et la cystamine ont inhibé la production de la mélanine, la tyrosinase et la formation des espèces réactives à l'oxygène. L'encapsulation du chlorhydrate de cystéamine a diminué légèrement l'effet de cette inhibition mais a augmenté la pénétration de la molécule dans la peau et sa rétention au niveau de l'épiderme. Toutefois, la cystamine n'a pas pénétré et n'a pas été détectée dans aucun compartiment de la peau.

Mot clés : cystéamine, cystamine, chromatographie par paires d'ions, effet dépigmentant, liposomes, lyophilisation, pénétration cutanée, stabilité.

Abstract

Cysteamine, an aminothiol compound synthetized by human body cells, presents several biological activities such as radioprotective and anticancer effects. It is the only treatment of cystinosis and can be used for Parkinson and Huntington treatments. This molecule also shows a depigmenting effect and has different forms like cysteamine hydrochloride. However, cysteamine is hygroscopic, presents poor organoleptic properties and pharmacokinetic profile. In addition, cysteamine is unstable in aqueous solutions because of its oxidation to its disulfide form cystamine. To overcome these problems, cysteamine and its hydrochloride form were encapsulated in liposomes, respectively. The liposomal suspensions were characterized for their size, homogeneity, zeta potential and the encapsulation efficiency of cysteamine and cysteamine hydrochloride were determined. The simultaneous quantification of cysteamine and cystamine by ion pair liquid chromatography was optimized. The stability of cysteamine and its hydrochloride form in the liposomes was also studied in different storage conditions. The freeze drying of the liposomal suspension was carried out to increase the shelf life of the formulations. The characterization after storage of the lyophilized form was also done. The liposomes were nanometric, monodisperse and a low encapsulation efficiency of the active product was obtained. The stability of cysteamine and cysteamine hydrochloride was increased after encapsulation especially after freeze-drying. Finally, the optimized formulations of cysteamine hydrochloride-loaded liposomes in liquid and dried forms were tested for their depigmenting effect. Their toxicity by the MTT assay, the dosage of melanin, the tyrosinase activity and the skin penetration of the free and the encapsulated cysteamine hydrochloride were evaluated. These tests showed that the selected formulations did not show cytotoxicity to the B16 murine melanoma cell line. Cysteamine hydrochloride and cystamine induced melanin, tyrosinase and reactive oxygen species inhibition. Encapsulation of cysteamine decreased the

effect of this inhibition but increased the penetration of the molecule into the skin and its retention in the epidermis. Cystamine did not penetrate and has not been found in skin layers.
Keywords: cysteamine, cystamine, ion pair chromatography, depigmenting effect, liposomes, freeze drying, skin penetration, stability.

Liste des abréviations

Chol : Cholestérol

CMC: Concentration micellaire critique

DLS : Dynamic Light Scattering, diffusion dynamique de la lumière

EDTA: Éthylènediaminetétraacétique

HPLC: High performance liquid chromatography

HP-β-CD : Hydroxypropyl-ß-cyclodextrine

MTT: Bromure de 3-(4,5-dimethylthiazol-2-yl)-2,5-diphenyl tetrazolium

pdI : polydispersity index, indice de polydispersité

PH 90H : Phospholipon 90H

SDS: Sodium dodecyl sulphate

TEM : Transmission Electronic Microscopy, microscopie électronique à transmission

Introduction générale

L'hyperpigmentation de la peau est une maladie qui se manifeste par une production excessive de mélanine conduisant à l'apparition de taches foncées (Grimes et al., 2018). Plusieurs traitements ont été développés mais présentent, pour la plupart, une certaine toxicité (Rendon & Gaviria, 2005). La cystéamine est une molécule synthétisée par le corps humain qui présente de nombreuses applications biologiques comme le traitement de la cystinose, des maladies de Huntington et de Parkinson, et autres (Besouw et al., 2013). Cette molécule et son produit d'oxydation la cystamine ont montré un effet dépigmentant en inhibant l'activité de la tyrosinase et par la suite l'inhibition de la production de mélanine (Chavin & Schlesinger, 1966). Malgré les effets bénéfiques que présente cette molécule, la cystéamine est hygroscopique et possède des propriétés organoleptiques défavorables, ainsi qu'une instabilité chimique en solution. Cette instabilité provient de la réaction d'oxydation de la cystéamine produisant la cystamine (Dixon et al., 2018). L'encapsulation de cette molécule peut être une solution pour surmonter ces problèmes et parvenir à l'effet souhaité. Les liposomes sont des vésicules nanométriques constitués de bicouches phospholipidiques capables d'encapsuler des molécules lipophiles, hydrophiles ou amphiphiles (Akbarzadeh et al., 2013). Afin d'augmenter la stabilité des suspensions liposomales, le processus de lyophilisation est proposé (Chen et al., 2010).

Plusieurs méthodes ont été mises au point pour détecter et quantifier la cystéamine. Cependant, sa quantification reste difficile en raison de l'absence de groupement chromophore au sein de sa structure ainsi que son instabilité en solution. Il apparait donc nécessaire de développer une technique analytique permettant le dosage simultané de la cystéamine et de la cystamine. Une étude de la stabilité des solutions durant l'analyse est aussi demandée.

Les liposomes encapsulant la cystéamine sous formes liquide et lyophilisée peuvent être utilisés afin d'augmenter la stabilité, la pénétration cutanée et l'efficacité de la cystéamine.

Ce travail de thèse a été réalisé au sein du Laboratoire de Molécules Bioactives (Faculté des Sciences, Section II, Université Libanaise) et du Laboratoire d'Automatique, de Génie des Procédés et de Génie Pharmaceutique (Université Claude Bernard Lyon 1). L'étude portant sur l'application cutanée a été effectuée à Bioexigence et à la plateforme en imagerie cellulaire Bourgogne/Franche Comté Site UFR Santé Besançon. L'objectif de cette thèse consiste à préparer et caractériser des liposomes encapsulant la cystéamine et le chlorhydrate de cystéamine sous formes liquide et lyophilisée afin d'étudier la stabilité de la molécule et son effet dépigmentant sur la peau.

Des liposomes constitués de deux types de lipides (Phospholipon 90H ou lipoïde S100) ainsi que de cholestérol et encapsulant la cystéamine et le chlorhydrate de cystéamine ont été préparés par la méthode d'injection éthanolique. La caractérisation des suspensions liposomales en termes de taille, indice de polydispersité et potentiel Zêta ainsi que le taux d'incorporation de cholestérol et de lipides a été réalisée. De plus, le taux et le rendement d'encapsulation de la cystéamine et du chlorhydrate de cystéamine dans les liposomes ont été déterminés après avoir optimisé la méthode de dosage de la cystéamine par la technique d'Ellman. La lyophilisation de ces suspensions liposomales et leurs caractérisations ont été menées. La méthode de dosage simultané de la cystéamine et la cystamine par chromatographie de paires d'ions a été optimisée. La stabilité des deux formes a été étudiée en variant les conditions de stockage. Les suspensions liposomales ont été testées pour leur effet dépigmentant. L'évaluation de la cytotoxicité ainsi que le dosage de la mélanine, la tyrosinase produites et la formation des espèces réactives à l'oxygène par les cellules de mélanome de souris, B16 en présence du chlorhydrate de cystéamine, la cystamine et des liposomes encapsulant le chlorhydrate de cystéamine ont été menés. Enfin, une étude de la pénétration

cutanée en utilisant la cellule de Franz du chlorhydrate de cystéamine libre et encapsulé a été réalisée.

Ce manuscrit est divisé en cinq chapitres dont quatre sont présentés sous formes d'articles. Le premier chapitre est une synthèse bibliographique portant sur la stabilisation, la quantification, les effets biologiques ainsi que les systèmes d'encapsulation de la cystéamine décrits dans la littérature. Le deuxième chapitre présente présentant les méthodes expérimentales utilisées au cours de cette thèse. Le troisième chapitre présente les résultats de la méthode développée pour la quantification simultanée de la cystéamine et la cystamine. Le quatrième chapitre décrit la préparation, la caractérisation et l'étude de stabilité des liposomes encapsulant la cystéamine sous formes liquide et poudre. Le cinquième chapitre porte sur l'application cutanée des liposomes encapsulant le chlorhydrate de cystéamine. Le manuscrit se termine par une conclusion et des perspectives.

Références

Akbarzadeh, A., Rezaei-Sadabady, R., Davaran, S., Joo, S. W., Zarghami, N., Hanifehpour, Y., Samiei, M., Kouhi, M., & Nejati-Koshki, K. (2013). Liposome: Classification, preparation, and applications. *Nanoscale Research Letters*, *8*(1), 102. https://doi.org/10.1186/1556-276X-8-102

Atallah, C., Charcosset, C., & Greige-Gerges, H. (2020). Challenges for cysteamine stabilization, quantification, and biological effects improvement. *Journal of Pharmaceutical Analysis*. https://doi.org/10.1016/j.jpha.2020.03.007

Besouw, M., Masereeuw, R., van den Heuvel, L., & Levtchenko, E. (2013). Cysteamine: An old drug with new potential. *Drug Discovery Today*, *18*(15), 785–792. https://doi.org/10.1016/j.drudis.2013.02.003

Chavin, W., & Schlesinger, W. (1966). Some potent melanin depigmentary agents in the black goldfish. *Die Naturwissenschaften*, *53*(16), 413–414.

Chen, C., Han, D., Cai, C., & Tang, X. (2010). An overview of liposome lyophilization and its future potential. *Journal of Controlled Release*, *142*(3), 299–311. https://doi.org/10.1016/j.jconrel.2009.10.024

Dixon, P., Powell, K., & Chauhan, A. (2018). Novel approaches for improving stability of cysteamine formulations. *International Journal of Pharmaceutics*, *549*(1), 466–475. https://doi.org/10.1016/j.ijpharm.2018.08.006

Grimes, P. E., Ijaz, S., Nashawati, R., & Kwak, D. (2018). New oral and topical approaches for the treatment of melasma. *International Journal of Women's Dermatology*, *5*(1), 30–36. https://doi.org/10.1016/j.ijwd.2018.09.004

Rendon, M. I., & Gaviria, J. I. (2005). Review of Skin-Lightening Agents. *Dermatologic Surgery*, *31*(s1), 886–890. https://doi.org/10.1111/j.1524-4725.2005.31736

Chapitre 1 : Synthèse bibliographique

Introduction

Ce chapitre est présenté sous forme d'une revue bibliographique intitulée « Challenges for cysteamine stabilization, quantification, and biological effects improvement » publiée en 2020 dans le journal « Journal of Pharmaceutical analysis ». Cette revue est constituée de plusieurs parties décrivant le métabolisme, les propriétés physico-chimiques et la stabilité de la cystéamine. Elle porte aussi sur les différentes méthodes analytiques utilisées pour quantifier la cystéamine et présente leurs avantages et leurs inconvénients. De plus, cette revue traite la pharmacocinétique et la pharmacodynamie de cette molécule en présentant les différentes applications biologiques et en soulignant l'effet dépigmentant. Aussi, la revue présente les systèmes d'encapsulation déjà utilisés dans la littérature pour améliorer les effets biologiques de la cystéamine.

Challenges for cysteamine stabilization, quantification, and biological effects improvement

Carla Atallah[a,b], Catherine Charcosset[b], and Hélène Greige-Gerges[a*]

[a]*Bioactive Molecules Research Laboratory, Doctoral School of Sciences and Technologies, Faculty of Sciences, Lebanese University, Lebanon*

[b]*Laboratoire d'Automatique, de Génie des Procédés et de Génie Pharmaceutique (LAGEPP), Université Claude Bernard Lyon 1, France.*

Journal of pharmaceutical analysis (2020)

Challenges for cysteamine stabilization, quantification, and biological effects improvement

Carla Atallah[a,b], Catherine Charcosset[b], and Hélène Greige-Gerges[a*]

[a]*Bioactive Molecules Research Laboratory, Doctoral School of Sciences and Technologies, Faculty of Sciences, Lebanese University, Lebanon*

[b]*Laboratoire d'Automatique, de Génie des Procédés et de Génie Pharmaceutique (LAGEPP), Université Claude Bernard Lyon 1, France.*

* Corresponding author: hgreige@ul.edu.lb; greigegeorges@yahoo.com

Abstract

The aminothiol cysteamine, deriving from coenzyme A degradation in mammalian cells, presents several biological applications. However, the bitter taste and sickening odor, the chemical instability, the hygroscopicity, and the poor pharmacokinetic profile of cysteamine limit its efficacy. The use of encapsulation systems is a good methodology to overcome these undesirable properties and improve the pharmacokinetic behavior of cysteamine. Besides, the conjugation of cysteamine to the surface of nanoparticles is generally proposed to improve the intra-oral delivery of cyclodextrin-drug inclusion complexes, as well as to enhance the colorimetric detection of compounds by a gold nanoparticle aggregation method. On the other hand, the detection and quantification of cysteamine is a challenging mission due to the lack of a chromophore in its structure and its susceptibility to oxidation before or during the analysis. Derivatization agents are therefore applied for the quantification of this molecule. To our knowledge, the derivatization techniques and the encapsulation systems used for cysteamine delivery were not reviewed previously. Thus, this review aims to compile all the

data on these methods as well as to provide an overview of the various biological applications of cysteamine focusing on its skin application.

Keywords

Cysteamine; detection; Encapsulation; Skin; Stability.

1. Introduction

Cysteamine (cys) or 2-mercaptoethylamine is an aminothiol endogenously synthesized by human body cells during the co-enzyme A metabolism cycle (**Fig. 1**).

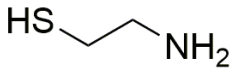

Figure 1: Structure of cys.

In 1953, cys was found to be one of the most potent thiol derivatives in the protection against ionizing radiation [1]. Numerous studies tested the radioprotective effect and the mechanism of action of this compound using human cell lines [2,3], bacteria [4], and mice models [5].

In 1976, it was first used for the treatment of cystinosis, was approved by the US Food and Drug Administration (FDA), and commercialized in the 1990s [6]. Till now, cys is the only specific targeted therapy available for patients with cystinosis. The latter is a rare autosomal recessive metabolic disease, characterized by the accumulation and crystallization of cystine within the lysosome, which eventually results in apoptosis and tissue damage in all organ systems including the cornea [7]. Following oral administration, cys enters the lysosome by an unknown transporter and breaks down cystine into cysteine and cysteine-cys disulfide, which are removed by specific transporters. Consequently, cys rapidly deplete cells and tissues of lysosomal cystine.

Another interesting application was recently discovered for cys, as it was shown to be clinically efficient in treating hyperpigmentation disorders [8,9]. Despite the presence of many potent depigmenting agents, namely hydroquinone and derivatives and kojic acid, however, they were found to possess local side effects (irritation, permanent depigmentation…) and presented mutagenic and carcinogenic potentials [10]. Cys has shown to be a well-tolerated compound, demonstrating its non-mutagenicity and non-carcinogenicity criteria [11]. Interestingly, it may

inhibit the mutagenic effect of some potent mutagens. Besides, it may exert an anti-cancer effect in several cancers, such as melanoma, in *in vivo* studies [12].

Regardless of its numerous and remarkable biological applications, the efficacy of cys may be limited by its unpleasant organoleptic properties, strong hygroscopicity, chemical instability, and its poor pharmacokinetic profile ($T_{1/2}$ = 1.75 h) [13]. Moreover, cys is often susceptible to degradation through its rapid oxidation in air or solution to its disulfide form cystamine (**Fig. 2**).

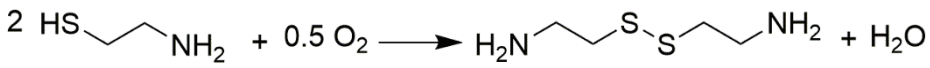

Figure 2: Oxidation of cys to cystamine.

Consequently, the encapsulation of this molecule into delivery systems has been commonly used as a good approach to overcome these problems [14–16]. Cys was mainly incorporated into three different types of encapsulating agents: liposomes, CDs, and emulsions. For example, its encapsulation in liposomes was used to selectively release cys in lysosomes [17] and to enhance its gastrointestinal absorption [15]. Besides, CDs and emulsions were successfully shown to remove cys odor [13] and to improve cys stability [18], respectively. On the other hand, cys was employed to modify the surface of encapsulation systems for many purposes. For example, cys was linked to the surface of CDs to improve intra-oral drug delivery [19,20] and to the surface of gold nanoparticles to enhance the colorimetric detection of compounds by these particles [21,22].

This review highlights the biosynthesis, the physicochemical properties, and the stability of cys. The quantification of this compound using different analytical methods, as well as the challenges encountered in these techniques will be for the first time analyzed. Then, we will discuss the biological activities of this compound emphasizing its topical effects. Finally, the

encapsulation of cys in different encapsulation systems and the use of cys to modify the surface of these carriers will be presented.

2. Metabolism of cys

Cys is an aminothiol that derives from coenzyme A (CoA) degradation. The degradation of CoA leads to the formation of pantetheine, which is hydrolyzed by pantetheinase to obtain cys and pantothenic acid (**Fig. 3 [24]**) [23,24]. Then, the oxidation of cys by cys dioxygenase produces hypotaurine. Later, cys is eliminated by the taurine pathway in the form of bile salts [25]. After the administration of a high dose of cys, an alternative catabolic route is manifested, involving its conversion to S-methylcys by a thiol-methyltransferase, which is consequently metabolized into methanethiol and acetamide by cytochrome P450. Then, methanethiol is converted to dimethylsulfide by another thiol-methyltransferase [26,27].

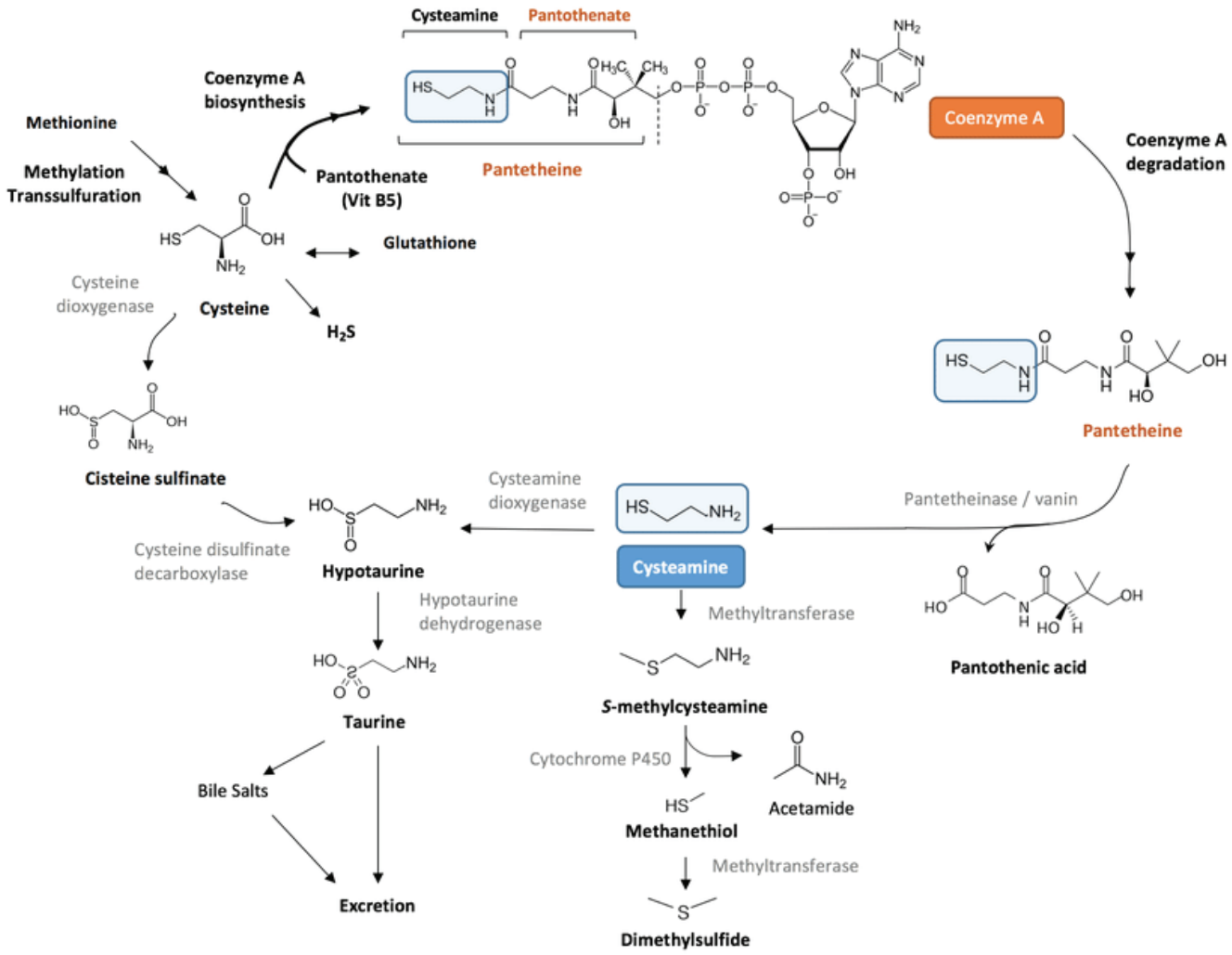

Figure 3: Metabolism of cys **[24]**.

3. Physicochemical properties and stability of cys

Cys possesses high aqueous solubility (23.5 g/L), a $pKa_{1(SH)}$= 8.19 and $pKa_{2(NH2)}$ =10.75 with a melting point of 67.3°C (**Table 1**;[16, 28-31]). This molecule exists in three ionic forms: the positively charged form (cys^{+}), the zwitterionic form (cys-ZW), and the negatively charged form (cys^{-}) (**Fig. 4**) [32].

Table 1. Physicochemical properties of cys.

Melting point	**67.3 °C** [16]
pKa values	pKa_1 = 8.19; pKa_2 = 10.75 [28]
Molecular Weight	77.15 g/mol [29]
Physical description	Solid [29]
Color	Crystal [29]
Odor	Disagreeable odor [29]
Chemical formula	$HSCH_2CH_2NH_2$
Boiling point	133.6 ± 23.0 °C at 760 mmHg (predicted)
Vapor pressure	0.03167 bar at 25°C [30]
Density	1.0 ± 0.1 g/mL (predicted)
Log*P*	0.1 [31]
Water solubility	23.5g/L [31]
Soluble in methanol, ethanol and freely soluble in alkaline media [31]	

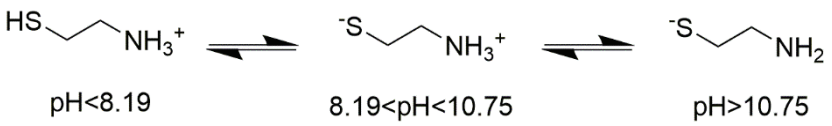

Figure 4: Chemical structures of cys forms obtained at different pHs.

Besides, cys, as a thiol compound, has a very offensive odor that makes it difficult its use as a depigmenting agent [9]. Different forms of cys have been used: cys hydrochloride (HCl), phosphocys, and cys bitartrate. Cys hydrochloride forms a eutectic equilibrium with water with a low eutectic temperature of 240 K. A eutectic mixture is composed of two or three components with a melting point significantly lower than that of its one component [33]. This low temperature causes the rapid dissolution of cys in the presence of water. The presence of a minor quantity of water vapor doesn't affect the stability state of cys hydrochloride, and cys

mass remains stable until a 35% relative humidity. In fact, above this water vapor pressure, cys hydrochloride melts immediately to form a very concentrated saturated solution of 0.85 mass fraction or 0.47-mole fraction of cys hydrochloride [31].

Cys is unstable in solution; a rapid conversion to cystamine occurs resulting from the rapid oxidation of the sulfhydryl group. The reactions of oxygen with thiols in aqueous solutions are presented in equations (1) and (2), according to which the reactions gave disulfides and hydrogen peroxide or water.

Alkaline pH stimulates the oxidation of cys because the thiolate anion (cys^-) is more reactive. Moreover, this reaction is catalyzed by metal ions such as Cu^{2+}, Fe^{3+}, and Zn^{2+}. In fact, the reduction reaction of cys by metal ions produces the reduced ion; the latter reacts with oxygen and peroxide. The following series of reactions would explain this fact.

The reaction between Cu^+ and oxygen produces superoxide (4), then superoxide reacts with a thiol to generate thiol radical (5) that reacts with itself to produce the disulfide (6).

On the other hand, oxygen consumption is stimulated by a reaction of a reduced metal ion with peroxide producing the potent hydroxyl radical (7), the latter will react with a thiol leading to its reduction to form water (8). The thiol radical reacts with itself to produce the disulfide (6) as described previously. Therefore, the use of a chelating agent, such as diethyldithiocarbamate, inhibits this reaction [34].

$$2\,RSH + O_2 \longrightarrow RSSR + H_2O_2 \quad (1)$$

$$4\,RSH + O_2 \longrightarrow 2\,RSSR + 2\,H_2O \quad (2)$$

$$RSH + 2\,Cu^{2+} \longrightarrow 2\,Cu^{+} + 1/2\,RSSR + H^{+} \quad (3)$$

$$Cu^{+} + O_2 \longrightarrow Cu^{+} + O_2^{\cdot} \quad (4)$$

$$RSH + O_2^{\cdot} + H^{+} \longrightarrow RS^{\cdot} + H_2O_2 \quad (5)$$

$$2\,RS^{\cdot} \longrightarrow RSSR \quad (6)$$

$$H_2O_2 + Cu^{+} \longrightarrow OH^{-} + OH^{\cdot} + Cu^{2+} \quad (7)$$

$$OH^{\cdot} + RSH \longrightarrow RS^{\cdot} + H_2O \quad (8)$$

The degradation of cys is a zero-order reaction indicating that the concentration of cys decreases linearly with time [35]. The removal of oxygen from a solution of cys by packing under nitrogen and the presence of ascorbic acid (antioxidant) increase the stability of the molecule but show a lower efficacy in comparison with chelating agents such as disodium edetate [36].

Pescina et al. (2016) examined the stability of cys after being dissolved in 0.9% NaCl at different pH, temperature, and in the presence of α-CD, ethylenediaminetetraacetic acid (EDTA), and sodium phosphate. They showed that cys oxidation is a pH-dependent reaction. It was very fast at pH 7.4 because of the presence of the ionized thiol groups while the oxidation decreases at an acidic pH of 4.2. As for the influence of the temperature (-20, 4, and 25°C), they found that the stability decreases when the temperature increases. While EDTA plays a crucial role in preventing cys oxidation, the presence of α-CD or sodium phosphate did not affect its stability [16].

The degradation of 0.1 mg/mL cys has been reached within 18 h in phosphate buffer saline (PBS) with a rate of degradation of 126 µg/h. A similar rate (132 µg/h) was also observed but with a higher concentration (4.4 mg/mL) [18]. In order to improve the stability of cys, the addition of different types of antioxidant to 0.1 mg/mL cys has been evaluated to out-compete cys for oxygen consumption and compared to the degradation rate of free cys (126 µg/h). Nevertheless, the presence of the hydrophilic antioxidant vitamin C increased the degradation rate of cys (523 µg/h). This rate was not also influenced by the presence of the hydrophobic antioxidants, vitamin E, and soybean oil since they are scarcely soluble in aqueous solution. Tween 80 surfactant has induced a reduction in degradation rate to 112 µg/h, suggesting some interaction with either dissolved cys or oxygen molecules. While, an emulsion of vitamin E, soybean oil, and tween 80 surfactant resulted in a greater decrease in cys degradation (101 µg/h). However, these results are not significant since the degradation rate of cys is not well

decreased. The use of catalase enzyme, which can revert peroxide species to diatomic oxygen and potentially starving the system of radicals essential to oxidize cys, reduces the degradation rate to 58 μg/h. On the other hand, a decline in the cys degradation rate to 20-30% was obtained after the addition of hydrophobic film (a soybean oil layer) to slow oxygen diffusion [18].

4. Analytical methods for cys detection

Different analytical methods have been suggested to detect and quantify cys in biological samples, such as plasma and urine in the literature such as enzymatic assay, high-voltage electrophoresis, ion-exchange column chromatography, high-performance liquid chromatography (HPLC) with fluorescence and ultraviolet (UV) detection, and gas chromatography with flame ionization and photometric detection. These methods will be for the time presented in this review.

4.1. Cys derivatization

Due to the lack of a chromophore in cys structure, the quantification of this compound using conventional analytical methods with UV absorbance or fluorescence detection is a challenging mission. Therefore, the derivatization of cys is used for cys separation or quantification. For this purpose, numerous derivatization agents were utilized and optimized according to the analytical method used. In Table 2 [37-53], the structure of all these agents, as well as the derivatization reactions with cys, is presented.

Table 2. Structure and reaction of derivatization agents with cys.

Derivatization agents	Structures	Reaction products	References
Pivaldehyde	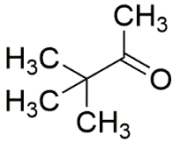	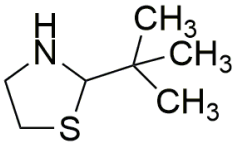	[37]
BSTFA	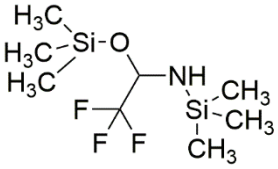	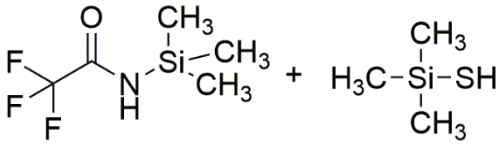	[38]
mBBr or QBBr	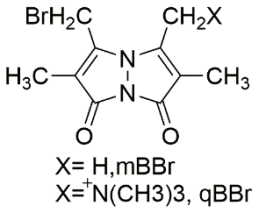	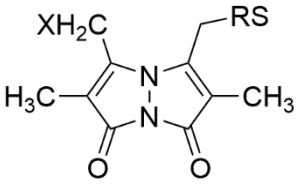	[39-42]
ABD-F	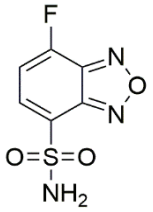	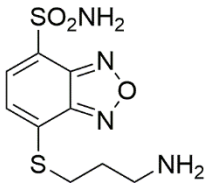	[43,44]
o-Phthalaldehyde	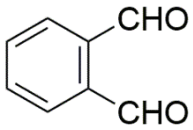	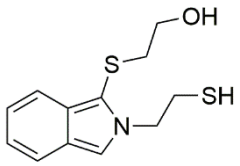	[45]
isoBCF	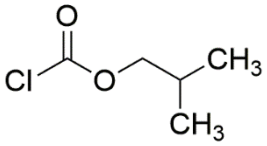	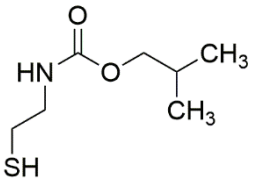	[46,47]
CMQT	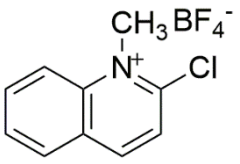		[48]

NPM	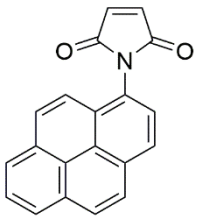	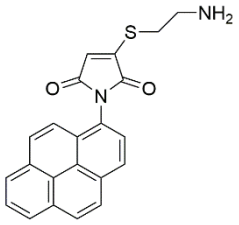	[49]
DAAB **D-Cl**	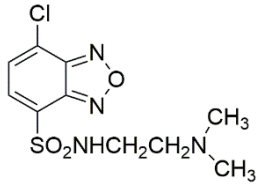	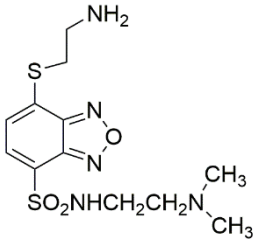	[50,51]
SBD-F	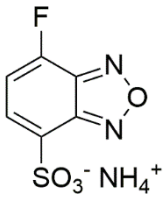	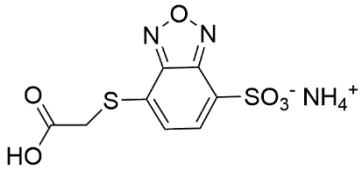	[52]
ACQ	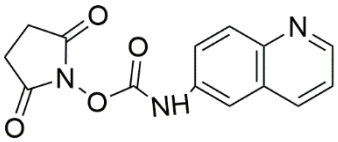	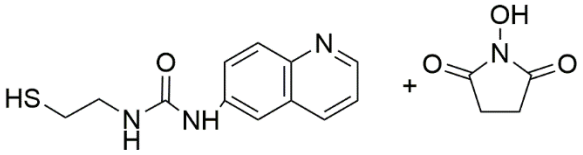	[53]

4.1.1. Pivaldehyde

Cys is derivatized with pivaldehyde before its analysis with gas chromatography [37].

4.1.2. Bis (trimethylsilyl) trifluoroacetamide (BSTFA)

The sample containing cys is placed in a screw-capped reaction vial, followed by the addition of dimethylformamide and BSTFA. The mixture is allowed to stand overnight before the analysis [38].

4.1.3. Monobromobimane (mBBr) or monobromotrimethylammoniobimane (qBBr)

mBBr or qBBr are dissolved in methanol, stored at 4°C, and protected from light for up to 4 months. This agent was used to quantify cys in plasma, red blood cells, and urine. A certain volume of this agent was added to cys solution and incubated for 15 min in the dark. For biological samples, perchloric acid was added to allow protein precipitation [39–42].

4.1.4. Ammonium 7-fluorobenzo-2-oxa-1,3-diazole-4-sulphonate (SBD-F)

SBD-F is prepared in borate buffer. Borate buffer (125 mM; pH 9.5) containing 4 mM EDTA was added to cys sample solution. After vortex-mixing for 30 s, the reaction mixture was heated at 60°C for 60 min and then cooled at 4°C for 15 min to stop the labeling reaction [43,44].

4.1.5. o-Phthalaldehyde

Cys solution is mixed with sodium hypochlorite followed by the addition of o-phthalaldehyde in the presence of 2-mercaptoethanol. The latter was used as an antioxidant. Sodium hypochlorite increased several times the fluorescence intensity of cys coupled to o-phthalaldehyde [45].

4.1.6. Isobutyl chloroformate (isoBCF)

IsoBCF and NaOH were added to cys sample, and the mixture was shaken at 300 rpm for 5 min at room temperature. The mixture was extracted with n-pentane, and the pentane extract was evaporated to dryness at 80°C. The residue was dissolved in ethyl acetate [46,47].

4.1.7. 2-chloro-1-methylquinolinium tetrafluoroborate (CMQT)

CMQT is synthetized as follows: 2-chloroquinoline, nitromethane, and trimethyloxonium tetrafluoroborate are mixed. Then, diethyl ether is added to the reaction mixture. The white precipitate is filtered off, washed with diethyl ether, and dried over phosphorus pentoxide under vacuum. Unfortunately, the synthesis reaction of CMQT was not presented.

Cys is derivatized by an excess of CMQT in tris buffer solution (pH 8.2), and hydrochloric acid is added to the mixture [48].

4.1.8. N-(1-pyrenyl) maleimide (NPM)

NPM solution is prepared in acetonitrile. Cys solutions are derivatized with 1.0 mM NPM solution and left to stand for 5 min at room temperature. HCl solution (2 N) is added to stop the reaction and stabilize the adducts at the end of the reaction time. The final pH of the solution is kept at about 2, which is necessary for the stability of the NPM-cys adduct [49].

4.1.9. 7-chloro-N-[2-(dimethylamino)ethyl]-2,1,3-benzoxadiazole-4-sulfonamide (DAABD-Cl)

DAABD-Cl is synthesized as follows (**Fig. 5**): 4-Chlorosulfonyl-7-chloro-2,1,3-benzoxadiazole is dissolved in CH_3CN. After the addition of N,N-dimethylethylenediamine, and triethylamine, the mixture is stirred at room temperature for 10 min. The reaction mixture is evaporated to dryness under reduced pressure to form DAABD-Cl [50].

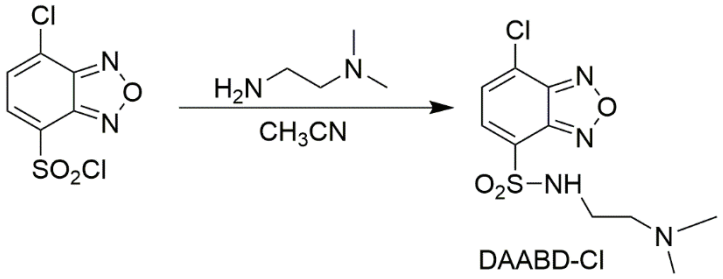

Figure 5: Synthetic route for DAABD-Cl.

DAABD-Cl is prepared in acetonitrile. A mixture of Tris (2-carboxyethyl) phosphine hydrochloride, EDTA, and 3-[(3-Cholamidoproryl) dimethylammonio] propanesulfonic acid is prepared in borate buffer. This mixture is added to cys solution, borate buffer, and DAABD-Cl. The reaction mixture is heated at 40°C, and aliquots of the reaction mixture are taken out at intervals of 5-20 min followed by the addition of 20% trifluoroacetic acid to stop the derivatization reaction [51].

4.1.10. 4-fluoro-7-sulfamoyl benzofurazan (ABD-F)

Cys solutions are directly derivatized with ABD-F reagent. The alkylation reaction is completed at 55°C for 15 min and stopped with HCl 12 N [52].

4.1.11. 6-aminoquinolyl-N-hydroxysuccinimidyl carbamate (ACQ)

Cys solutions are derivatized with ACQ in the presence of borate buffer and heated at 55°C for 10 min. The mixture was allowed to cool at room temperature before HPLC analysis [53].

4.2. Analytical methods

4.2.1. Enzymatic assay

This assay consists of the inhibition of D-amino acid oxidase enzyme activity by the product of the reaction occurring between cys and bromopyruvate (9). The enzyme activity is proportional to the amount of cys [54].

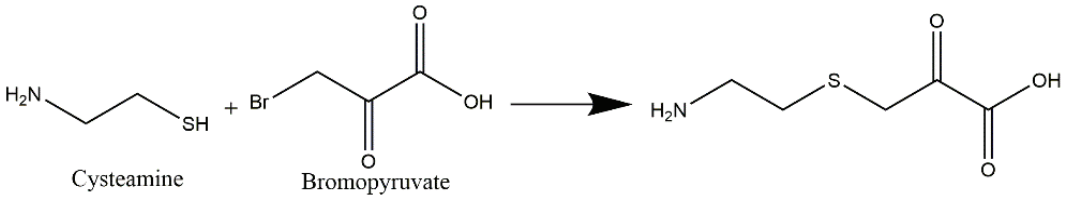

(9)

Another method described by Duffel et al. (1987) involved the oxidation of cys to hypotaurine by cys dioxygenase (10). Therefore the quantification of oxygen uptake is proportional to cys concentration with standard solutions between 10 and 100 nmol [55].

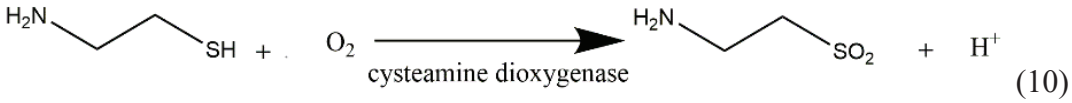

(10)

4.2.2. Ion-exchange column chromatography

Hsiung et al. (1978) worked on the detection of cys by ion-exchange column chromatography using an amino acid analyzer with a short column of Beckman analyzer. Cys was detected after 268 min, a long time that may lead to the oxidation of the product during the analysis and therefore, an underestimation of the product concentration [56].

Derivatization of cys with monobromotrimethylammoniobimane and monobromobimane has been realized by Fahey et al. (1981), followed by separation of the derivatives by cation-exchange chromatography and detection by fluorometry. The principal limitation of this method is the time required for sample analysis, 3-4 h for each of the bromobimane derivatives [39].

Later, Ida et al. (1984) used as derivatization agent the o-phthalaldehyde in the presence of 2-mercaptoethanol and sodium hypochlorite. Cation-exchange chromatography, using cation

exchange resin (ISC-05/S0504), sodium borate buffer (pH 11.10) as mobile phase, 70°C as temperature with a linearity range of 2-200 pmol, was used to separate the derivatives and the elution time was decreased to attain 7.5 min based on a fluorometric detection [45]. For the application of this assay method to biological materials, the pretreatment with a cation exchange column (Dowex 5OWX8) was essential to remove interfering o-phthalaldehyde-reactive substances. This method was found to be suitable for evaluating the cys plus cystamine content in various organs and tissues because cys was quantitatively converted to cystamine in biological materials during these sampling procedures.

4.2.3. HPLC

The detection of cys by HPLC was performed using fluorescence, UV, and electrochemical detections. Electrochemical detection doesn't require any derivatization, while cys needs to be derivatized when using fluorescence and UV detections (Table 3 [40-44,48,49,50-53]). Herein, we will present the two methods of HPLC that use derivatization agents.

Table 3. Detection of cys by HPLC.

Derivatization agent	Flow rate (mL/min)	Stationary phase	Mobile phase	T (°C)	Elution time (min)	Limit of detection	References
CMQT[a]	1	C_{18} (5µm; 4.6 mm×150 mm)	Gradient elution or isocratic elution (trichloro acetic acid and acetonitrile)	25	9	0.1 µM	[48]
	1.5	C_{18} (5 µm; 4.6 mm×150 mm)	Gradient elution (methanol, acetic acid and water)	RT*	12.5	nmol	[40]
mBBr[b]	1.5	C_{18} (3 µm; 4.6 mm×150 mm)	Acetonitrile	RT*	4.3	50 nM	[41]
	0.3	C_{18} (5 µm; 2.1 mm×100 mm)	Water: methanol (65:35)	-	11	2 nM	[42]
SBD-F[b]	1	C_{18} (8-10 µm; 3.9 mm×300 mm)	Gradient elution (methanol and sodium acetate)	RT*	10	0.07 pmol	[43]

	0.3	C_{18} (5µm; 2.0 mm×250 mm)	Phosphate buffer: CH_3CN (96:4)	30	5	0.47 µM	[44]
NPM[b]	1	C_{18} (5µm; 4.6 mm×250 mm)	Acetonitrile: water (70:30)	RT*	10	0.01 nM	[49]
DAABD-Cl[b]	0.6	C_{18} (2 nm, 4.6 mm×150 mm)	Gradient elution (water, acetonitrile and trifluoroacetic acid)	50	6.4	154 fmol	[51]
ABD-F[b]	1	C_{18} (3µm; 3.9 mm×150 mm)	2.5 % methanol and ammonium acetate	-	-	-	[52]
ACQ[b]	0.3	C_{18} (5µm; 2.1 mm×150 mm)	Gradient elution (sodium acetate and trimethyl- amine, acetonitrile and water)	RT*	29	0.77 pmol	[53]

**RT: Room temperature; a: HPLC coupled with UV detection; b: HPLC coupled with fluorescence detection*

4.2.3.1.Fluorescence detection

HPLC using fluorescence detection is widely used to detect cys. Many derivatization agents were used inducing different analysis conditions and eluting times. For example, monobromobimane [40–42], ammonium 7-fluorobenzo-2-oxa-1.3-diazole-4-sulphonate [43,44], N-(1-pyrenyl) maleimide [49], 7-chloro-N-[2-(dimethylamino)ethyl]-2,1,3-benzoxadiazole-4-sulfonamide (DAABD-Cl) [51], 4-fluoro-7-sulfamoylbenzofurazan [52], and ACQ [53] were all selected to detect cys. **Table 3** resumes the analytical conditions and elution times for each derivatization agent.

4.2.3.2.UV detection

2-chloro-1-methylquinolinium tetrafluoroborate was synthesized and used as a derivatization agent for UV detection of cys. The elution time was 25 min, the limit of detection was 0.1, and 0.2 µmol/L, and the detection wavelength was 355 nm. This method is highly sensitive and specific. But, it is labor-intensive, as the derivatization reagent has to be synthesized initially for the preparation of stable derivatives [48].

4.2.4. Gas chromatography

Gas chromatography with flame ionization and photometric detection were used to quantify cys (Table 4 [37,38,46,47]).

Table 4. Gas chromatography detection of cys.

Derivatization agent	Carrier gas	Column used	T (°C)	Internal standard	Limit of detection	References
Pivaldehyde[a]	Helium (35 mL/min)	5' x 1/8" column	From 80° to 250°C at 10°/min	-	8 pmole	[37]
(Trimethylsilyl) trifluoro acetamide[a]	Helium (80 mL/min)	6 ft. ¼ column	From 75°-230° at 8°/min	-	Sub nanomole	[38]
Isobutyl chloroformate[b]	Nitrogen (10 mL/min)	15 m x 0.53 mm column	From 170° to 250°C at 5°/min	*p*-Toluene sulphonyl anilide	2 pmole	[46]
	Nitrogen (8 mL/min)	15 m x 0.53 mm column	From 170° to 250°C at 5°/min	Thianthrene	2 pmole	[47]

4.2.4.1. Flame ionization

Pivaldehyde (2,2-dimethylpropanal) [37] and (trimethylsilyl) trifluoracetamide [38] were used as derivative agents of cys. The conditions used in the analysis are presented in **table 4**.

4.2.4.2. Flame photometric detection:

The detection of cys in mouse tissues [46], in urine, and plasma samples [47] using isobutylchloroformate as a derivatization agent was studied. It is a sensitive and selective method but requires the preparation of stable derivatives, which is a time-consuming procedure.

4.2.5. UHPLC-ESI-MS/MS

5-Aminoisoquinolyl-N-hydroxysuccinimidyl carbamate (5-AIQC) and **N**-(acridin-9-yl)-2-bromoacetamide (AYBA) were used as derivatization agents for cys quantification using UHPLC-ESI-MS/MS. The different conditions of the analysis are described in table 5 [57-58].

Table 5. UHPLC-ESI-MS/MS detection of cys.

Derivatization agent	Mobile phase	Stationary phase	Flow rate (mL/min)	T(°C)	Gas flow (L/min)	Gas T(°C)	LOD (fmol)	References
5-AIQC	Gradient elution (ultra-pure water and methanol containing 0.1% formic acid)	C_{18} (1.8 µm; 2.1mm×100 mm)	0.6	50 °C	10	315	4	[57]
AYBA	Gradient elution (0.1% (v/v 1:999) HCOOH and MeOH)	C_{18} (1.7 µm; 2.1 mm×100 mm)	0.4	N.D.	3	250	0.0120	[58]

[58] *(N.D.: not determined)*

4.2.6. Colorimetric method using Ellman's reagent

In 1958, George Ellman described a method for the determination of mercaptan based on interchange of bis(*p*-nitrophenyl) disulfide and mercaptan anions (S^-) at pH 8.0 (**Fig. 6**). The kinetics of the reaction between cys and bis(*p*-nitrophenyl) disulfide showed that the full absorbance is settled after 60-90 min [59].

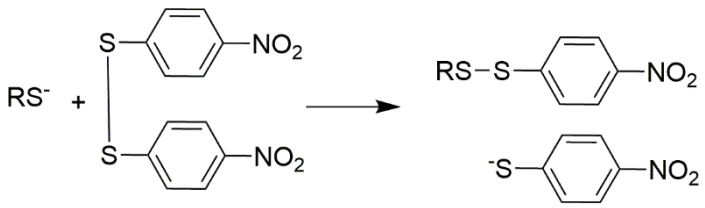

Figure 6: Reaction between bis(*p*-nitrophenyl) disulfide and mercaptan anion.

In 1959, bis(*p*-nitrophenyl) disulfide was replaced by its carboxylated derivative 5,5'-dithiobis (2-nitrobenzoique acid) (DTNB) because of its poor solubility in water (**Fig. 7**) [60].

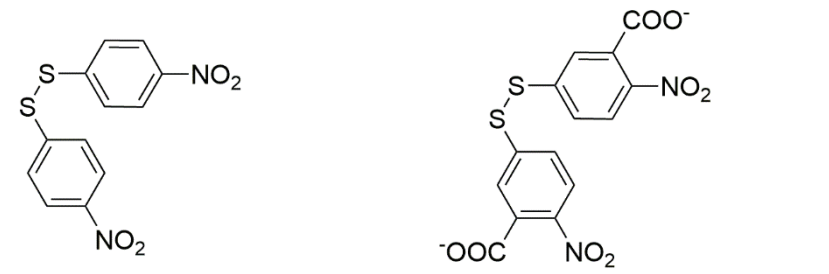

bis-(p-nitrophenyl) disulfide 5,5'-Dithiobis(2-nitrobenzoic acid)

Figure 7: Structure difference between bis(*p*-nitrophenyl) disulfide and DTNB.

An easy and rapid method was developed by Ellman (1959) to quantify sulfhydryl groups based on colorimetric detection after a reaction between sulfhydryl groups and DTNB, resulting in a yellow-colored product (2-nitro-5-thiobenzoic acid). The absorbance of the latter is measured spectrophotometrically at a wavelength of 412 nm, reflecting the concentration of cys.

The detection and quantification of cys using Ellman's reagent can be achieved using many techniques such as UV-visible spectroscopy [15], HPLC [61], ultra-performance liquid chromatography-tandem mass spectrometer [62], and using microtiter plate [63]. This method is easy to be applied since it doesn't need any synthesis of the reactive agent, could be used with different analytical techniques from the simplest to the most complicated ones and the reaction between the reactive and the sulfhydryl group is rapid without the requirement of heat or enzyme (**Fig. 8**).

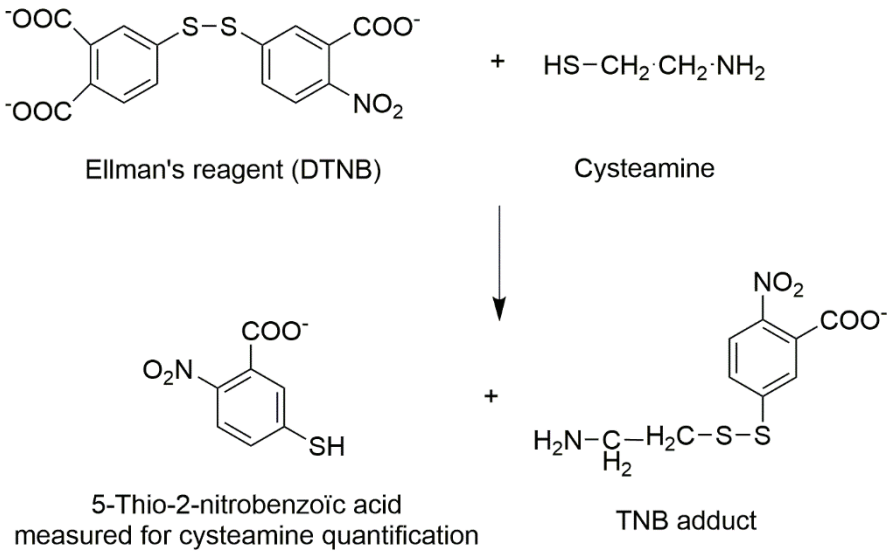

Figure 8: Reaction between cys and Ellman's reagent.

Some difficulties could be faced in the detection of cys by this method in some samples, for example in cloudy solutions such as liposomes loading cys. This issue is not well elaborated in the literature, however, Butler et al. (1978) tried to overcome this problem by adding 2% deoxycholate solution in the assay buffer to solubilize liposomes and/or by using matching amounts of liposomes suspension in the reference cuvette [17]. Besides, this method is not selective since many compounds possessing a sulfhydryl group may react with DTNB.

4.2.7. Ion pair and micellar chromatography

The quantification of cys was also assessed with the addition of a surfactant into the mobile phase which interacts with cys affecting its retention through a reversed-phase column. The addition of sodium dodecyl phosphate (40 mM) using micellar chromatography and sodium 1-heptanesulfonate (4 mM) using the ion pair chromatography to the mobile phase were able to separate and quantify cys and cystamine (Table 6 [16,64]).

Table 6. Cys detection using ion pair and micellar chromatography.

Method	Surfactant	Mobile phase	Stationary phase	Flow rate (mL/min)	T(°C)	LOD (µM)	References
Micellar chromatography	Sodium dodecyl phosphate (40 mM)	Water: acetonitrile: methanol (38:30:32) with phosphoric acid, and sodium dodecyl sulfate	C_{18} (5 µm; 4.6 mm x 250 mm)	1.6	50	4.15	[16]
Ion pair chromatography	Sodium 1-heptanesulfonate (4 mM)	Acetonitrile: water (0.1% phosphoric acid + Sodium 1-heptanesulfonate) (85:15)	C_{18} (5 µm; 4.6 mm x 250 mm)	1	25	12.9	[64]

4.2.8. Electrochemical detection of cys

Electrochemical reactions involve the loss or gain of electrons followed by subsequent rearrangements or reactions. If these reactions occur on physically separated metals in a conducting medium, a difference in electrical potential is generated; the electrical signal depends on the analyte concentration [65]. Cys is known for its oxidation to cystamine and therefore can be detected electrochemically. This was realized in literature using different types of electrodes. Cys was first analyzed by HPLC with an electrochemical detector using platinum electrode [66] or a single gold/mercury electrode [67,68]. However, the use of unmodified electrodes has proved a high overpotential and low electrical signal. Therefore, the electrochemical determination of cys was assessed using modified electrodes such as single-wall carbon nanotube modified glassy carbon electrode [69], carbon paste electrode [70-74], multiwall carbon nanotubes paste electrode [75-78], and screen-printed electrode [79]. The

electrooxidation of cys was catalyzed using different types of mediators cited in table 7 [69-79].

Table 7. The different electrochemical detection methods.

Electrode	Mediator	Concentrations range (µM)	LOD (µM)	Samples	References
Single-wall carbon nanotube modified glassy carbon electrode	1,2-Naphthoquinone-4-sulfonic acid sodium	5.0-270	3.0	-	[69]
Carbon paste electrode	N,Ndimethylaniline/ferrocyanide	80-1140	79.7	Capsules	[70]
	(9, 10-dihydro-9, 10-ethanoanthracene-11, 12-dicarboximido)-4-Ethylbenzene-1, 2-diol and nickel-oxide-carbon nanotube	0.01– 250	0.007	Tablet and urine	[71]
	Ferrocene carboxaldehyde and nickel-oxide nanoparticle	0.09-300	0.06	Urine and capsule	[72]
	N-(4-hydroxyphenyl)-3,5-Dinitrobenzamide and magnesium oxide nanoparticles	0.03–600	0.009	capsule and pharmaceutical serum	[73]
	Acetylferrocene and Nickel-oxide-Carbon nanotube	0.1-600	0.07	drug and pharmaceutical serum	[74]
Multiwall carbon nanotubes paste electrode	Ferrocene	0.7-200	0.3	Pharmaceutical, serum, and urine samples	[75]

	3,4-Dihydroxycinnamic acid	0.25-400	0.09	-	[76]
	Isoproterenol	0.3–450.0	0.09	Urine and drug	[77]
	Promazine hydrochloride	Two dynamic ranges of 2.0-346.5 µM and 346.5-1,912.5 µM	0.8	Urine and drug	[78]
Screen printed electrode	La_2O_3/Co_3O_4	1.0–700.0	0.3	Urine and capsule	[79]

The electrocatalytic mechanism for cys determination at the surface of an electrode in the presence of the mediator is illustrated in Fig. 9. Each method was applied in a certain range of cys concentration where the catalytic oxidation peak current showed a linear relationship with the concentration of cys. The limit of detection was determined for each method and the quantification was evaluated in different biological samples such as urine, tablet, capsules, and serum.

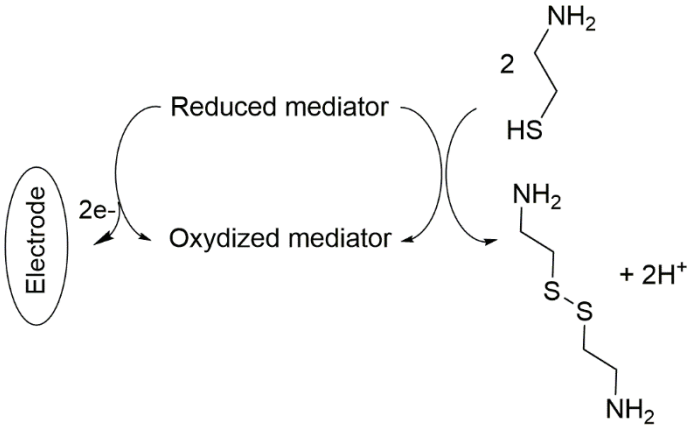

Figure 9: Electrocatalytic mechanism for cys determination at the surface of an electrode in the presence of a mediator.

Herein, we presented the different methods of cys quantification. The choice of an adequate method is hard, and it's based on various parameters. First, the type of sample used should be widely considered. For example, the Ellman method cannot be applied to plasma samples because of the interference of other thiol compounds during cys detection. Moreover, some derivatization agents (CMQT and cystine thiosulfonate) are not commercialized, and thus they should be synthesized. Additionally, the time required to detect cys seems to be crucial. For instance, the use of ACQ as derivatization agent elutes cys after 29 min while SBD-F elutes cys after 5 min using HPLC with fluorescence detection.

5. Pharmacokinetics of cys

Limited information is available on the pharmacokinetics of cys. The bioavailability of cys is less than 10%. After the ingestion of cys (15 mg/kg) by children with nephropathic cystinosis, a peak concentration (0.03-0.07 mM) in plasma is reached around one hour later [80]. The absorption of this molecule in the small intestine is much better than in the stomach or colon [81]. In addition, this bioavailability could be affected by the type of food administered as this drug could potentially bind to food such as fats and high-protein meals. A study showed that taking cys with foods may reduce its absorption by 30%, particularly with a high-protein diet [82]. Cys absorption is enhanced by iron in the proximal duodenum, iron loading accelerates, and iron depletion slows [^{14}C] cys uptake in intestinal epithelial cells [83]. Armas et al. showed that the pharmacokinetics of cys bitartrate delayed-release capsules are not affected by co-administration with orange juice, water only, or omeprazole (with water) [84].

Cys, after oral administration in rats, is primarily distributed in the kidney, the gastrointestinal tract (mainly the duodenum), and the liver. Regardless of the way of administration, cys uptake reaches a maximum in the duodenum after 6 h, which is maintained for up to 12 h, and the efflux is observed only after 24 h. At a concentration higher than 20 mM, cys uptake was

blocked, suggesting that the uptake system is saturable. Two studies suggested a carrier-mediated system for cys uptake. Based on an *in vitro* system, the first study suggested the presence of an unknown cys carrier for the human fibroblast lysosomes [85]. The second one confirmed that cys uptake by intestinal epithelial cells is mediated by an organic cation transport (OCT) system. The latter is inhibited by cys analogs and modulated by inhibitors of the organic cation transporters OCT and by suppression of OCT gene expression [83]. Moreover, these studies showed that cellular uptake of cys is more favorable at alkaline pH compared to pH 5 due to the pK_a of NH_2; the protonated form is presumably less well transported into the lysosome and intestinal epithelial cells, compared to its thiolate form [83,85].

After being metabolized to taurine and bile salts, cys is eliminated from the body after 6 h of administration, and this is the main cause behind cys administration every 6 h for patients with cystinosis. The problem of repeated administration of cys was resolved in 2013, where Cystagon®, an immediate release cys approved by FDA in 1994, was replaced by PROCYSBI® (Horizon Pharma) an enteric-coated delayed-release cys bitartrate formulation. This formulation bypasses absorption in the stomach, resulting in sustained absorption in the small intestine and thus improving gastro-intestinal tolerability [82]. Consequently, the drug was eliminated after 12 h reducing the drug administration and thus the treatment side effects [86].

Table 8 shows the pharmacokinetic parameters after the oral and gastrointestinal administration of cys in human body cells. T_{max} is the time corresponding to C_{max}, half-life ($t_{1/2}$), the area under the curve between time 0 and the last sample ($AUC_{0-\infty}$), and clearance (CL) are represented in this table [87,88]. The best pharmacokinetic values were obtained for gastro-intestinal administration in humans, more specifically in the small intestine.

Table 8. Pharmacokinetic parameters of cys after different routes of administration.

Route of administration of cys		C_{max} (mg/L)	T_{max} (min)	$t_{1/2}$ (min)	$AUC_{0-\infty}$ (mg.min/L)	CL (L/min)
Oral (450 mg cys)[a]		2.86	72	222	9.62	1.5
Gastro-intestinal (500 mg cys)[b]	Stomach	8.8	50	94.5	880	N.D.
	Small intestine	11	21	112	983	N.D.
	Caecum	5.2	64	98	713	N.D.
	Mid-ileum	11	30	124	1034	N.D.

[a][87]; [b][88] *(N.D.: not determined)*

6. Biological applications of cys

A low concentration of cys induces the transport of cysteine into cells. The latter is a precursor of glutathione (GSH) synthesis, an important antioxidant, thus influencing the oxidative state of a cell [89]. The oxidative state regulates several signaling pathways involved in cell proliferation and influences the gene expression of several redox-sensitive genes [90]. Moreover, the thiol group of cys can react with free thiol or the disulfide bonds of peptides and proteins, ending by interference with their function [91]. The alteration in gene expression and the interference with the protein function are the main causes behind the ability of cys to treat Huntington and Parkinson diseases. At high concentration, the oxidation of cys in the presence of transition metals produces hydrogen peroxide (H_2O_2) molecules, responsible for oxidative stress. Additionally, it induces the inhibition of GSH peroxidase responsible for cys toxicity at high concentrations (10^{-4} to 10^{-3} M) [92]. Therefore, the dose selection is very important to avoid any complication in the treatment of any disease by cys.

Cys has shown several biological applications: treatment of cystinosis, Huntington and Parkinson disease, malaria, neuropsychiatric disorders, cancer, and non-alcoholic fatty liver disease and is used as a radioprotective agent (**Fig. 10**). Many reviews profoundly discussed

these applications [7,23,24]. We will focus on the main applications of cys as a radioprotective agent, in the treatment of cystinosis, and for anti-tumor proliferation. However, the topical application of cys, for the treatment of hyperpigmentation, hasn't yet been well elaborated and reviewed. Consequently, all the data in the literature concerning this topic was collected and described below.

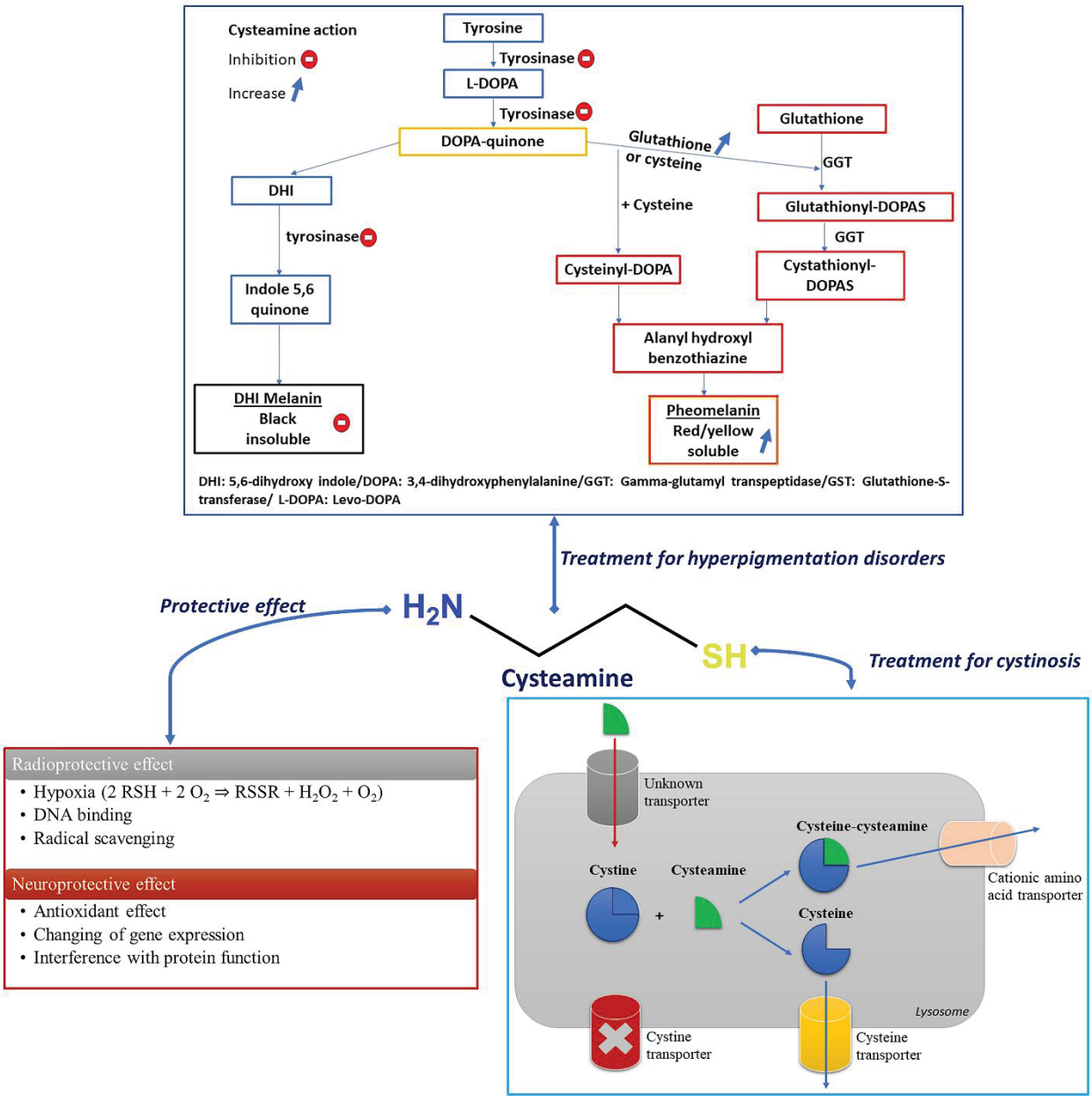

Figure 10: Cys pharmacodynamics.

6.1.Radioprotective effect

Cys was first used in 1954 as a radioprotective agent [1]. This radioprotective effect is attributed to its sulfhydryl group. It is a great scavenger of hydroxyl radical (·OH). It also reacts slowly with hydrogen peroxide (H_2O_2), but this reaction can lead to significant rates of H_2O_2 removal if high concentrations of cys are present [93]. Cys enters the cells rapidly and provides the maximum level of protection within 10 min [94]. Cys radioprotection *in vitro* is based on three different mechanisms [4]. First, cys can undergo an oxidation reaction with molecular oxygen in the cells leading to hypoxia. Besides, cys donate hydrogen atoms to hydroxyl radicals (·OH), decreasing by that their indirect radiation effect. Moreover, cys activates specific repressor molecules that interrupt the DNA templates activity necessary for DNA replication. A metabolically active DNA molecule is more sensitive to ionizing radiation; thus cys leads to the diminishment of radiation injury to the DNA molecule [5,95].

6.2.Treatment of cystinosis

Cystinosis is a rare autosomal recessive metabolic disorder characterized by a defect in lysosomal cystine transport leading to the intralysosomal accumulation of cystine crystals in many tissues (kidneys, bone marrow, intestine, etc.) including the eye (retina, conjunctiva, iris, and cornea) [96], affecting muscles and the central nervous system [86]. This disease can cause a generalized proximal tubular damage (called renal Fanconi syndrome), resulting in polyuria, polydipsia, and a development failure within the first year of life [97]. If left untreated, cystinosis can cause end-stage renal disease around the age of ten years.

In 1976, cys in the form of cys bitartrate was introduced as a treatment of cystinosis [98]. Cys is a weak base that enters the lysosome and reacts with cystine to form a mixed disulfide of half-cystine and cys. The mixed disulfide has a stearic resemblance to the amino acid lysine consequently, it rapidly leaves the lysosomes via lysine transporter [99]. However, this treatment presents many side effects such as gastrointestinal complaints, disagreeable breath,

and sweat odor, developing of lupus nephritis, proliferative vascular lesions on their elbows, skin striae, and bone and muscular pain [23]. These side effects are mainly caused by the metabolism of 3% of cys to dimethyl sulfide (**Fig. 3**) [100].

6.3.Treatment of cancer

Cys has been shown to inhibit gastric [101] and mammary [12] tumors formation. Besides, a study conducted by Wan et al. (2011) demonstrated that cys caused autophagosome accumulation in cancer cells and sensitized doxorubicin-elicited chemotherapeutic killing in HeLa, B16 melanoma, doxorubicin-resistant MCF-7 cells, and in a mouse melanoma model [102]. Besides, cys inhibits matrix metalloproteinases conducting to the suppression of invasion, metastasis, and prolonging survival in a mouse model of human pancreatic cancer [103] and human ovarian cancer [104].

6.4.Treatment of hyperpigmentation

There are three types of skin color alteration: darkening, lightening, and the occurrence of unusual skin color [105]. Eumelanin and pheomelanin are the two forms of melanin. Eumelanin is responsible for the brown pigmentation of the skin while pheomelanin produces yellow and red colorations [106]. Pigmentary disorders can occur after an increase or decrease in melanocyte activity. They are divided into two different categories: hyperpigmentation and hypopigmentation [107]. Hyperpigmentation is divided into three main types: melasma, post-inflammatory hyperpigmentation, and sun damage or sunspots. Melasma is a psychologically distressing skin disorder divided into three types: epidermal, dermal, and mixed melasma. Epidermal and dermal melasma is the accumulation of melanin in the epidermis and the dermis, respectively, and mixed melasma is a combination of epidermal and dermal melasma [108]. Post-inflammatory hyperpigmentation is an acquired hypermelanosis occurring after cutaneous inflammation or injury that can arise in all skin types [109] and sunspots are usually light brown

(generally called freckles) and appear mostly on the face, neck, chest, and hands, which are primarily exposed to UV rays [110].

Several natural and synthetic skin depigmenting agents have been developed. Their mechanisms of action may occur before, during or after the melanin synthesis. Moreover, depigmentation by any exogenous agent is induced by the destruction or the loss of melanocytes, alteration of the melanin present in melanosomes, and the interference with (i) the biosynthesis of premelanosomes and melanosomes, (ii) the conversion of tyrosine to DOPA (3,4-dihydroxyphenylalanine) to melanin, (iii) the biosynthesis of tyrosinase or the active center of the enzyme, and (iv) the transfer of melanosomes to keratinocytes (**Fig. 11 [111]**) [111].

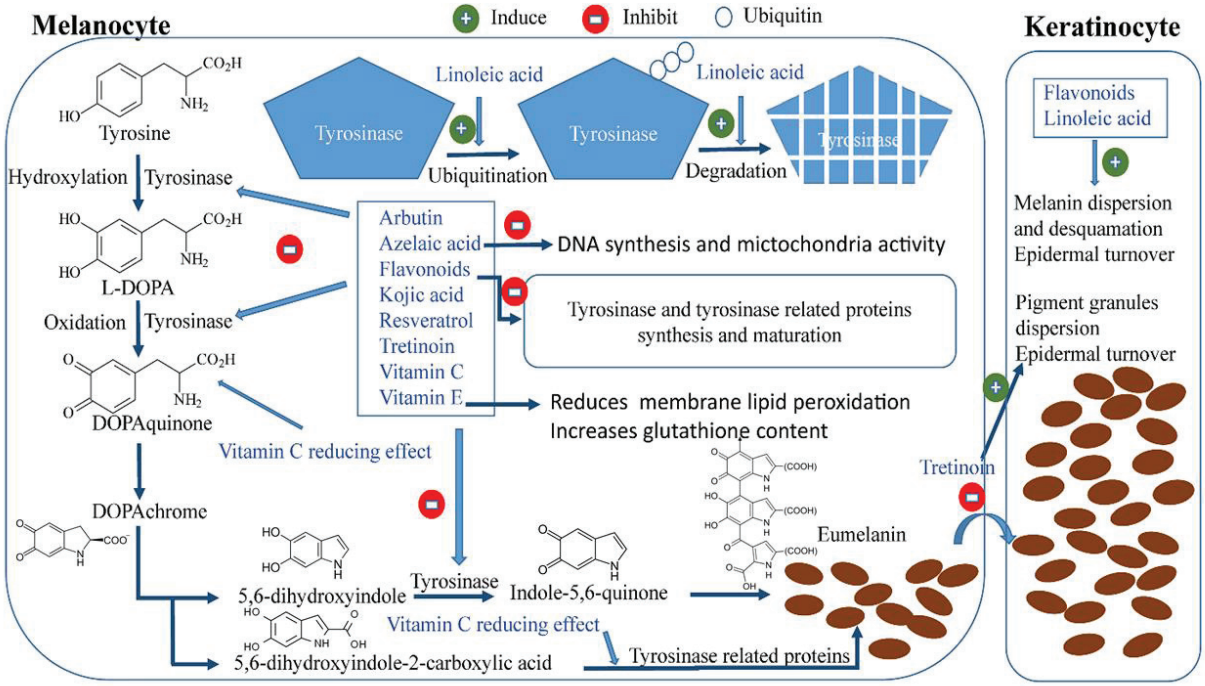

Figure 11: Schematic illustration of the mechanism of action of skin whitening agent [111].

Cys hydrochloride has been known to be a potent depigmenting molecule for over 5 decades. Chavin et al. (1966) examined, for the first time, the ability of several compounds (quinhydrone, cys, N-(2 mercaptoethyl)-dimethylamine HCI, sodium cys-S-phosphate, cystamine, 3-methylcatechol, fluphenazine, hydroquinone, etc…) to induce a specific destructive effect in

the melanin synthesizing cells (melanocytes and melanophores). These compounds were injected by subcutaneous injection in black goldfish. They found that all the molecules induced lysis of melanophores and melanocytes locally and systemically, however, hydroquinone was the most potent anti-pigmentary compound [112]. Another study demonstrated that cys was an effective depigmenting agent when applied to the skin of black guinea pigs, and conversely to the previous result was shown to be more potent than hydroquinone [113]. In fact, melanocytes are the specific target of cys since a noticeable decrease of the epidermal melanocyte was observed after the topical application of this compound to the skin of black guinea pigs. The treatment with cys did not affect the keratinocytes cells adjacent to melanocytes cells [114]. The minimum dose required for depigmentation is 100 μM, and this concentration decreased the percentage of melanin by 21% [11].

The mechanism of cys as a depigmenting agent is not yet deeply studied. It might act through the inhibition of tyrosinase and peroxidase and the increase of intracellular GSH levels.

6.4.1. Inhibition of tyrosinase and peroxidase activity

Tyrosinase is responsible for the conversion of tyrosine to DOPA and of DOPA to DOPA quinone. As for peroxidase, it catalyzes the final step of the oxidative polymerization reaction of the formed indoles to eumelanin pigments [115]. Thiolic depigmenting agents such as cys and GSH [116], are known to be inhibitors of tyrosinase and peroxidase, the two key enzymes involved in melanin biosynthesis [117]. The inhibition of tyrosinase will produce the scavenging of DOPA quinone affecting the production of melanin. Arbutin, azelaic acid, flavonoids, kojic acid resveratrol, tretinoin, and vitamins C and E act by the same mechanism [111]. Qiu et al. (2000) reported that the depigmenting action of cys is due to its interaction with the products of the reactions catalyzed by tyrosinase activity (DOPA oxidation products are isolated) inhibiting pigment synthesis. They confirmed that the cys mechanism of action is a melanogenesis inhibition, and not melanocytotoxicity, in contrast to hydroquinone [11].

6.4.2. Increase in the level of intracellular GSH

The interaction of DOPA-quinone with the thiol groups of GSH or cysteine shifts the melanogenesis from eumelanin to phaeomelanin synthesis (**Fig. 10**) [118]. Cys enhances the intracellular levels of GSH, thus leading in delaying the melanogenesis procedure. Among the different depigmenting agents, only vitamin E exhibited this action as well [111]. Djurhuus et al. (1990) demonstrated the enhancement of GSH content in C3H/10T1/2 cells after the addition of cys. De Matos and Furnus (2000) proved that the addition of cys to the culture medium during *in vitro* maturation of bovine oocytes increased the GSH levels in the mature oocytes while Wilmer et al. (2011) showed that cys increases total GSH and restore GSH redox status in a renal cystinosis cell mode [89,119–121]. Cys stimulates GSH synthesis by increasing the rate of cellular cysteine uptake through the formation of mixed disulfides with cysteine. Mixed disulfides of cysteine and cys enter cells via transport system L and are reduced intracellularly to release both thiol compounds. The cysteine is then used in GSH synthesis [122].

Several skin whitening agents such as retinoic acid, kojic acid or hydroquinone proved high efficacy. However, they present numerous side effects like hypersensitivity to the sun, skin irritation, inhibition of new melanin formation, and they are responsible for itching, peeling, dryness, and redness of the skin [123]. Cysteamine is a natural skin whitening agent as powerful as hydroquinone, does not present any risk, and is compatible with light exposure. The main obstacle in the use of cys as a depigmenting agent is its fast oxidation once in contact with air as well as the strongly unpleasant organoleptic features of this molecule [13], which could not be covered by perfumes [124]. Recently, Scientis Pharma© developed a new technology that stabilizes cys molecules and significantly reduces its odor. Cys Cream® was eventually the first and only depigmenting agent commercially available based on cys molecule. Hsu et al. (2013) applied cys cream® to the ear of black female guinea pigs. Evaluation with dermatoscopic,

chromametric, and histologic instruments was performed, and the cys cream® showed a potent depigmenting effect in guinea pig skin [124]. Then, Mansouri et al. (2015) evaluated the efficacy and safety of cys cream® for the treatment of epidermal melasma in a randomized, double-blind vehicle-controlled clinical trial. After an evaluation of melanin content and erythema levels, they conclude that the treatment with cys cream® decreased the content of melanin and consequently it was a good treatment for epidermal melasma [8,9].

7. Cys and encapsulation systems

Cys encapsulation into liposomes, CDs, and emulsions was conducted to enhance its effects; studies dealing with encapsulation are addressed in this section. Moreover, the conjugation of cys to the surface of CD induces the formation of disulfide bonds with cysteine-rich substructures of the ocular and glycoproteins mucus providing a prolonged residence time of the incorporated drugs at the site of action. On the other hand, the conjugation of cys to the surface of gold nanoparticles improves the colorimetric detection of compounds using the gold nanoparticles aggregation method by decreasing the electrostatic repulsion force between the nanoparticles.

7.1.Liposomes

Liposomes are enclosed spherical vesicles that are organized in one or several concentric phospholipidic bilayers with an internal aqueous phase. Liposomes can entrap lipophilic drugs within the lipid membrane, hydrophilic agents in their internal aqueous compartment, or amphiphilic ones at the water-lipid interface [125]. These carriers are biodegradable, biocompatible, and non-immunogenic [126]. Since liposomes mimic natural membranes, their use in topical applications is generally favorable [127]. Liposomes can be prepared by classical and large-scale techniques [125,128]. In fact, cys was first encapsulated in liposomes by Butler et al. (1978), to reduce cystine accumulation in cells [17]. Since cys is a water-soluble

compound, it can be incorporated in the internal aqueous cavity of the liposomes, thus facilitating the selective uptake of cys by endocytic target cells. The authors compared different types of liposomes formed from saturated and unsaturated or positively and negatively charged lipids. The best type of liposomes selected for subsequent experiments was those containing saturated dipalmitoyl phosphatidylcholine and negative charge by the inclusion of phosphatidic acid. This is explained as follows: saturated fatty acids are not subject to autoxidation as are unsaturated one; the use of dipalmitoylphosphatidylcholine liposomes avoids some of the toxic effects of peroxides or epoxides on cells in tissue culture and negatively charged liposomes made with phosphatidic do not present any aggregation contrary to those with positive charge. The encapsulation of cys in liposomes provides a better efficacy to reduce cystine in cystinotic cells in tissue culture [17]. In addition, liposomes serve as targeting agent to the lysosome since cys incorporated into liposomes will be mainly taken up by phagocytic cells and concentrated in lysosomes. They confirmed that the liposomes were disrupted by lysosomal enzymes releasing cys intralysosomally followed by the diffusion of mixed disulfide from lysosome [17]. Roman et al. (1982) reported the encapsulation of cys in liposomes. It was delivered orally in mice with an evaluation of its radioprotective effect. They found that the liposome encapsulating cys protects the drug up to 3 h after administration in contrast to free cys [129]. In order to investigate the effect of liposome-encapsulation on cys absorption through the intestinal wall, the distribution of the molecule after *in vivo* administration was studied by Jaskierowicz et al. (1985). They used mixed egg yolk lecithin and cholesterol (4:1 mol/mol) and reported that radioactivity was higher and more persistent in blood, plasma, liver, and spleen in encapsulated cys than in the free form. The digestive absorption of cys is more important when entrapped, and the drug is protected from digestive degradation [15].

On the other hand, the encapsulation of cys in liposomes formed from egg yolk phospholipid and cholesterol (4:1) extended the presence and duration of action of cys in pituitary glands, after oral administration. It leads to reduce tumor proliferation through the modification of hormone status where cys was able to reduce somatostatin and/or prolactin levels near the tumor. 10.8% of the initial cys were encapsulated in liposomes. Cys loaded liposomes were stable during storage for six days [130]. **Table 9** shows the different studies conducted to encapsulate cys in liposomes [15,17,130].

Table 9. Liposomes prepared by thin lipid film hydration method encapsulating cys.

Liposomes composition	Model used	Administration routes	Biological effects	References
Mixed egg yolk lecithin and cholesterol (4:1)	*In vivo*	Intragastric	Enhancement of cys absorption through the intestinal wall	[15]
Negatively charged, saturated phosphatidyl choline cholesterol-phosphatidic acid (7:2:1)	- Cystinotic cells in tissue culture - *In vivo*	Intravenously	Reducing cystine contents and improvement of uptake into target tissues	[17]
Mixed egg yolk and cholesterol (4:1)	*In vivo*	Orally	Enhancement of prolactin depletion action period	[130]

Unfortunately, liposome's characteristics (size, shape, homogeneity, encapsulation efficiency, and loading rate) were not investigated in these studies.

7.2.Cyclodextrins

CDs are a family of cyclic oligosaccharides composed of α-(1,4) linked glucopyranose subunits [131]. Three native CDs are known: α-CD, β-CD, and γ-CD composed of six, seven, and eight α-(1,4)-linked glycosyl units, respectively [132]. CDs possess a lipophilic inner cavity and a

hydrophilic outer surface that allow the formation of non-covalent inclusion complexes with numerous type of guests [133].

Table 10 shows the methods of preparation and the effects of different CD: cys molar ratios on cys properties. In fact, the presence of hydroxyl groups (OH) outside the molecule prevents the inclusion of hydrophilic drugs in CDs. To evaluate if the complexation between cys and CDs can be realized, Lahiani-Skiba et al. (2007) studied the interaction between lyophilized complexes of cys hydrochloride and α-CDs. Inclusion complexes were prepared from solutions obtained by the dissolution of cys hydrochloride in α-CD solution. Lyophilized products were obtained with molar ratio 1:1, 2:1, 3:1, and 4:1 (cys hydrochloride/α-CD). After the analysis of the lyophilized products by differential scanning calorimetry, mass spectrometry analysis, ^{1}H-nuclear magnetic resonance (NMR), and Fourier transform infrared spectroscopy, they affirmed the complex formation. The nuclear over Hauser effect spectroscopy technique showed the proximity of the methylene groups of cys protons with protons H2 and H4, located at the outside of α-CD (**Fig. 12 [13]**). They obtained odorless powder of cys with moderate flavor, storable at room temperature [13].

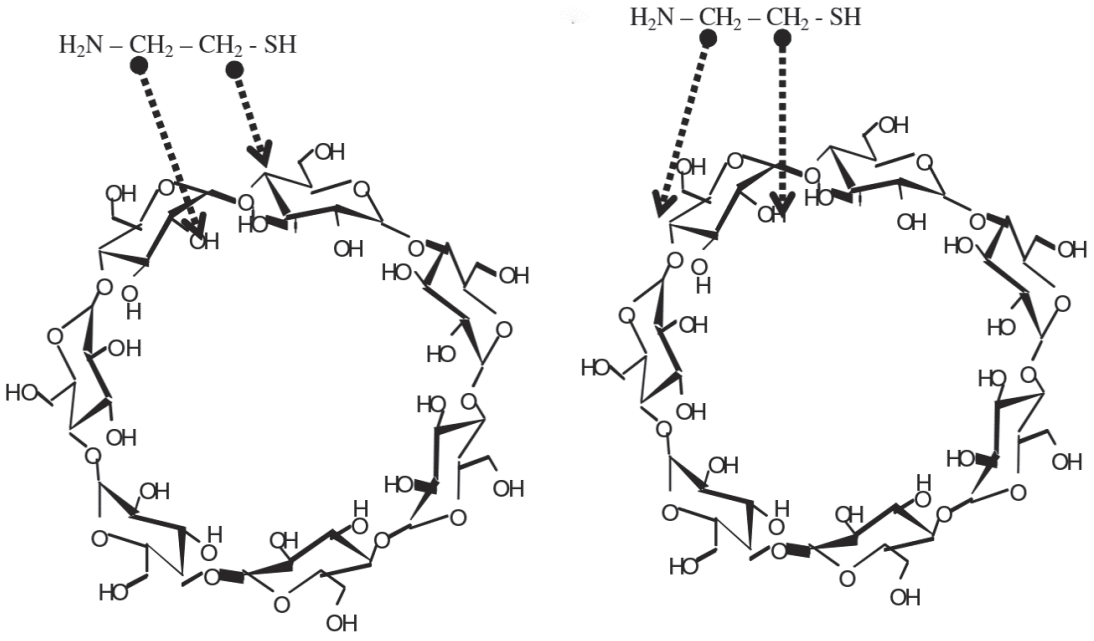

Figure 12: Representation proposed for the interaction between cys and α-CD according to the results of NMR technique (A) interactions of CH_2 of cys with H2 and H4 of two different glucopyranose (B) interactions of CH_2 of cys with H2 and H4 of a same glucopyranose [13].

Pescina et al. (2016) reported the encapsulation of cys in α-CD to improve the trans-corneal permeation of cys. An increase of permeation was observed when CD concentration was added at a concentration range between 3 and 5.5%. The increase of permeation was CD concentration-dependent, for example, a 5.5% concentration of CD increased the amount permeated up to 20 times compared to free cys [16].

7.3.Emulsions

Emulsions are metastable colloids made out of two immiscible fluids, one being dispersed in the other, in the presence of surface-active agents [134].

Gresham et al. (1971) reported the use of sustained-release multiple emulsion to extend the period of cys radioprotection. They compared the radioprotective effect in irradiated mice protected by cys with those that are unprotected. They found that emulsions prolonged the radioprotective effect of cys from 15 min obtained using free cys to 1.5 h when cys was administrated in an emulsion [14].

Recently, Dixon et al. (2018) tried to enhance cys stability using an emulsion of vitamin E, soybean oil, and tween 80 surfactants [18] since emulsions have been shown to decrease the transport of oxygen and increase the stability of other hydrophilic antioxidants [135]. Vitamin E and/or soybean oil were prepared at the solubility limit by adding an excess of the hydrophobic component(s) to PBS and stirring at 300 rpm for 24 h, followed by the addition of cys (0.1 mg/mL). The emulsion formulation was prepared by first mixing vitamin E (0.45 mg/mL) and soybean oil (0.45 mg/mL), followed by the addition of the surfactant solution tween 80 (0.1 mg/mL) with sonication for 30 min. The degradation rate of cys decreases from 126 µg/h for free cys (0.1 mg/mL) to 111 µg/h for cys, oil, and vitamin E at the solubility limit

in PBS. This rate was decreased to 101 μg/h for cys in the emulsion. The solubilization of the antioxidants increases their concentrations in the formulation and consequently allows the stabilization of cys [18].

7.4.Modification of encapsulation systems by cys

7.4.1. Cyclodextrins

The synthesis and characterization of thiolated β- and α- CD [19,20] as a novel mucoadhesive excipient for intra-oral drug delivery was studied. The synthesis of the thiolated CD was achieved in two steps: the oxidation of CD and the covalent coupling of cys via reductive amination (**Fig. 13**).

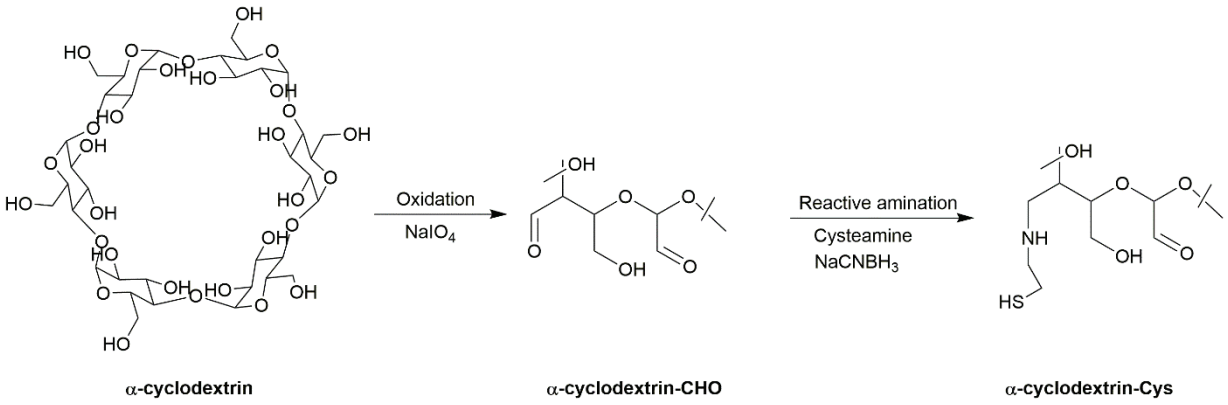

Figure 13: Synthetic pathway for the generation of thiolated α-CD.

α-CD-Cys and β-CD-Cys conjugates displayed an increase in the retention time of cetirizine on the ocular mucosal surface and miconazole nitrate on porcine intestinal and buccal mucosa. This could be due to the improvement of CD drug encapsulation properties after being thiolated, where the solubility of miconazole nitrate is enhanced. In addition, local mucosal irritating effects of cetirizine have been significantly reduced after being complexed with α-CD-Cys and applied on the rabbit's ocular mucosa (**Table 10**). These findings could be a promising tool for the delivery of poorly water-soluble therapeutic agents.

Table 10. Interaction of cys with CDs.

	CD type	Molar ratio (Cys: CD)	Preparation method	Freeze dried	Effect	References
Encapsulation	α-CD	1:1	Direct dissolution of cys hydrochloride in α-CD solution	Freeze-dried on a shelf at 50°C for 3 h at least.	An odorless powder and moderate flavor of cys is obtained, storable at room temperature	[13]
		2:1				
		3:1				
		4:1 (best ratio)				
		1:7	Dissolution of cys in α-CD solution	–	Increase in the permeation of the trans corneal diffusion of cys (*ex vivo* model)	[16]
		1:10				
		1:11				
		1:12.5 (best ratio)				
Modification	β-CD	1:2	The oxidation of CD prior to the covalent coupling of cys via reductive amination	–	Improved water solubility and retention time of miconazole nitrate on porcine intestinal and buccal mucosa	[19]
	α-CD	10:3			Prolong drug residence time of cetirizine on the ocular mucosal surface	[20]

7.4.2. Gold nanoparticles

7.4.2.1.Synthesis

Gold nanoparticles (AuNPs) are a diverse group of nanomaterials ranging in size from 5 to 110 nm with different forms, including spheres, cubes, nanorods, and nanoribbons [136].

There is a variety of methods to synthesize gold nanoparticles (AuNPs). We can find chemical methods of synthesis based on the chemical reduction of gold salt in aqueous or/and organic phase. The physical methods involve the γ-irradiation technique, the technique of microwave irradiation, and heat or photochemical reduction. Finally, the biological method was also reported using citrus fruit juice extracts or edible mushrooms [137].

Cys modified-gold nanoparticles are prepared by the attachment of cys mercapto group to the surface of the gold nanoparticles (AuNPs) by the formation of Au–S bonds with the –NH2 groups exposed on the outer surface of the citrate-capped AuNPs [138].

7.4.2.2.Colorimetric detection of compounds via cys-gold nanoparticles

The use of gold nanoparticles as a colorimetric reporter to detect several compounds of large numbers of samples, such as in milk products, eggs, and feeds, has received a great attention in the last few years, to substitute the classical techniques like HPLC and gas chromatography which are expensive and need dedicated instruments. This method was developed since AuNPs possess a surface plasmon resonance (SPR) changing from red to blue corresponding to their dispersion or aggregation state. The development of a more sensitive assay involves the modification of the AuNPs surface by cys to decrease the electrostatic repulsion force between AuNPs. The cys-AuNPs (cys-gold nanoparticles) solution is wine-red and displays an absorption peak at 524 nm. An electrostatic repulsion is occurred because of the positive charge of cys-AuNPs inhibiting the aggregation of the latter. When the compound is added to the cys-AuNPs solution, the absorption spectrum exhibits an obvious decrease at 524 nm and a strong increase at 650 nm. The color of the conjugates changes from wine-red to purple within several minutes, indicating the aggregation of cys-AuNPs (**Fig. 14**) [21,22].

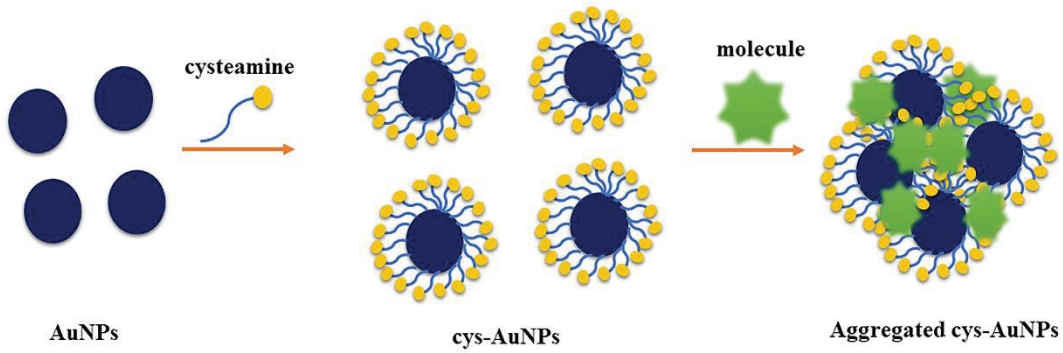

Figure 14: Colorimetric detection strategy of molecules based on cys modified AuNPs.

The colorimetric detection of gentamycin melamine [21,139], heparin [139], lipopolysaccharides [140], mercury (II) [21], glyphosate [22], trinitrotoluene [141], clenbuterol [142], and sulfate [143] using cys modified gold nanoparticles has been reported.

This method presents a lot of advantages like simplicity of preparation and manipulation and high sensitivity. It is more robust, with lower cost compared to the conventional methods.

8. Conclusion and perspective

Due to the important role of cys in medical and cosmetic fields, it was extensively studied in literature. However, this molecule suffers from different drawbacks mainly related to its instability, its organoleptic and pharmacokinetic properties. The quantification of this agent is also challenging because of its low absorptivity. This review presents a broad overview of cys characteristics; it could serve as reference for novel works focusing on the improvement of cys properties through encapsulation in delivery systems which may enlarge cys application.

Acknowledgments

Authors thank the Research Funding Program at the Lebanese University and the "Agence Universitaire de la Francophonie, projet PCSI" for supporting the project (2018-2020).

References

[1] Z.M. Bacq, G. Dechamps, P. Fischer, et al., Protection against x-rays and therapy of radiation sickness with beta-mercaptoethylamine, Science. 117 (1953) 633–636.

[2] P. Eker, A. Pihl, Studies on the growth-inhibiting and radioprotective effect of cystamine, cysteamine, and AET on mammalian cells in tissue culture, Radiat. Res. 21 (1964) 165–179. https://doi.org/10.2307/3571556.

[3] Y. Takagi, M. Shikita, T. Terasima, et al., Specificity of radioprotective and cytotoxic effects of cysteamine in HeLa S3 cells: generation of peroxide as the mechanism of paradoxical toxicity, Radiat. Res. 60 (1974) 292–301.

[4] Y.N. Korystov, F.B. Vexler, Mechanisms of the radioprotective effect of cysteamine in Escherichia coli, Radiat. Res. 114 (1988) 550–555.

[5] P. Mitznegg, M. Säbel, On the mechanism of radioprotection by cysteamine. I. Relationship between cysteamine-induced mitotic inhibition and radioprotective effects in the livers of young and senile white mice, Int. J. Radiat. Biol. Relat. Stud. Phys. Chem. Med. 24 (1973) 329–337.

[6] S. Cherqui, Cysteamine therapy: a treatment for cystinosis, not a cure, Kidney Int. 81 (2012) 127–129. https://doi.org/10.1038/ki.2011.301.

[7] W.A. Gahl, Early oral cysteamine therapy for nephropathic cystinosis, Eur. J. Pediatr. 162 (2003) S38–S41. https://doi.org/10.1007/s00431-003-1349-x.

[8] S. Farshi, P. Mansouri, B. Kasraee, Efficacy of cysteamine cream in the treatment of epidermal melasma, evaluating by Dermacatch as a new measurement method: a randomized double blind placebo controlled study, J. Dermatol. Treat. (2017) 1–8. https://doi.org/10.1080/09546634.2017.1351608.

[9] P. Mansouri, S. Farshi, Z. Hashemi, et al., Evaluation of the efficacy of cysteamine 5% cream in the treatment of epidermal melasma: a randomized double-blind placebo-controlled trial, Br. J. Dermatol. 173 (2015) 209–217. https://doi.org/10.1111/bjd.13424.

[10] D. McGregor, Hydroquinone: an evaluation of the human risks from its carcinogenic and mutagenic properties, Crit. Rev. Toxicol. 37 (2007) 887–914. https://doi.org/10.1080/10408440701638970.

[11] L. Qiu, M. Zhang, R.A. Sturm, et al., Inhibition of melanin synthesis by cystamine in human melanoma cells, J. Invest. Dermatol. 114 (2000) 21–27. https://doi.org/10.1046/j.1523-1747.2000.00826.x.

[12] M. Tatsuta, H. Iishi, H. Yamamura, et al., Inhibitory effect of prolonged administration of cysteamine on experimental carcinogenesis in rat stomach induced by N-methyl-N'-nitro-N-nitrosoguanidine, Int. J. Cancer. 41 (1988) 423–426.

[13] M. Lahiani-Skiba, Y. Boulet, I. Youm, et al., Interaction between hydrophilic drug and α-cyclodextrins: physico-chemical aspects, J. Incl. Phenom. Macrocycl. Chem. 57 (2007) 211–217. https://doi.org/10.1007/s10847-006-9194-y.

[14] P.A. Gresham, M. Barnett, S.V. Smith, et al., Use of a sustained-release multiple emulsion to extend the period of radio protection conferred by cysteamine, Nature. 234 (1971) 149–150.

[15] D. Jaskierowicz, F. Genissel, V. Roman, et al., Oral administration of liposome-entrapped Cysteamine and the distribution pattern in blood, liver and spleen, Int. J. Radiat. Biol. Relat. Stud. Phys. Chem. Med. 47 (1985) 615–619. https://doi.org/10.1080/09553008514550851.

[16] S. Pescina, F. Carra, C. Padula, et al., Effect of pH and penetration enhancers on cysteamine stability and trans-corneal transport, Eur. J. Pharm. Biopharm. 107 (2016) 171–179. https://doi.org/10.1016/j.ejpb.2016.07.009.
[17] J.D. Butler, F. Tietze, F. Pellefigue, et al., Depletion of cystine in cystinotic fibroblasts by drugs enclosed in liposomes, Pediatr. Res. 12 (1978) 46–51. https://doi.org/10.1203/00006450-197801000-00012.
[18] P. Dixon, K. Powell, A. Chauhan, Novel approaches for improving stability of cysteamine formulations, Int. J. Pharm. 549 (2018) 466–475. https://doi.org/10.1016/j.ijpharm.2018.08.006.
[19] M. Ijaz, B. Matuszczak, D. Rahmat, et al., Synthesis and characterization of thiolated β-cyclodextrin as a novel mucoadhesive excipient for intra-oral drug delivery, Carbohydr. Polym. 132 (2015) 187–195. https://doi.org/10.1016/j.carbpol.2015.06.073.
[20] M. Ijaz, M. Ahmad, N. Akhtar, et al., Thiolated α-Cyclodextrin: The Invisible Choice to Prolong Ocular Drug Residence Time, J. Pharm. Sci. 105 (2016) 2848–2854. https://doi.org/10.1016/j.xphs.2016.04.021.
[21] Y. Ma, L. Jiang, Y. Mei, et al., Colorimetric sensing strategy for mercury(ii) and melamine utilizing cysteamine-modified gold nanoparticles, The Analyst. 138 (2013) 5338-5343. https://doi.org/10.1039/c3an00690e.
[22] J. Zheng, H. Zhang, J. Qu, et al., Visual detection of glyphosate in environmental water samples using cysteamine-stabilized gold nanoparticles as colorimetric probe, Anal Methods. 5 (2013) 917–924. https://doi.org/10.1039/C2AY26391B.
[23] M. Besouw, R. Masereeuw, L. van den Heuvel, et al., Cysteamine: an old drug with new potential, Drug Discov. Today. 18 (2013) 785–792. https://doi.org/10.1016/j.drudis.2013.02.003.
[24] L. Gallego-Villar, L. Hannibal, J. Häberle, et al., Cysteamine revisited: repair of arginine to cysteine mutations, J. Inherit. Metab. Dis. 40 (2017) 555–567. https://doi.org/10.1007/s10545-017-0060-4.
[25] H. Ripps, W. Shen, Review: taurine: a “very essential” amino acid, Mol. Vis. 18 (2012) 2673–2686.
[26] M. Besouw, H. Blom, A. Tangerman, et al., The origin of halitosis in cystinotic patients due to cysteamine treatment, Mol. Genet. Metab. 91 (2007) 228–233. https://doi.org/10.1016/j.ymgme.2007.04.002.
[27] W.A. Gahl, J. Ingelfinger, P. Mohan, et al., Intravenous cysteamine therapy for nephropathic cystinosis, Pediatr. Res. 38 (1995) 579–584. https://doi.org/10.1203/00006450-199510000-00018.
[28] E.P. Serjeant, B. Dempsey, Ionisation constants of organic acids in aqueous solution, Pergamon Press, Oxford ; New York, 1979.
[29] M.J. O’Neil, The Merck index : an encyclopedia of chemicals, drugs, and biologicals, 13th ed, Whitehouse Station, N.J. : Merck, 2001. https://trove.nla.gov.au/version/13531769 (accessed January 23, 2020).
[30] I. Gana, M. Barrio, C. Ghaddar, et al., An integrated view of the influence of temperature, pressure, and humidity on the stability of trimorphic cysteamine hydrochloride, Mol. Pharm. 12 (2015) 2276–2288. https://doi.org/10.1021/mp500830n.
[31] PubChem, Cysteamine, https://pubchem.ncbi.nlm.nih.gov/compound/6058 (accessed January 23, 2020).
[32] L. Riauba, G. Niaura, O. Eicher-Lorka, et al., A study of cysteamine ionization in solution by raman spectroscopy and theoretical modeling, J. Phys. Chem. A. 110 (2006) 13394–13404. https://doi.org/10.1021/jp063816g.

[33] Q. Zhang, K. De Oliveira Vigier, S. Royer, et al., Deep eutectic solvents: syntheses, properties and applications, Chem. Soc. Rev. 41 (2012) 7108-7146. https://doi.org/10.1039/c2cs35178a.
[34] J.E. Biaglow, R.W. Issels, L.E. Gerweck, et al., Factors influencing the oxidation of cysteamine and other thiols: implications for hyperthermic sensitization and radiation protection, Radiat. Res. 100 (1984) 298–312.
[35] A. Brodrick, H.M. Broughton, R.M. Oakley, The stability of an oral liquid formulation of cysteamine, J. Clin. Pharm. Ther. 6 (1981) 67–70. https://doi.org/10.1111/j.1365-2710.1981.tb00889.x.
[36] R. Purkiss, Stability of cysteamine hydrochloride in solution, J. Clin. Pharm. Ther. 2 (1977) 199–203. https://doi.org/10.1111/j.1365-2710.1977.tb00090.x.
[37] E. Jellum, V.A. Bacon, W. Patton, et al., Quantitative determination of biologically important thiols and disulfides by gas-liquid chromatography, Anal. Biochem. 31 (1969) 339–347. https://doi.org/10.1016/0003-2697(69)90274-7.
[38] R.T. Lofberg, Gas chromatographic analysis of aminothiol radioprotective compounds, Anal. Lett. 4 (1971) 77–86. https://doi.org/10.1080/00032717108058594.
[39] R.C. Fahey, G.L. Newton, R. Dorian, et al., Analysis of biological thiols: quantitative determination of thiols at the picomole level based upon derivatization with monobromobimanes and separation by cation-exchange chromatography, Anal. Biochem. 111 (1981) 357–365.
[40] G.L. Newton, R. Dorian, R.C. Fahey, Analysis of biological thiols: derivatization with monobromobimane and separation by reverse-phase high-performance liquid chromatography, Anal. Biochem. 114 (1981) 383–387.
[41] A. Pastore, R. Massoud, C. Motti, et al., Fully automated assay for total homocysteine, cysteine, cysteinylglycine, glutathione, cysteamine, and 2-mercaptopropionylglycine in plasma and urine, Clin. Chem. 44 (1998) 825–832.
[42] M. Stachowicz, B. Lehmann, A. Tibi, et al., Determination of total cysteamine in human serum by a high-performance liquid chromatography with fluorescence detection, J. Pharm. Biomed. Anal. 17 (1998) 767–773. https://doi.org/10.1016/S0731-7085(97)00248-3.
[43] T. Toyo'oka, K. Imai, High-performance liquid chromatography and fluorometric detection of biologically important thiols, derivatized with ammonium 7-fluorobenzo-2-oxa-1,3-diazole-4-sulphonate (SBD-F), J. Chromatogr. 282 (1983) 495–500.
[44] S. Ichinose, M. Nakamura, M. Maeda, et al., A validated HPLC-fluorescence method with a semi-micro column for routine determination of homocysteine, cysteine and cysteamine, and the relation between the thiol derivatives in normal human plasma, Biomed. Chromatogr. 23 (2009) 935–939. https://doi.org/10.1002/bmc.1205.
[45] S. Ida, Y. Tanaka, S. Ohkuma, et al., Determination of cystamine by high-performance liquid chromatography, Anal. Biochem. 136 (1984) 352–356.
[46] H. Kataoka, Y. Imamura, H. Tanaka, et al., Determination of cysteamine and cystamine by gas chromatography with flame photometric detection, J. Pharm. Biomed. Anal. 11 (1993) 963–969.
[47] H. Kataoka, H. Tanaka, M. Makita, Determination of total cysteamine in urine and plasma samples by gas chromatography with flame photometric detection, J. Chromatogr. B Biomed. Appl. 657 (1994) 9–13.
[48] K. Kuśmierek, R. Głowacki, E. Bald, Determination of total cysteamine in human plasma in the form of its 2-S-quinolinium derivative by high performance liquid chromatography, Anal. Bioanal. Chem. 382 (2005) 231–233. https://doi.org/10.1007/s00216-005-3166-8.

[49] J. Ogony, S. Mare, W. Wu, et al., High performance liquid chromatography analysis of 2-mercaptoethylamine (cysteamine) in biological samples by derivatization with N-(1-pyrenyl) maleimide (NPM) using fluorescence detection, J. Chromatogr. B. 843 (2006) 57–62. https://doi.org/10.1016/j.jchromb.2006.05.027.
[50] M. Masuda, C. Toriumi, T. Santa, et al., Fluorogenic derivatization reagents suitable for isolation and identification of cysteine-containing proteins utilizing high-performance liquid chromatography−tandem mass spectrometry, Anal. Chem. 76 (2004) 728–735. https://doi.org/10.1021/ac034840i.
[51] H. Asamoto, T. Ichibangase, H. Saimaru, et al., Existence of low-molecular-weight thiols in Caenorhabditis elegans demonstrated by HPLC-fluorescene detection utilizing 7-chloro-N-[2-(dimethylamino)ethyl]-2,1,3-benzoxadiazole-4-sulfonamide, Biomed. Chromatogr. 21 (2007) 999–1004. https://doi.org/10.1002/bmc.814.
[52] M. Bousquet, C. Gibrat, M. Ouellet, et al., Cystamine metabolism and brain transport properties: clinical implications for neurodegenerative diseases: Cystamine in neurodegenerative diseases, J. Neurochem. 114 (2010) 1651–1658. https://doi.org/10.1111/j.1471-4159.2010.06874.x.
[53] B.D. Soriano, L.-T.T. Tam, H.S. Lu, et al., A fluorescent-based HPLC assay for quantification of cysteine and cysteamine adducts in Escherichia coli-derived proteins, J. Chromatogr. B Analyt. Technol. Biomed. Life. Sci. 880 (2012) 27–33. https://doi.org/10.1016/j.jchromb.2011.11.011.
[54] G. Ricci, M. Nardini, R. Chiaraluce, et al., Detection and determination of cysteamine at the nanomole level., J. Appl. Biochem. 5 (1983) 320–329.
[55] M.W. Duffel, D.J. Logan, D.M. Ziegler, Cysteamine and cystamine, in: Methods Enzymol., Academic Press, 1987: pp. 149–154. https://doi.org/10.1016/0076-6879(87)43027-9.
[56] M. Hsiung, Y.Y. Yeo, K. Itiaba, et al., Cysteamine, penicillamine, glutathione, and their derivatives analyzed by automated ion exchange column chromatography, Biochem. Med. 19 (1978) 305–317. https://doi.org/10.1016/0006-2944(78)90032-7.
[57] J. Wang, L. Zhou, H. Lei, et al., Simultaneous quantification of amino metabolites in multiple metabolic pathways using ultra-high performance liquid chromatography with tandem-mass spectrometry, Sci. Rep. 7 (2017) 1423. https://doi.org/10.1038/s41598-017-01435-7.
[58] H.-M. Xiao, X. Wang, Q.-L. Liao, et al., Sensitive analysis of multiple low-molecular-weight thiols in a single human cervical cancer cell by chemical derivatization-liquid chromatography-mass spectrometry, The Analyst. 144 (2019) 6578–6585. https://doi.org/10.1039/C9AN01566C.
[59] G.L. Ellman, A colorimetric method for determining low concentrations of mercaptans, Arch. Biochem. Biophys. 74 (1958) 443–450.
[60] G.L. Ellman, Tissue sulfhydryl groups, Arch. Biochem. Biophys. 82 (1959) 70–77. https://doi.org/10.1016/0003-9861(59)90090-6.
[61] E.B. Belldina, M.Y. Huang, J.A. Schneider, et al., Steady-state pharmacokinetics and pharmacodynamics of cysteamine bitartrate in paediatric nephropathic cystinosis patients: Pharmacokinetics of cysteamine, Br. J. Clin. Pharmacol. 56 (2003) 520–525. https://doi.org/10.1046/j.1365-2125.2003.01927.x.
[62] A. Luaces-Rodríguez, V. Díaz-Tomé, M. González-Barcia, et al., Cysteamine polysaccharide hydrogels: Study of extended ocular delivery and biopermanence time by PET imaging, Int. J. Pharm. 528 (2017) 714–722. https://doi.org/10.1016/j.ijpharm.2017.06.060.

[63] B. Coulomb, F. Robert-Peillard, E. Palacio, et al., Fast microplate assay for simultaneous determination of thiols and dissolved sulfides in wastewater, Microchem. J. 132 (2017) 205–210. https://doi.org/10.1016/j.microc.2017.01.022.
[64] Y. Kim, D.H. Na, Simultaneous Determination of Cysteamine and Cystamine in Cosmetics by Ion-Pairing Reversed-Phase High-Performance Liquid Chromatography, Toxicol. Res. 35 (2019) 161–165. https://doi.org/10.5487/TR.2019.35.2.161.
[65] S. Li, ed., Molecularly imprinted sensors: overview and applications, 1st ed, Elsevier, Amsterdam; Boston, 2012.
[66] M.J. Kelly, D. Perrett, S.R. Rudge, The determination of cysteamine in physiological fluids by HPLC with electrochemical detection, Biomed. Chromatogr. BMC. 2 (1987) 216–220. https://doi.org/10.1002/bmc.1130020509.
[67] L.A. Smolin, J.A. Schneider, Measurement of total plasma cysteamine using high-performance liquid chromatography with electrochemical detection, Anal. Biochem. 168 (1988) 374–379. https://doi.org/10.1016/0003-2697(88)90332-6.
[68] R.A.G. Garcia, L.L. Hirschberger, M.H. Stipanuk, Measurement of cyst(e)amine in physiological samples by high performance liquid chromatography, Anal. Biochem. 170 (1988) 432–440. https://doi.org/10.1016/0003-2697(88)90655-0.
[69] J.B. Raoof, R. Ojani, F. Chekin, Fabrication of functionalized carbon nanotube modified glassy carbon electrode and its application for selective oxidation and voltammetric determination of cysteamine, J. Electroanal. Chem. 633 (2009) 187–192. https://doi.org/10.1016/j.jelechem.2009.05.011.
[70] R. Ojani, J.-B. Raoof, E. Zarei, Electrocatalytic oxidation and determination of Cysteamine by poly- *N,N* -dimethylaniline/ferrocyanide film modified carbon paste electrode, Electroanalysis. 21 (2009) 1189–1193. https://doi.org/10.1002/elan.200804530.
[71] H. Karimi-Maleh, P. Biparva, M. Hatami, A novel modified carbon paste electrode based on NiO/CNTs nanocomposite and (9, 10-dihydro-9, 10-ethanoanthracene-11, 12-dicarboximido)-4-ethylbenzene-1, 2-diol as a mediator for simultaneous determination of cysteamine, nicotinamide adenine dinucleotide and folic acid, Biosens. Bioelectron. 48 (2013) 270–275. https://doi.org/10.1016/j.bios.2013.04.029.
[72] H. Karimi-Maleh, M. Salimi-Amiri, F. Karimi, et al., A voltammetric sensor based on NiO nanoparticle-modified carbon-paste electrode for determination of cysteamine in the presence of high concentration of tryptophan, J. Chem. (2013). https://doi.org/10.1155/2013/946230.
[73] V. Arabali, H. Karimi-Maleh, Electrochemical determination of cysteamine in the presence of guanine and adenine using a carbon paste electrode modified with N-(4-hydroxyphenyl)-3,5-dinitrobenzamide and magnesium oxide nanoparticles, Anal. Methods. 8 (2016) 5604–5610. https://doi.org/10.1039/C6AY01591C.
[74] S. Salmanpour, M. Abbasghorbani, F. Karimi, et al., Electrocatalytic determination of cysteamine uses a nanostructure based electrochemical sensor in pharmaceutical samples, Curr. Anal. Chem. 13 (2016) 40–45. https://doi.org/10.2174/1573411012666160601143003.
[75] A. Taherkhani, H. Karimi-Maleh, A.A. Ensafi, et al., Simultaneous determination of cysteamine and folic acid in pharmaceutical and biological samples using modified multiwall carbon nanotube paste electrode, Chin. Chem. Lett. 23 (2012) 237–240. https://doi.org/10.1016/j.cclet.2011.10.023.
[76] M. Keyvanfard, S. Sami, H. Karimi-Maleh, et al., Electrocatalytic determination of cysteamine using multiwall carbon nanotube paste electrode in the presence of 3,4-dihydroxycinnamic acid as a homogeneous mediator, J. Braz. Chem. Soc. 24 (2013) 32–39. https://doi.org/10.1590/S0103-50532013000100006.

[77] M. Keyvanfard, M. Ahmadi, F. Karimi, et al., Voltammetric determination of cysteamine at multiwalled carbon nanotubes paste electrode in the presence of isoproterenol as a mediator, Chin. Chem. Lett. 25 (2014) 1244–1246. https://doi.org/10.1016/j.cclet.2014.05.018.
[78] B. Rezaei, H. Khosropour, A.A. Ensafi, Sensitive voltammetric determination of cysteamine using promazine hydrochloride as a mediator and modified multi-wall carbon nanotubes carbon paste electrodes, Ionics. 20 (2014) 1335–1342. https://doi.org/10.1007/s11581-013-1059-y.
[79] S.Z. Mohammadi, S. Tajik, H. Beitollahi, et al., Sensitive Cysteamine Determination Using Disposable Electrochemical Sensor Based on Modified Screen Printed Electrode, Biquarterly Iran. J. Anal. Chem. 6 (2019). https://doi.org/10.30473/ijac.2019.45800.1142.
[80] L.A. Smolin, K.F. Clark, J.G. Thoene, et al., A comparison of the effectiveness of cysteamine and phosphocysteamine in elevating plasma cysteamine concentration and decreasing leukocyte free cystine in nephropathic cystinosis, Pediatr. Res. 23 (1988) 616–620. https://doi.org/10.1203/00006450-198806000-00018.
[81] R. Dohil, M. Fidler, B.A. Barshop, et al., Understanding intestinal cysteamine bitartrate absorption, J. Pediatr. 148 (2006) 764–769. https://doi.org/10.1016/j.jpeds.2006.01.050.
[82] R. Dohil, B.L. Cabrera, J. Gangoiti, et al., The Effect of Food on Cysteamine Bitartrate Absorption in Healthy Participants, Clin. Pharmacol. Drug Dev. 1 (2012) 170–174. https://doi.org/10.1177/2160763X12454423.
[83] T. Khomenko, J. Kolodney, J.T. Pinto, et al., New mechanistic explanation for the localization of ulcers in the rat duodenum: role of iron and selective uptake of cysteamine, Arch. Biochem. Biophys. 525 (2012) 60–70. https://doi.org/10.1016/j.abb.2012.05.013.
[84] D. Armas, R.J. Holt, N.F. Confer, et al., A phase 1 pharmacokinetic study of cysteamine bitartrate delayed-release capsules following oral administration with orange juice, water, or omeprazole in cystinosis, Adv. Ther. 35 (2018) 199–209. https://doi.org/10.1007/s12325-018-0661-9.
[85] R.L. Pisoni, G.Y. Park, V.Q. Velilla, et al., Detection and characterization of a transport system mediating cysteamine entry into human fibroblast lysosomes. Specificity for aminoethylthiol and aminoethylsulfide derivatives, J. Biol. Chem. 270 (1995) 1179–1184.
[86] G. Medic, M. van der Weijden, A. Karabis, et al., A systematic literature review of cysteamine bitartrate in the treatment of nephropathic cystinosis, Curr. Med. Res. Opin. 33 (2017) 2065–2076. https://doi.org/10.1080/03007995.2017.1354288.
[87] G. Devereux, S. Steele, K. Griffiths, et al., An open-label investigation of the pharmacokinetics and tolerability of oral cysteamine in adults with cystic fibrosis, Clin. Drug Investig. 36 (2016) 605–612. https://doi.org/10.1007/s40261-016-0405-z.
[88] M.C. Fidler, B.A. Barshop, J.A. Gangoiti, et al., Pharmacokinetics of cysteamine bitartrate following gastrointestinal infusion, Br. J. Clin. Pharmacol. 63 (2007) 36–40. https://doi.org/10.1111/j.1365-2125.2006.02734.x.
[89] D.G. de Matos, C.C. Furnus, The importance of having high glutathione (GSH) level after bovine in vitro maturation on embryo development effect of beta-mercaptoethanol, cysteine and cystine, Theriogenology. 53 (2000) 761–771. https://doi.org/10.1016/S0093-691X(99)00278-2.
[90] P.D. Ray, B.-W. Huang, Y. Tsuji, Reactive oxygen species (ROS) homeostasis and redox regulation in cellular signaling, Cell. Signal. 24 (2012) 981–990. https://doi.org/10.1016/j.cellsig.2012.01.008.

[91] V.S. Chopra, L.E. Chalifour, H.M. Schipper, Differential effects of cysteamine on heat shock protein induction and cytoplasmic granulation in astrocytes and glioma cells, Mol. Brain Res. 31 (1995) 173–184. https://doi.org/10.1016/0169-328X(95)00049-X.
[92] T.M. Jeitner, D.A. Lawrence, Mechanisms for the cytotoxicity of cysteamine, Toxicol. Sci. Off. J. Soc. Toxicol. 63 (2001) 57–64.
[93] O.I. Aruoma, B. Halliwell, B.M. Hoey, et al., The antioxidant action of taurine, hypotaurine and their metabolic precursors, Biochem. J. 256 (1988) 251–255.
[94] J.W. Purdie, A comparative study of the radioprotective effects of cysteamine, WR-2721, and WR-1065 in cultured human cells, Radiat. Res. 77 (1979) 303–311.
[95] C.K. Nair, D.K. Parida, T. Nomura, Radioprotectors in radiotherapy, J. Radiat. Res. (Tokyo). 42 (2001) 21–37.
[96] M.A. Elmonem, K.R. Veys, N.A. Soliman, et al., Cystinosis: a review, Orphanet J. Rare Dis. 11 (2016) 47. https://doi.org/10.1186/s13023-016-0426-y.
[97] M.J. Wilmer, J.P. Schoeber, L.P. van den Heuvel, et al., Cystinosis: practical tools for diagnosis and treatment, Pediatr. Nephrol. Berl. Ger. 26 (2011) 205–215. https://doi.org/10.1007/s00467-010-1627-6.
[98] J.G. Thoene, R.G. Oshima, J.C. Crawhall, et al., Cystinosis. Intracellular cystine depletion by aminothiols in vitro and in vivo, J. Clin. Invest. 58 (1976) 180–189. https://doi.org/10.1172/JCI108448.
[99] S. Bozdağ, K. Gümüş, O. Gümüş, et al., Formulation and in vitro evaluation of cysteamine hydrochloride viscous solutions for the treatment of corneal cystinosis, Eur. J. Pharm. Biopharm. 70 (2008) 260–269. https://doi.org/10.1016/j.ejpb.2008.04.010.
[100] M. Besouw, A. Tangerman, E. Cornelissen, et al., Halitosis in cystinosis patients after administration of immediate-release cysteamine bitartrate compared to delayed-release cysteamine bitartrate, Mol. Genet. Metab. 107 (2012) 234–236. https://doi.org/10.1016/j.ymgme.2012.06.017.
[101] H. Inano, M. Onoda, K. Suzuki, et al., Inhibitory effects of WR-2721 and cysteamine on tumor initiation in mammary glands of pregnant rats by radiation, Radiat. Res. 153 (2000) 68–74.
[102] X.-M. Wan, F. Zheng, L. Zhang, et al., Autophagy-mediated chemosensitization by cysteamine in cancer cells, Int. J. Cancer. 129 (2011) 1087–1095. https://doi.org/10.1002/ijc.25771.
[103] T. Fujisawa, B. Rubin, A. Suzuki, et al., Cysteamine Suppresses Invasion, Metastasis and Prolongs Survival by Inhibiting Matrix Metalloproteinases in a Mouse Model of Human Pancreatic Cancer, PLOS ONE. 7 (2012) e34437. https://doi.org/10.1371/journal.pone.0034437.
[104] A. Suzuki, R. Bhardwaj, P. Leland, et al., Cysteamine suppresses tumor metastasis by inhibiting activity of matrix metalloproteases without inducing toxicity in mouse models of human ovarian cancer, Cancer Res. 77 (2017) 4900–4900. https://doi.org/10.1158/1538-7445.AM2017-4900.
[105] J.J. Nordlund, R.E. Boissy, V.J. Hearing, et al., eds., The Pigmentary System: Physiology and Pathophysiology, 1 edition, Oxford University Press, New York, 1998.
[106] P.T. Rose, Pigmentary disorders, Med. Clin. North Am. 93 (2009) 1225–1239. https://doi.org/10.1016/j.mcna.2009.08.005.
[107] E. Bastonini, D. Kovacs, M. Picardo, Skin Pigmentation and Pigmentary Disorders: Focus on Epidermal/Dermal Cross-Talk, Ann. Dermatol. 28 (2016) 279-289. https://doi.org/10.5021/ad.2016.28.3.279.

[108] D. Rigopoulos, S. Gregoriou, A. Katsambas, Hyperpigmentation and melasma, J. Cosmet. Dermatol. 6 (2007) 195–202. https://doi.org/10.1111/j.1473-2165.2007.00321.x.
[109] E.C. Davis, V.D. Callender, Postinflammatory Hyperpigmentation, J. Clin. Aesthetic Dermatol. 3 (2010) 20–31.
[110] L. Nieuweboer-Krobotova, Hyperpigmentation: types, diagnostics and targeted treatment options: Hyperpigmentation, J. Eur. Acad. Dermatol. Venereol. 27 (2013) 2–4. https://doi.org/10.1111/jdv.12048.
[111] E. Ephrem, H. Elaissari, H. Greige-Gerges, Improvement of skin whitening agents efficiency through encapsulation: Current state of knowledge, Int. J. Pharm. 526 (2017) 50–68. https://doi.org/10.1016/j.ijpharm.2017.04.020.
[112] W. Chavin, W. Schlesinger, Some potent melanin depigmentary agents in the black goldfish, Naturwissenschaften. 53 (1966) 413–414.
[113] M.A. Pathak, E. Frenk, G. Szabó, et al., Cutaneous depigmentation, Clin. Res. 14 (1966).
[114] E. Frenk, M.A. Pathak, G. Szabó, et al., Selective action of mercaptoethylamines on melanocytes in mammalian skin: experimental depigmentation, Arch. Dermatol. 97 (1968) 465–477.
[115] C. Niu, H.A. Aisa, Upregulation of Melanogenesis and Tyrosinase Activity: Potential Agents for Vitiligo, Molecules. 22 (2017) 1303. https://doi.org/10.3390/molecules22081303.
[116] C.D. Villarama, H.I. Maibach, Glutathione as a depigmenting agent: an overview, Int. J. Cosmet. Sci. 27 (2005) 147–153. https://doi.org/10.1111/j.1467-2494.2005.00235.x.
[117] B. Kasraee, Peroxidase-Mediated Mechanisms Are Involved in the Melanocytotoxic and Melanogenesis-Inhibiting Effects of Chemical Agents, Dermatology. 205 (2002) 329–339. https://doi.org/10.1159/000066439.
[118] E. Karg, G. Odh, A. Wittbjer, et al., Hydrogen peroxide as an inducer of elevated tyrosinase level in melanoma cells, J. Invest. Dermatol. 100 (1993) 209S-213S.
[119] R. Djurhuus, A.M. Svardal, P.M. Ueland, Cysteamine increases homocysteine export and glutathione content by independent mechanisms in C3H/10T1/2 cells., Mol. Pharmacol. 38 (1990) 327–332.
[120] M.J. Wilmer, L.A.J. Kluijtmans, T.J. van der Velden, et al., Cysteamine restores glutathione redox status in cultured cystinotic proximal tubular epithelial cells, Biochim. Biophys. Acta BBA - Mol. Basis Dis. 1812 (2011) 643–651. https://doi.org/10.1016/j.bbadis.2011.02.010.
[121] N.P. Smit, H. Van der Meulen, H.K. Koerten, et al., Melanogenesis in cultured melanocytes can be substantially influenced by L-tyrosine and L-cysteine, J. Invest. Dermatol. 109 (1997) 796–800. https://doi.org/10.1111/1523-1747.ep12340980.
[122] T. Meier, R.D. Issels, [11] Promotion of cyst(e)ine uptake, in: Methods Enzymol., Academic Press, 1995: pp. 103–112. https://doi.org/10.1016/0076-6879(95)52013-9.
[123] M.I. Rendon, J.I. Gaviria, Review of Skin-Lightening Agents, Dermatol. Surg. 31 (2005) 886–890. https://doi.org/10.1111/j.1524-4725.2005.31736.
[124] C. Hsu, H.A. Mahdi, M. Pourahmadi, et al., Cysteamine cream as a new skin depigmenting product, J. Am. Acad. Dermatol. 68 (2013). https://doi.org/10.1016/j.jaad.2012.12.781.
[125] A. Laouini, C. Jaafar-Maalej, I. Limayem-Blouza, et al., Preparation, Characterization and Applications of Liposomes: State of the Art, J. Colloid Sci. Biotechnol. 1 (2012) 147–168. https://doi.org/10.1166/jcsb.2012.1020.

[126] C. Zylberberg, S. Matosevic, Pharmaceutical liposomal drug delivery: a review of new delivery systems and a look at the regulatory landscape, Drug Deliv. 23 (2016) 3319–3329. https://doi.org/10.1080/10717544.2016.1177136.
[127] A. Akbarzadeh, R. Rezaei-Sadabady, S. Davaran, et al., Liposome: classification, preparation, and applications, Nanoscale Res. Lett. 8 (2013) 102. https://doi.org/10.1186/1556-276X-8-102.
[128] R. Gharib, H. Greige-Gerges, S. Fourmentin, et al., Liposomes incorporating cyclodextrin–drug inclusion complexes: Current state of knowledge, Carbohydr. Polym. 129 (2015) 175–186. https://doi.org/10.1016/j.carbpol.2015.04.048.
[129] V. Roman, F. Bocquier, F. Leterrier, et al., Radioprotective effect of cysteamine entrapped in liposomes orally administered to the mouse, Comptes Rendus Seances Acad. Sci. Ser. III Sci. Vie. 295 (1982) 191–193.
[130] T.M. Jeitner, J.R. Oliver, Possible oncostatic action of cysteamine on the pituitary glands of oestrogen-primed hyperprolactinaemic rats, J. Endocrinol. 127 (1990) 119–127. https://doi.org/10.1677/joe.0.1270119.
[131] R. Challa, A. Ahuja, J. Ali, et al., Cyclodextrins in drug delivery: An updated review, AAPS PharmSciTech. 6 (2005) E329–E357. https://doi.org/10.1208/pt060243.
[132] E.M.M. Del Valle, Cyclodextrins and their uses: a review, Process Biochem. 39 (2004) 1033–1046. https://doi.org/10.1016/S0032-9592(03)00258-9.
[133] S. Ramnik, B. Nitin, M. Jyotsana, et al., Characterization of cyclodextrin inclusion complexes – a review, J. Pharm. Sci. Technol. 2 (2010) 171-183.
[134] J. Bibette, F.L. Calderon, P. Poulin, Emulsions: basic principles, Rep. Prog. Phys. 62 (1999) 969-1033. https://doi.org/10.1088/0034-4885/62/6/203.
[135] J.N. Coupland, D.J. McClements, Lipid oxidation in food emulsions, Trends Food Sci. Technol. 7 (1996) 83–91. https://doi.org/10.1016/0924-2244(96)81302-1.
[136] H. Bridle, Chapter Nine - Nanotechnology for detection of waterborne pathogens, in: Waterborne Pathog., Academic Press, Amsterdam, 2014: pp. 291–318. https://doi.org/10.1016/B978-0-444-59543-0.00009-8.
[137] K. Alaqad, T.A. Saleh, Gold and silver nanoparticles: synthesis methods, characterization routes and applications towards drugs, J. Environ. Anal. Toxicol. 6 (2016). https://doi.org/10.4172/2161-0525.1000384.
[138] X. Liang, H. Wei, Z. Cui, et al., Colorimetric detection of melamine in complex matrices based on cysteamine-modified gold nanoparticles, The Analyst. 136 (2011) 179–183. https://doi.org/10.1039/C0AN00432D.
[139] R. Cao, B. Li, A simple and sensitive method for visual detection of heparin using positively-charged gold nanoparticles as colorimetric probes, Chem. Commun. 47 (2011) 2865-2867. https://doi.org/10.1039/c0cc05094f.
[140] J. Sun, J. Ge, W. Liu, et al., A facile assay for direct colorimetric visualization of lipopolysaccharides at low nanomolar level, Nano Res. 5 (2012) 486–493. https://doi.org/10.1007/s12274-012-0234-1.
[141] Y. Jiang, H. Zhao, N. Zhu, et al., A Simple Assay for Direct Colorimetric Visualization of Trinitrotoluene at Picomolar Levels Using Gold Nanoparticles, Angew. Chem. Int. Ed. 47 (2008) 8601–8604. https://doi.org/10.1002/anie.200804066.
[142] J. Kang, Y. Zhang, X. Li, et al., A Rapid Colorimetric Sensor of Clenbuterol Based on Cysteamine-Modified Gold Nanoparticles, ACS Appl. Mater. Interfaces. 8 (2016) 1–5. https://doi.org/10.1021/acsami.5b09079.

[143] D. Zhao, C. Chen, L. Lu, et al., A label-free colorimetric sensor for sulfate based on the inhibition of peroxidase-like activity of cysteamine-modified gold nanoparticles, Sens. Actuators B Chem. 215 (2015) 437–444. https://doi.org/10.1016/j.snb.2015.04.010.

Objectifs et stratégie du travail expérimental

L'application de la cystéamine en tant qu'agent dépigmentant est limitée par son instabilité chimique en solution. Afin de contourner ce problème, divers systèmes d'encapsulation à base de lipides ont été développés pour améliorer les propriétés physico-chimiques des composés. Nous nous sommes intéressés à l'encapsulation de la cystéamine dans des vésicules lipidiques (liposomes) afin d'augmenter sa stabilité et par la suite sa pénétration à travers la peau.

Pour atteindre notre objectif, notre travail a été divisé en trois axes principaux :

- La cystéamine ne présentant pas de groupement chromophore, sa détection directe est problématique. La dérivatisation par le réactif d'Ellman est la méthode la plus utilisée pour quantifier la cystéamine en utilisant l'acide 5,5'-dithiobis(2-nitrobenzoïque) ou DTNB. Cette méthode se base sur la réaction entre le DTNB et le groupement thiol pour produire un disulfure et l'acide 2-nitro-5-thiobenzoïque (TNB^{2-}). Ce dernier a une couleur jaune et sa concentration peut être mesurée par spectrophotométrie à 412 nm. Nous avons eu recours à cette méthode pour le dosage de la cystéamine dans les suspensions liposomales. Toutefois, un chevauchement dans les pics d'absorbance des lipides et ceux du TNB^{2-} a été observé, d'où le recours à l'optimisation de cette méthode afin de solubiliser les vésicules lipidiques. Pour cela, le triton X-100 (1%) a été ajouté au mélange réactionnel pour solubiliser les liposomes. De plus, des solvants organiques (méthanol, éthanol, acétone, acétonitrile et diméthyl sulfoxyde) ont été testés et ajoutés au mélange réactionnel à différents rapports de volume solvant organique : mélange réactionnel (100:0 ; 50:50 et 10:90). Malgré l'optimisation de cette méthode, elle est limitée à la quantification de la cystéamine où le produit de dégradation, la cystamine, ne peut pas être quantifié simultanément. Pour cela nous avons optimisé et comparé deux méthodes chromatographiques : la chromatographie par paires d'ions et la

chromatographie micellaire en ajoutant du SDS dans la phase mobile. En outre, différentes tentatives ont été appliquées pour stabiliser et éviter l'oxydation de la cystéamine pendant l'analyse. Une étude de stabilité a été menée dans des solutions tamponnées et non tamponnées à différentes températures et conditions d'exposition à la lumière.

- Le deuxième axe de notre étude porte sur la préparation des liposomes blancs et chargés en cystéamine, composés de PH90H et de Lipoïde S100 par la méthode d'injection éthanolique afin d'améliorer les propriétés physico-chimiques de la cystéamine. Les suspensions liposomales ont été caractérisées par leur taille, leur indice de polydispersité et leur potentiel zêta ainsi que par leur morphologie. Les concentrations de la cystéamine, de phospholipides et de cholestérol dans les liposomes ont été mesurées. L'efficacité d'encapsulation (EE%) et le taux de charge (LR %) de cystéamine dans les liposomes ont également été déterminés. La lyophilisation des liposomes PH 90H a été réalisée et les caractéristiques des liposomes resuspendus ont été déterminées. De plus, la stabilité de la cystéamine libre et encapsulée a été évaluée à différentes températures (4, 25 et 37 °C) et en présence et absence de la lumière. Enfin, la stabilité de la forme lyophilisée de la cystéamine encapsulée a été évaluée après quatre mois de stockage à 4 °C.
- Dans le troisième axe de notre étude, le chlorhydrate de cystéamine a été utilisé en raison de sa meilleure stabilité en comparaison avec la forme basique de la cystéamine. Des liposomes blancs et des liposomes chargés de chlorhydrate de cystéamine ont été préparés par la méthode d'injection d'éthanol et caractérisés pour leur taille, leur indice de polydispersité et leur potentiel zêta. L'efficacité de l'encapsulation du chlorhydrate de cystéamine (EE%) dans les liposomes a également été calculée. Les liposomes blancs

et les liposomes chargés de chlorhydrate de cystéamine ont été lyophilisés. La stabilité du chlorhydrate de cystéamine libre et encapsulé en suspension et sous forme lyophilisée a été évaluée à 4°C pendant 6 mois. La cytotoxicité du chlorhydrate de cystéamine et de la cystamine, des liposomes blancs et des liposomes chargés de chlorhydrate de cystéamine en suspension et des formes lyophilisées remises en suspension a ensuite été évaluée par le test MTT. En outre, l'activité *in vitro* de la mélanine et de la tyrosinase a été mesurée après avoir traité les cellules avec les différentes formulations. Enfin, la pénétration cutanée du chlorhydrate de cystéamine libre et encapsulé dans les liposomes a été comparée à l'aide de la cellule de diffusion de Franz.

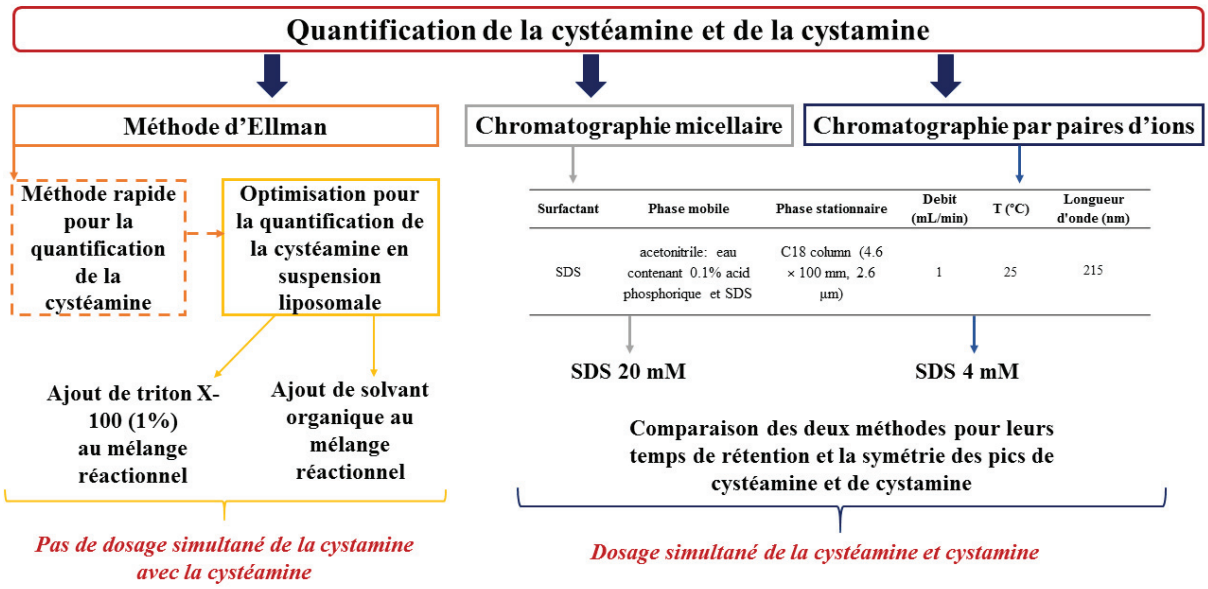

Schéma 1 : Méthodologie suivie pour la quantification de la cystéamine et la cystamine.

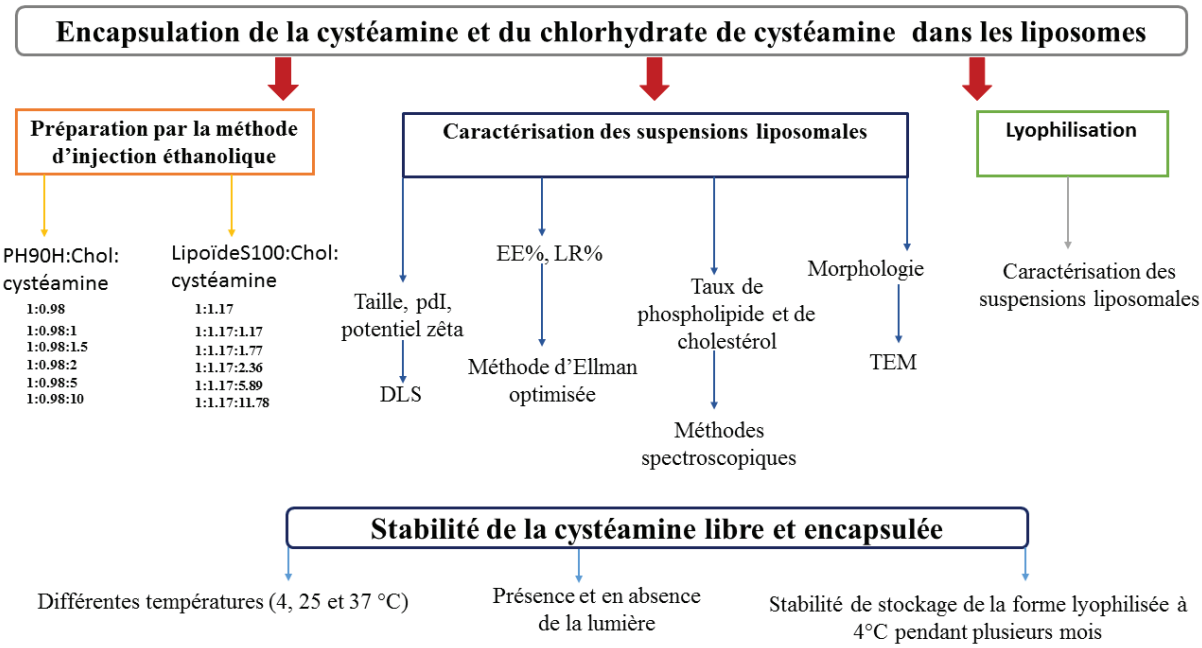

Schéma 2 : Méthodologie suivie pour la préparation, caractérisation, lyophilisation et l'étude de stabilité de la cystéamine et le chlorhydrate de cystéamine dans des liposomes.

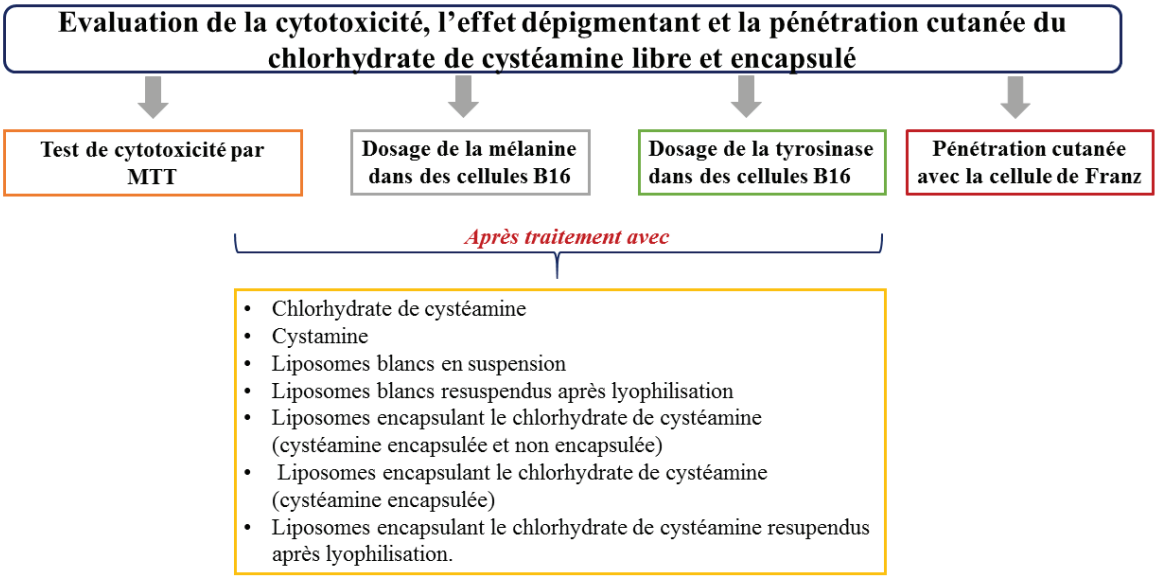

Schéma 3 : Méthodologie suivie pour l'évaluation de l'effet dépigmentant et la pénétration cutanée du chlorhydrate de cystéamine libre et encapsulé.

Chapitre 2 : Méthodes

Ce chapitre présente les principales techniques expérimentales utilisées dans ce travail de thèse. Nous verrons successivement la méthode d'Ellman (la méthode classique et son optimisation pour la quantification de la cystéamine présente dans des suspensions liposomales) puis les méthodes chromatographiques (chromatographie de paires d'ions et chromatographie liquide micellaire) qui ont été mises au point comme alternatives à la méthode d'Ellman. Puis, nous ferons quelques rappels sur la lyophilisation des liposomes qui permet une stabilité à long terme de ces systèmes d'encapsulation et la quantification de l'éthanol présent dans les suspensions liposomales par résonance magnétique nucléaire (RMN). L'éthanol, composant clé de la méthode d'injection éthanolique, présente une certaine toxicité sur les cellules, il est donc important d'en connaitre la concentration. Enfin, nous verrons les différentes méthodologies qui ont été mises en œuvre pour déterminer les effets potentiels des liposomes chargés en cystéamine lors d'un traitement de l'hyperpigmentation.

1) Spectroscopie UV-Visible (méthode d'Ellman)

a) Principe

La méthode d'Ellman est une méthode simple et rapide pour quantifier les groupements sulfhydryles (Ellman, 1959). Elle est basée sur la détection colorimétrique après une réaction entre les groupements sulfhydryles et le 5,5-dithio-bis-2-acide nitrobenzoïque (DTNB) donnant un produit de couleur jaune qui est le 5-thio-2-acide nitrobenzoïque (TNB) **(Figure 1)**. L'absorbance de cette molécule est mesurée par spectrophotométrie à une longueur d'onde de 412 nm, afin de déterminer la concentration de la cystéamine grâce à ses groupements sulfhydryles.

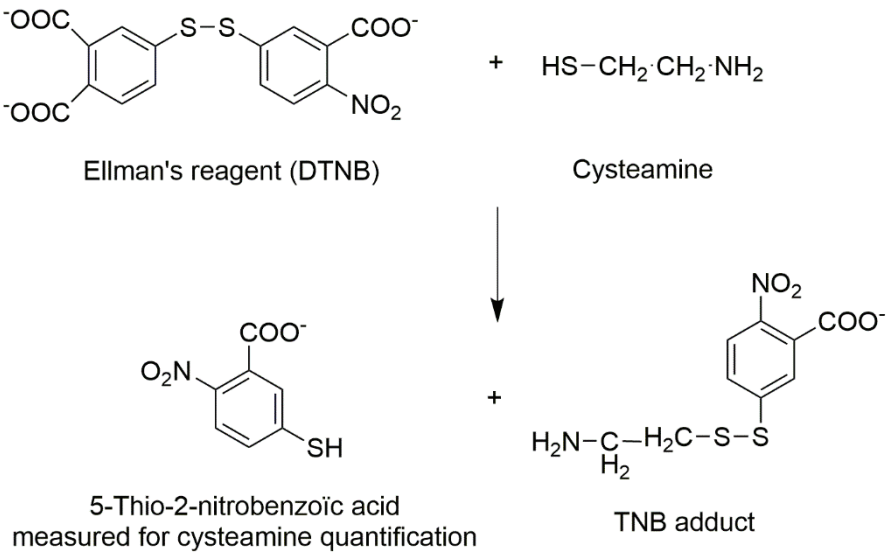

Figure 1: Réaction entre la cystéamine et le réactif d'Ellman. DTNB: 5,5-dithio-bis-2-acide nitrobenzoïque, TNB: 5-thio-2-acide nitrobenzoïque.

La détection et la quantification de la cystéamine à l'aide du réactif d'Ellman peuvent être réalisées à l'aide de nombreuses techniques telles que la spectroscopie UV-visible (Jaskierowicz et al., 1985), la chromatographie en phase liquide à haute performance (Belldina et al., 2003), la chromatographie liquide à haute résolution couplée à la spectrométrie de masse en tandem (Luaces-Rodríguez et al., 2017), et en utilisant une plaque de microtitration (Coulomb et al., 2017).

b) Méthode classique d'Ellman

Une solution mère de cystéamine a été préparée dans l'eau (1 mg / ml) puis diluée pour obtenir des concentrations finales de cystéamine comprises entre 2,5 et 100 µg/ml. Le réactif d'Ellman a été préparé en dissolvant 4 mg de DTNB dans 1 ml de tampon de réaction (pH 8,0). Ce dernier est composé de phosphate de sodium 0,1 M et d'EDTA 1 mM. 250 µL d'eau (blanc) ou de solution de cystéamine ont été ajoutés à 2,5 ml de tampon de réaction et 50 µL de solution de réactif d'Ellman. Ce mélange réactionnel a ensuite été vortexé et incubé à température ambiante

pendant 15 min. L'absorbance a été mesurée à 412 nm en utilisant le spectrophotomètre UV5 Mettler Toledo (Columbus Ohio, USA).

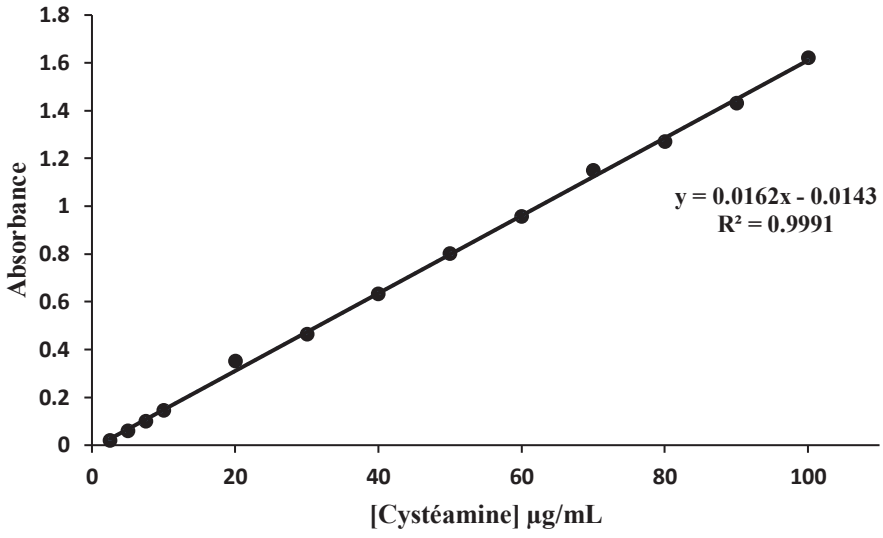

Figure 2: Courbe d'étalonnage de la cystéamine en utilisant la méthode Ellman.

La courbe d'étalonnage a été construite en traçant l'absorbance de la cystéamine par rapport à la concentration de la cystéamine allant de 2,5 à 100 µg / mL. La relation linéaire a été évaluée par analyse de régression avec la méthode des moindres carrés, le coefficient de corrélation déterminé était de 0,9997 (**Figure 2**). La limite de détection de la cystéamine était de 2,5 µg / mL.

c) Optimisation de la méthode d'Ellman pour la quantification de la cystéamine dans les suspensions liposomales

Préparation de la suspension liposomale

Les liposomes ont été préparés par la méthode d'injection d'éthanol (Jaafar-Maalej et al., 2010; Sebaaly et al., 2015; Shaker et al., 2017). Cette technique met en œuvre la nanoprécipiation lorsqu'une solution éthanolique de lipides entre en contact avec une phase aqueuse. Par

réorganisation des fragments lipidiques formés lors de l'injection, des liposomes sont obtenus. La Figure 3 montre une structure typique de liposome, constituée d'une bicouche lipidique entourant un cœur aqueux. La cystéamine, qui est une molécule hydrophile, est représenté dans le cœur aqueux du liposome.

Le protocole utilisé dans notre étude expérimentale reprend la méthodologie décrite par exemple par Sebaaly et al. (2015) (Sebaaly et al., 2015). Les principales étapes sont les suivantes. Le phospholipide (PH 90H) et le cholestérol (5 mg / ml) ont été dissous dans de l'éthanol absolu pour obtenir la phase organique (10 ml). Ensuite, la phase organique a été injectée dans la phase aqueuse (20 mL) à l'aide d'une pompe à seringue (Fortuna optima, GmbH-Germany), à une température supérieure à la température de transition du phospholipide (55 ° C pour PH 90H) et sous agitation magnétique à 400 tr / min. Le contact entre la solution éthanolique et la phase aqueuse conduit à une formation spontanée de liposomes. Les suspensions liposomales ont ensuite été laissées 15 min à 25 ° C sous agitation (400 rpm) **(Figure 3)**. L'éthanol a été éliminé par évaporation rotative (Heidolph GmbH, Allemagne) sous pression réduite à 40 ° C et les solutions liposomales obtenues ont été stockées à 4 ° C.

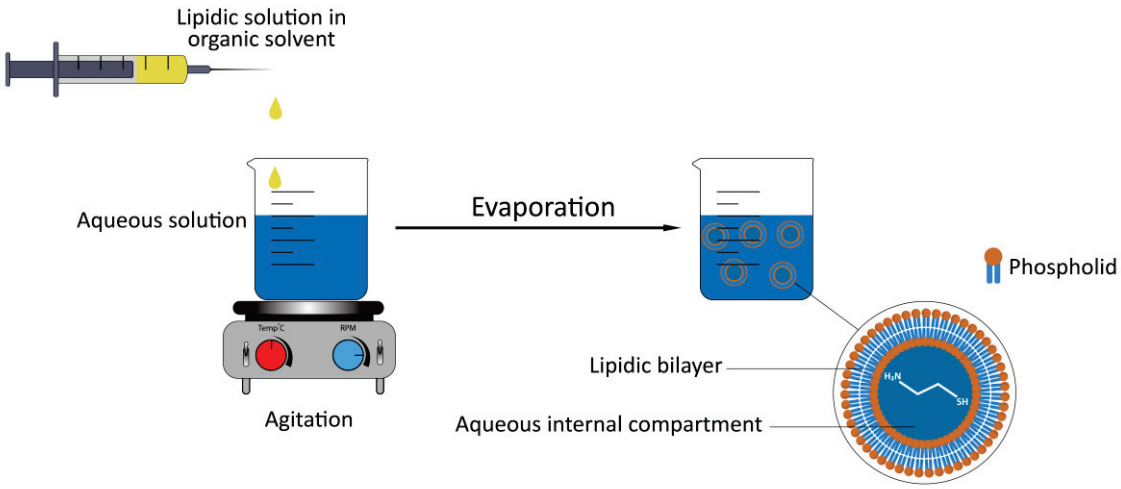

Figure 3 : Méthode d'injection éthanolique, représentation d'un liposome chargé en cystéamine.

Optimisation de la méthode d'Ellman

La méthode classique d'Ellman, décrite ci-dessus, ne convient pas à la quantification de la cystéamine dans les suspensions liposomales en raison de l'interférence entre la courbe d'absorbance des molécules lipidiques et celle de la cystéamine. Par conséquent, une méthode Ellman modifiée a été optimisée pour surmonter ce problème. Pour cela, du triton X-100 (1%) a été ajouté à la solution tampon phosphate pour solubiliser les liposomes. De plus, des solvants organiques (méthanol, éthanol, acétone, acétonitrile et diméthylsulfoxyde) ont été testés et ajoutés au mélange réactionnel à différents rapports volumiques solvant organique: mélange réactionnel (100: 0; 50:50 et 10:90).

Les suspensions liposomales ont montré une absorption à 412 nm même après dilution; pour cela, une optimisation des conditions expérimentales a donc été nécessaire. La problématique a été d'éliminer l'absorbance de la suspension liposomale sans affecter le dosage de la cystéamine

par la méthode d'Ellman. Premièrement, comme on peut le voir sur la figure 4, les suspensions liposomales ont montré une absorbance même après l'addition de Triton X (1%). L'utilisation de Triton X (1%) n'était donc pas appropriée pour dissoudre complètement les structures liposomales. Deuxièmement, divers solvants organiques miscibles à l'eau (méthanol, éthanol, acétone, acétonitrile et diméthylsulfoxyde) ont été testés. Le méthanol était le seul solvant organique éliminant l'absorbance des suspensions liposomales lorsqu'il était ajouté à un petit volume (inférieur à 2 ml) (**Figure 4**). L'utilisation d'un volume équivalent de méthanol (1,25 ml) et de tampon phosphate contenant de l'EDTA (1,25 ml) avec une suspension liposomale (préalablement diluée à 1/10 ou plus dans l'eau) et 50 µL de réactif d'Ellman a été déterminée comme étant l'approche la plus appropriée pour la quantification de la cystéamine dans les suspensions liposomales.

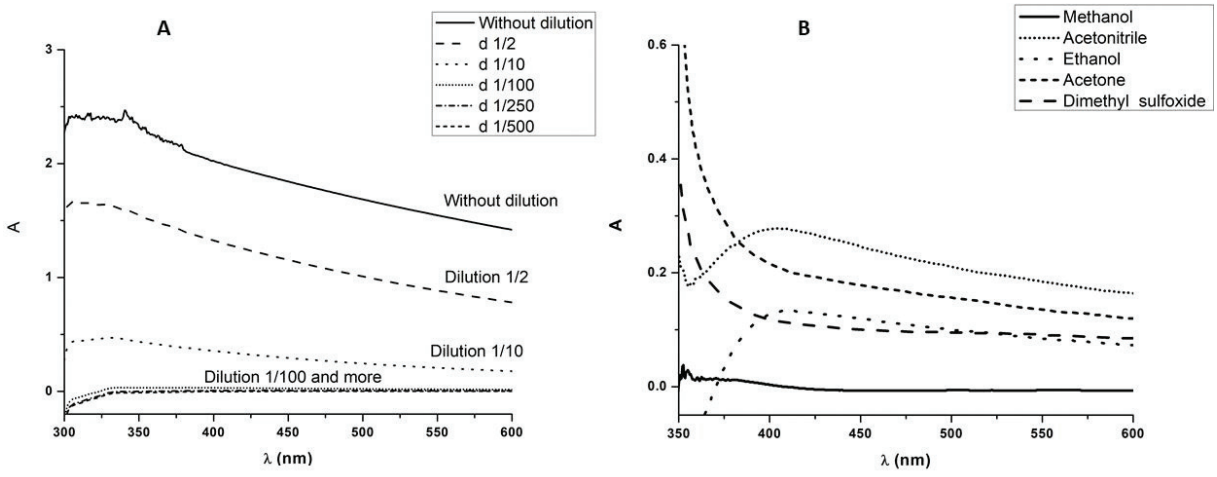

Figure 4: Spectres d'absorbance des liposomes blancs dilués (½; 1/10; 1/100; 1/250; 1/500) ou non dans l'eau suivi de l'ajout de 2,5 mL de solution tampon phosphate contenant 1% de triton X- 100 (A) et des liposomes blancs dilués au 1/10 dans l'eau suivi de l'ajout de 1,25 mL de différents solvants organiques et 1,25 mL de tampon phosphate et 50 µL de réactif d'Ellman (B).

La courbe d'étalonnage de la cystéamine utilisant la méthode d'Ellman modifiée pour déterminer la concentration de cystéamine dans les suspensions liposomales est présentée dans

la figure 5. Les équations de la courbe d'étalonnage de la cystéamine utilisant les méthodes classique et modifiée d'Ellman étaient similaires.

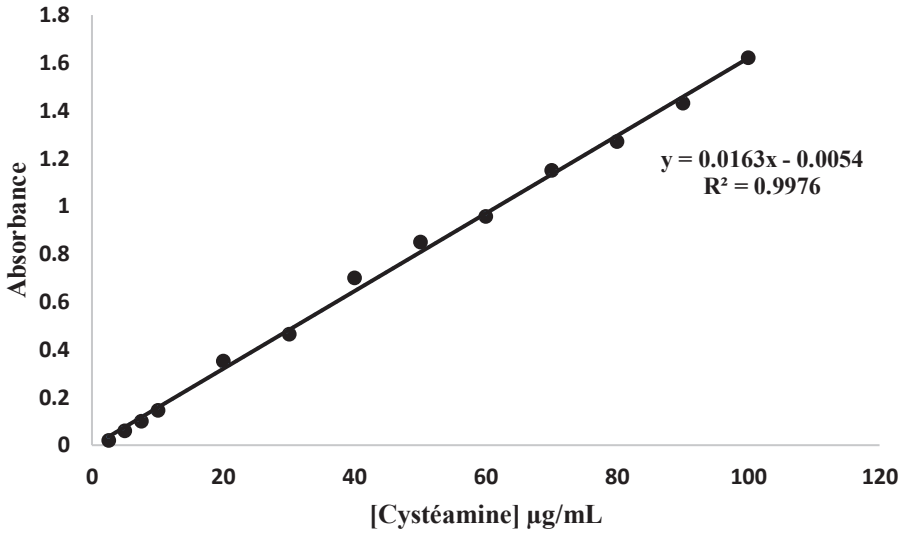

Figure 5: Courbe d'étalonnage de la cystéamine en utilisant la méthode Ellman modifiée.

2) **Méthodes chromatographiques (chromatographie de paires d'ions et chromatographie liquide micellaire)**

a) **Chromatographie de paires d'ions**

La chromatographie de paires d'ions (CPI) est une technique de chromatographie liquide haute performance à phase inversée (RP-CLHP) efficace pour la séparation des ions organiques et des analytes organiques partiellement ionisés en utilisant les mêmes types de phases stationnaires et de phases mobiles que la RP- CLHP (Snyder et al., 2011). Un réactif de pair d'ions ou un contre-ion est ajouté à la phase mobile. Les ions à analyser forment une paire d'ions à l'aide du contre-ion qui possède une ou des chaînes alkyles. Grâce à la présence de ces chaînes alkyles, le contre-ion a une affinité avec les molécules hydrophobes (la colonne hydrophobique) **(Figure 6)**. Ces contre-ions sont généralement du tétraalkylammonium pour des analytes à charge négative (acides) ou de l'alkylsufonate pour des analytes à charge positive (bases). La

longueur de la chaîne alkyle est importante en chromatographie de paires d'ions. Elle influence le ratio de contre-ions dans la phase stationnaire par rapport à la phase mobile. La concentration en contre-ions est plus importante si la chaîne alkyle est plus longue, ceci peut être expliqué par le fait que le caractère hydrophobe du contre-ion et de la paire d'ions est plus grand lorsque la chaîne alkyle est longue, donc le contre-ion se liera plus facilement à la phase stationnaire.

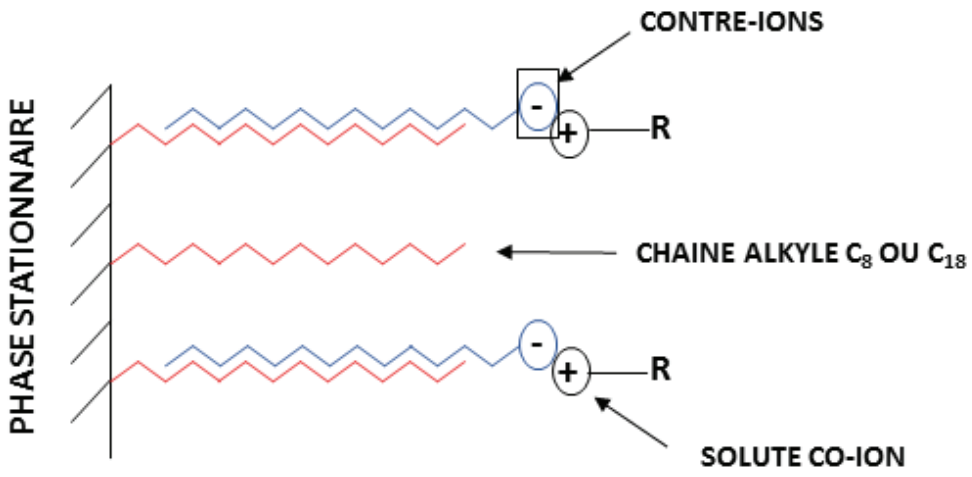

Figure 6: Chromatographie de paires d'ions.

b) Chromatographie liquide micellaire

Les tensioactifs, composés amphiphiles, contiennent une queue de chaîne hydrophobe et une tête polaire qui peuvent être cationiques, anioniques, neutres ou zwitterioniques. Les monomères de tensioactifs interagissent pour former des micelles dans des solutions aqueuses, à des concentrations supérieures à la concentration micellaire critique (CMC). Les queues hydrophobes restent dans le noyau pour éviter le contact avec l'eau, tandis que les têtes polaires sont orientées vers l'eau **(Figure 7)**. La chromatographie liquide micellaire (CLM) est une RP-CLHP, où la phase mobile est une solution micellaire (Berthod & Garcia-Alvarez-Coque,

2000). Les colonnes les plus utilisées sont celles contenant une phase de silice liée octadécyle (C18). Les micelles et les monomères tensioactifs libres affectent les propriétés des phases stationnaire et mobile. L'adsorption des monomères sur la phase stationnaire avec le groupe polaire orienté vers l'eau crée une structure similaire à une micelle ouverte. Sur la phase stationnaire, une couche externe polaire et éventuellement chargée apparaît, tandis que la couche interne devient plus hydrophobe. La distribution de l'analyte est influencée par l'hydrophobicité, la charge et le facteur stérique des solutés, la phase stationnaire et les micelles. Ces paramètres dépendent des réactions secondaires acide/basique, par conséquent, un tampon doit être ajouté pour ajuster le pH à la valeur appropriée et le maintenir constant pendant tout le cycle chromatographique. Les mécanismes de rétention en CLM dépendent de nombreux éléments expérimentaux, tels que le type de colonne, le pH, la nature et la quantité de tensioactif.

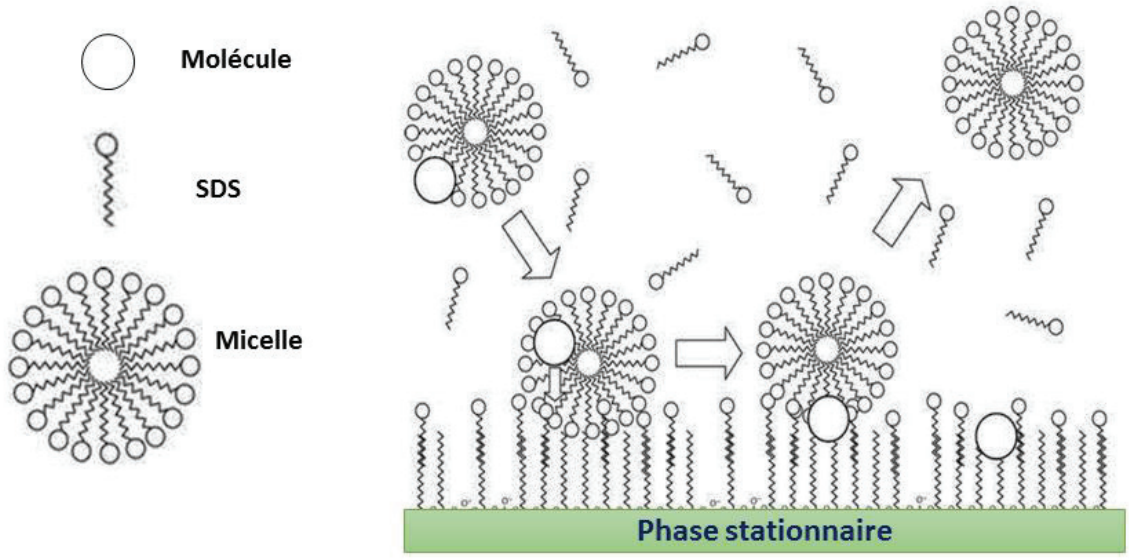

Figure 7: Chromatographie liquide micellaire.

3) La lyophilisation des liposomes

Pour pouvoir surmonter les problèmes d'instabilité chimique et physique des liposomes dans un milieu aqueux et les conserver à long-terme, la lyophilisation des liposomes a été proposée par de nombreuses auteurs (par exemple Chen et al., 2010, Stark et al., 2010, Sebaaly et al., 2015, Gharib et al., 2018). La lyophilisation est constituée de trois étapes principales :

- La congélation qui permet la transformation de l'eau libre en cristaux de glace.
- Le séchage primaire, aussi appelé dessiccation primaire, où l'eau est éliminée progressivement par sublimation de la glace grâce au vide créé.
- Le séchage secondaire, aussi appelé dessiccation secondaire, où l'eau congelée et retenue sur le produit par adsorption est éliminée.

La lyophilisation de suspensions liposomales peut présenter plusieurs problèmes comme l'altération des bicouches lipidiques avec la formation de la glace après l'étape de congélation ou des phénomènes d'agrégation ou de fusion des vésicules et une perte du principe actif encapsulé après l'étape de déshydratation (Chen et al., 2010). L'utilisation d'un agent cryoprotecteur comme les carbohydrates (saccharose, glucose, lactose, tréhalose, mannitol, dextrose et cyclodextrines) ou des polyalcools comme le glycérol est alors nécessaire (Stark et al., 2010).

Le protocole expérimental que nous avons utilisé dans notre étude est similaire à celui mis en œuvre par Gharib et al. 2018 (Gharib et al., 2018). Le cryoprotecteur choisi est l'hydroxypropyl β-cyclodextrine (HP-β-CD).

4) La quantification de l'éthanol par résonance magnétique nucléaire (RMN)

Il est important de connaitre la concentration résiduelle en éthanol dans les suspensions liposomales finales en raison de la toxicité éventuelle de ce composé. Plusieurs méthodes de quantification sont possibles comme la réfractométrie, la chromatographie gazeuse et la RMN.

Dans note étude, la quantification de l'éthanol dans les suspensions liposomales est réalisée par la technique de RMN. L'éthanol donne un signal triplet à 1,19 ppm, correspondant aux protons du groupe méthyle, CH_3–, et un signal multiplet à 3,66 ppm, produit par les protons du groupe méthylène, –CH_2– **(Figure 8)** (Zuriarrain et al., 2015). Le triméthylsilylpropanoate de sodium (TSP) est utilisée comme étalon interne car il est soluble dans l'eau, stable dans le milieu de l'échantillon, est disponible en haute pureté et a un spectre RMN 1H très simple constitué d'un singulet unique de neuf protons (Del Campo et al., 2006), qui ne chevauche jamais avec un autre signal de l'éthanol. Ce singulet est utilisé simultanément pour fixer le déplacement chimique à 0,0 ppm dans les spectres RMN 1H.

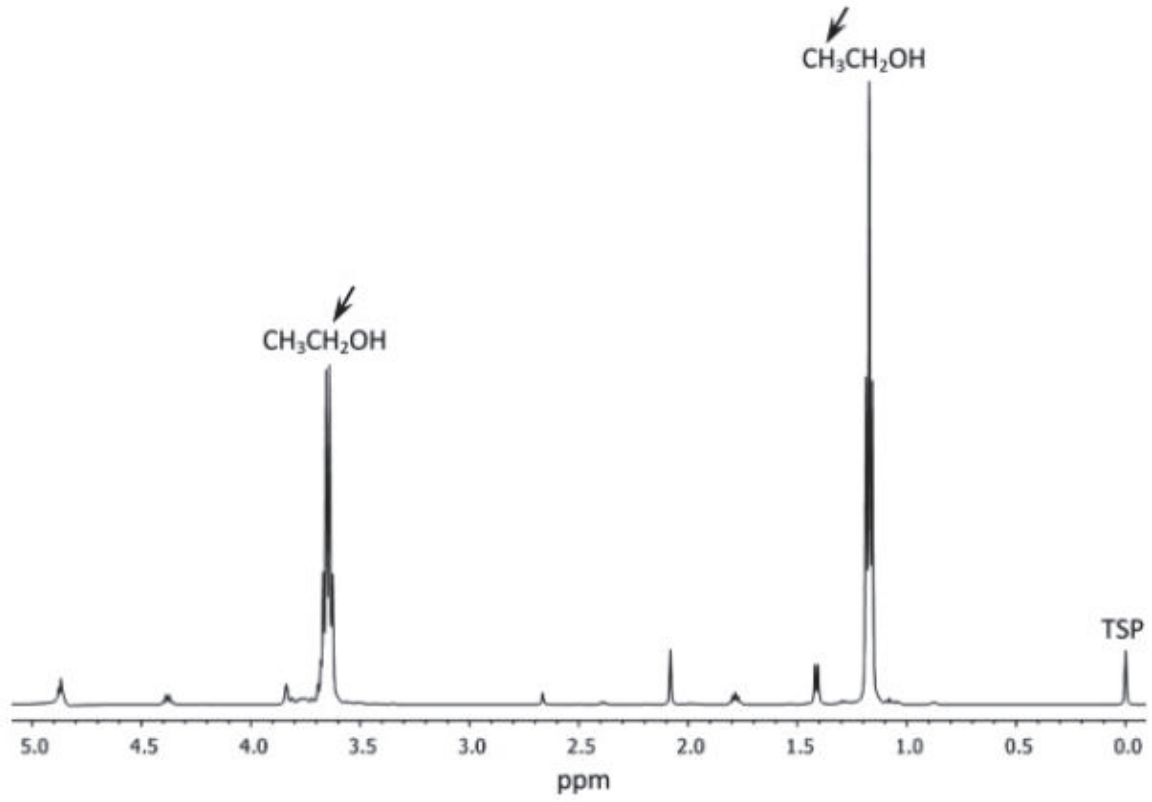

Figure 8 : Spectre RMN 1H de l'éthanol. Les signaux de l'éthanol et du TSP sont indiqués. Les protons impliqués dans les signaux de l'éthanol sont pointés vers le haut avec des flèches (Zuriarrain et al., 2015).

Préparation de la suspension liposomale pour l'analyse RMN

Les suspensions liposomales ont été centrifugées pendant 10 min à 10 000 rpm. L'étalon interne utilisé était le sel de sodium de l'acide (triméthylsilyl) -2,2,3,3-tétradeutepropropionique (TSP) $(CH_3)_3SiCD_2CD_2CO_2Na$. 10 mg de TSP ont été dissous dans 400 µL de D_2O et 300 µL du surnageant de suspension liposomale. Le nombre de moles d'éthanol est calculé directement à partir du spectre RMN en utilisant l'équation suivante:

$$n_{EtOH} = \frac{H_{IS}}{H_{CH2}} \times n_{IS} \times \frac{I_{CH2}}{I_{IS}}$$

Où H_{IS} et H_{CH2} sont le nombre d'hydrogène présent dans l'étalon interne (H_{IS} =9) et dans le groupe CH_2 (H_{CH2}=2) de l'éthanol, n_{IS} est le nombre de mole de l'étalon interne (n_{IS} =5.78 × 10^{-5} mole) et I_{CH2} et I_{IS} sont l'intégration du groupe CH_2 de l'éthanol et des pics de l'étalon interne.

Pour simplifier l'équation précédente, H_{IS}, H_{CH2} et n_{IS} sont remplacées par leurs valeurs pour obtenir l'équation suivante:

$n_{EtOH} = 0.00026 \times \frac{I_{CH2}}{I_{IS}}$.

Les expériences ont été effectuées en utilisant un spectromètre Avance 300 Bruker équipé d'une sonde BBFO standard. Des impulsions à 90 degrés ont été appliquées avec un temps de relaxation de 30 s pour assurer des analyses quantitatives.

5) Tests sur les cellules de mélanome B16 et la pénétration cutanée

Plusieurs méthodes ont été réalisées pour caractériser les effets d'une suspension liposomale chargée en cystéamine sur les cellules de mélanome B16 et la peau humaine, afin d'envisager l'utilisation de ce système d'encapsulation comme agent de traitement de l'hyperpigmentation.

Ainsi, nous avons mis en œuvre un test de cytotoxicité (test MTT), le dosage de la mélanine par spectrophotométrie, le dosage de l'activité de la tyrosinase, le dosage de l'activité antioxydante et des mesures de perméation sur cellules de Franz.

a) Le test de cytotoxicité (test MTT)

Le test MTT est un test colorimétrique qui est utilisé pour évaluer l'activité métabolique cellulaire. Les enzymes oxydoréductases cellulaires dépendantes du nicotinamide adenine dinucleotide phosphate (NADPH) peuvent, dans des conditions définies, refléter le nombre de cellules viables présentes. Ces enzymes sont capables de réduire le 3- (4,5-diméthylthiazol-2-yl) -2,5-diphényltétrazolium (MTT) en son formazan insoluble, qui a une couleur violette **(Figure 9)**.

Le MTT, un tétrazole jaune, est réduit en formazan violet dans les cellules vivantes. Un solvant (généralement soit du diméthylsulfoxyde, une solution d'éthanol acidifiée ou une solution du détergent dodécylsulfate de sodium dans de l'acide chlorhydrique dilué) est ajoutée pour dissoudre le formazan violet insoluble dans une solution colorée. L'absorbance de cette solution colorée peut être quantifiée en mesurant à une certaine longueur d'onde (généralement entre 500 et 600 nm) par un spectrophotomètre. Le degré d'absorption de la lumière dépend du degré de concentration de formazan accumulé à l'intérieur de la cellule et à la surface de la cellule. Plus la concentration de formazan est élevée, plus la couleur violette est profonde et donc plus l'absorbance est élevée (Supino, 1995).

Figure 9 : Réduction du MTT en formazan.

b) Dosage de la mélanine par spectrophotométrie

Le terme mélanine désigne de nombreux pigments biologiques foncés qui sont notamment responsable de de la couleur de la peau; cette coloration dépend principalement de son type et de sa concentration. Le dosage de la mélanine au spectrophotomètre permet de quantifier la mélanine totale. La mélanine intracellulaire a été extraite en solubilisant les culots cellulaires dans du NaOH 1N contenant 10% de DMSO pendant 2 h à 80 ° C. La teneur en mélanine des surnageants de lysat cellulaire a été mesurée par spectrophotométrie à une absorbance de 405 nm. Une courbe d'étalonnage de mélanine synthétique a été établie. La quantité de protéine dans le culot cellulaire a été déterminée par la méthode de Bradford. La teneur en mélanine intracellulaire a été ajustée par la quantité de protéine (Wang et al., 2018).

c) Dosage de l'activité de la tyrosinase

La tyrosinase est une enzyme qui catalyse la formation de la L-dopaquinone puis du dopachrome à partir de la L-Dopa **(Figure 10)**. Le dopachrome est un composé coloré quantifiable par spectrophotométrie visible à 490 nm. Une courbe d'étalonnage de la tyrosinase de champignon a été établie. L'activité de la tyrosinase a été normalisée à la quantité de protéine en divisant la quantité de tyrosinase et celui de protéine (déterminée en utilisant le test de

Bradford). L'utilisation d'un actif capable de modifier l'activité enzymatique se traduit par une variation de la densité optique à 490 nm (Moonrungsee et al., 2012).

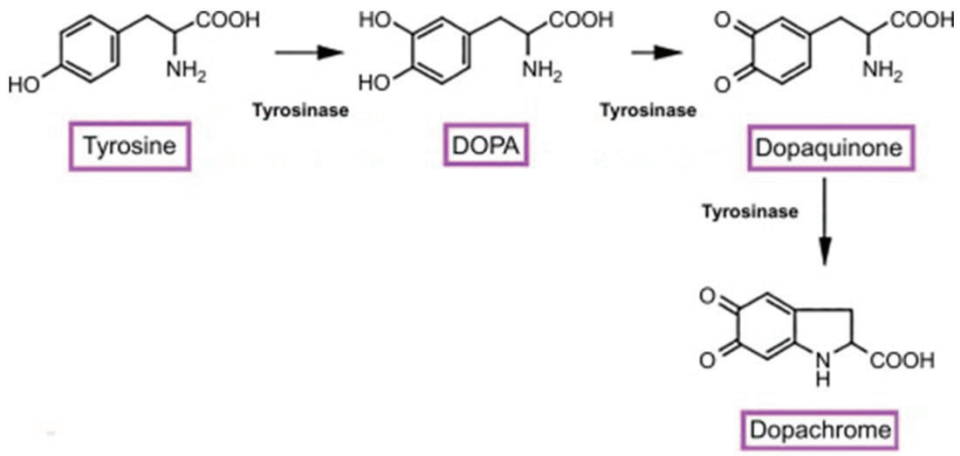

Figure 10 : La réaction de formation du dopachrome catalysée par la tyrosinase**.**

d) Dosage de l'activité antioxydante

Le 2,7-Dichlorodihydrofluorescéine (DCF) est souvent utilisé comme indicateur fluorescent de la formation des espèces réactives de l'oxygène (ROS) à la fois dans des dosages d'antioxydants biochimiques simples et dans des dosages d'antioxydants basés sur des cultures cellulaires (Shaaban, 2011). Le DCF peut être oxydé par le peroxynitrite, les radicaux hydroxyles et la peroxydase pour générer un produit final hautement fluorescent **(Figure 11)**. Lorsqu'il est utilisé dans des tests basés sur la culture cellulaire, il est utilisé sous forme de diacétate (DCF-DA). Sous cette forme, le DCF-DA peut pénétrer la membrane cellulaire et une fois à l'intérieur de la cellule, les enzymes estérases intracellulaires cliveront les groupes acétate piégeant le DCF dans la cellule. Les cellules peuvent ensuite être exposées à des conditions qui génèrent des ROS, telles que l'irradiation UV. Étant donné que le colorant n'a pas d'impact sur la viabilité cellulaire, la formation de ROS peut ensuite être suivie en temps réel en effectuant des mesures de fluorescence périodiques des cellules avec un fluoromètre. Cela permet non seulement de

mesurer les effets immédiats des dommages oxydatifs, mais cela permet également de poursuivre les mesures lorsque que les cellules se rétablissent (Shaaban, 2011).

Les cellules ont été traitées avec 100 µL de substances testées, puis avec du peroxyde d'hydrogène H_2O_2 (100 µM dans le milieu de culture) pendant 6 h. Ensuite, une solution de DCFH-DA (1 uM dans du milieu de culture) a été ajoutée aux cellules pendant 30 min à 37 ° C. Immédiatement après le lavage au PBS, la fluorescence a été quantifiée à l'aide d'un spectrofluorophotomètre (BioTek, Synergy H1) avec une excitation de 495 nm et des filtres d'émission de 527 nm. Les ROS ont été observés sous un microscope à fluorescence inversée (Olympus, DP50).

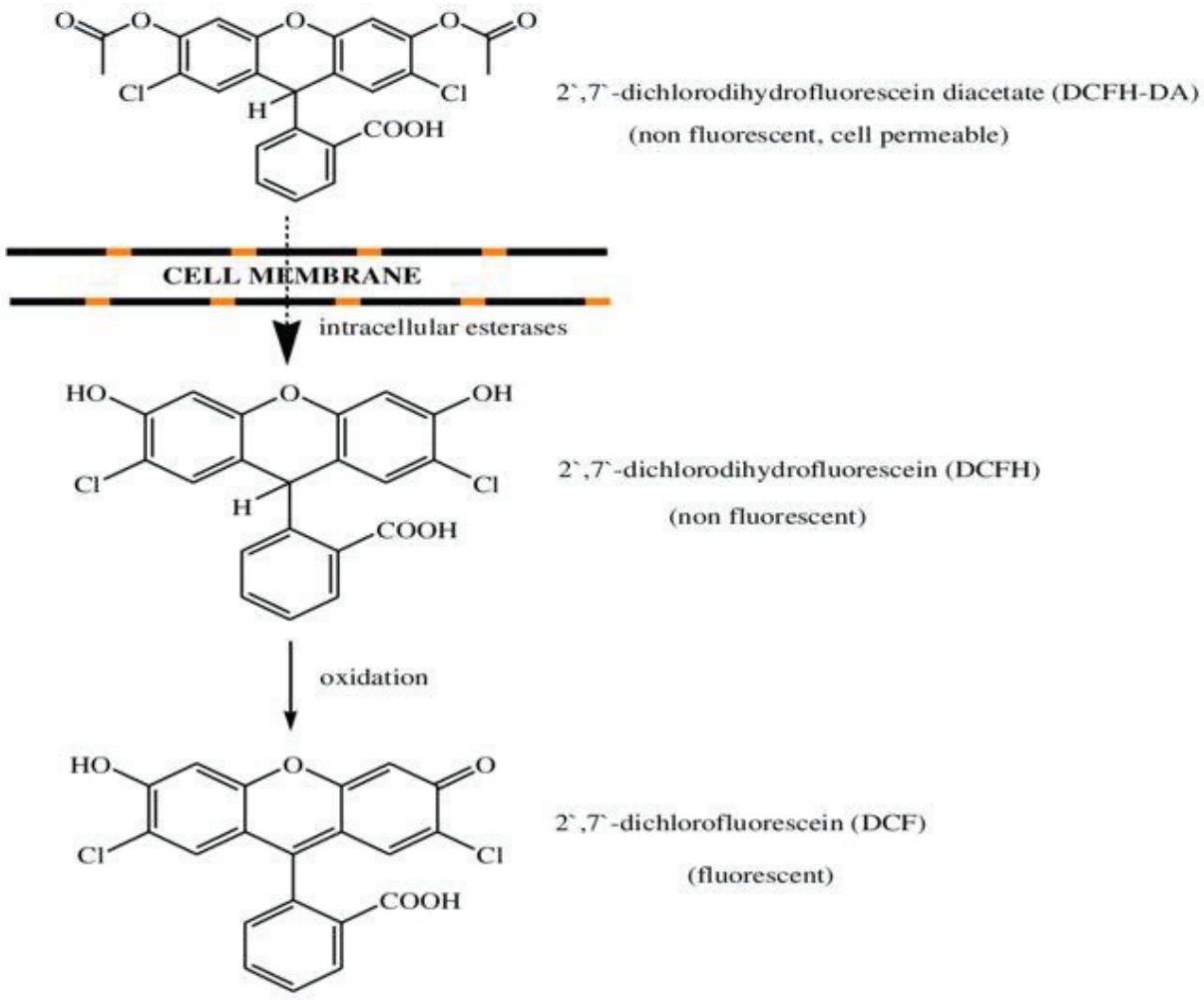

Figure 11 : Détection de ROS avec la sonde DCFH-DA ; DCFH-DA est clivé par des estérases intracellulaires en DCFH et oxydé par ROS en molécule hautement fluorescente DCF (Shaaban, 2011).

e) Cellules de Franz

Les cellules de Franz (**Figure 12**) sont des dispositifs permettant d'évaluer le passage d'un composé à travers une membrane naturelle ou synthétique. Il s'agit d'une cellule de diffusion composée de deux compartiments : un donneur, qui contient la molécule d'intérêt destinée à être appliqué sur la peau, et un receveur, où des prélèvements à intervalles de temps définis vont être faits, afin d'étudier la quantité de molécule d'intérêt libérée en fonction du temps. Les différents prélèvements peuvent ensuite être dosés par différentes techniques comme la spectroscopie Ultra-Violet Visible ou encore la CLHP. Afin de s'affranchir d'un ralentissement de diffusion, il est important de s'assurer que la solubilité du principe actif (PA) ne sera pas un facteur limitant sa libération. Pour cela, il faut respecter les conditions « sink » : la concentration du PA dans le milieu receveur devra être 3 à 10 fois inférieure à celle de saturation du PA.

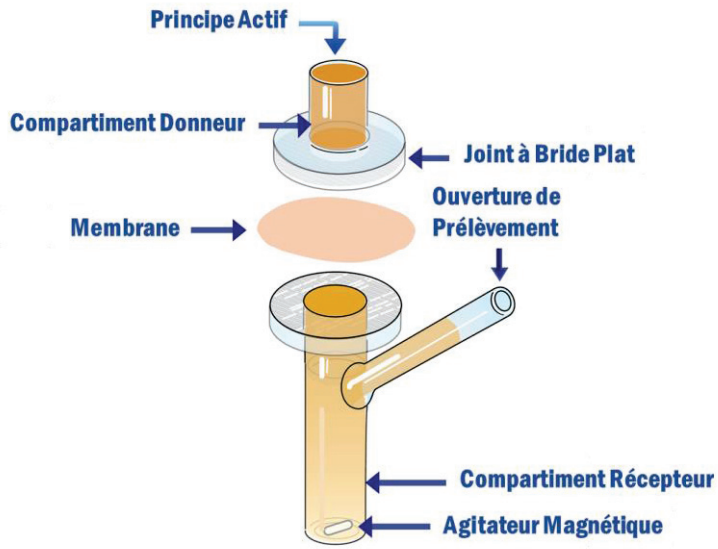

Figure 12 : Cellule de Franz.

La perméation percutanée ex vivo du chlorhydrate de cystéamine a été réalisée sur la peau décongelée d'une donneuse caucasienne. La peau a été dégraissée à l'aide d'un scalpel puis dermatomée avec un dermatome (Zimmer Biomet Electric® Dermatome). Les disques de peau ont été réalisés à l'aide d'un couteau encerclé et la plage d'épaisseur était comprise entre 400 et 600 µm. Les disques cutanés ont été montés sur un système de cellules de Franz (PermeGear). Les cellules de Franz étaient auparavant remplies de fluide récepteur (RF) constitué de PBS-EDTA 0,1% à pH 7,4. Les disques cutanés ont été équilibrés pendant 1 h avant la mesure de TEWL (Trans Epidermal Water Loss) à l'aide d'un tewameter TM300 (MDD 4, Courage & Khazaka). Les formulations testées étaient une solution de chlorhydrate de cystéamine, des liposomes chargés de chlorhydrate de cystéamine total et encapsulé et des liposomes chargés de chlorhydrate de cystéamine lyophilisés remis en suspension. 1 mL de chaque formulation diluée pour obtenir 1200 µM de chlorhydrate de cystéamine en tant que concentration finale a été déposé sur la peau. Le RF a été échantillonné à différents moments 0, 1, 4, 18 et 24h. A 24 h, les formulations ont été retirées et les disques cutanés ont été lavés avec RF (1 ml). Les compartiments cutanés ont été séparés à l'aide de forceps afin d'obtenir l'épiderme et le derme. Des échantillons (lavage, épiderme et derme) ont été pesés puis l'ingrédient actif a été extrait dans un mélange méthanol: eau (50:50, v / v) après agitation pendant 24 h. Enfin, les extraits ont été quantifiés par chromatographie de paires d'ions.

Références

Belldina, E. B., Huang, M. Y., Schneider, J. A., Brundage, R. C., & Tracy, T. S. (2003). Steady-state pharmacokinetics and pharmacodynamics of cysteamine bitartrate in paediatric nephropathic cystinosis patients: Pharmacokinetics of cysteamine. *British Journal of*

Clinical Pharmacology, *56*(5), 520–525. https://doi.org/10.1046/j.1365-2125.2003.01927.x

Berthod, A., & Garcia-Alvarez-Coque, C. (2000). *Micellar Liquid Chromatography*. CRC Press.

Chen, C., Han, D., Cai, C., & Tang, X. (2010). An overview of liposome lyophilization and its future potential. *Journal of Controlled Release*, *142*(3), 299–311. https://doi.org/10.1016/j.jconrel.2009.10.024

Coulomb, B., Robert-Peillard, F., Palacio, E., Di Rocco, R., & Boudenne, J.-L. (2017). Fast microplate assay for simultaneous determination of thiols and dissolved sulfides in wastewater. *Microchemical Journal*, *132*, 205–210. https://doi.org/10.1016/j.microc.2017.01.022

del Campo, G., Berregi, I., Caracena, R., & Santos, J. I. (2006). Quantitative analysis of malic and citric acids in fruit juices using proton nuclear magnetic resonance spectroscopy. *Analytica Chimica Acta*, *556*(2), 462–468. https://doi.org/10.1016/j.aca.2005.09.039

Ellman, G. L. (1959). Tissue sulfhydryl groups. *Archives of Biochemistry and Biophysics*, *82*(1), 70–77. https://doi.org/10.1016/0003-9861(59)90090-6

Gharib, R., Greige-Gerges, H., Fourmentin, S., & Charcosset, C. (2018). Hydroxypropyl-ß-cyclodextrin as a membrane protectant during freeze-drying of hydrogenated and non-hydrogenated liposomes and molecule-in-cyclodextrin-in- liposomes: Application to trans-anethole. *Food Chemistry*, *267*, 67–74. https://doi.org/10.1016/j.foodchem.2017.10.144

Jaafar-Maalej, C., Diab, R., Andrieu, V., Elaissari, A., & Fessi, H. (2010). Ethanol injection method for hydrophilic and lipophilic drug-loaded liposome preparation. *Journal of Liposome Research*, *20*(3), 228–243. https://doi.org/10.3109/08982100903347923

Jaskierowicz, D., Genissel, F., Roman, V., Berleur, F., & Fatome, M. (1985). Oral Administration of Liposome-entrapped Cysteamine and the Distribution Pattern in Blood, Liver and Spleen. *International Journal of Radiation Biology and Related Studies in Physics, Chemistry and Medicine*, *47*(6), 615–619. https://doi.org/10.1080/09553008514550851

Luaces-Rodríguez, A., Díaz-Tomé, V., González-Barcia, M., Silva-Rodríguez, J., Herranz, M., Gil-Martínez, M., Rodríguez-Ares, M. T., García-Mazás, C., Blanco-Mendez, J., Lamas, M. J., Otero-Espinar, F. J., & Fernández-Ferreiro, A. (2017). Cysteamine polysaccharide hydrogels: Study of extended ocular delivery and biopermanence time by PET imaging. *International Journal of Pharmaceutics*, *528*(1–2), 714–722. https://doi.org/10.1016/j.ijpharm.2017.06.060

Moonrungsee, N., Shimamura, T., Kashiwagi, T., Jakmunee, J., Higuchi, K., & Ukeda, H. (2012). Sequential injection spectrophotometric system for evaluation of mushroom tyrosinase-inhibitory activity. *Talanta*, *101*, 233–239. https://doi.org/10.1016/j.talanta.2012.09.015

Sebaaly, C., Jraij, A., Fessi, H., Charcosset, C., & Greige-Gerges, H. (2015). Preparation and characterization of clove essential oil-loaded liposomes. *Food Chemistry*, *178*, 52–62. https://doi.org/10.1016/j.foodchem.2015.01.067

Shaaban, S. (2011). *Synthesis and Biological Activity of Multifunctional Sensor/Effector Catalysts*.

Shaker, S., Gardouh, A. R., & Ghorab, M. M. (2017). Factors affecting liposomes particle size prepared by ethanol injection method. *Research in Pharmaceutical Sciences*, *12*(5), 346–352. https://doi.org/10.4103/1735-5362.213979

Snyder, L. R., Kirkland, J. J., & Dolan, J. W. (2011). *Introduction to Modern Liquid Chromatography*. John Wiley & Sons.

Stark, B., Pabst, G., & Prassl, R. (2010). Long-term stability of sterically stabilized liposomes by freezing and freeze-drying: Effects of cryoprotectants on structure. *European Journal of Pharmaceutical Sciences*, *41*(3), 546–555. https://doi.org/10.1016/j.ejps.2010.08.010

Supino, R. (1995). MTT Assays. In S. O'Hare & C. K. Atterwill (Eds.), *In Vitro Toxicity Testing Protocols* (pp. 137–149). Humana Press. https://doi.org/10.1385/0-89603-282-5:137

Wang, Y., Tissot, M., Rolin, G., Muret, P., Robin, S., Berthon, J.-Y., He, L., Humbert, P., & Viennet, C. (2018). Development and validation of a simple method for the extraction of human skin melanocytes. *Cytotechnology*, *70*(4), 1167–1176. https://doi.org/10.1007/s10616-018-0207-7

Zuriarrain, A., Zuriarrain, J., Villar, M., & Berregi, I. (2015). Quantitative determination of ethanol in cider by 1H NMR spectrometry. *Food Control*, *50*, 758–762. https://doi.org/10.1016/j.foodcont.2014.10.024

Chapitre 3 : Dosage de la cystéamine par spectroscopie UV-visible et par chromatographie de paires d'ions

Introduction

Le dosage de la cystéamine est problématique en raison de l'absence de groupement chromophore au sein de sa structure et de son instabilité en solutions, d'où le recours à une méthode qui soit, à la fois, rapide et efficace. L'utilisation de la spectroscopie UV-Visible nécessite l'emploi d'un agent de dérivatisation. La méthode d'Ellman (Ellman, 1959) qui se base sur l'utilisation du 5,5-dithio-bis-2-acide nitrobenzoïque ou DTNB connu sous le terme réactif d'Ellman a été utilisée afin de quantifier la cystéamine en solution. Lors de la quantification de la molécule dans des suspensions liposomales, l'absorbance des vésicules liposomales chevauche avec celle de la cystéamine. L'ajout de méthanol dans le réactif d'Ellman permet de solubiliser les liposomes et d'éliminer le problème de chevauchement. Mais, l'importance de la méthode reste limitée parce qu'elle permet le dosage de la cystéamine seulement.

L'HPLC est couramment utilisée pour quantifier simultanément plusieurs molécules en se basant sur l'interaction entre la molécule et la phase stationnaire (la colonne) (Thammana, 2016). La HPLC en phase inverse est basée sur l'utilisation d'une phase stationnaire non polaire et d'une phase mobile polaire. Par conséquent, la cystéamine et la cystamine, des molécules hydrophiles, sont directement éliminées dans le temps mort de la colonne. Le recours à la chromatographie par paires d'ions ou la chromatographie micellaire est donc nécessaire. Ces deux méthodes sont basées sur l'ajout au niveau de la phase stationnaire d'un contre-ion qui possède une ou des chaînes alkyles. Par la présence de ces derniers, le contre-ion présente une affinité avec les molécules hydrophobes. Ces contre-ions sont généralement du tétra-alkylammonium pour des analytes à charge négative ou de l'alkylsufonate pour des analytes à charge positive. Cette charge va interagir avec la molécule afin d'augmenter sa rétention dans la phase stationnaire (Kord & Khaledi, 1992).

Le dodécylsulfate de sodium (SDS) est un détergent et tensioactif ionique fort fréquemment utilisé en chimie et biochimie (Tan et al., 2002). Afin de quantifier la cystéamine et la cystamine simultanément, le SDS a été testé en utilisant deux concentrations différentes. Une concentration supérieure à la concentration micellaire critique (CMC) pour l'utilisation de la chromatographie micellaire et une autre inferieure à la CMC pour l'utilisation de la chromatographie par paires d'ions. Ces deux méthodes ont été comparées pour la forme et la symétrie des pics de la cystéamine et de la cystamine obtenus. La chromatographie par paires d'ions a été choisie comme méthode de quantification et une étude de stabilité des échantillons pendant l'analyse a été menée. Enfin, une étude de stabilité de la cystéamine dans différentes conditions a été réalisée.

Ce chapitre est constitué de l'article portant sur le dosage simultané de la cystéamine et la cystamine par la chromatographie par paire d'ions.

Références

Ellman, G. L. (1959). Tissue sulfhydryl groups. *Archives of Biochemistry and Biophysics*, *82*(1), 70–77. https://doi.org/10.1016/0003-9861(59)90090-6

Kord, A. S., & Khaledi, M. G. (1992). Chromatographic characteristics of surfactant-mediated separations: Micellar liquid chromatography vs ion pair chromatography. *Analytical Chemistry*, *64*(17), 1901–1907. https://doi.org/10.1021/ac00041a027

Tan, A., Ziegler, A., Steinbauer, B., & Seelig, J. (2002). Thermodynamics of Sodium Dodecyl Sulfate Partitioning into Lipid Membranes. *Biophysical Journal*, *83*(3), 1547–1556. https://doi.org/10.1016/S0006-3495(02)73924-6

Thammana, M. (2016). A Review on High Performance Liquid Chromatography (HPLC). *Research & Reviews: Journal of Pharmaceutical Analysis*, *5*(2), 1–7.

Simultaneous determination of cysteamine and cystamine by ion pair chromatography: Application to the stability study of cysteamine

Carla Atallah[a,b], Catherine Charcosset[b], and Hélène Greige-Gerges[a]

[a]*Bioactive Molecules Research Laboratory, Faculty of Sciences, Lebanese University, Lebanon.*

[b]*Laboratoire d'Automatique, de Génie des Procédés et de Génie Pharmaceutiques (LAGEPP), Université Claude Bernard Lyon 1, France.*

To be submitted

Simultaneous determination of cysteamine and cystamine by ion pair chromatography: Application to the stability study of cysteamine

Carla Atallah[a,b], Catherine Charcosset[b], and Hélène Greige-Gerges*[a]

[a]*Bioactive Molecules Research Laboratory, Faculty of Sciences, Lebanese University, Lebanon.*

[b]*Laboratoire d'Automatique, de Génie des Procédés et de Génie Pharmaceutiques (LAGEPP), Université Claude Bernard Lyon 1, France.*

**Corresponding author: Faculty of Sciences, Section II, Bioactive Molecules Research Laboratory, Lebanese University, B.P. 90656 Jdaidet El-Matn, Lebanon.*

Tel.: +961 3 341011; fax: +961 1 689647.

E-mail addresses: greigegeorges@yahoo.com, hgreige@ul.edu.lb (H. Greige-Gerges).

Abstract

The aminothiol cysteamine presents several biological applications; however, it is unstable in aqueous solution due to its conversion to its disulfide form cystamine. Ion pair- and micellar-chromatography methods allowing simultaneous quantification of cysteamine and cystamine in solutions were performed on a reverse-phase Kinetex C18 column (4.6 × 100 mm, 2.6 µm) using a mobile phase composed of acetonitrile and water containing 0.1% phosphoric acid and sodium dodecyl sulfate. The flow rate was set at 1.0 mL/min, the column temperature was maintained at 25°C, and the detection wavelength was 215 nm. Metformin was used as an internal standard. The ion pair chromatography was more efficient than micellar chromatography because it showed better peak symmetry and higher theoretical plates for cysteamine. Moreover, the stability of the samples containing cysteamine and cystamine during the analysis was evaluated in the presence of different concentrations of ethylenediaminetetraacetic acid (EDTA). The addition of EDTA (0.1%) preserved the ratio of cysteamine/cystamine concentrations during the analysis as well as the shape of cysteamine and cystamine peaks. The stability of cysteamine was evaluated in different experimental conditions where the buffer type and its concentration, the temperature, and the light exposure were affecting the stability of cysteamine.

Keywords: Cysteamine; cystamine; ion-pair chromatography; micellar chromatography; stability.

1. Introduction

Cysteamine is an aminothiol compound deriving from coenzyme A degradation in mammalian cells. It is used for the treatment of cystinosis, cancer, Parkinson, and Huntington diseases [1]. The quantification of cysteamine is a challenging mission due to the lack of a chromophore in its structure and its ability for oxidation during the analysis. Many methods were employed to quantify cysteamine. These methods were mainly based on the derivatization of the molecule using different derivatization agents such as Ellman reagent, pyvaldehyde, bis (trimethylsilyl) trifluoroacetamide, o-phthalaldehyde, and others using spectrophotometric and chromatographic methods [2].

One of the significant drawback of cysteamine uses is its instability in solutions. Cysteamine is converted to its disulfide form cystamine via a very rapid oxidation reaction (126 µg/h when 0.1 mg/mL of the drug was prepared in phosphate buffer saline) [3]. Many factors seem to affect the stability of cysteamine like the presence of metal ions such as Cu^{2+}, Fe^{3+}, and Zn^{2+} and the pH of the medium [4]. In parallel, cystamine can be converted to cysteamine after the addition of a reducing agent such as β-mercaptoethanol and dithiothreitol [5]. Therefore, the simultaneous quantification of these two molecules is crucial to analyze the results obtained in pharmaceutical and cosmetic fields.

Ion pair chromatography (IPC) and micellar liquid chromatography (MLC) are based on the addition of ionic surfactant to a reversed-phase chromatography system. It is applied for the separation and quantification of analytes that contain ionizable or strongly polar groups having poor retention on hydrophobic columns [6]. The main difference between these two methods is the concentration of the surfactant; the latter should be below or above the critical micelle concentration (CMC) in IPC or MLC, respectively [7].

Sodium dodecyl sulfate (SDS) is the most studied anionic surfactant with a CMC value of 8.2 mM. This surfactant was used in IPC for the quantification of the hydrolysis products of cisplatin [8], metformin [9], stachydrine, leonurine [10], desloratadine and its derivatives [11], and vildagliptin [12]. Also, SDS was used in MLC to quantify a large number of sedative and hypnotic drugs such as ethosuximide, primidone, phenobarbital and different benzodiazepine derivatives like diazepam and lorazepam [13]. It was also used to quantify risedronate [14], different alkaloids such as morphine [15], anti-diabetic drugs such as metformin and gliclazide [16], and antihypertensive drugs such as atenolol [17].

The quantification of cysteamine and cystamine in aqueous solutions (containing NaCl, benzalkonium chloride, EDTA, alpha cyclodextrin and sulfonic acid buffering agent) by MLC using SDS as a surfactant was studied by Pescina et al. (2016). The column used was C18 (250 mm × 4.6 mm, 5 µm) thermostated at 50°C. The mobile phase consisted of water: acetonitrile: methanol (38:30:32), containing 1.4 mL phosphoric acid 85%, and 11.52 g sodium dodecyl sulfate (40 mM) with a flow rate of 1.6 mL/min. Retention times were 4 and 14 min for cysteamine and cystamine, respectively. Linearity was between 50 µg/mL and 2000 µg/mL for both compounds [18]. Recently, Kim & Na (2019) studied the quantification of cysteamine and cystamine by IPC in cosmetic products such as cream using sodium 1-heptanesulfonate. They used a C18 column (250 mm × 4.6 mm, 5 µm) and a mobile phase composed of aqueous 4.0 mM sodium 1-heptanesulfonate 0.1% phosphoric acid: acetonitrile (85:15). The retention times were 6.4 and 15.9 min for cysteamine and cystamine, respectively. The analysis was done without any internal standard, and the stability of the compounds was not assessed during the analysis [19].

In this study, IPC and MLC methods using SDS as a surfactant allowing simultaneous quantification of cysteamine and cystamine in solutions were compared for their peak shapes.

Besides, different attempts were applied to stabilize and avoid oxidation of cysteamine during the analysis. A stability study of cysteamine was conducted in buffered and unbuffered solutions at different temperatures and light exposure conditions.

2. Materials and Methods

2.1. Materials

Cysteamine, cystamine dihydrochloride, DL-dithiothreitol, and metformin hydrochloride were purchased from Sigma-Aldrich (Buchs, Switzerland). Ethylenediaminetetraacetic acid (EDTA) was purchased from Sigma-Aldrich (Steinheim, Germany). SDS, sodium carbonate and bicarbonate were obtained from Sigma-Aldrich (China), phosphoric acid and trizma base were purchased from Sigma-Aldrich (USA) and hydrochloric acid was purchased from Sigma-Aldrich (Austria). All other chemicals were of analytical grade.

2.2. Methods

2.2.1. Preparation of standard solutions

Stock solutions of cysteamine or cystamine (0.5 mg/mL) were prepared in ultra-pure water and then diluted in water to obtain final concentrations ranging between 1 and 100 µg/mL (1; 2.5; 5; 7.5; 10; 25; 50; 75; 100 µg/mL). To evaluate the effect of the anti-oxidant dithiothreitol (DTT) on the stability of the cysteamine solutions during analysis, a stock solution of cysteamine (0.5 mg/mL) was prepared and diluted in DTT solution (0.8 mg/mL prepared in ultra-pure water) to obtain final concentrations ranging between 1 and 100 µg/mL. Also, a stock solution (1 mg/mL) of metformin was prepared in ultra-pure water and diluted to obtain a metformin solution of 10 µg/mL.

100 µL of the different concentrations of cysteamine prepared in water or in DTT was added to 100 µL of metformin (10 µg/mL) and 800 µL of water or DTT to obtain the calibration curve of cysteamine. To obtain the calibration curve of cystamine, 100 µL of the different concentrations of cystamine prepared in water was added to 100 µL of metformin (10 µg/mL) and 800 µL of water.

2.2.2. High-performance liquid chromatography analysis

High-performance liquid chromatography (HPLC) experiments were conducted using an Agilent 1200 series HPLC system equipped with a vacuum degasser, a binary pump, an autosampler, a thermostatted column compartment (heating up to 80°C), and a diode array detector. All data were collected and analyzed using chemStation software. An isocratic mode, consisting of acetonitrile: water containing 0.1% phosphoric acid was used for the analysis of cysteamine and cystamine where the volume ratios of 49:51 with SDS (20 mM) and 45:55 with SDS (4 mM) were used for MLC and IPC, respectively. Phosphoric acid was added to acidify the mobile phase, to improve the interaction between the positively charged amino group of cysteamine and the negatively charged sulfate group of SDS. The reverse-phase Kinetex C18 column (4.6 × 100 mm, 2.6 µm) (Phenomenex, Torrance, CA, USA) was used and the injection volume was of 20 µL. The flow rate was set at 1.0 mL/min, the column temperature was maintained at 25 °C, and the detection wavelength was 215 nm.

2.2.3. Precision and system suitability studies

The precision of the analytical method was evaluated by intra- and inter-day reproducibility assays (the intraday data were collected from 6 samples and the interday date were collected from a three day period (n=3)). The number of theoretical plates, reflecting the column performance, was also determined.

$N = 16\,(\frac{tr}{W})^2$ Where N is the number of theoretical plates, tr is the retention time and w is the peak width.

The column is divided into theoretical plates. Each plate is the distance over which the sample components achieve one equilibration between the stationary and mobile phase in the column. Therefore, the more theoretical plates available within a column, the more equilibrations are possible inducing a better quality of the separation [20]. The limit of detection (LOD) and the limit of quantification (LOQ) can be determined by different ways based on signal to noise ratios that is given by the software of the HPLC system (LOD= 3.3 S/N; LOQ=10 S/N), on the slope of the calibration curve, or on laboratory fortified blank. In this article, the LOD and the LOQ were determined using the signal to noise ratios. The peak symmetry, the signal to noise ratios to determine the LOD and the LOQ and the theoretical plate numbers data were collected from the chemstation software of the HPLC system (United States Pharmacopeia).

2.2.4. Effect of EDTA on the maintenance of cysteamine/cystamine ratio during analysis

Solutions of cysteamine (100 µg/mL) containing EDTA at different percentages (0, 0.1, 0.25, 0.5, 0.75, and 1%) were prepared and analyzed for their peak shapes after preparation by IPC method. Then, solutions containing cysteamine (100 µg/mL) and cystamine (100 µg/mL) were prepared in water in absence or in presence of 0.1% of EDTA and kept in the autosampler chamber of the HPLC system before analysis. The concentrations of cysteamine and cystamine were measured at different time intervals during 18 h. The ratios between the concentrations of remaining cysteamine and formed cystamine were determined at different times.

2.2.5. Stability study of cysteamine

2.2.5.1. pH and buffer effects

Cysteamine solutions (1 mg/ml) were prepared in water, tris-HCl buffer (0.1 M; pH 7.4) and carbonate buffer (0.1 M; pH 9.5). The solutions were vortexed for 1 min and stored at 4°C, 25°C and 37°C in the dark.

2.2.5.2. Buffer concentration effect

Cysteamine solutions (0.5 mg/ml) were prepared in tris-HCl buffer with different concentrations (0.01; 0.05; 0.1 M), and stored at 4°C in the dark.

2.2.5.3. Light effect

To evaluate the effect of light, cysteamine solutions (1 mg/mL) were prepared in water and in tris-HCl buffer and stored at 25°C in dark and light.

The concentrations of cysteamine remaining in all the solutions described above were measured after being diluted to be in the concentrations range of the calibration curve at different times during 350 h. Each experiment was done in triplicate.

3. Results

3.1. IPC and MLC analytical methods development

The use of a mobile phase composed of water with 0.1% phosphoric acid and acetonitrile prepared at different volume ratios (water (0.1% phosphoric acid):acetonitrile; 10: 90; 70: 85; 85: 15) led to the elution of cysteamine and cystamine within the column dead time (**Figure S1**).

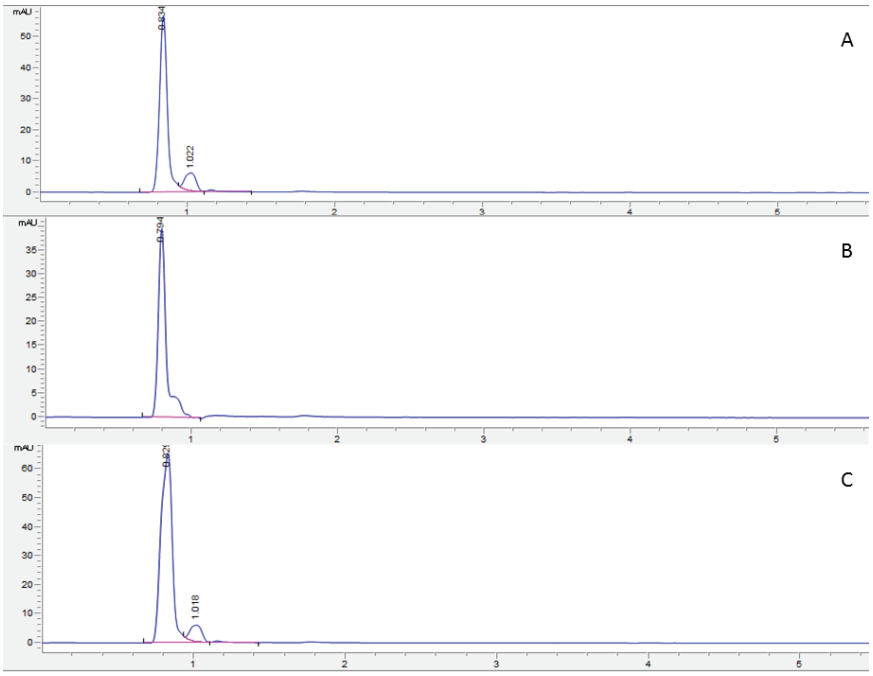

Figure S1: Chromatogram of cysteamine (100 µg/mL prepared in water) (A), cystamine (100 µg/mL prepared in water) (B) and a mixture of cysteamine (100 µg/mL) and cystamine (100 µg/mL) obtained with a mobile phase composed of acetonitrile: water with 0.1% phosphoric acid (45:55) without an ion-pairing agent.

Hence, the use of an ionic surfactant like SDS in the mobile phase of reversed phase HPLC method was mandatory for the analysis of cysteamine and cystamine. Two concentrations of SDS were chosen; for the IPC and MLC methods, the concentration was below the CMC (4 mM) or above it (20 mM), respectively. SDS allowed the separation of cysteamine and cystamine peaks in IPC and MLC **(Figure S2, Figure 1)**. Metformin was used as an internal standard after a screening of different molecules such as dopamine hydrochloride, ascorbic acid, glutamic acid, and histidine; the mentioned molecules were not retained by the column. Lysine hydrochloride was retained by the column but presented an asymmetric peaks shape.

Figure S2 shows that the retention times of cysteamine, metformin, and cystamine in MLC were 1.8, 3.8, and 7.4 min, respectively. Despite the symmetric shape of cystamine (1.29 as asymmetry factor) and metformin peaks, the peak shape of cysteamine using the MLC method was asymmetric with an asymmetry factor of 0.62. The number of theoretical plates of

cysteamine was low (2325) but high for cystamine peaks (11710). MLC has the major drawback of low chromatographic efficiency due to resistance to mass transfer when using micelles [21]. However, an improvement of the peak symmetry was obtained when using the IPC compared to the MLC **(Figure 1)**.

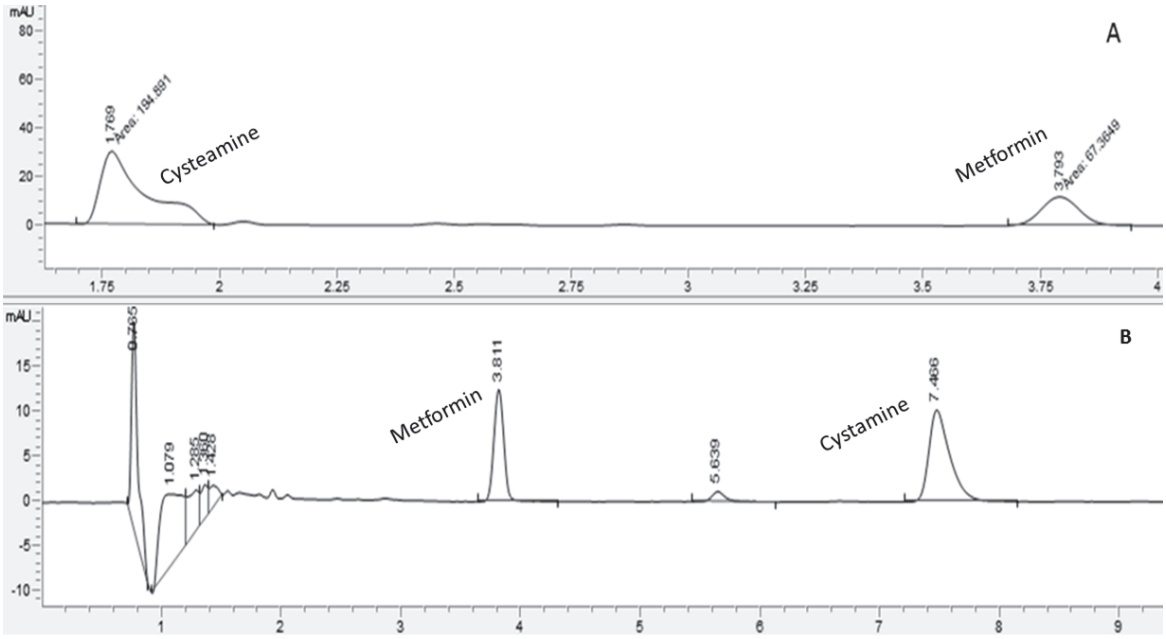

Figure S2: Chromatograms of 100 µg/mL cysteamine (tr=1.7 min) and 1 µg/mL metformin (tr=3.8 min) prepared in DTT solution (A); 1 µg/mL metformin (tr=3.8 min) and 100 µg/mL cystamine (tr= 7.4 min) prepared in water (B) using micellar chromatography.

The peaks of cysteamine, metformin, and cystamine were symmetrical using the IPC (**Figure 1)**. A peak asymmetry of 0.9 and 1 was obtained for cysteamine and cystamine, respectively. Therefore, IPC was selected in the rest of the study.

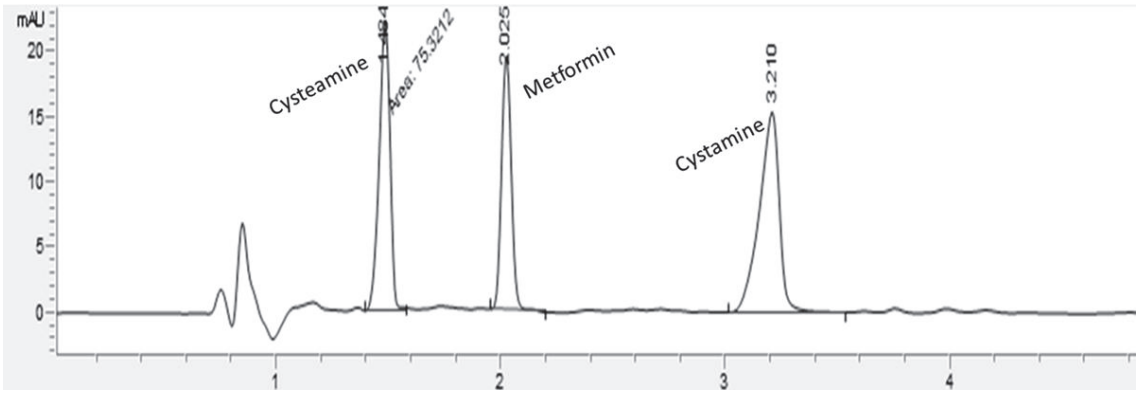

Figure 1: Chromatograms of 75 µg/mL cysteamine (tr=1.48 min), 1 µg/mL metformin (tr=2.0

min) and 10 µg/mL cystamine (tr= 3.2 min) prepared in water in the absence of EDTA using IPC.

The retention times of cysteamine, cystamine, and metformin in IPC were 1.48, 2.05, and 3.21 min, respectively (**Figure 1**). A higher area under curve (AUC) of cysteamine was obtained for the solutions prepared in DTT (0.8 mg/mL) compared to the solutions prepared in water. For example, the AUC of cysteamine in the presence of DTT was 216 while it was 148 in absence of DTT for a cysteamine concentration of 100 µg/mL. This result can be explained by the conversion of cysteamine to cystamine when cysteamine was prepared in water. Therefore, the solutions of cysteamine were prepared in DTT to obtain the calibration curve of cysteamine. The calibration curves were constructed by plotting the cysteamine or cystamine AUCs over the metformin AUC ratio against the concentrations of cysteamine or cystamine expressed in µg/ml. The correlation coefficients of linear regressions (R^2) over a concentration range of 2.5-100 µg/mL and 5-100 µg/mL for cysteamine and cystamine, respectively, were higher than 0.998. The LOD of cysteamine and cystamine were 1.16 and 1.5 µg/mL, and the LOQ were 5.39 and 13.76 µg/mL, respectively **(Table 1)**. The number of theoretical plates of cysteamine (5323) was higher in IPC than in MLC.

Table 1: Linear regression, retention time (tr) and internal standard of the IPC method developed for cysteamine and cystamine quantification in aqueous solutions.

Parameters	Cysteamine	Cystamine
Regression equation	y = 0.042x + 0.0295	y = 0.02x + 0.0377
R^2	0.9994	0.9989
tr (min)	1.48	3.21
Linearity (µg/mL)	2.5-100	5-100
LOD (µg/mL)	1.16	1.50
LOQ (µg/mL)	5.39	13.76
Internal standard	Metformin (1 µg/mL; tr=2.05 min)	

The method precision was then determined by measuring the intra- and inter-day precisions. The precision was expressed as the percentage of the relative standard deviation (% RSD). RSD % was less than 2.51% for the intra- and inter-day variations (**Table 2**).

Table 2: Inter and Intra-day precision studies for cysteamine and cystamine peaks using IPC.

Compounds	Concentrations (µg/mL)	Intra-day precision		Inter-day precision	
		Peak area	RSD (%)	Peak area	RSD (%)
Cysteamine	75	161.66	2.51	160.33	2.31
	50	108.33	1.52	110.62	1.64
	5	12.39	0.53	12.43	0.52
Cystamine	75	110.43	0.40	112.33	0.47
	50	75.10	0.17	76.66	0.23
	5	9.86	0.28	10.33	1.22

3.2. Maintenance of cysteamine/cystamine ratio during analysis

The addition of an antioxidant to cysteamine solutions led to the conversion of cystamine to cysteamine and thus altered the results. Pescina et al. (2016) showed that EDTA alone or combined with sodium phosphate plays a crucial role in preventing cysteamine oxidation [18]. The addition of EDTA (0.1 or 0.25%) to the solutions containing cysteamine, cystamine, and metformin did not affect the shape or the retention times of these three molecules (**Figure S3**). The AUC of cysteamine was higher in presence of 0.1% EDTA than in absence of EDTA. For example, for a mixture containing 10 µg/mL of cystamine and 50 µg/mL of cysteamine the AUC of cysteamine and cysteamine was 86 and 41, respectively in the presence of EDTA and 48 and 69, respectively in the absence of EDTA. While, when EDTA at 0.5 % or above was added, the peak of cysteamine was deformed.

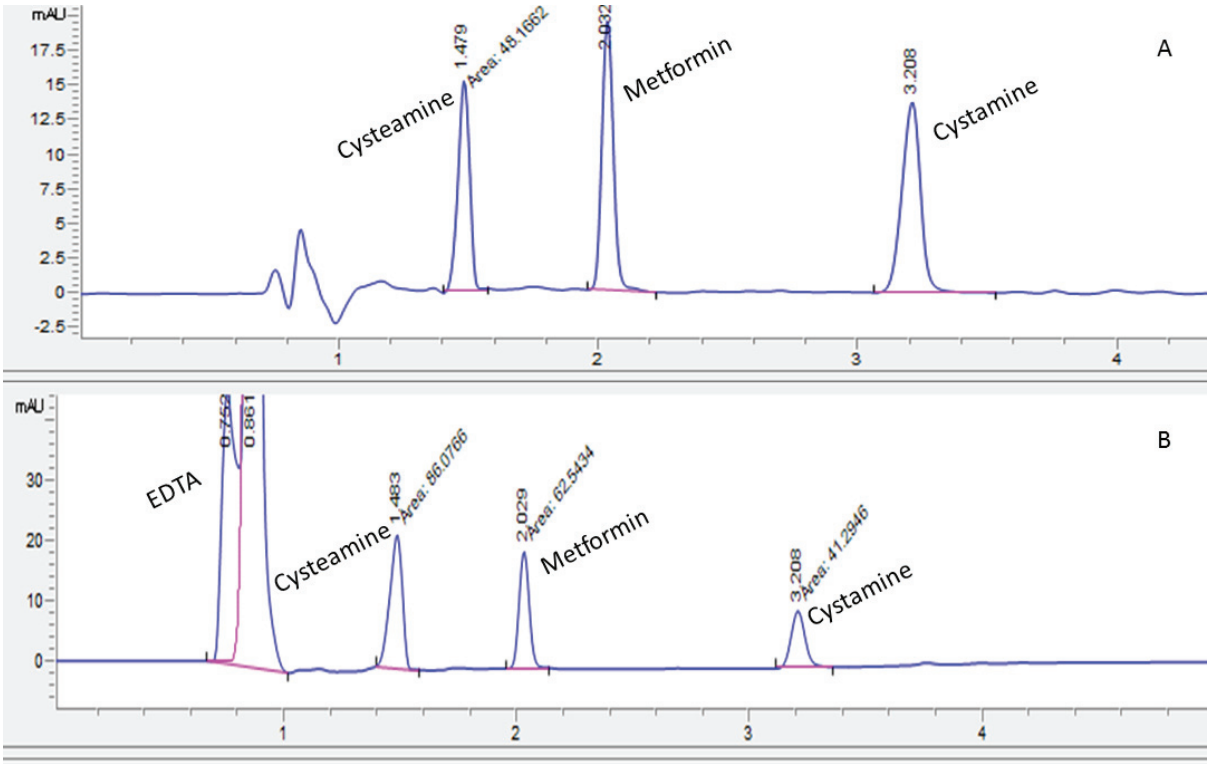

Figure S3: Chromatograms showing the cysteamine (1.48 min), metformin (2 min) and cystamine (3.2 min) peaks using ion pair chromatography for a solution containing cysteamine (50 µg/mL), cystamine (10 µg/mL) and metformin (1 µg/mL) in absence (A) or presence (B) of EDTA (0.1%).

As shown in **figure 2**, the addition of 0.1% of EDTA maintained the cysteamine to cystamine concentrations ratio for 18 h while a total conversion of cysteamine to cystamine was observed in the absence of EDTA.

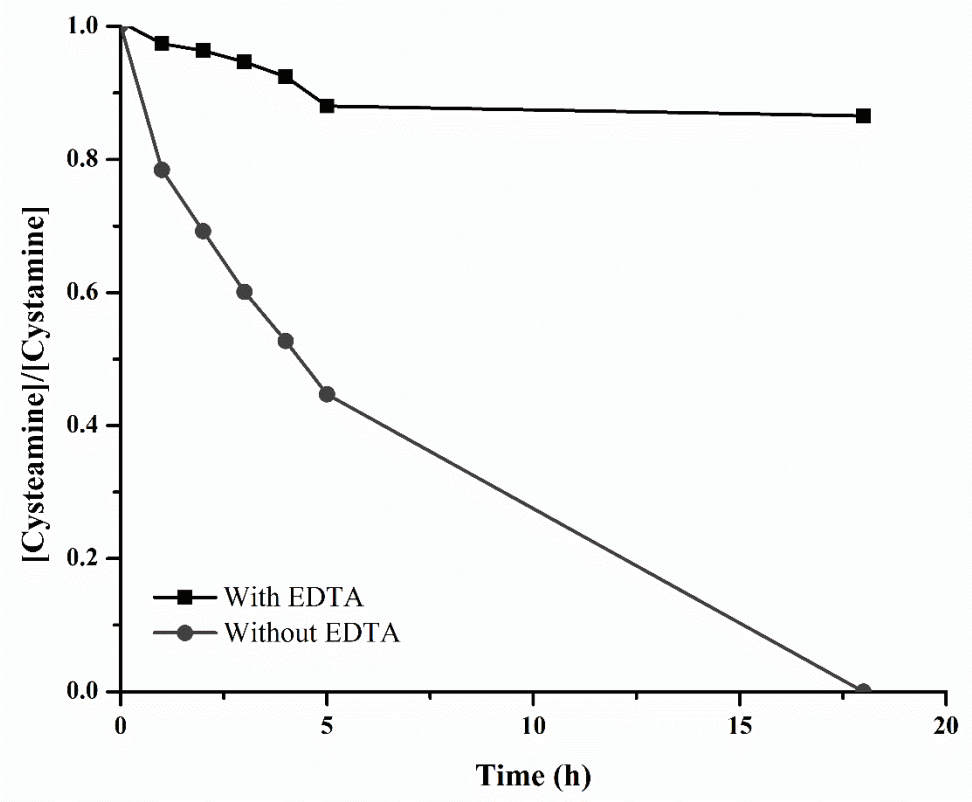

Figure 2: The variation of cysteamine to cystamine concentrations ratios during analysis in the absence and presence of EDTA (0.1%) versus time (h). The initial concentration of cysteamine and cystamine was 100 µg/mL.

3.3. Stability study of cysteamine

3.3.1. Effect of buffered solution on cysteamine stability in dark

The stability of 1 mg/mL cysteamine was evaluated in water, tris-HCl and carbonate buffers after being diluted to be included in the calibration curve of cysteamine. The prepared solutions were stored in dark. Cysteamine was noticeably more stable in water than in tris-HCl (pH 7.4). After 144 h, the total degradation of cysteamine was observed in tris-HCl buffer, while 80 % of cysteamine concentration was remained in water **(Figure 3)**. The pH of the aqueous solution of cysteamine prepared in water was 9.5. This pH was due to the zwitterionic form of cysteamine. The pH at the isoelectric point is approximately equal to the average of the two pKa of cysteamine ($pKa_{1(SH)}$= 8.19 and $pKa_{2(NH2)}$ =10.75). Consequently, at pH 9.5, the molecule has one negative and one positive electrical charge, and the net charge was zero. While

at pH 7.4, the molecule was positively charged. Cysteamine was more stable in water than in buffer solution because the zwitterionic form of cysteamine is known to be the most stable form in solid-state and in aqueous solution [22,23]. At the end of the degradation, the pH of the cysteamine solution prepared in water decreased from 9.5 to 8.5, which corresponds to the pKa of the amino group of cystamine.

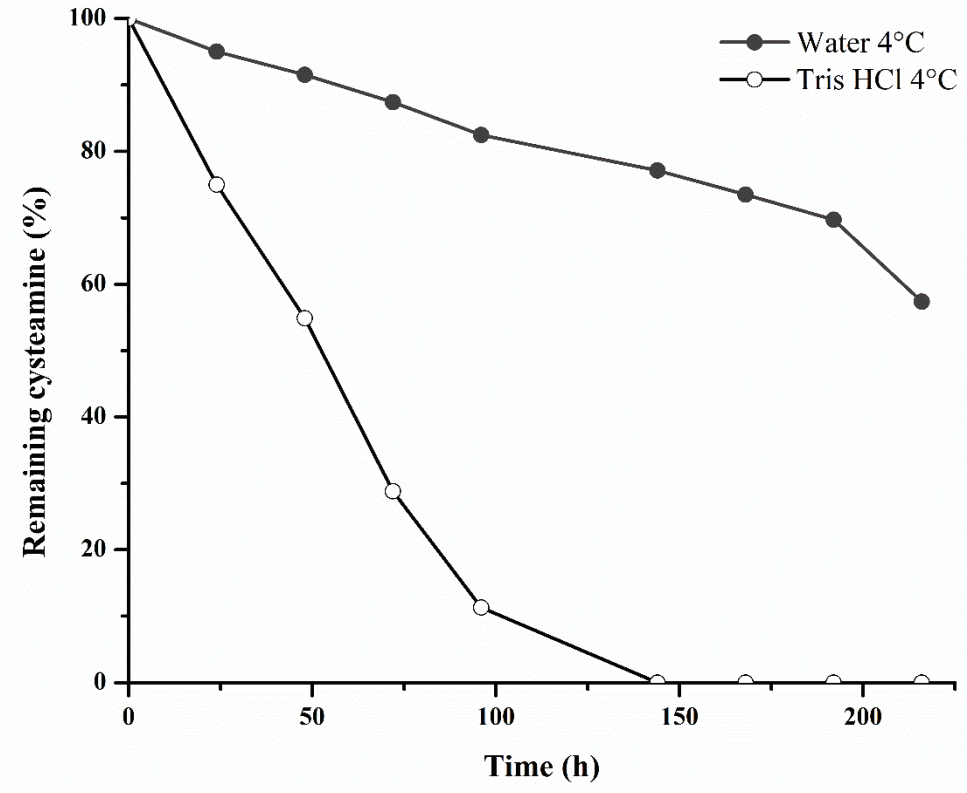

Figure 3: Remaining percentage of cysteamine (1 mg/mL) prepared in water and in tris-HCl buffer (0.1M; pH 7.4) and stored at 4°C in dark versus time (h).

To determine if the stability of cysteamine was affected by the presence of the buffer salts or by the pH variation, cysteamine was prepared in carbonate buffer (pH 9.5). The oxidation of cysteamine was faster in carbonate buffer than in water, in the dark at 4°C and in light at 25°C but it was lower than in tris-HCl buffer **(Figure 4)**. Therefore, cysteamine is more stable in water than in the studied buffered solutions.

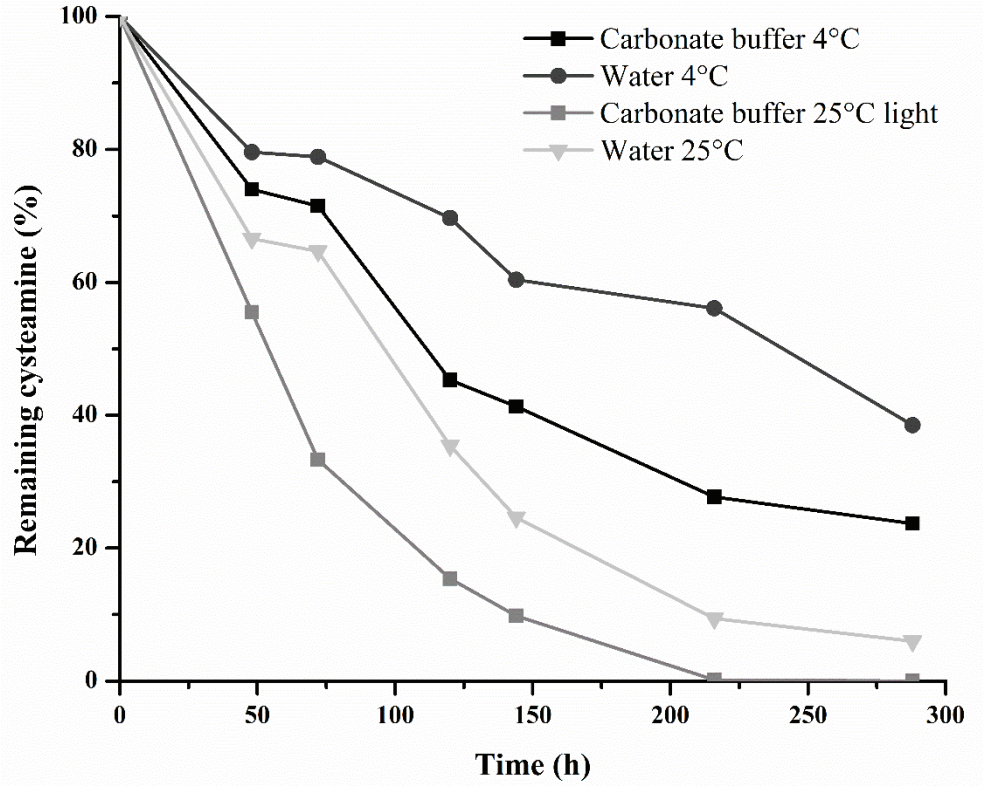

Figure 4: Remaining percentage of cysteamine (1 mg/mL) prepared in water and in carbonate buffer (0.1 M; pH 7.4) and stored at 4°C in dark and 25°C in light versus time (h).

3.3.2. Effect of buffer concentration

To evaluate the effect of the buffer concentration on the stability of cysteamine, cysteamine solutions were prepared in Tris HCl buffer of different concentrations (0.01; 0.05; 0.1M) and stored at 4°C in dark. A solution of cysteamine (0.5 mg/mL) was totally oxidized after 8 h when it was prepared in 0.1M and 0.05M Tris HCl buffer while the oxidation was delayed to 16 h when the solution of cysteamine (0.5 mg/mL) was prepared in 0.01M Tris HCl buffer. Cysteamine was more stable in the less concentrated Tris-HCl buffer solution.

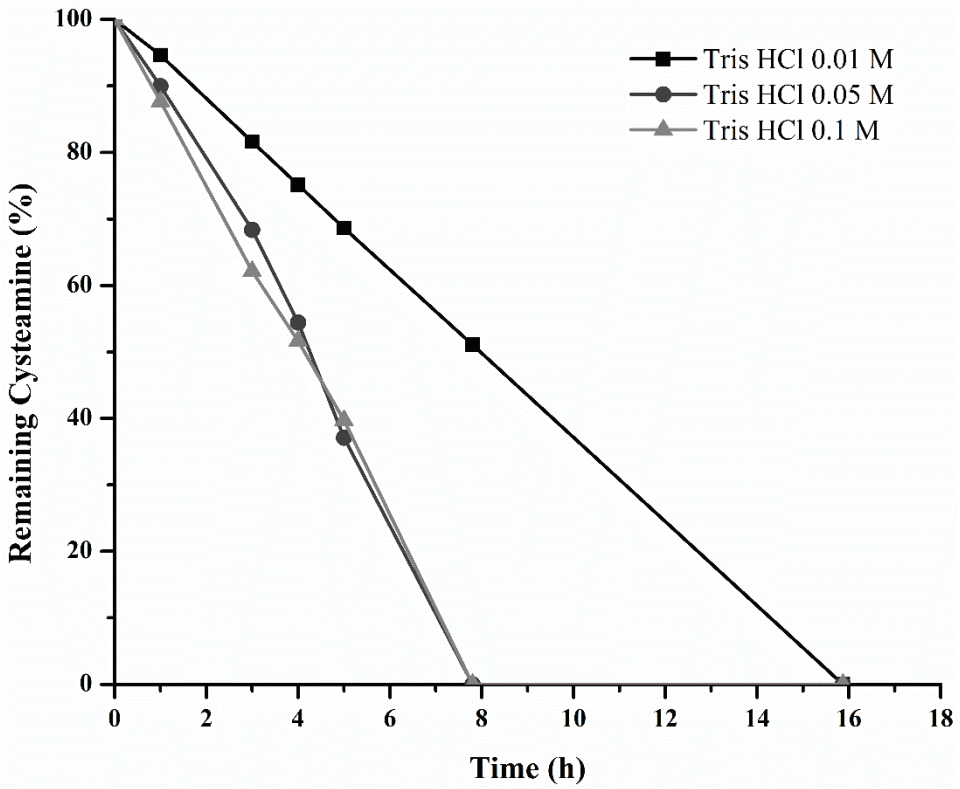

Figure 5: Remaining percentage of cysteamine (0.5 mg/mL) in tris-HCl buffer of different concentrations (0.01; 0.05 and 0.1 M) at 4°C in dark versus time (h).

3.3.3. Effect of temperature on cysteamine stability in dark

The temperature has an important influence on the stability of cysteamine. The increase of the temperature resulted in a higher degradation rate of the molecule. In water, a total degradation of cysteamine was observed after 144 h at 37°C while 80% and 40% of cysteamine concentration were remained at 4°C and 25°C, respectively. At pH 7.4, the same trend was observed. After 48 h, 55% and 45% were remained at 4°C and 25°C, respectively, while the total degradation of cysteamine was observed at 37°C (**Figure 6**).

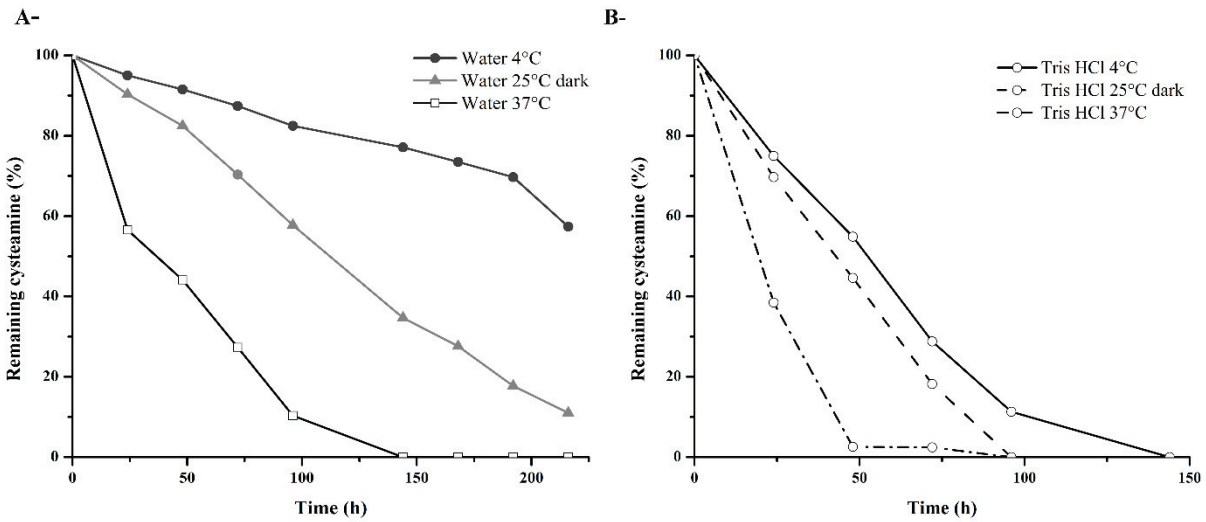

Figure 6: Temperature effect on cysteamine (1 mg/mL) stability in water (initial pH of cysteamine solution was of 9.5) (A) and in tris-HCl buffer (0.1 M; pH 7.4) (B) stored in dark.

3.3.4. Effect of light

Finally, the exposure of cysteamine to room light slightly increased its degradation. In an aqueous solution of cysteamine stored at 25°C and after 144 min, 20% of cysteamine has remained at room light conditions while 35% of cysteamine remained in the dark (**Figure 7**).

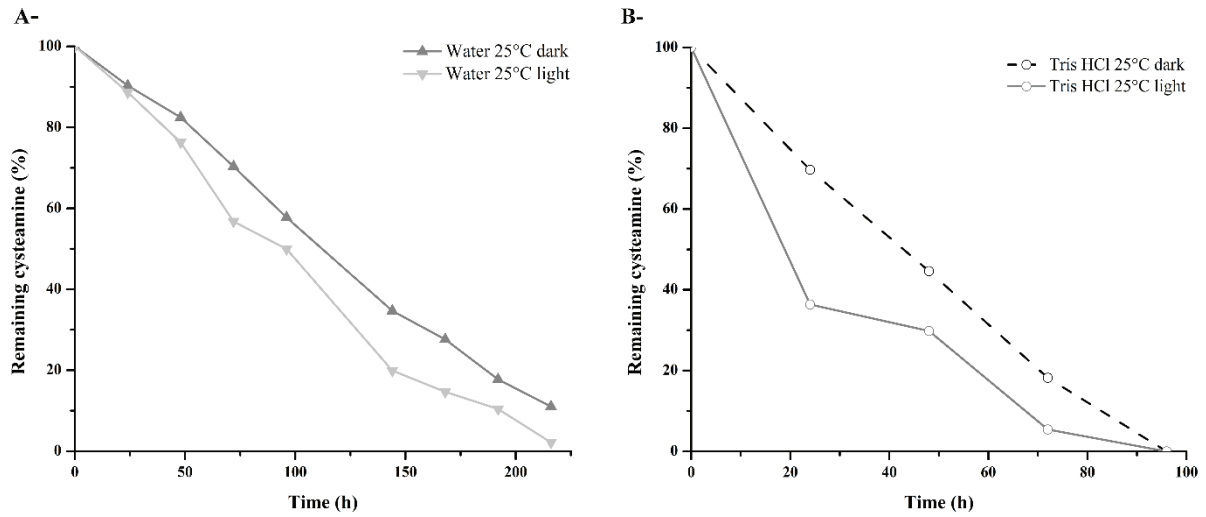

Figure 7: Effect of the room light on the stability of cysteamine (1mg/mL) in water (initial pH value of 9.5) (A) and in tris-HCl buffer (0.1 M; pH 7.4) (B).

4. Discussion

In the present study, we developed a new method for the simultaneous quantification of cysteamine and cystamine. Two chromatographic methods, IPC and MLC methods, were examined through the addition of two different concentrations of SDS to the mobile phase. IPC showed the best results regarding the symmetry of the peaks. The complete analysis of each sample took less than 5 min, and there was no need for derivatization procedures that are usually time-consuming. For example, the use of 2-chloro-1-methylquinolinium tetrafluoroborate as a derivatization agent for the detection of cysteamine by HPLC is labor-intensive since the agent should be synthesized prior to the analysis [24]. In addition, cysteamine was also detected using ion-exchange chromatography after its derivatization with monobromotrimethylammoniobimane and monobromobimane but the time required for the sample analysis was 3 to 4 h for each sample [25]. o-Phthalaldehyde in the presence of 2-mercaptoethanol and sodium hypochlorite was also used as derivatization agent to detect the presence of cystamine. However, when this method was applied for biological materials, a pretreatment with a cation exchange column was mandatory to remove interfering o-phthalaldehyde-reactive substances inducing the conversion of cysteamine to cystamine during the sampling procedure. Therefore, this method was able to quantify the mixture of cysteamine converted to cystamine and cystamine [26]. Besides, IPC is more efficient than ion-exchange chromatography because of the high efficiency of reverse-phase columns when compared with columns used in ion-exchange chromatography [27]. The MLC technique was already adopted for the simultaneous quantification of cysteamine and cystamine where the SDS was used as surfactant [18]. The aim of the mentioned study was not the development of analytical method for the quantification of these two compounds but to study the effect of pH and penetration enhancers on cysteamine stability and trans-corneal transport. Therefore, this study did not

show the chromatograms obtained for cysteamine and cystamine. The IPC technique was also used with the sodium 1-heptanesulfonate as surfactant [19]. The chromatographic results showed a good peak symmetry with a good retention time. However, the sodium 1-heptanesulfonate is more expensive and less used in the laboratory than SDS.

A stability study of cysteamine in different conditions was also assessed. Cysteamine was more stable in water where the initial pH value was of 9.5 than in tris-HCl (pH 7.4) or carbonate (pH 9.5) buffers. This difference was not explained by the pH variation of the solution since even at the same pH, cysteamine prepared in water was more stable. The stability of cysteamine was also affected by the concentration of the buffer. The degradation of many drugs can be affected by the presence of a buffer; the hydrolysis rates of these drugs is faster in buffered than in unbuffered solutions. Therefore, the influence of buffer components and buffer concentration on the degradation rates of these drugs has to be critically measured [28]. The degradation of spironolactone was faster in presence of buffer and with the increase of the buffer concentration [29] and the rate of degradation of lansoprazole, omeprazole and pantoprazole had a direct relationship with the H^+ and the salt concentrations [30]. The stability of cysteamine in different buffer solutions is studied for the first time. It is important to insure that the compounds will be stable under laboratory handling and biological assays, thus, pH and bioassay buffer are important conditions to test for stability [31]. The temperature and the exposure to light affected the stability of cysteamine as well. A study evaluated the stability of cysteamine in aqueous solutions containing NaCl, benzalkonium chloride, EDTA, NaH_2PO_4, alpha cyclodextrin and sulfonic acid buffering agent at -20, 4, and 25°C showing that the increase of the temperature affects the stability of cysteamine [18].

5. Conclusion

In this paper, a new method for the simultaneous quantification of cysteamine and cystamine was developed. IPC was better than MLC in terms of peak shapes and retention times of cysteamine and cystamine. The addition of an anionic surfactant to the mobile phase resulted in a better retention and separation of these two molecules. Furthermore, EDTA prevented the oxidation of cysteamine and maintained the cysteamine to cystamine concentrations ratio during the analysis. A stability study of cysteamine in different conditions was assessed, showing that the buffer nature and concentration, the temperature, and the light can affect the stability of cysteamine.

Acknowledgments

Authors thank the "Agence Universitaire de la Francophonie, projet PCSI" for supporting the project (2018-2020).

Bibliography

[1] M. Besouw, R. Masereeuw, L. van den Heuvel, et al., Cysteamine: an old drug with new potential, Drug Discovery Today. 18 (2013) 785–792. https://doi.org/10.1016/j.drudis.2013.02.003.

[2] C. Atallah, C. Charcosset, H. Greige-Gerges, Challenges for cysteamine stabilization, quantification, and biological effects improvement, Journal of Pharmaceutical Analysis. (2020). https://doi.org/10.1016/j.jpha.2020.03.007.

[3] P. Dixon, K. Powell, A. Chauhan, Novel approaches for improving stability of cysteamine formulations, International Journal of Pharmaceutics. 549 (2018) 466–475. https://doi.org/10.1016/j.ijpharm.2018.08.006.

[4] J.E. Biaglow, R.W. Issels, L.E. Gerweck, et al., Factors Influencing the Oxidation of Cysteamine and Other Thiols: Implications for Hyperthermic Sensitization and Radiation Protection, Radiation Research. 100 (1984) 298–312. https://doi.org/10.2307/3576351.

[5] W. Konigsberg, [13] Reduction of disulfide bonds in proteins with dithiothreitol, in: Methods in Enzymology, Academic Press, 1972: pp. 185–188. https://doi.org/10.1016/S0076-6879(72)25015-7.

[6] Şerban Moldoveanu, V. David, Essentials in modern HPLC separations, Elsevier, Waltham, MA, 2013.

[7] A.S. Kord, M.G. Khaledi, Chromatographic characteristics of surfactant-mediated separations: micellar liquid chromatography vs ion pair chromatography, Anal. Chem. 64 (1992) 1901–1907. https://doi.org/10.1021/ac00041a027.

[8] M. El-Khateeb, T.G. Appleton, B.G. Charles, et al., Development of HPLC conditions for valid determination of hydrolysis products of cisplatin, J Pharm Sci. 88 (1999) 319–326. https://doi.org/10.1021/js980287m.

[9] S. AbuRuz, J. Millership, J. McElnay, Determination of metformin in plasma using a new ion pair solid phase extraction technique and ion pair liquid chromatography, Journal of Chromatography B. 798 (2003) 203–209. https://doi.org/10.1016/j.jchromb.2003.09.043.

[10] Z. Chao, L. Ma, X. Zhou, Determination of stachydrine and leonurine in Herba Leonuri by ion- pair reversed-phase high-performance liquid chromatography, Di Yi Jun Yi Da Xue Xue Bao. 24 (2004) 1223–1226.

[11] J. Zheng, A.M. Rustum, Rapid separation of desloratadine and related compounds in solid pharmaceutical formulation using gradient ion-pair chromatography, Journal of

Pharmaceutical and Biomedical Analysis. 51 (2010) 146–152. https://doi.org/10.1016/j.jpba.2009.08.024.

[12] M. Attimarad, S.H. Nagaraja, B.E. Aldhubaib, et al., Development of a rapid reversed phase-high performance liquid chromatography method for simultaneous determination of metformin and vildagliptin in formulation and human plasma, Journal of Young Pharmacists. 6 (2014) 40–46. https://doi.org/10.5530/jyp.2014.4.7.

[13] M.R. Hadjmohammadi, A. Shariphi Aghili, Separation of Sedative – Hypnotic Drugs with Mixed Micellar Liquid Chromatography, Iranian Journal of Chemistry and Chemical Engineering (IJCCE). 24 (2005) 59–63.

[14] M. Walash, M. Metwally, M. Eid, et al., Development and Validation of a Micellar High-Performance Liquid Chromatographic Method for Determination of Risedronate in Raw Material and in a Pharmaceutical Formulation: Application to Stability Studies, J AOAC Int. 93 (2010) 1228–1235. https://doi.org/10.1093/jaoac/93.4.1228

[15] A. U. Kulikov, A. P. Boichenko, A. G. Verushkin, Optimization of micellar LC conditions for separation of opium alkaloids and their determination in pharmaceutical preparations, Analytical Methods. 3 (2011) 2749–2757. https://doi.org/10.1039/C1AY05389B.

[16] D.R. El-Wasseef, Simultaneous Determination of Metformin, Nateglinide and Gliclazide in Pharmaceutical Preparations Using Micellar Liquid Chromatography, Int J Biomed Sci. 8 (2012) 144–151.

[17] S.S.G. Yadav, J.R. Rao, Micellar liquid chromatographic analysis for simultaneous determination of atenolol and hydrochlorothiazide in tablet dosage form, Int. J. Pharm. Pharm. Sci. 5 (2013) 63-67.

[18] S. Pescina, F. Carra, C. Padula, et al., Effect of pH and penetration enhancers on cysteamine stability and trans-corneal transport, European Journal of Pharmaceutics and Biopharmaceutics. 107 (2016) 171–179. https://doi.org/10.1016/j.ejpb.2016.07.009.

[19] Y. Kim, D.H. Na, Simultaneous Determination of Cysteamine and Cystamine in Cosmetics by Ion-Pairing Reversed-Phase High-Performance Liquid Chromatography, Toxicol Res. 35 (2019) 161–165. https://doi.org/10.5487/TR.2019.35.2.161.

[20] P.M. Doran, Bioprocess Engineering Principles, Elsevier, 1995.

[21] M. Rambla-Alegre, Retention Behaviour in Micellar Liquid Chromatography, Chromatography Research International. (2012). https://doi.org/10.1155/2012/402635.

[22] H. Fleischer, Y. Dienes, B. Mathiasch, et al., Cysteamine and Its Homoleptic Complexes with Group 12 Metal Ions. Differences in the Coordination Chemistry of Zn^{II}, Cd^{II}, and Hg^{II} with a Small N,S-Donor Ligand, Inorganic Chemistry. 44 (2005) 8087–8096. https://doi.org/10.1021/ic050814m.

[23] L. Riauba, G. Niaura, O. Eicher-Lorka, et al., A Study of Cysteamine Ionization in Solution by Raman Spectroscopy and Theoretical Modeling, The Journal of Physical Chemistry A. 110 (2006) 13394–13404. https://doi.org/10.1021/jp063816g.

[24] K. Kuśmierek, R. Głowacki, E. Bald, Determination of total cysteamine in human plasma in the form of its 2-S-quinolinium derivative by high performance liquid chromatography, Analytical and Bioanalytical Chemistry. 382 (2005) 231–233. https://doi.org/10.1007/s00216-005-3166-8.

[25] R.C. Fahey, G.L. Newton, R. Dorian, et al., Analysis of biological thiols: quantitative determination of thiols at the picomole level based upon derivatization with

monobromobimanes and separation by cation-exchange chromatography, Anal. Biochem. 111 (1981) 357–365.

[26] S. Ida, Y. Tanaka, S. Ohkuma, et al., Determination of cystamine by high-performance liquid chromatography, Anal. Biochem. 136 (1984) 352–356.

[27] J. Ståhlberg, CHROMATOGRAPHY: LIQUID | Ion Pair Liquid Chromatography, in: I.D. Wilson (Ed.), Encyclopedia of Separation Science, Academic Press, Oxford, 2000: pp. 676–684. https://doi.org/10.1016/B0-12-226770-2/01591-X.

[28] T.K. Ghosh, B.R. Jasti, Theory and Practice of Contemporary Pharmaceutics, CRC Press, 2004.

[29] Y. Pramar, V.D. Gupta, Preformulation studies of spironolactone: Effect of pH, two buffer species, ionic strength, and temperature on stability, Journal of Pharmaceutical Sciences. 80 (1991) 551–553. https://doi.org/10.1002/jps.2600800611.

[30] A. Ekpe, T. Jacobsen, Effect of Various Salts on the Stability of Lansoprazole, Omeprazole, and Pantoprazole as Determined by High-Performance Liquid Chromatography, Drug Development and Industrial Pharmacy. 25 (1999) 1057–1065. https://doi.org/10.1081/DDC-100102270.

Chapitre 4 : Préparation et caractérisation des liposomes encapsulant la cystéamine sous formes liquide et poudre.

Introduction

Malgré les nombreux effets biologiques que présente la cystéamine (Besouw et al., 2013), son instabilité chimique en solution rend son application problématique. Cette instabilité chimique provient de l'oxydation rapide de la cystéamine en cystamine. L'encapsulation peut être une solution afin d'augmenter la stabilité de la cystéamine. Cette molécule a été encapsulée dans des liposomes pour augmenter son absorption intestinale (Jaskierowicz et al., 1985), son efficacité dans le traitement de la cystinose (Butler et al., 1978) et dans l'inhibition de la prolactine (Jeitner & Oliver, 1990). Cependant, dans ces études, les liposomes encapsulant la cystéamine n'ont pas été caractérisés et la stabilité de la cystéamine encapsulée n'a pas été évaluée. Dans notre étude, les liposomes encapsulant la cystéamine ont été préparés par la méthode d'injection éthanolique. Cette méthode se base sur la formation spontanée des liposomes après le contact entre la solution organique, composée de phospholipides et de cholestérol préparée dans de l'éthanol, et la solution aqueuse. Dans cette étude, deux types de phospholipides ont été utilisés : un phospholipide saturé (Phospholipon 90H) et un phospholipide insaturé (Lipoïde S100). La préparation des liposomes se fait à une température supérieure à la température de transition qui est de 55°C pour le Phospholipon 90H et -20°C pour le Lipoïde S100. Différentes concentrations en cystéamine ont été testées afin d'évaluer l'effet de ce paramètre sur la formulation. Les liposomes obtenus sont caractérisés pour leur taille, pdI et potentiel Zêta en utilisant la diffusion dynamique de la lumière (DLS) et leur morphologie a été observée par microscopie électronique à transmission (TEM). Le taux d'incorporation du lipide ainsi que celui du cholestérol ont été déterminés par la méthode de Bartlett et en utilisant le kit cholestérol CHOD-POD, respectivement. Le taux et le rendement

d'encapsulation de la cystéamine ont été déterminés par la méthode d'Ellman préalablement optimisée.

La stabilité des suspensions liposomales contenant la cystéamine a été évaluée par rapport à la stabilité de la solution aqueuse de cystéamine. Elle a été étudiée à 4°C, 25°C et 37°C en absence et présence de la lumière. L'encapsulation a amélioré la stabilité de la molécule dans toutes les conditions mentionnées.

Afin d'augmenter la stabilité des suspensions liposomales et les conserver pour une longue durée, la lyophilisation de ces dernières a été appliquée (Stark et al., 2010). La lyophilisation est constituée de trois étapes principales (Khairnar et al., 2012):

- La congélation qui consiste à transformer l'eau libre en cristaux de glace.
- Le séchage primaire, aussi appelé dessiccation primaire, où l'eau est éliminée progressivement par sublimation de la glace grâce au vide créé.
- Le séchage secondaire, aussi appelé dessiccation secondaire, où l'eau congelée et retenue sur le produit par adsorption est éliminée.

L'hydroxypropyl-β-cyclodextrine (HP-β-CD) a été ajouté comme agent protecteur afin de conserver les caractéristiques des liposomes après la phase de déshydratation/réhydratation (Gharib et al., 2018). Les liposomes blancs et les liposomes encapsulant la cystéamine constitués de PH 90H ont été lyophilisés et caractérisés en termes de taille, pdI et potentiel Zêta avant et après lyophilisation par DLS. De plus, la stabilité de stockage à 4°C des liposomes lyophilisés a été étudiée après 4 mois.

Ce chapitre est présenté sous forme d'article intitulée « Development of cysteamine loaded liposomes in liquid and dried forms for improvement of cysteamine stability » publiée en 2020 dans le journal « International Journal of Pharmaceutics».

Références

Besouw, M., Masereeuw, R., van den Heuvel, L., & Levtchenko, E. (2013). Cysteamine: An old drug with new potential. *Drug Discovery Today*, *18*(15), 785–792. https://doi.org/10.1016/j.drudis.2013.02.003

Butler, J. D., Tietze, F., Pellefigue, F., Spielberg, S. P., & Schulman, J. D. (1978). Depletion of Cystine in Cystinotic Fibroblasts by Drugs Enclosed in Liposomes. *Pediatric Research*, *12*(1), 46–51. https://doi.org/10.1203/00006450-197801000-00012

Gharib, R., Greige-Gerges, H., Fourmentin, S., & Charcosset, C. (2018). Hydroxypropyl-ß-cyclodextrin as a membrane protectant during freeze-drying of hydrogenated and non-hydrogenated liposomes and molecule-in-cyclodextrin-in- liposomes: Application to trans-anethole. *Food Chemistry*, *267*, 67–74. https://doi.org/10.1016/j.foodchem.2017.10.144

Jaskierowicz, D., Genissel, F., Roman, V., Berleur, F., & Fatome, M. (1985). Oral Administration of Liposome-entrapped Cysteamine and the Distribution Pattern in Blood, Liver and Spleen. *International Journal of Radiation Biology and Related Studies in Physics, Chemistry and Medicine*, *47*(6), 615–619. https://doi.org/10.1080/09553008514550851

Jeitner, T. M., & Oliver, J. R. (1990). Possible oncostatic action of cysteamine on the pituitary glands of oestrogen-primed hyperprolactinaemic rats. *Journal of Endocrinology*, *127*(1), 119–127. https://doi.org/10.1677/joe.0.1270119

Khairnar, S., Kini, R., Harwalkar, M., Salunkhe, K., & Chaudhari, S. (2012). A Review on Freeze Drying Process of Pharmaceuticals. *International Journal of Research in Pharmacy and Science*, *IJRPS 2013*, 76–94.

Stark, B., Pabst, G., & Prassl, R. (2010). Long-term stability of sterically stabilized liposomes by freezing and freeze-drying: Effects of cryoprotectants on structure. *European Journal of Pharmaceutical Sciences*, *41*(3), 546–555. https://doi.org/10.1016/j.ejps.2010.08.010

Development of cysteamine loaded liposomes in liquid and dried forms for improvement of cysteamine stability

Carla Atallah[a,b], Hélène Greige-Gerges[a], and Catherine Charcosset[b]

[a]*Bioactive Molecules Research Laboratory, Faculty of Sciences, Lebanese University, Lebanon*

[b]*Laboratoire d'Automatique, de Génie des Procédés et de Génie Pharmaceutique (LAGEPP), Université Claude Bernard Lyon 1, France.*

International Journal of Pharmaceutics (2020)

Development of cysteamine loaded liposomes in liquid and dried forms for improvement of cysteamine stability

Carla Atallah[a,b], Hélène Greige-Gerges[a], and Catherine Charcosset*[b]

[a]*Bioactive Molecules Research Laboratory, Faculty of Sciences, Lebanese University, Lebanon*

[b]*Laboratoire d'Automatique, de Génie des Procédés et de Génie Pharmaceutique (LAGEPP), Université Claude Bernard Lyon 1, France.*

***Corresponding Author:**
Claude Bernard Lyon 1 University
Laboratory of Automatic Control, Chemical and Pharmaceutical Engineering
308 G Bldg., CPE
43 Bd du 11 Novembre 1918
69 622 Villeurbanne Cedex, France
Tel: 04 72 43 18 34
Fax: 04 72 43 16 99
E-mail : catherine.charcosset@univ-lyon1.fr

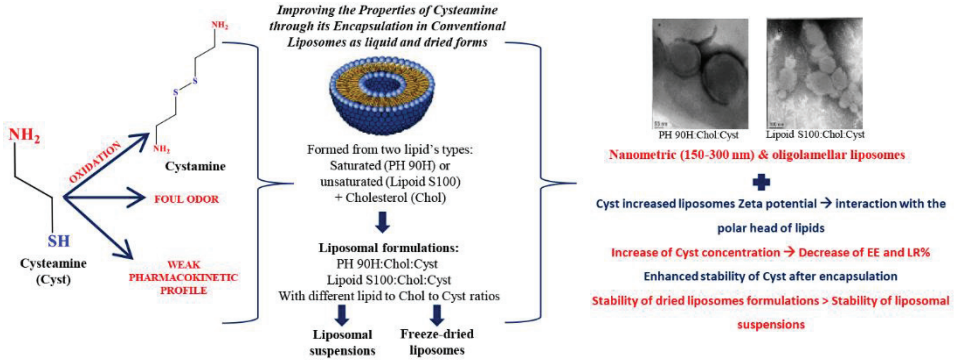

Abstract

Despite the high aqueous solubility of cysteamine, its unpleasant organoleptic properties, hygroscopicity, instability in solutions, and poor pharmacokinetic profile are the main drawbacks that limit its use for medical and cosmetic purposes. In this study, cysteamine-loaded liposomes were prepared using the ethanol injection method. Liposomes were characterized for their size, homogeneity, surface charge, and morphology. The incorporation ratios of cholesterol and phospholipids, the encapsulation efficiency and the loading ratio of cysteamine in liposomes were determined. Moreover, the stability of free and encapsulated cysteamine was assessed at different temperatures (4, 25, and 37°C) in the presence and absence of light. Cysteamine-loaded liposomes were freeze-dried and reconstituted liposomes were characterized. Finally, the storage stability of the freeze-dried cysteamine-loaded liposomes was studied. Liposomes were nanometric, oligolamellar, and spherical. The encapsulation efficiency and the loading ratio of cysteamine varied between 12 and 40% in the different formulations. The encapsulation improved the stability of cysteamine in the various storage conditions. The dried form of cysteamine-loaded liposomes conserved the size of the vesicles and retained 33% of cysteamine present in the liposomal suspension before lyophilization. The freeze-dried liposomes formulations were stable after four months of storage at 4°C.

Keywords: Cysteamine; Encapsulation; Freeze-drying; Liposomes; Stability.

1. Introduction

Cysteamine (Cyst) is an aminothiol compound synthesized by human body cells and derives from coenzyme A degradation (Besouw et al., 2013; Gallego-Villar et al., 2017). Cyst is described to have a radioprotective (Bacq et al., 1953), an anti-cancer (Apffel et al., 1975), and anti-malarial (Min-Oo et al., 2010) effects. It can be used for hyperprolactinemia treatment by reducing the size of pituitary glands and depleting plasma prolactin (Sagar et al., 1985). This molecule represents the only treatment of cystinosis disease, which is characterized by cystine accumulation in many tissues (Elmonem et al., 2016). In lysosomes, Cyst reacts with cystine to form a mixed disulfide of half-cystine and Cyst, which then leaves the cells via a lysine transporter (Bozdağ et al., 2008). It can also be used as a depigmenting agent (Chavin and Schlesinger, 1966; Farshi et al., 2018; Frenk et al., 1968; Mansouri et al., 2015). Cyst is freely soluble in water (23.5 mg/mL), has a foul odor and a bitter taste, and presents a weak pharmacokinetic profile (Lahiani-Skiba et al., 2007). Besides, Cyst is unstable in aqueous solutions due to the rapid oxidation of the sulfhydryl group, leading to the formation of cystamine. This reaction is catalyzed by metal ions such as Cu^{2+}, Fe^{3+}, and Zn^{2+} and is stimulated in alkaline pH (Atallah et al., 2020). To increase its stability and improve its biological effects, Cyst has been encapsulated in liposomes (Butler et al., 1978; Jaskierowicz et al., 1985; Jeitner and Oliver, 1990), cyclodextrins (Lahiani-Skiba et al., 2007), and emulsions (Gresham et al., 1971).

Liposomes are spherical vesicles that comprise one or more lipid bilayer structures enclosing an aqueous core. They are used to encapsulate active compounds for various applications (Laouini et al., 2012). Their biocompatibility, biodegradability, and low toxicity make them very appropriate carriers for many drugs (Zylberberg and Matosevic, 2016). Cyst has been encapsulated in liposomes to enhance its absorption through the intestinal wall (Butler et al.,

1978), its effectiveness in cystinosis (Jaskierowicz et al., 1985), and the period of prolactin depletion action (Jeitner and Oliver, 1990). To the best of our knowledge, the liposomes encapsulating Cyst were not characterized in previous studies, and the effect of encapsulation on Cyst stability was not evaluated.

The freeze-drying is a promising approach to increase the shelf life of liposomes incorporating active agents. Among several cryoprotectants (sucrose, trehalose, glucidex 6D and 19D), *Sebaaly et al.* demonstrated that hydroxypropyl beta-cyclodextrin (HP-β-CD) was the most effective cryoprotectant of liposomes during the freeze-drying of eugenol-loaded Phospholipon 90H (PH 90H) liposomes (Sebaaly et al., 2016). Besides, *Gharib et al.* proved that HP-β-CD protects hydrogenated but not unsaturated liposomes during freeze-drying (Gharib et al., 2018). In this study, blank and Cyst-loaded liposomes composed of PH 90H and Lipoid S100 were prepared by the ethanol injection method. The liposomal suspensions were characterized for their size, polydispersity index (PdI), and zeta potential by diffusion light scattering (DLS) as well as for their morphology using transmission electron microscopy (TEM). The concentrations of Cyst, phospholipid, and cholesterol (Chol) in liposomes were determined spectrophotometrically by the Ellman method with some modifications, Bartlett method and Chol quantitation kit, respectively. The encapsulation efficiency (EE%) and the loading ratio (LR %) of Cyst in liposomes were also determined. Freeze-drying of PH 90H liposomes was realized according to the optimized protocol previously described (Gharib et al., 2018), and the characteristics of the reconstituted vesicles were determined. Moreover, the stability of free and encapsulated Cyst was assessed at different temperatures (4, 25, and 37°C) and in the presence and absence of room light. Finally, the storage stability of the freeze-dried form of encapsulated Cyst was evaluated after four months of storage at 4°C.

2. Materials and methods

2.1.Materials

Cyst, monobasic phosphate, cystamine dihydrochloride, DL-dithiothreitol, and metformin hydrochloride were purchased from Sigma-Aldrich (Buchs, Switzerland). 5,5′- Dithiobis(2-nitrobenzoic acid) (DTNB), ammonium molybdate were purchased from Sigma-Aldrich (St Louis, Missouri, USA). Ethylenediaminetetraacetic acid (EDTA), dibasic phosphate, sulfuric acid, and hydrogen peroxide were purchased from Sigma-Aldrich (Steinheim, Germany). PH 90 H (90% soybean PC, 4% lysoPC, 2% triglycerides, 2% water, and 0.5% ethanol) and Lipoid S100 (94% soybean PC, 3% lysoPC, 0.5% N-acyl-PE, 0.1% PE, 0.1% phosphatidylinositol, 2% water, 0.2% ethanol) were obtained from Lipoid GmbH (Ludwigshafen, Germany). Chol was obtained from the Fisher chemical (Loughborough, UK), and sodium bisulfite was purchased from Combi Blocks (San Diego, California, USA). 4-Amino-3-hydroxy-1-naphthalene sulfonic acid was purchased from Sigma-Aldrich (Bangalore, India). Chol quantitation kit was purchased from SPINREACT (Barcelona, Spain). HP-β-CD-oral grade (MS=0.85) was purchased from Roquette (Lestrem, France). Sodium dodecyl phosphate and phosphoric acid were obtained from Sigma-Aldrich (China). All other chemicals were of analytical grade.

2.2.Cyst quantification

The quantification of Cyst was done using two methods. For the quantification of Cyst in liposomal suspension, a modified Ellman method was used. First, a stock solution of Cyst was prepared in water (1 mg/mL) and then diluted to obtain final concentrations of Cyst ranging between 2.5 and 100 µg/mL. Ellman's reagent was prepared by dissolving 4 mg DTNB in 1 mL of reaction buffer (pH 8.0). The latter is composed of 0.1 M sodium phosphate and 1 mM EDTA. 250 µL of water (blank) or Cyst solution was added to 1.25 mL reaction buffer, 1.25

mL of methanol, and 50 µL Ellman's reagent solution. This reaction mixture was then vortexed and incubated at room temperature for 15 min. The absorbance was measured at 412 nm using the Spectrophotometer UV5 Mettler Toledo (Columbus Ohio, USA). The calibration curve was constructed by plotting the absorbance against the concentration of Cyst ranging from 2.5 to 100 µg/mL.

For the stability studies, the simultaneous quantification of Cyst and its degradation product cystamine was needed. An ion-pair chromatography with an isocratic mode consisting of acetonitrile: water containing 0.1% phosphoric acid and SDS (4 mM) (v/v, 45:55) was used. 20 µL of the samples were injected into a reverse-phase Kinetex C18 column (4.6 × 100 mm, 2.6 µm). The flow rate was set at 1.0 mL/min, the column temperature was maintained at 25°C, and the detection wavelength was 215 nm. Metformin was used as an internal standard with a concentration of 1 µg/mL. Linearity was between 2.5 and 100 µg/mL for Cyst and between 5 and 100 µg/mL for cystamine.

2.3.Preparation of liposomes

Liposomes were prepared by the ethanol injection method, as described by Sebaaly et al. (2016). Saturated (PH 90H) or unsaturated lipids (Lipoid S100) (10 mg/mL) and Chol (5 mg/mL) were dissolved in absolute ethanol to obtain the organic phase (10 mL). Then, the organic phase was injected into the aqueous phase (20 mL) containing different concentrations of Cyst (0; 0.5; 0.75; 1; 2.5; 5 mg/mL), using a syringe pump (Fortuna optima, GmbH-Germany), at a temperature above the transition temperature of the phospholipid (55°C for PH 90H and -20°C for Lipoid S100) and under magnetic stirring at 400 rpm. The phospholipid:Chol:Cyst molar ratios ranged between 1:0.98:1 and 1:0.98:10; for PH 90H and between 1:1.17:1.17 and 1:1.17:11.7 for Lipoid S100. The contact between the organic solution

and the aqueous phase leads to a spontaneous liposome formation. The liposomal suspensions were then left for 15 min at 25 °C under stirring (400 rpm). The ethanol was removed by rotary evaporation (Heidolph GmbH, Germany) under reduced pressure at 40 °C and the obtained liposomal solutions were stored at 4 °C for further characterization. Each preparation was performed in triplicate.

2.4.Characterization of the liposomal suspensions

2.4.1. Determination of size, pdI and zeta potential by dynamic light scattering

Malvern Zetasizer Nanoseries (Zetasizer Nano ZS; Malvern Instruments Ltd, France) was used to determine the intensity average of the vesicles mean size. All batches were diluted with ultrapure water. The particle-size distribution data were collected using the DTS (nano) software (version 5.10) provided with the instrument. The polydispersity index, which indicates the particle size distribution, ranges from 0 (monodispersed) to 1 (very broad distribution). Zeta potential was calculated using Smoluchowski's equation from the electrophoretic mobility of liposomes. All measurements were carried out at 25°C after 2 min of equilibration and were performed in triplicate. Data were expressed as the mean values ± SD.

2.4.2. Morphological characterization by transmission electron microscopy

The morphology of the liposomal suspensions was imaged by transmission electron microscope (TEM) (CM 120; Philips, Eindhoven, Netherlands) operating at an accelerating voltage of 120 kV. A drop of a solution of the liposomal suspension with or without dilution was placed onto a carbon-coated copper grid for 2 min, and the remaining liquid was removed using a filter paper. The grid was placed on negative staining using a 1% sodium silico-tungstate solution during 30 s. The excess amount of sodium silicotungstate solution was removed using a filter paper, and dried samples were observed.

2.4.3. Determination of phospholipid:Chol:Cyst molar ratios in the final liposome structures

The concentrations of incorporated compounds (phospholipids, Chol, and Cyst) in lipid vesicles were obtained by subtracting the concentrations of free compounds from their total concentrations determined in the suspensions. The suspensions underwent centrifugation at 21382xg during 1 h at 4°C using Vivaspin 500 centrifugal concentrator (Sartorius Stedim Biotech, Germany, MWCO = 10 kDa). The filtrates contained the free compounds.

2.4.4. Phospholipid quantification assay

Bartlett's method was used to determine free and total concentrations of phospholipids in the various liposomal suspensions. This method is based on several steps; first, the digestion of the organic phosphate (0.5 mL from total liposomal suspensions, filtrates, and standard solutions of phosphorus) using diluted sulfuric acid (5 mM) at 200°C for 1h. Then, the oxidation to the inorganic phosphates was done in the presence of 10% hydrogen peroxide (0.1 mL) for 30 min at 200°C. A phosphomolybdic complex was formed after the addition of ammonium molybdate (4.6 mL) and the reduction of this complex by the 4-amino-3-hydroxyl-1-naphthalene sulfonic acid (0.2 mL) at 100°C for 15 min. A blue solution appeared and was measurable at 815 nm spectrophotometrically.

The incorporation ratio (IR) of phospholipids was calculated as follows:

$$\text{IR } \% = \frac{\text{Incorporated mass of phospholipids}}{\text{Initial added mass of phospholipids}} \times 100 \quad \text{Eq. (1)}$$

where the incorporated mass of phospholipids stands for the phospholipid mass determined in the liposome structure; the initial mass of phospholipids represents the mass initially used to prepare liposomes.

2.4.5. Chol quantification assay

The quantification of Chol (free form or total amount present in the suspension) was performed after its enzymatic hydrolysis and oxidation using the Chol CHOD-POD kit (SPINREACT, Spain). Chol in the samples was oxidized by Chol oxidase into 4-cholestenona and hydrogen peroxide. The latter reacts with 4-aminophenazone in the presence of peroxidase to form the colorimetric indicator quinonimine, having an absorbance proportional to Chol concentration in the sample. Standard solutions (0 to 2 mg/mL) were prepared from Chol stock solution (2 mg/mL); the latter was prepared in 10% Triton X-100. Samples from the liposome suspensions were diluted in 10% Triton X-100 and sonicated for 20 min at room temperature to ensure the dissolution of vesicles and the release of incorporated Chol. 1 mL of the working reagent containing buffer and enzyme was then added to 10 µL of each sample (liposome suspension, filtrate, and Chol standard solution) and incubated for 10 min at room temperature. The absorbance was monitored at a wavelength of 505 nm.

The incorporation ratio (IR) of Chol was calculated as follows:

$$\text{IR } \% = \frac{\text{Incorporated mass of Chol}}{\text{Initial added mass of Chol}} \times 100 \quad \text{Eq. (2)}$$

Where the incorporated mass of Chol stands for the Chol mass determined in the liposome structure, the initial mass of Chol represents the mass initially used to prepare liposomes.

2.4.6. Encapsulation efficiency and loading ratio of Cyst

The EE and LR% of Cyst in liposomes were determined using the optimized Ellman method. 250 µL of the Cyst standard solution, the filtrate containing free Cyst, or the diluted solution of the liposomal suspension were added to 1.25 mL phosphate buffer, 1.25 mL of methanol, and 50 µL of Ellman's reagent. This method allows the determination of the free ($[Cyst]_{free}$) and the total ($[Cyst]_{tot}$) Cyst concentrations. EE% was calculated as the following equation:

$$EE_{cyst}\% = \frac{[Cyst]_{tot} - [Cyst]_{free}}{[Cyst]_{tot}} \times 100 \quad \text{Eq. (3)}$$

where $[Cyst]_{tot}$ and $[Cyst]_{free}$ correspond to the concentration of total and free Cyst in the liposomal suspension, respectively.

LR% of Cyst was calculated as follows:

$$LR\% = \frac{m_{total} - m_{free}}{m_{initial}} \times 100 \quad \text{Eq. (4)}$$

where m_{total} and m_{free} are the mass of total and free Cyst in the liposomal suspension and $m_{initial}$ is the mass of Cyst initially added to the aqueous phase during the preparation of the liposomes.

2.5.Stability study

The formulation PH 90H: Chol: Cyst (1:0.98:10) was selected to compare the stability of Cyst loaded in liposome to that of free Cyst. The liposomal suspension (5 mL) was centrifuged, the supernatant was eliminated, and the pellet was re-suspended in water. The concentration of the encapsulated Cyst was determined after the destruction of liposomes by sonication; Cyst solutions with a similar concentration were prepared in water and placed at 4, 25, and 37°C in the dark. Also, the same concentration of free Cyst was placed in light at 25°C. At different times, aliquots were removed, and the concentration of Cyst remaining in solution and that of formed cystamine were determined by ion-pair chromatography.

The percentage of remaining Cyst was calculated as follows:

$$\text{Remaining Cyst (\%)} = \frac{[Cyst]_t}{[Cyst]_{t0}} \times 100 \quad \text{Eq. (5)}$$

where $[Cyst]_t$ is the concentration of remaining Cyst determined at time t and $[Cyst]_{t0}$ is the initial Cyst concentration.

The percentage of formed cystamine was calculated as follows:

$$\text{Formed cystamine (\%)} = \frac{[\text{Cystamine}]_t}{[\text{Cystamine}]_f} \times 100 \quad \text{Eq. (6)}$$

where $[\text{Cystamine}]_t$ is the concentration of formed cystamine determined at time t and $[\text{Cystamine}]_f$ is the final cystamine concentration obtained after the total conversion of Cyst to cystamine.

2.6.Freeze-drying of liposomes

The freeze-drying of blank and Cyst loaded liposomes composed of PH 90H and Chol was performed according to *Gharib et al.* (Gharib et al., 2018). Blank liposomes and Cyst loaded liposomes (PH 90H: Chol: Cyst molar ratios of 1:0.98:1 and 1:0.98:10) were freshly prepared; 5 mL were then ultracentrifuged at 170000 g for 1 h at 4°C. The supernatant was removed, and the pellet was reconstituted in an aqueous solution of 50 mM HP-β-CD (2 mL). The samples were kept at -20°C overnight then placed into the drying chamber of Cryonext 23020 freeze-dryer (Trappes, France), pre-cooled to -20°C, then lowered to -40°C with a slow cooling profile of 0.5°C/min. The product was stabilized for 30 min at -38°C before the vacuum was applied. Primary drying was executed at a pressure of 150 µbar for 3 h at -10°C, then the temperature of the drying chamber was progressively increased to 5°C for 6 h at 250 µbar, to reach finally 10°C at 350 µbar for 9 h. The temperature was adjusted at a product temperature higher than that of the sublimation temperature of the water. During primary drying, the ice crystals are sublimated, resulting in the porous cake of the freeze-concentrated matrix. A secondary drying step for 10 h at 20°C and 100 µbar pressure was applied. This step is crucial to decrease the residual water content of the amorphous matrix. Finally, the vials were removed from the freeze-dryer, closed with rubber caps, and stored at 4°C. The lyophilized liposomes were then reconstructed with ultra-pure water to its original volume (5 mL) before characterization and further analysis.

2.7.Storage stability of freeze-dried forms

After four months of storage at 4°C, freeze-dried liposomes were resuspended in 5 mL water; the particle size, PdI, and zeta potential values of the obtained suspensions were determined. The remaining Cyst concentrations were measured using ion-pair chromatography. The following equation was used to determine the percentage of remaining Cyst:

$$\text{Percentage of remaining Cyst} = \frac{[\text{Cyst}]_t}{[\text{Cyst}]_{t0}} \times 100 \quad \text{Eq. (7)}$$

where $[Cyst]_t$ and $[Cyst]_{t0}$ are the total concentrations of Cyst in the liposomal suspension before and after storage of dried liposomes at 4°C for 4 months. The experiment was carried out in triplicate.

3. Results and Discussion

3.1.Liposomes characterization

3.1.1. Size, polydispersity index, and zeta potential

The characterization of liposomes composed of saturated (PH 90H) and unsaturated (Lipoid S100) phospholipids and Chol was realized by DLS. The mean particle size, polydispersity index (PdI), and zeta potential values were determined (**Table 1**).

Table 1: Size, pdI, and zeta potential of blank and Cyst loaded PH 90H and Lipoid S100 liposomes.

Formulation	Lipid:Chol: Cyst molar ratio	Size				Zeta potential (mV)	PdI
		Population 1		Population 2			
		%	Mean size (nm)	%	Mean size (µm)		
Blank liposomes (PH 90H:Chol)	1:0.98	99 ± 0.4	211 ± 8	0.9 ± 0.4	5 ± 0.1	-17.9 ± 4.0	0.2 ± 0.0
Cyst-loaded liposomes (PH 90H:Chol:Cyst)	1:0.98:1	98 ± 1.3	301 ± 56	2 ± 1.3	5 ± 0.3	-35.8 ± 0.8	0.2 ± 0.0
	1:0.98:1.5	98 ± 1.1	318 ± 47	2 ± 1.1	5 ± 0.3	-37.1 ± 0.7	0.2 ± 0.1
	1:0.98:2	98 ± 1.7	248 ± 86	2 ± 1.7	5 ± 3.0	-37.0 ± 1.2	0.2 ± 0.1
	1:0.98:5	97 ± 2.7	278 ± 55	3 ± 2.7	5 ± 2.9	-45.0 ± 2.8	0.2 ± 0.1
	1:0.98:10	95 ± 0.7	262 ± 33	5 ± 0.7	5 ± 0.1	-45.0 ± 1.0	0.2 ± 0.1
Blank liposomes (Lipoid S100:Chol)	1:1.17	98 ± 0.7	151 ± 11	2 ± 0.0	5 ± 0.0	-24.0 ± 0.1	0.2 ± 0.0
Cyst loaded liposomes (Lipoid S100:Chol:Cyst)	1:1.17:1.17	94 ± 2.0	156 ± 13	6 ± 2.0	5 ± 0.2	-32.0 ± 0.41	0.3 ± 0.0
	1:1.17:1.77	97 ± 1.0	150 ± 3	3 ± 1.0	5 ± 0.3	-34.0 ± 3.70	0.3 ± 0.0
	1:1.17:2.36	97 ± 1.0	149 ± 1	3 ± 1.0	5 ± 1.0	-34.3 ± 1.45	0.3 ± 0.0
	1:1.17:5.89	97 ± 1.0	152 ± 11	3 ± 1.0	5 ± 0.2	-42.5 ± 1.17	0.3 ± 0.1
	1:1.17:11.78	97 ± 1.6	160 ± 8	3 ± 1.8	4 ± 0.2	-39.2 ± 1.30	0.2 ± 0.0

Two populations were observed in blank and Cyst-loaded liposomes. The first population was nanometric and represented more than 94% of the suspensions. The second population was of a micrometric size and represented a negligible percentage varying between 1 and 6%.

The size of blank PH 90H liposomes was 211 ± 8 nm, while that of blank Lipoid S100 liposomes was lower (151 ± 11 nm). Similar results were obtained by *Gharib et al.* (Gharib et al., 2017).

The PdI values were close to 0.2 for all the formulations, signifying that the liposomes had homogeneous size. The zeta potential indicates the vesicle's surface charge; this parameter reflected the liposome stability since it shows repulsive forces between particles (Domingues et al., 2008). All liposomal formulations had a negative charge due to the presence of the phosphate group at the surface of the vesicles (Ascenso et al., 2013). Liposomes incorporating Cyst presented zeta potential values lower than blank ones. A variation of the pH between the supernatants of blank liposomal formulation (pH 7) and Cyst loaded liposomes (pH 9.5) was noticed. Also, the positively charged amino group of Cyst can interact with the negative charges of phosphate groups of lipid membranes. The decrease of zeta potential values could be due to the negative sulfur group of Cyst attached to the surface. Indeed, after the incubation of Cyst with the blank liposomes, the centrifugation of the mixture, and the reconstitution of the pellet with water, the vesicles presented lower zeta potential values than blank liposomes indicating that electrostatic interaction between Cyst and liposomes surface may occur.

Berleur et al. studied the interaction of Cyst with dipalmitoylphosphatidylcholine (DPPC) using differential scanning calorimetry, electron spin resonance, and turbidimetry. They demonstrated that Cyst interacts with the DPPC membranes in their polar head region. At a low concentration (10^{-4} M), Cyst behaved like a divalent cation (amine and SH groups), creating electrostatic bridges with the negatively charged phosphate groups of the polar heads of lipids leading to an increase in membrane stability. These bridges are disrupted when Cyst is present at high concentration (10^{-2} and 10^{-1} M) inducing a decrease in the lipid membrane rigidity; Cyst acted like a monovalent cation and displacement of the slightly charged SH extremity by the amine of Cyst is occurred (Berleur et al., 1985).

3.1.2. Incorporation ratios of phospholipid and Chol, encapsulation efficiency and loading ratio of Cyst

The quantification of phospholipids showed a high incorporation ratio of phospholipids in all the formulations since the IR values were above 94 ± 1.41% (**Table 2**). Our results are in accordance with those of *Sebaaly et al.* for blank PH 90 liposomes (Sebaaly et al., 2016). Cyst did not affect the incorporation ratio of phospholipids since it is a hydrophilic molecule, and therefore, it is expected to be encapsulated in the aqueous core of the liposomes. Concerning Chol incorporation, the IR of Chol was higher for Lipoid S100 blank liposome (95 ± 2.0%) than for PH 90H blank liposome (80 ± 0.0%). Similar results were reported by *Azzi et al.*, where the IR values of Chol were higher for Lipoid S100 (85.2 ± 2.4%) when compared to PH 90H liposomes (84.2 ± 3.8%) (Azzi et al., 2018). Regarding Chol incorporation into Cyst-loaded liposomes, the IR% values were slightly decreased for Cyst-loaded PH 90H liposomes compared to blank liposomes. While for Lipoid S100-liposomes, a noticeable decrease of the IR of Chol was observed at high Cyst to lipid molar ratios (phospholipid:Chol:Cyst of 1:1.17:5.89 and 1:1.17:11.78). The mechanism underlying this decrease is unclear.

Table 2: Incorporation ratios of phospholipids (%) and Chol (%), EE%, and LR% values of Cyst in liposomes suspensions.

Formulations	Lipid:Chol:Cyst molar ratios	IR % of phospholipid	IR % of Chol	EE%	LR%	Final liposome composition (Lipid:Chol:Cyst molar ratio)
Blank liposomes (PH 90H:Chol)	1:0.98	94 ± 1.4	80 ± 0.0			0.94:0.81
Cyst-loaded liposomes (PH 90H:Chol:Cyst)	1:0.98:1	97 ± 0.8	74 ± 0.5	29 ± 3.0	24 ± 2	0.97:0.72:0.24
	1:0.98:1.5	100 ± 0.0	74 ± 1.5	26 ± 6.0	22 ± 6	1:0.72:0.33
	1:0.98:2	98 ± 0.5	72 ± 3.7	23 ± 4.0	20 ± 4	0.98:0.70:0.40
	1:0.98:5	94 ± 3.6	72 ± 2.0	24 ± 2.0	18 ± 3	0.94:0.70:0.90
	1:0.98:10	94 ± 2.5	74 ± 2.5	21 ± 5.0	16 ± 4	0.94:0.73:0.16
Blank liposomes (Lipoid S100:Chol)	1:1.17	99 ± 1.0	95 ± 2.0			0.99:1.11
Cyst loaded liposomes (Lipoid S100:Chol:Cyst)	1:1.17:1.17	100 ± 1.0	99 ± 2.0	40 ± 4.0	30 ± 2	0.99:1.16:0.35
	1:1.17:1.77	100 ± 2.0	91 ± 3.8	29 ± 4.0	24 ± 4	1:1.06:0.42
	1:1.17:2.36	99 ± 0.7	97 ± 5.0	22 ± 0.4	20 ± 1	0.99:1.13:0.47
	1:1.17:5.89	99 ± 1.0	35 ± 2.7	13 ± 2.0	12 ± 2	0.94:0.34:0.71
	1:1.17:11.78	99 ± 1.3	12 ± 0.0	13 ± 2.0	12 ± 2	0.94:0.12:1.41

On the other hand, EE and LR% of Cyst decreased while increasing the concentration of Cyst in both types of liposomes. The higher EE and LR% values were obtained for the liposomal suspensions containing the lowest concentration of Cyst **(Table 2)**. At this same Cyst concentration, the EE and the LR% of Cyst were higher for unsaturated liposomes when compared to saturated ones. The preparation of PH 90H liposomes required heating above the main transition temperature of the phospholipid (55°C), which could accelerate the oxidation of the product. The EE% values of Cyst were generally lower (less than 40%) than those determined for hydrophobic bioactive molecules (Azzi et al., 2018; Sebaaly et al., 2015) using the same liposome formulations. A low encapsulation efficiency usually results when encapsulating a hydrophilic drug (Eloy et al., 2014) because of its diffusion in and out of the lipid membrane. Thus, the drug is difficultly retained inside the liposomes (Çağdaş et al., 2014). The EE% values of caffeine were 7, 18, and 30% in Lipoid S100, Phospholipon 90G

(phosphatidylcholine 95%) liposomes (Tuncay Tanriverdi, 2018), and egg or soy lecithin (Budai, 2013). Also, the EE% value of ciprofloxacin was 9% in liposomes composed of 1,2-distearoyl-sn-glycero-3-phosphoglycerol-distearoylphosphatidylcholine-Chol (5:5:5 molar ratio) (Oh et al., 1995); that of mitomycin C was 31% in Phospholipon 80:Chol (9:6 molar ratio) (Chetoni et al., 2007) and the EE% value of ascorbic acid was 40% in phosphatidylcholine liposomes (Serrano et al., 2015).

Liposomes are known to increase the bioavailability of drugs by protecting them in the gastrointestinal tract, increasing cellular contact and residence time in the blood circulation. They protect the drug from the first pass metabolism, decrease drug efflux and increase the diffusion across the mucosal and epithelial layers (Daeihamed et al., 2017). Compared to free drugs, the encapsulation of apigenin in PH 90H (mean particle size of 107 nm) increased its oral bioavailability in rats by 1.5 fold (Telange et al., 2017); also the freeze-dried Eudragit-coated liposomes (mean particle size of 204 nm) increased the bioavailability of docetaxel by 3-fold (Kim et al., 2018). Compared to carboxymethyl cellulose suspension containing baicalin, the encapsulation of baicalin in PH 90H liposomes (373 nm) increased its bioavailability threefold; the baicalin concentrations were significantly increased in the liver (5.59-fold), kidney (2.33-fold), and lung (1.25-fold) in the case of baicalin-liposome (Wei et al., 2014). In addition, the encapsulation protects Cyst from digestive degradation (Jaskierowicz et al., 1985).

3.1.3. Liposomes morphology

TEM images of blank liposomes and Cyst-loaded liposomes are shown in **Fig. 1**. These images correlated with the DLS results and showed the formation of nanometer-sized vesicles. Oligolamellar spherical-shaped vesicles were obtained for blank and Cyst-loaded liposomes.

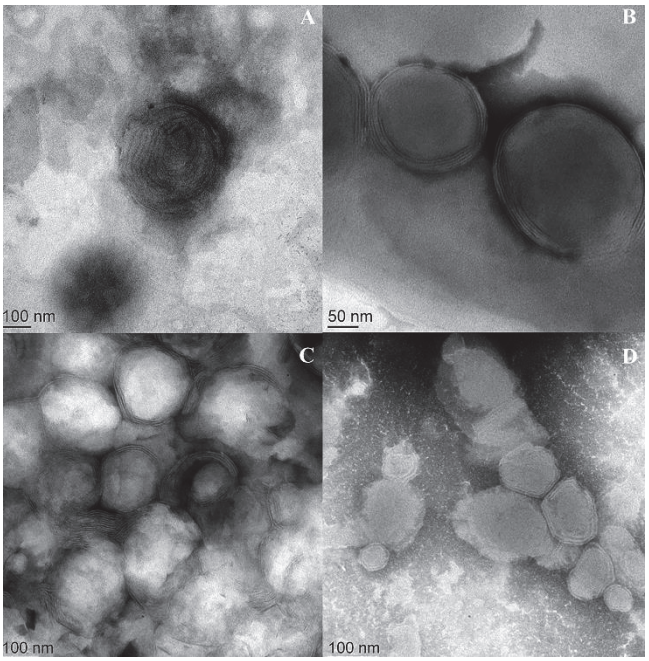

Figure 1: TEM images for blank PH 90H liposomes (A), Cyst-loaded PH 90H liposomes (PH 90H: Chol: Cyst 1:0.98:1) (B) blank Lipoid S100 liposomes (C), Cyst-loaded Lipoid S100 liposomes (Lipoid S100: Chol: Cyst 1: 1.17: 1.77) (D).

3.2. *Stability study*

The stability of free and encapsulated Cyst was assessed at different temperatures (4, 25, and 37°C) and in dark and light. Aliquots were withdrawn at different time intervals, and the concentration of Cyst was determined by ion-pair chromatography. The results were expressed as the percentage of Cyst remaining in the solution as a function of time. The plots showed a straight line indicating that the oxidation of Cyst followed a zero-order reaction, and the slope corresponds to –k.

The stability of Cyst decreased when the temperature increased **(Fig. 2)**. Cyst was oxidized after 15 h at 4°C in the dark with a degradation rate of 5.25 ± 0.09 $\mu g.mL^{-1}.h^{-1}$ (**Table 3**). Whereas at 37°C in the dark, the total oxidation of Cyst was achieved after 8h of incubation with a degradation rate of 11.52 ± 0.16 $\mu g.mL^{-1}.h^{-1}$. *Pescina et al.* confirmed the temperature

dependence of Cyst oxidation after measuring the stability of the molecule at -20, 4, and 25°C (Pescina et al., 2016).

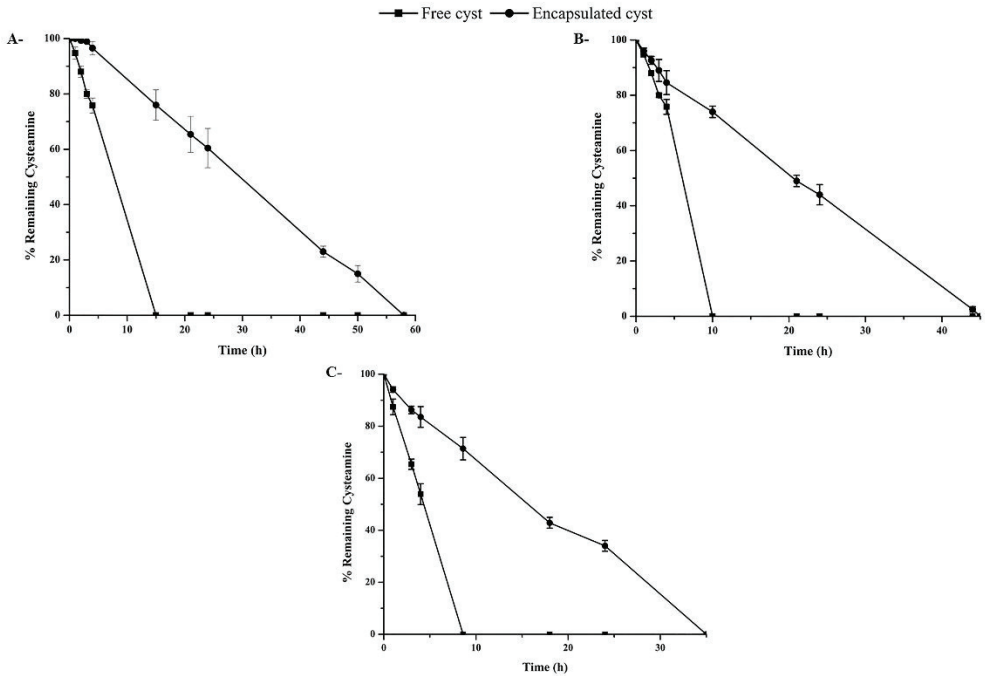

Figure 2: Stability study of free and encapsulated Cyst in the dark at 4°C (A), 25°C (B), and 37°C (C).

Table 3: Degradation rate constants of free and encapsulated Cyst at 4°C (dark), 25°C (dark and light), and 37°C (dark).

Formulations	Temperature (°C)	Degradation rate constant k ($\mu g.\ mL^{-1}.h^{-1}$)	Protection factor
Free Cyst	4 (dark)	5.25 ± 0.09	-
Cyst loaded liposome		1.77 ± 0.18	2.96
Free Cyst	25 (dark)	10.06 ± 0.07	-
Cyst loaded liposome		2.14 ± 0.12	4.7
Free Cyst	25 (light)	10.68 ± 0.57	-
Cyst loaded liposome		2.12 ± 0.07	5
Free Cyst	37 (dark)	11.52 ± 0.16	-
Cyst loaded liposome		2.78 ± 0.05	4.14

The effect of light on Cyst stability was also evaluated, and the results showed that there wasn't any significant difference between the stability of incubated Cyst in light or dark **(Fig. 3)**. The degradation rate of Cyst was slightly higher at 25°C in light (10.68 ± 0.57 $\mu g.mL^{-1}.h^{-1}$) than in dark (10.06 ± 0.07 $\mu g.mL^{-1}.h^{-1}$).

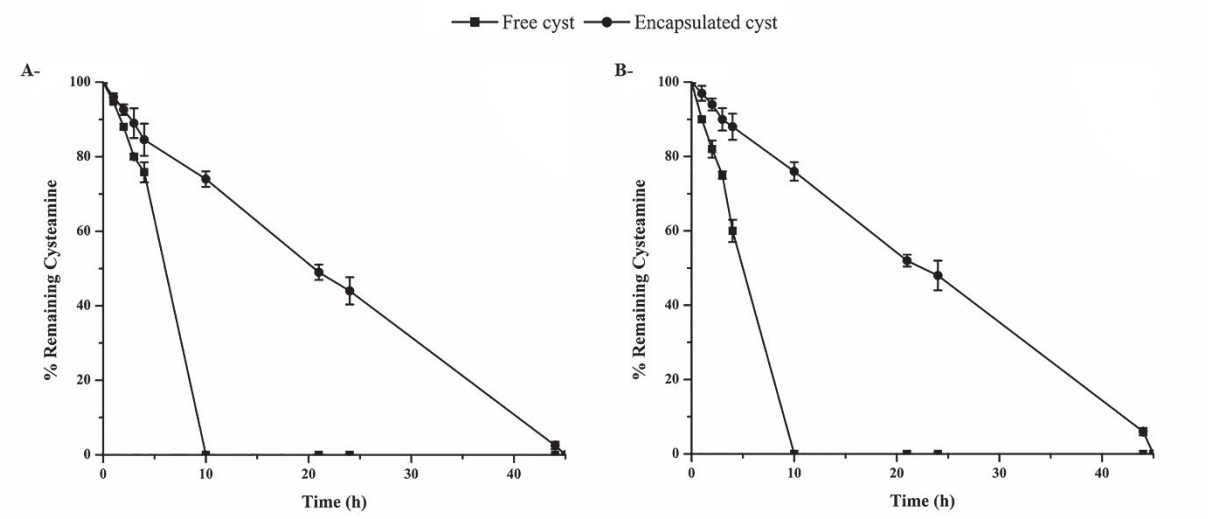

Figure 3: Stability study of free and encapsulated Cyst at 25°C in the dark (A) and in light (B).

The encapsulation of Cyst slowed down the oxidation of Cyst in all the studied conditions. For example, at 4°C in the dark, the total oxidation was delayed for 43 h for the encapsulated Cyst compared to the free Cyst. The protection factor, defined as the degradation rate of the free Cyst divided by the degradation rate of the encapsulated Cyst, was also calculated. Following the encapsulation of Cyst in liposomes, protection factors from its oxidation were of 2.96, 4.7, 5, and 4.14 after storage at 4°C, 25°C at dark, 25°C in light, and 37°C, respectively (**Table 3**). This protection is probably due to the decrease of the contact between Cyst and oxygen. The fraction of the free volume or intermolecular voids in the middle of the lipid bilayer increases with the increase of the unsaturation of the acyl chains (Rabinovich et al., 2005) and decreases with the increase of Chol content (Falck et al., 2004). The major barrier for oxygen permeability is located in the headgroup region. The addition of Chol to the saturated phosphatidylcholine

membrane reduces the oxygen transport in and near the headgroup region of the lipid bilayer by enhancing the *trans* configuration of the alkyl chains of phospholipids, thus reducing their gauche-*trans* isomerization (Subczynski et al., 1991). In this study, we demonstrated that the liposome formulations made of saturated lipids (PH 90H) and presenting a high incorporation rate of Chol (Table 2) were able to stabilize Cyst. Kaddah et al. proved that the permeability of DPPC bilayer decreases with the increase of Chol content (Kaddah et al., 2018). This may explain the lower diffusion of oxygen through the PH 90H/Chol membrane and thus the higher stability of Cyst. Cyst is encapsulated in liposomes and the diffusion of the drug is limited by the presence of Chol in the membrane. Large polar or ionic molecules cannot easily cross the phospholipid bilayer. Very small polar molecules, like water, can cross via simple diffusion. Charged atoms or molecules of any size cannot cross the cell membrane via simple diffusion as the charges are repelled by the hydrophobic tails in the interior of the phospholipid bilayer (Cooper, 2000).

In our experimental conditions, Cyst is charged and its diffusion is limited. Moreover, the incorporation of Chol in the phospholipid bilayer reduced the leakage of contents from liposomes by increasing the membrane rigidity (Kaddah et al., 2018). Figure 4 was added to explain the findings.

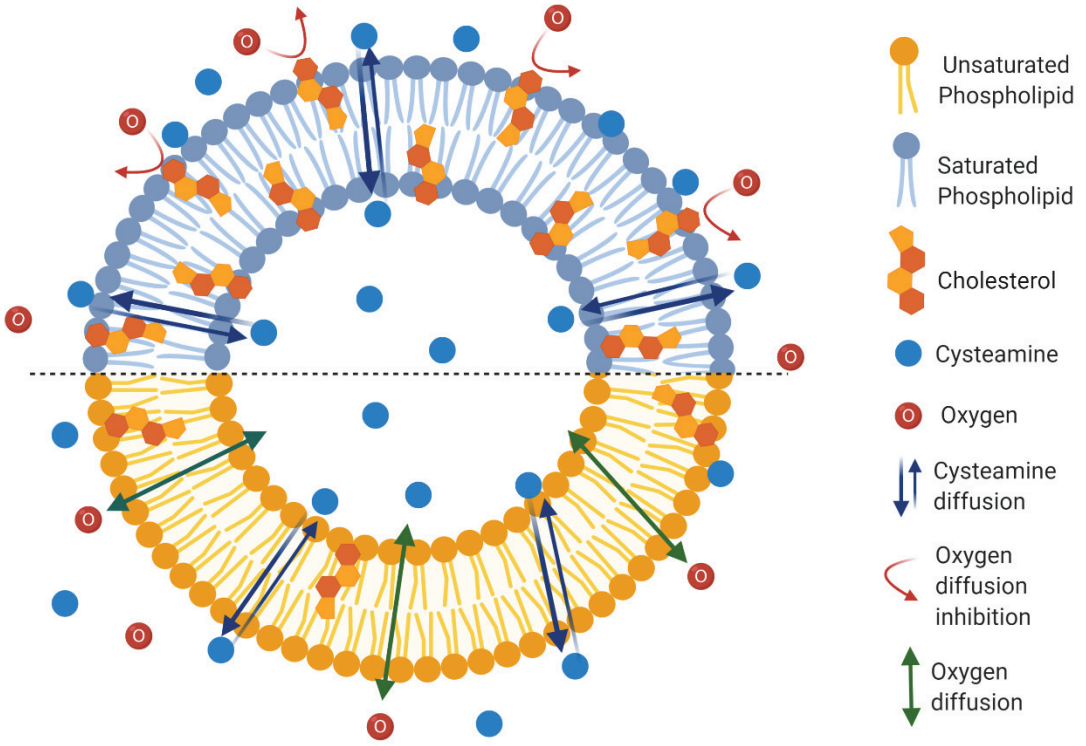

Figure 4: Representative schema of Cyst and oxygen diffusion across the liposomes containing saturated with high cholesterol content and unsaturated lipids with low cholesterol content.

Whereas, the use of cyclodextrin didn't affect the stability of Cyst (Pescina et al., 2016). Besides, *Dixon et al.* found that the addition of antioxidants except the enzyme catalase had an insignificant effect on the prevention of Cyst oxidation (Dixon et al., 2018).

To our knowledge, the quantification of Cyst and its degradation product cystamine is done for the first time in liposomal suspension. Cyst was totally converted to cystamine. The latter was the only product present in the liposomal suspension after the total oxidation of Cyst. The encapsulation delayed this conversion in all the studied conditions **(Fig. 5)**.

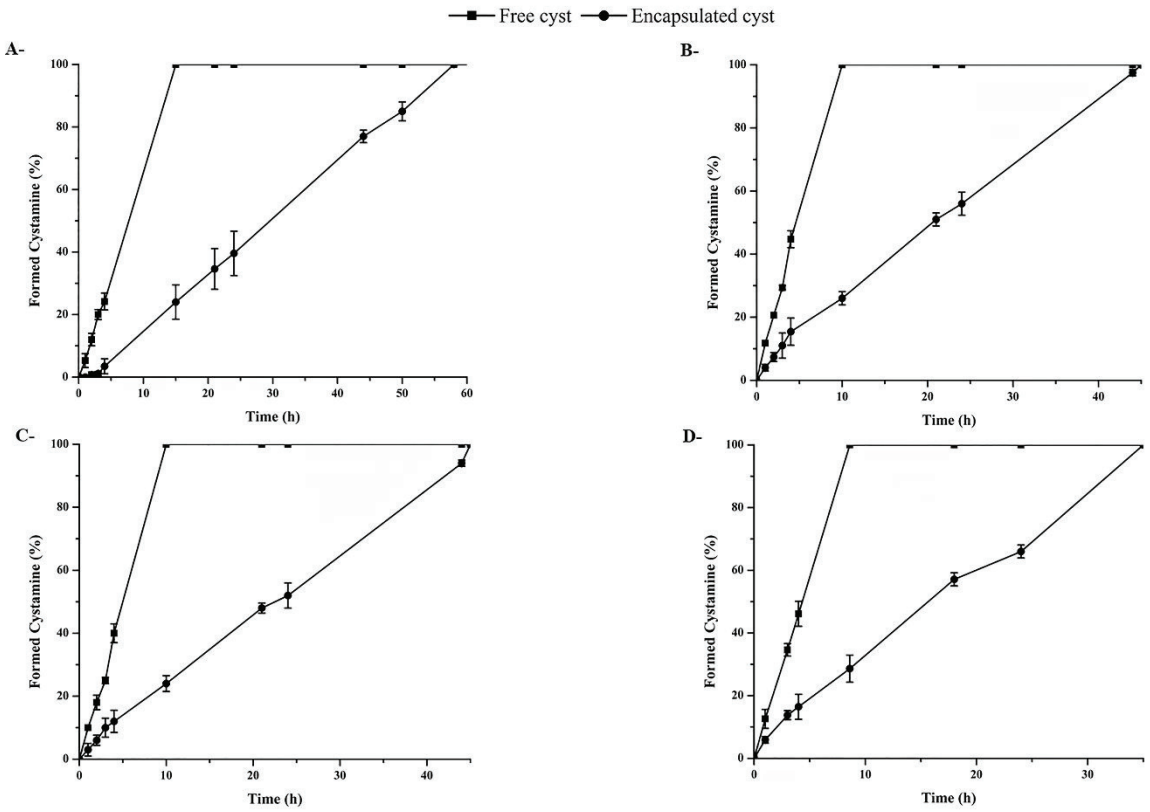

Figure 5: Percentage of formed cystamine in free and Cyst-loaded liposomes in the dark at 4°C (A), 25°C (dark (B), and light (C)), and 37°C (D).

3.3.Freeze-drying

Gharib et al. succeeded to freeze-dry PH 90H liposomes formulations using HP-β-CD (50 mM) as a cryoprotectant (Gharib et al., 2018). Two formulations of Cyst loaded liposomes (PH 90H:Chol:Cyst 1:0.98:1 and 1:0.98:10 molar ratios) were selected for freeze-drying. The liposomes were then reconstituted in water and characterized for their morphology, homogeneity, size, surface charge, and LR% (**Table 4**).

Table 4: Size, polydispersity index, zeta potential values for blank and Cyst-loaded liposomes and loading rate of Cyst in liposomes made from PH 90H before and after freeze-drying at t_0 and after four months of storage in powder form **(bold)**. The values obtained after lyophilization were compared to those before lyophilization.

	Before freeze-drying				After freeze-drying			
	Size (nm)	**pdI**	**Zeta potential (mV)**	**LR%**	**Size (nm)**	**pdI**	**Zeta potential (mV)**	**LR%**
Blank PH 90H liposome	187 ± 42	0.15 ± 0.08	-17 ± 2.8		172 ± 14	0.23 ± 0.03	-18 ± 2.5	
PH 90H:Chol:Cyst 1:0.98:1	181 ± 19	0.12 ± 0.01	-37 ± 0.2	24 ± 2	166 ± 2 **231 ± 36**	0.15 ± 0.05 **0.29 ± 0.05**	-19 ± 0.8 **-18 ± 3.5**	8 ± 1.2 **0 ± 0**
PH 90H:Chol:Cyst 1:0.98:10	187 ± 18	0.18 ± 0.06	-48 ± 4	16 ± 4	193 ± 27 **226 ± 15**	0.32 ± 0.02 **0.23 ± 0.02**	-33 ± 1.4 **-34 ± 0.5**	5 ± 0.5 **0.8 ±0.11**

The morphology of the liposomes was preserved after lyophilization (**Fig. 6**); the vesicles appeared to be oligolamellar and spherical. The presence of HP-β-CD did not affect liposome lamellarity or morphology.

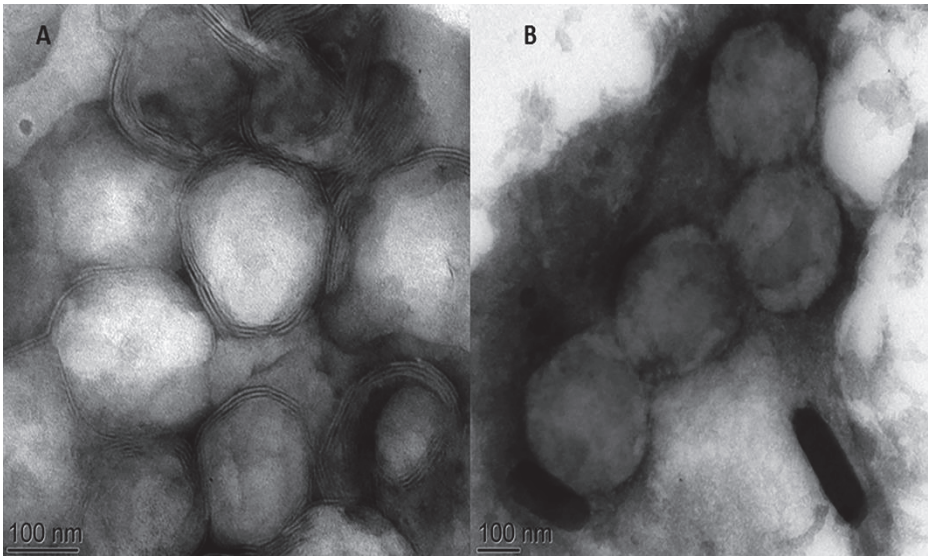

Figure 6: TEM images for blank (A) and Cyst-loaded-PH 90H liposomes (B) after freeze-drying and reconstitution with water.

The size of blank and Cyst PH 90H loaded liposomes was maintained after lyophilization regardless of the concentration of Cyst. A slight increase of the pdI values was observed after lyophilization and reconstitution for blank and Cyst-loaded liposomes. The zeta potential value was conserved for the blank liposomes; nevertheless, it significantly decreased for Cyst-loaded liposomes from -42 to -19 mV for the formulation PH 90H:Chol:Cyst molar ratio of 1:0.98:1 and from -48 to -33 mV for the formulation PH 90H:Chol:Cyst molar ratio of 1:0.98:10. The variation of the zeta potential was due to the loss of Cyst bound to the outer side of the membranes of the vesicles during lyophilization. Furthermore, the loading ratio of Cyst after the freeze-drying decreased from 24 to 8% in PH 90H:Chol:Cyst (1:0.98:1) and from 16 to 5% in PH 90H:Chol:Cyst (1:0.98:10). After lyophilization, liposomal suspension retained 33% of Cyst present in the PH 90H liposomal suspension. A significant decrease in the loading rate of anethole after freeze-drying in anethole loaded liposomes was also observed previously (Gharib et al., 2018).

3.4.Storage stability of freeze-dried forms

The mean particle size, PdI, and zeta potential values of the reconstituted liposomes after freeze-drying and after four months of storage at 4°C were evaluated (**Table 4**). The two formulations used in this study were stable with adequate size, PdI, and zeta potential values.

Besides, the total concentrations of Cyst in the reconstituted liposomes after freeze-drying were determined after four months and compared to those obtained at t_0. The percentage of remaining Cyst was 16% for the formulation PH 90H:Chol:Cyst (1:0.98:10). This result was satisfactory, especially when considering the high instability of Cyst; Cyst was oxidized entirely to Cystamine after 15 h in aqueous solution and 60 h in liposomal suspensions after storage at 4°C (**Fig. 2A**).

The storage conditions are critical in the case of Cyst. Taking into account its instability, the eye-drop Cystaran™ (Cyst ophthalmic solution 0.44%) has to be stored at -20°C, and administered hourly during the daytime. After its opening, it should be used within one week (Huynh et al., 2013). Cyst hydrochloride (0.5%) formulated ophthalmic preparation is easily oxidized within the first week after storage at +4°C, rendering the preparation less effective (Reda et al., 2017). In comparison with the aqueous liposomal suspension, the freeze-dried form conserved Cyst for a more extended period. The elimination of the water from the liposomal suspension is the factor that induced this improvement of Cyst stability. The presence of water will lead to the degradation of Cyst to cystamine (Gana et al., 2015).

The freeze-drying of pharmaceutical formulations increases their shelf life (Chen et al., 2010). It is relevant for liposomal formulations as liposomes tend to aggregate in aqueous media forming larger liposome particles. In aqueous dispersion, liposomes have limited physical stability and shelf life. In addition, the encapsulated molecule could diffuse to the dispersing solution and therefore be lost due to bacteriological, enzymatic, and/or chemical reactions facilitated by the dispersing medium (Ickenstein et al., 2006).

The encapsulation of Cyst improves its pharmacokinetic profile; indeed, compared to free Cyst, the encapsulated form was more stable in gastro-intestinal tract, more absorbed when administered via enteral route, and remained in blood circulation for a longer period (Jaskierowicz et al., 1985).

4. Conclusion

In this study, we proved that the encapsulation of Cyst in conventional liposomes improved its stability. Cyst-loaded liposomes were nanometric and presented a negative surface charge. In addition to its incorporation in vesicles, Cyst binds to the surface of the vesicle. The loading ratio of Cyst in liposomes varied between 12 and 24% depending on Cyst to lipid molar ratio. Besides, in this work, we succeeded in preparing freeze-dried liposomes that retain a noticeable amount of Cyst after four months of storage at 4°C. These results could help to develop various pharmaceutical forms of Cyst and enlarge its applications.

Acknowledgements

Authors thank the Research Funding Program at the Lebanese University and the "Agence Universitaire de la Francophonie, projet PCSI" for supporting the project (2018-2020). Authors also thank Géraldine Agusti for the TEM measurements. Electron microscopy studies have been done at the "Centre Technologique des Microstructures" – Claude Bernard University of Lyon.

Declaration of Competing Interest

The authors declare that they have no known competing financial interests or personal relationships that could have appeared to influence the work reported in this paper.

References

Apffel, C.A., Walker, J.E., Issarescu, S., 1975. Tumor Rejection in Experimental Animals Treated with Radioprotective Thiols. Cancer Res 35, 429–437.

Ascenso, A., Cruz, M., Euletério, C., Carvalho, F.A., Santos, N.C., Marques, H.C., Simões, S., 2013. Novel tretinoin formulations: a drug-in-cyclodextrin-in-liposome approach. Journal of Liposome Research 23, 211–219. https://doi.org/10.3109/08982104.2013.788026

Atallah, C., Charcosset, C., Greige-Gerges, H., 2020. Challenges for cysteamine stabilization, quantification, and biological effects improvement. Journal of Pharmaceutical Analysis. https://doi.org/10.1016/j.jpha.2020.03.007

Azzi, J., Auezova, L., Danjou, P.-E., Fourmentin, S., Greige-Gerges, H., 2018. First evaluation of drug-in-cyclodextrin-in-liposomes as an encapsulating system for nerolidol. Food Chemistry 255, 399–404. https://doi.org/10.1016/j.foodchem.2018.02.055

Bacq, Z.M., Dechamps, G., Fischer, P., Herve, A., Le Bihan, H., Lecomte, J., Pirotte, M., Rayet, P., 1953. Protection against x-rays and therapy of radiation sickness with beta-mercaptoethylamine. Science 117, 633–636.

Berleur, F., Roman, V., Jaskierowicz, D., Fatome, M., Leterrier, F., Ter-Minassian-Saraga, L., Madelmont, G., 1985. The binding of the radioprotective agent cysteamine with the phospholipidic membrane headgroup-interface region. Biochem. Pharmacol. 34, 3071–3080.

Besouw, M., Masereeuw, R., van den Heuvel, L., Levtchenko, E., 2013. Cysteamine: an old drug with new potential. Drug Discovery Today 18, 785–792. https://doi.org/10.1016/j.drudis.2013.02.003

Bozdağ, S., Gümüş, K., Gümüş, O., Unlü, N., 2008. Formulation and in vitro evaluation of cysteamine hydrochloride viscous solutions for the treatment of corneal cystinosis. Eur J Pharm Biopharm 70, 260–269. https://doi.org/10.1016/j.ejpb.2008.04.010

Budai, L., 2013. Liposomes for Topical Use: A Physico-Chemical Comparison of Vesicles Prepared from Egg or Soy Lecithin. Scientia Pharmaceutica 81, 1151–1166. https://doi.org/10.3797/scipharm.1305-11

Butler, J.D., Tietze, F., Pellefigue, F., Spielberg, S.P., Schulman, J.D., 1978. Depletion of Cystine in Cystinotic Fibroblasts by Drugs Enclosed in Liposomes. Pediatric Research 12, 46–51. https://doi.org/10.1203/00006450-197801000-00012

Çağdaş, M., Sezer, A.D., Bucak, S., 2014. Liposomes as Potential Drug Carrier Systems for Drug Delivery. Application of Nanotechnology in Drug Delivery. https://doi.org/10.5772/58459

Chavin, W., Schlesinger, W., 1966. Some potent melanin depigmentary agents in the black goldfish. Naturwissenschaften 53, 413–414.

Chen, C., Han, D., Cai, C., Tang, X., 2010. An overview of liposome lyophilization and its future potential. Journal of Controlled Release 142, 299–311. https://doi.org/10.1016/j.jconrel.2009.10.024

Chetoni, P., Burgalassi, S., Monti, D., Najarro, M., Boldrini, E., 2007. Liposome-encapsulated mitomycin C for the reduction of corneal healing rate and ocular toxicity. Journal of Drug Delivery Science and Technology 17, 43–48. https://doi.org/10.1016/S1773-2247(07)50006-7

Cooper, G.M., 2000. Transport of Small Molecules. The Cell: A Molecular Approach. 2nd edition.

Daeihamed, M., Dadashzadeh, S., Haeri, A., Faghih Akhlaghi, M., 2017. Potential of Liposomes for Enhancement of Oral Drug Absorption. Current Drug Delivery 14, 289–303.
Dixon, P., Powell, K., Chauhan, A., 2018. Novel approaches for improving stability of cysteamine formulations. International Journal of Pharmaceutics 549, 466–475. https://doi.org/10.1016/j.ijpharm.2018.08.006
Domingues, M.M., Santiago, P.S., Castanho, M.A.R.B., Santos, N.C., 2008. What can light scattering spectroscopy do for membrane-active peptide studies? Journal of Peptide Science 14, 394–400. https://doi.org/10.1002/psc.1007
Elmonem, M.A., Veys, K.R., Soliman, N.A., van Dyck, M., van den Heuvel, L.P., Levtchenko, E., 2016. Cystinosis: a review. Orphanet Journal of Rare Diseases 11, 47. https://doi.org/10.1186/s13023-016-0426-y
Eloy, J.O., Claro de Souza, M., Petrilli, R., Barcellos, J.P.A., Lee, R.J., Marchetti, J.M., 2014. Liposomes as carriers of hydrophilic small molecule drugs: Strategies to enhance encapsulation and delivery. Colloids and Surfaces B: Biointerfaces 123, 345–363. https://doi.org/10.1016/j.colsurfb.2014.09.029
Falck, E., Patra, M., Karttunen, M., Hyvönen, M.T., Vattulainen, I., 2004. Impact of cholesterol on voids in phospholipid membranes. The Journal of Chemical Physics 121, 12676. https://doi.org/10.1063/1.1824033
Farshi, S., Mansouri, P., Kasraee, B., 2018. Efficacy of cysteamine cream in the treatment of epidermal melasma, evaluating by Dermacatch as a new measurement method: a randomized double blind placebo controlled study. Journal of Dermatological Treatment 29, 182–189. https://doi.org/10.1080/09546634.2017.1351608
Frenk, E., Pathak, M.A., Szabó, G., Fitzpatrick, T.B., 1968. Selective action of mercaptoethylamines on melanocytes in mammalian skin: experimental depigmentation. Arch Dermatol 97, 465–477.
Gallego-Villar, L., Hannibal, L., Häberle, J., Thöny, B., Ben-Omran, T., Nasrallah, G.K., Dewik, A.-N., Kruger, W.D., Blom, H.J., 2017. Cysteamine revisited: repair of arginine to cysteine mutations. Journal of Inherited Metabolic Disease 40, 555–567. https://doi.org/10.1007/s10545-017-0060-4
Gana, I., Barrio, M., Ghaddar, C., Nicolaï, B., Do, B., Tamarit, J.-L., Safta, F., Rietveld, I.B., 2015. An Integrated View of the Influence of Temperature, Pressure, and Humidity on the Stability of Trimorphic Cysteamine Hydrochloride. Molecular Pharmaceutics 12, 2276–2288. https://doi.org/10.1021/mp500830n
Gharib, R., Auezova, L., Charcosset, C., Greige-Gerges, H., 2017. Drug-in-cyclodextrin-in-liposomes as a carrier system for volatile essential oil components: Application to anethole. Food Chem 218, 365–371. https://doi.org/10.1016/j.foodchem.2016.09.110
Gharib, R., Greige-Gerges, H., Fourmentin, S., Charcosset, C., 2018. Hydroxypropyl-ß-cyclodextrin as a membrane protectant during freeze-drying of hydrogenated and non-hydrogenated liposomes and molecule-in-cyclodextrin-in- liposomes: Application to trans-anethole. Food Chemistry 267, 67–74. https://doi.org/10.1016/j.foodchem.2017.10.144
Gresham, P.A., Barnett, M., Smith, S.V., Schneider, R., 1971. Use of a sustained-release multiple emulsion to extend the period of radio protection conferred by cysteamine. Nature 234, 149–150.
Huynh, N., Gahl, W.A., Bishop, R.J., 2013. Cysteamine ophthalmic solution 0.44% for the treatment of corneal cystine crystals in cystinosis. Expert Review of Ophthalmology 8, 341–345. https://doi.org/10.1586/17469899.2013.814885

Ickenstein, L.M., Sandström, M.C., Mayer, L.D., Edwards, K., 2006. Effects of phospholipid hydrolysis on the aggregate structure in DPPC/DSPE-PEG2000 liposome preparations after gel to liquid crystalline phase transition. Biochimica et Biophysica Acta (BBA) - Biomembranes 1758, 171–180. https://doi.org/10.1016/j.bbamem.2006.02.016

Jaskierowicz, D., Genissel, F., Roman, V., Berleur, F., Fatome, M., 1985. Oral Administration of Liposome-entrapped Cysteamine and the Distribution Pattern in Blood, Liver and Spleen. International Journal of Radiation Biology and Related Studies in Physics, Chemistry and Medicine 47, 615–619. https://doi.org/10.1080/09553008514550851

Jeitner, T.M., Oliver, J.R., 1990. Possible oncostatic action of cysteamine on the pituitary glands of oestrogen-primed hyperprolactinaemic rats. Journal of Endocrinology 127, 119–127. https://doi.org/10.1677/joe.0.1270119

Kaddah, S., Khreich, N., Kaddah, F., Charcosset, C., Greige-Gerges, H., 2018. Cholesterol modulates the liposome membrane fluidity and permeability for a hydrophilic molecule. Food and Chemical Toxicology 113, 40–48. https://doi.org/10.1016/j.fct.2018.01.017

Kim, J.H., Shin, D.H., Kim, J.-S., 2018. Preparation, characterization, and pharmacokinetics of liposomal docetaxel for oral administration. Arch. Pharm. Res. 41, 765–775. https://doi.org/10.1007/s12272-018-1046-y

Lahiani-Skiba, M., Boulet, Y., Youm, I., Bounoure, F., Vérité, P., Arnaud, P., Skiba, M., 2007. Interaction between hydrophilic drug and α-cyclodextrins: physico-chemical aspects. Journal of Inclusion Phenomena and Macrocyclic Chemistry 57, 211–217. https://doi.org/10.1007/s10847-006-9194-y

Laouini, A., Jaafar-Maalej, C., Limayem-Blouza, I., Sfar, S., Charcosset, C., Fessi, H., 2012. Preparation, Characterization and Applications of Liposomes: State of the Art. Journal of Colloid Science and Biotechnology 1, 147–168. https://doi.org/10.1166/jcsb.2012.1020

Mansouri, P., Farshi, S., Hashemi, Z., Kasraee, B., 2015. Evaluation of the efficacy of cysteamine 5% cream in the treatment of epidermal melasma: a randomized double-blind placebo-controlled trial. Br. J. Dermatol. 173, 209–217. https://doi.org/10.1111/bjd.13424

Min-Oo, G., Fortin, A., Poulin, J.-F., Gros, P., 2010. Cysteamine, the Molecule Used To Treat Cystinosis, Potentiates the Antimalarial Efficacy of Artemisinin. Antimicrobial Agents and Chemotherapy 54, 3262–3270. https://doi.org/10.1128/AAC.01719-09

Oh, Y.K., Nix, D.E., Straubinger, R.M., 1995. Formulation and efficacy of liposome-encapsulated antibiotics for therapy of intracellular Mycobacterium avium infection. Antimicrob. Agents Chemother. 39, 2104–2111. https://doi.org/10.1128/aac.39.9.2104

Pescina, S., Carra, F., Padula, C., Santi, P., Nicoli, S., 2016. Effect of pH and penetration enhancers on cysteamine stability and trans-corneal transport. European Journal of Pharmaceutics and Biopharmaceutics 107, 171–179. https://doi.org/10.1016/j.ejpb.2016.07.009

Rabinovich, A.L., Balabaev, N.K., Alinchenko, M.G., Voloshin, V.P., Medvedev, N.N., Jedlovszky, P., 2005. Computer simulation study of intermolecular voids in unsaturated phosphatidylcholine lipid bilayers. The Journal of Chemical Physics 122, 084906. https://doi.org/10.1063/1.1850903

Reda, A., Van Schepdael, A., Adams, E., Paul, P., Devolder, D., Elmonem, M.A., Veys, K., Casteels, I., van den Heuvel, L., Levtchenko, E., 2017. Effect of Storage Conditions on Stability of Ophthalmological Compounded Cysteamine Eye Drops. JIMD Rep 42, 47–51. https://doi.org/10.1007/8904_2017_77

Sagar, S.M., Millard, W.J., Martin, J.B., Murchison, S.C., 1985. The mechanism of action of cysteamine in depleting prolactin immunoreactivity. Endocrinology 117, 591–600. https://doi.org/10.1210/endo-117-2-591

Sebaaly, C., Greige-Gerges, H., Stainmesse, S., Fessi, H., Charcosset, C., 2016. Effect of composition, hydrogenation of phospholipids and lyophilization on the characteristics of eugenol-loaded liposomes prepared by ethanol injection method. Food Bioscience 15, 1–10. https://doi.org/10.1016/j.fbio.2016.04.005

Sebaaly, C., Jraij, A., Fessi, H., Charcosset, C., Greige-Gerges, H., 2015. Preparation and characterization of clove essential oil-loaded liposomes. Food chemistry 178, 52–62. https://doi.org/10.1016/j.foodchem.2015.01.067

Serrano, G., Almudéver, P., Serrano, J.-M., Milara, J., Torrens, A., Expósito, I., Cortijo, J., 2015. Phosphatidylcholine liposomes as carriers to improve topical ascorbic acid treatment of skin disorders. Clin Cosmet Investig Dermatol 8, 591–599. https://doi.org/10.2147/CCID.S90781

Subczynski, W.K., Hyde, J.S., Kusumi, A., 1991. Effect of alkyl chain unsaturation and cholesterol intercalation on oxygen transport in membranes: a pulse ESR spin labeling study. Biochemistry 30, 8578–8590. https://doi.org/10.1021/bi00099a013

Telange, D.R., Patil, A.T., Pethe, A.M., Fegade, H., Anand, S., Dave, V.S., 2017. Formulation and characterization of an apigenin-phospholipid phytosome (APLC) for improved solubility, in vivo bioavailability, and antioxidant potential. European Journal of Pharmaceutical Sciences, Use of phospholipids in oral drug delivery 108, 36–49. https://doi.org/10.1016/j.ejps.2016.12.009

Tuncay Tanriverdi, S., 2018. Preparation and Characterization of Caffeine Loaded Liposome and Ethosome Formulations for Transungual Application. The Turkish Journal of Pharmaceutical Sciences 15, 178–183. https://doi.org/10.4274/tjps.22931

Wei, Y., Guo, J., Zheng, X., Wu, J., Zhou, Y., Yu, Y., Ye, Y., Zhang, L., Zhao, L., 2014. Preparation, pharmacokinetics and biodistribution of baicalin-loaded liposomes. Int J Nanomedicine 9, 3623–3630. https://doi.org/10.2147/IJN.S66312

Zylberberg, C., Matosevic, S., 2016. Pharmaceutical liposomal drug delivery: a review of new delivery systems and a look at the regulatory landscape. Drug Deliv 23, 3319–3329. https://doi.org/10.1080/10717544.2016.1177136

Chapitre 5 : Evaluation de l'effet dépigmentant du chlorhydrate de cystéamine encapsulé dans des liposomes

Introduction

L'hyperpigmentation est une production excessive de mélanine induisant des tâches foncées plus ou moins grande sur la peau (Grimes et al., 2018). La cystéamine et la cystamine présentent un effet dépigmentant en inhibant l'activité de la tyrosinase et en stimulant l'activité de la glutathionne (Qiu et al., 2000). Ces effets induisent ainsi l'augmentation de la production de la phéomélanine, responsable de la coloration rouge/jaune de la peau, et la diminution de celle du 5,6-dihydroxyindole, responsable de la coloration noire de la peau (Mansouri et al., 2015). Afin d'évaluer l'influence de la cystéamine encapsulée dans les liposomes sur son effet dépigmentant, des tests d'efficacité et de pénétration cutanée ont été réalisés.

La cystéamine peut se trouver sous différentes formes : le chlorhydrate de cystéamine, la phosphocystéamine et le bitartrate de cystéamine (Atallah et al., 2020). Dans ce chapitre, le chlorhydrate de cystéamine a été utilisé parce qu'il présente une stabilité plus élevée que celle de la cystéamine. Les suspensions liposomales contenant du chlorhydrate de cystéamine ont été préparées et caractérisées pour leur taille, pdI et leur potentiel Zêta. La stabilité de ces suspensions a été étudiée après stockage à 4°C. L'effet de la lyophilisation de ces suspensions sur l'efficacité et la pénétration cutanée de la cystéamine a été aussi évalué.

Premièrement, des tests de cytotoxicité ont été effectués par MTT sur la lignée cellulaire mélanome B16 en présence du chlorhydrate de cystéamine, la cystamine, des liposomes blancs en suspension et lyophilisés et des liposomes contenant le chlorhydrate de cystéamine en suspension et lyophilisés. Pour cela, différents facteurs de dilution ont été étudiés, afin de choisir une concentration adéquate pour les différents échantillons précédemment cités. Une fois les concentrations choisies, les dosages de la mélanine, la tyrosinase et les espèces réactives à l'oxygène ont été effectués en présence des différents échantillons en utilisant la lignée

cellulaire mélanome B16. De plus, la pénétration cutanée du chlorhydrate de cystéamine et de la cystamine des différents échantillons a été évaluée en utilisant une cellule de Franz.

Références

Atallah, C., Charcosset, C., & Greige-Gerges, H. (2020). Challenges for cysteamine stabilization, quantification, and biological effects improvement. *Journal of Pharmaceutical Analysis*. https://doi.org/10.1016/j.jpha.2020.03.007

Grimes, P. E., Ijaz, S., Nashawati, R., & Kwak, D. (2018). New oral and topical approaches for the treatment of melasma. *International Journal of Women's Dermatology*, *5*(1), 30–36. https://doi.org/10.1016/j.ijwd.2018.09.004

Mansouri, P., Farshi, S., Hashemi, Z., & Kasraee, B. (2015). Evaluation of the efficacy of cysteamine 5% cream in the treatment of epidermal melasma: A randomized double-blind placebo-controlled trial. *The British Journal of Dermatology*, *173*(1), 209–217. https://doi.org/10.1111/bjd.13424

Qiu, L., Zhang, M., Sturm, R. A., Gardiner, B., Tonks, I., Kay, G., & Parsons, P. G. (2000). Inhibition of melanin synthesis by cystamine in human melanoma cells. *The Journal of Investigative Dermatology*, *114*(1), 21–27. https://doi.org/10.1046/j.1523-1747.2000.00826.x

Effect of cysteamine hydrochloride-loaded liposomes on skin depigmenting, antioxidant effect and penetration

Carla Atallah[a,b], Celine Viennet[c], Sophie Robin[d], Sami Ibazizen[d], Hélène Greige-Gerges[a], and Catherine Charcosset[b]

[a]*Bioactive Molecules Research Laboratory, Faculty of Sciences, Lebanese University, Lebanon.*

[b]*Laboratoire d'Automatique, de Génie des Procédés et de Génie Pharmaceutiques (LAGEPP), Université Claude Bernard Lyon 1, France.*

[c]*Laboratory of Engineering and Cutaneous Biology, UMR 1098, Bourgogne Franche-Comté University, 19 rue Ambroise Paré, 25000, Besançon, France*

[d]*Bioexigence SAS, Espace Lafayette, Besançon, France*

En cours de préparation

Effect of cysteamine hydrochloride-loaded liposomes on skin depigmenting, antioxidant effect and penetration

Carla Atallah[a,b], Celine Viennet[c], Sophie Robin[d], Sami Ibazizen[d], Hélène Greige-Gerges[a], and Catherine Charcosset[b]

[a]*Bioactive Molecules Research Laboratory, Faculty of Sciences, Lebanese University, Lebanon.*

[b]*Laboratoire d'Automatique, de Génie des Procédés et de Génie Pharmaceutiques (LAGEPP), Université Claude Bernard Lyon 1, France.*

[c]*Laboratory of Engineering and Cutaneous Biology, UMR 1098, Bourgogne Franche-Comté University, 19 rue Ambroise Paré, 25000, Besançon, France*

[d]*Bioexigence SAS, Espace Lafayette, Besançon, France*

Abstract

Hyperpigmentation is a skin disorder known for the excessive production of melanin. Cysteamine, an aminothiol compound physiologically synthetized in human body cells, has been known as depigmenting agent. The aim of this study was to evaluate the impact of liposome formulations encapsulating cysteamine hydrochloride on its depigmenting effect and skin penetration. First, cysteamine hydrochloride-loaded liposomes were prepared and characterized for their size, polydispersity index, zeta potential and the encapsulation efficiency of the active molecule. The stability of cysteamine hydrochloride in the prepared liposome formulations in suspension and freeze-dried forms was then assessed. The *in vitro* cytotoxicity of cysteamine and cysteamine-loaded liposome suspensions (either original or freeze-dried) was evaluated in B16 murine melanoma cells. The measurement of melanin and tyrosinase activities was assessed after cells treatment with free and encapsulated cysteamine. The antioxidant activity of the free and encapsulated cysteamine was also evaluated by the measurement of ROS formation in treated cells. The *ex vivo* human skin penetration study was also performed using Franz diffusion cell. The stability of cysteamine hydrochloride was improved after encapsulation in liposomal suspension. In addition, for the liposome re-suspended after freeze-drying, a significant increase of vesicle stability was observed. The free and the encapsulated cysteamine in suspension (either original or freeze-dried) did not show any cytotoxic effect, inhibited the melanin formation as well as the tyrosinase activity. An antioxidant activity was observed for the free and the encapsulated cysteamine hydrochloride. The encapsulation enhanced the skin penetration of cysteamine hydrochloride. The penetration of this molecule was better for the re-suspended freeze-dried form than the original liposomal suspension where the drug was found retained in the epidermis layer of the skin.

Keywords: Cysteamine hydrochloride, cystamine, cytotoxicity, liposome, melanin, skin penetration, tyrosinase.

1 Introduction

Many compounds such as hydroquinone, kojic acid, and arbutin are used to treat hyperpigmentation; however, their use was associated with cytotoxic effects (Ephrem et al., 2017; Rendon & Gaviria, 2005; Solano et al., 2006). Cysteamine (Cyst), an aminiothiol synthetized by human body cells; and its disulfide form, cystamine, have shown to possess a depigmenting effect on black gold fish (Chavin & Schlesinger, 1966; Frenk et al., 1968). Besides, the application of cysteamine Cream® on the ear of black female guinea pigs demonstrated a high depigmenting effect (Hsu et al., 2013). A randomized, double-blind vehicle-controlled clinical trial was also conducted to evaluate the efficacy and safety of this cream to treat epidermal melasma; the treatment with cysteamine cream® decreased the content of melanin (Farshi et al., 2017; Mansouri et al., 2015). It was reported that the depigmenting action of Cyst and cystamine is due to the inhibition of tyrosinase activity which is the enzyme that plays a crucial role in the melanogenesis. Unlike hydroquinone, Cyst and cystamine mechanisms of action are a melanogenesis inhibition and not a melanocytotoxicity (Qiu et al., 2000). Qiu et al. reported that 100 µM of Cyst inhibited 21% of melanin and 87% of tyrosinase while 50 µM of cystamine inhibited 5% of melanin and 89% of tyrosinase (Qiu et al., 2000). These molecules could also reduce the reactive oxygen species generation and enhance the intracellular glutathione (Lee et al., 2017; Okamura et al., 2014; Ribeiro et al., 2013; Shin et al., 2011; Sun et al., 2010). The production of reactive oxygen species (ROS) was significantly suppressed by low dose of Cyst on 1-methyl-4-phenyl-1,2,3,6-tetrahydropyridine-induced dopaminergic neurodegeneration mice (Sun et al., 2010). Cyst also inhibited tert-butyl hydroperoxide-induced ROS production in human corneal endothelial cells (Shin et al., 2011). It reduced ROS production by 33% in phorbol 12-myristate-13-acetate stimulated macrophages (Okamura et al., 2014). In addition, Cyst inhibited vascular endothelial growth factor-induced

ROS generation in a concentration-dependent manner, with maximum effect at 50 µM (Lee et al., 2017). Moreover, cystamine decreased ROS levels evoked by H_2O_2 or staurosporine in mutant cells (Ribeiro et al., 2013).

However, Cyst presents an offensive odor and is unstable in solutions where it undergoes oxidation to cystamine (Atallah, Charcosset, et al., 2020). The encapsulation of many skin whitening agents in delivery systems improved their stability (Ephrem et al., 2017). Moreover, it increases their concentration at the targeted site by improving skin permeation, penetration or distribution (Ephrem et al., 2017). Liposomes are nanometric spherical vesicles able to encapsulate hydrophilic, hydrophobic and amphiphilic molecules. They are biodegradable, biocompatible and present a low toxicity (Zylberberg & Matosevic, 2016).

Cyst can be used in different forms such as Cyst (base form), Cyst hydrochloride (cyst HCl), phosphoCyst, and Cyst bitartrate (**Figure 1**). An increase of the stability of the base form of Cyst was previously demonstrated after encapsulation in liposomes suspension (original and from freeze-dried form) compared to free Cyst (base form) during storage at 4°C (Atallah, Greige-Gerges, et al., 2020). However, after 60 h, the remaining Cyst in liposome suspension was very low. Therefore, cyst HCl was used in this study because the salt form of this molecule is more stable than its base form (Wiedmann & Naqwi, 2016).

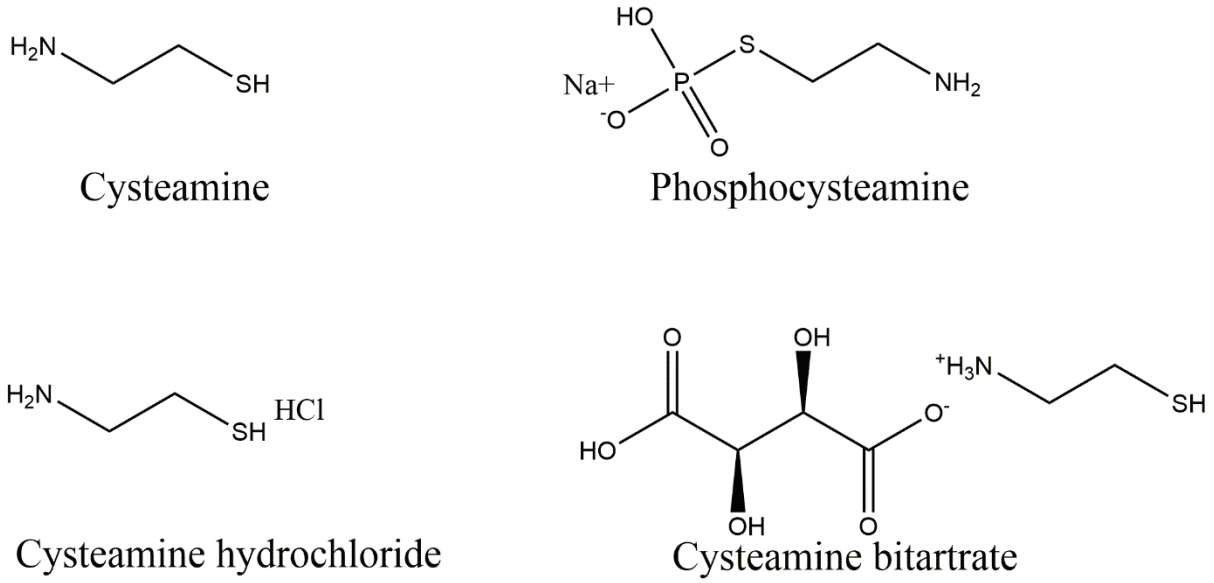

Figure 1: The structure of the different forms of cysteamine.

In this study, blank and cyst HCl-loaded liposomes were prepared by the ethanol injection method and characterized for their size, polydispersity index and zeta potential. The encapsulation efficiency of cyst HCl (EE%) in liposomes was also calculated. The amount of residual ethanol in the blank liposomes was determined by Nuclear Magnetic Resonance (NMR) technique. Blank and cyst HCl-loaded liposomes were freeze-dried according to the optimized protocol previously described (Gharib et al., 2018). The lyophilized liposomes were then re-suspended with ultra-pure water. The stability of free cysteamine dissolved in water and that of the cyst HCl-loaded liposome suspensions (original or freeze-dried form) was evaluated at 4°C during 6 months. The cytotoxicity of free cyst HCl, cystamine and the suspensions of blank- and cyst HCl-loaded liposomes (original or freeze-dried) were evaluated by MTT assay. In addition, the effects of the same formulations on the *in vitro* melanin content and tyrosinase activity were measured. Moreover, the antioxidant activity of the free and the encapsulated cyst HCl was assessed by the measurement of ROS formation induced by the presence of H_2O_2 in B16 cells. Finally, the skin penetration of free- and cyst HCl-loaded liposomes was compared using the Franz diffusion cell.

2 Materials and Methods

2.1 Materials

Cyst HCl, cystamine dihydrochloride, metformin hydrochloride, (3-(4, 5-dimethylthiazol-2-yl)-2, 5-diphenyltetrazolium bromide), DMSO, L-DOPA and NaOH were purchased from Sigma-Aldrich (Buchs, Switzerland). Phospholipon 90H (90% soybean PC, 4% lysoPC, 2% triglycerides, 2% water, and 0.5% ethanol) was obtained from Lipoid GmbH (Ludwigshafen, Germany). Cholesterol was obtained from Fisher Chemical (Loughborough, UK). HP-β-CD-oral grade (MS=0.85) was purchased from Roquette (Lestrem, France). Sodium dodecyl phosphate and phosphoric acid were obtained from Sigma-Aldrich (China). (trimethylsilyl)-2,2,3,3-tetradeutepropropionic acid sodium salt was purchased form Sigma-Aldrich (USA). Deuterium oxide (D_2O) was purchased from Acros organics (USA). Dulbecco's Modified Eagle Medium (DMEM), fetal bovine serum (FBS), penicillin, and streptomycin were purchased from Dominique Dutscher (France). All other chemicals were of analytical grade.

2.2 Cyst HCl-loaded liposomes suspensions preparation (original and re-suspended after freeze-drying)

Liposomes were prepared by the ethanol injection method, as described by Sebaaly et al. (2016). The organic phase was prepared by dissolving Phospholipon 90H (saturated lipid) (100 mg) and cholesterol (50 mg) in absolute ethanol (10 mL). Then, the organic phase was injected into the aqueous phase (20 mL) containing 5 mg/mL of cyst HCl, using a syringe pump (Fortuna optima, GmbH-Germany), at a temperature above the transition temperature of the phospholipid (55°C) and under magnetic stirring at 400 rpm. The contact between the organic solution and the aqueous phase leads to a spontaneous liposome formation. The liposomal suspensions were then left for 15 min at 25°C under stirring (400 rpm). The ethanol was removed by rotary evaporation (Heidolph GmbH, Germany) under reduced pressure at 40°C

and the obtained liposomal solutions were stored at 4°C. Each preparation was performed in triplicate.

The freeze drying of blank- and cyst HCl-loaded liposomes was done as previously reported (Atallah, Greige-Gerges, et al., 2020). In brief, blank liposomes and cyst HCl-loaded liposomes (PH 90H: Chol: Cyst molar ratios 1:0.98:10) were freshly prepared; 5 mL of these suspensions were then ultracentrifuged at 170,000g for 1 h at 4 °C. The supernatant was removed, and the pellet was re-dissolved in an aqueous solution of 50 mM HP-β-CD (2 mL). The samples were kept at −20 °C overnight then placed into the drying chamber of Cryonext 23,020 freeze-dryer (Trappes, France), pre-cooled to -20°C, then lowered to -40°C with a slow cooling profile of 0.5°C/min. The product was stabilized for 30 min at -38 °C before the vacuum was applied. Primary drying was executed at a pressure of 150 µbar for 3 h at -10°C, then the temperature of the drying chamber was progressively increased to 5 °C for 6 h at 250 µbar, to reach finally 10°C at 350 µbar for 9 h. A secondary drying step for 10 h at 20°C and 100 µbar pressure was applied. Finally, the vials were removed from the freeze-dryer, closed with rubber caps, and stored at 4°C. The lyophilized liposomes were then re-suspended with ultra-pure water to the original volume (5 mL).

2.3 Cyst HCl-loaded liposomes characterization

The size, polydispersity index and zeta potential were determined using Malvern Zetasizer Nanoseries (Zetasizer Nano ZS; Malvern Instruments Ltd, France). All batches were diluted with ultrapure water. The particle-size distribution data were collected using the DTS (nano) software (version 5.10) provided with the instrument. Zeta potential was calculated using Smoluchowski's equation from the electrophoretic mobility of liposomes. All measurements were carried out at 25°C after 2 min of equilibration and were performed in triplicate. Data were expressed as the mean values ± SD.

For the calculation of EE%, liposomal suspensions (5 mL) were ultra-centrifuged (OptimaTM Ultracentrifuge, Beckman Coulter, USA) at 170,000g for 1 h at 4°C to separate the free cyst HCl (supernatant) from the liposomes loading cyst HCl (pellet). The pellet was re-suspended in water (5 mL). The total liposomal suspension as well as the re-suspended pellet were sonicated and then analyzed by ion pair chromatography method as described below. This allows to determine the total and encapsulated cyst HCl concentrations in the liposomal suspensions.

The encapsulation efficiency (EE %) of cyst HCl was calculated using the formula:

$$EE_{\text{Cyst HCl}}\% = \frac{[\text{Cyst HCl}]_{\text{encapsulated}}}{[\text{Cyst HCl}]_{\text{total}}} \times 100$$

Where $[\text{Cyst HCl}]_{\text{encapsulated}}$ and $[\text{Cyst HCl}]_{\text{total}}$ represent the concentration of encapsulated cyst HCl (pellet) and the concentration of the total cyst HCl present in the liposomal suspension, respectively.

2.4 Cyst HCl and cystamine quantification

To quantify cyst HCl and cystamine in the different formulations, an ion-pair chromatography with an isocratic mode consisting of acetonitrile:water containing 0.1% phosphoric acid and sodium dodecyl phosphate (4 mM) (v/v, 45:55) was used. The column was a reverse-phase Kinetex C18 column (4.6 × 100 mm, 2.6 µm; phenomenex). 20 µL were injected in the column maintained at 25°C with a flow rate of 1.0 mL/min, and the detection wavelength was 215 nm. Metformin (1 µg/mL) was used as an internal standard. Linearity was between 2.5 and 100 µg/mL for cyst HCl and between 5 and 100 µg/mL for cystamine. This method was previously used for the quantification of cysteamine in its base form; the same chromatographic results were obtained as for cyst HCl (retention time, limits of detection and quantification).

2.5 Ethanol quantification in the blank liposomal suspension

The quantity of ethanol present in the blank liposomal suspension was also determined by NMR technique according to Zuriarrain et al. (Zuriarrain et al., 2015). Blank liposomal suspensions were centrifuged for 10 min at 11200g. The residual ethanol is supposed to be present in the upper phase. The internal standard used was (trimethylsilyl)-2,2,3,3-tetradeutepropropionic acid sodium salt (TSP) $(CH_3)_3SiCD_2CD_2CO_2Na$. 10 mg of TSP was dissolved in 400 µL D_2O and 300 µL of the supernatant of the liposomal suspension. The number of moles of ethanol is calculated from the NMR spectrum using the following equation:

$$n_{EtOH} = \frac{H_{IS}}{H_{CH2}} \times n_{IS} \times \frac{I_{CH2}}{I_{IS}}$$

Where H_{IS} and H_{CH2} are the numbers of hydrogen atoms present in the internal standard structure (equals to 9) and in CH_2 group of ethanol (equals to 2), n_{IS} is the number of moles of the internal standard (equals to 5.78×10^{-5} mole) and I_{CH2} and I_{IS} are the integration of the CH_2 group of ethanol and the internal standard peaks.

To simplify, we replaced H_{IS}, H_{CH2} and n_{IS} by their values to obtain the following equation:

$$n_{EtOH\ (mole)} = 0.00026 \times \frac{I_{CH2}}{I_{IS}}$$

Experiments were run on an Avance 300 Bruker spectrometer equipped with a standard BBFO probe. 90 degrees pulses were applied with 30s relaxation time to ensure quantitative analyses.

2.6 Stability of free cyst HCl in solution, suspended cyst HCl-loaded liposomes (original and freeze-dried)

The stability of cyst HCl-loaded liposomes was compared to that of free cyst HCl. The liposomal suspension (5 mL) was centrifuged, the supernatant was eliminated, and the pellet was re-suspended in water. The concentration of the encapsulated cyst HCl was determined after the destruction of liposomes by sonication. A solution of cyst HCl with the same

concentration of the encapsulated cyst HCl was also prepared in water and stored at 4°C. After 6 months of storage at 4 °C, the concentration of the remaining cyst HCl in free cyst HCl solution and the suspensions of liposomes loading cyst HCl was determined. Also, after 3 months of storage at 4 °C, freeze-dried liposomes were re-suspended in 5 mL water and the remaining cyst HCl concentration was measured using ion-pair chromatography.

2.7 Cell culture

B16 murine melanoma cells (Elabscience, CliniSciences, Nanterre, France) were grown in Dulbecco's Modified Eagle Medium (DMEM) supplemented with 10% heat-inactivated fetal bovine serum (FBS), 100 U/mL penicillin, and 100 µg/mL streptomycin. Cells were maintained in an incubator at 37 °C in a humidified 5% CO_2 atmosphere and passaged weekly using 1% trypsin to maintain the optimum conditions for exponential growth.

2.8 Preparation of the formulations used in the cytotoxicity tests, melanin and tyrosinase assays

Different concentrations of cyst HCl and cystamine (50; 60; 100 and 500 µM) were prepared in culture medium. Blank liposomes (original and re-suspended after freeze-drying) were prepared between 0.1 to 5.7% v/v in culture medium to evaluate their cytotoxic effect. The suspensions containing total cyst HCl-loaded liposome (encapsulated and non-encapsulated) were centrifuged and the pellet was re-suspended to obtain the encapsulated cyst HCl-loaded liposome suspensions. The total (present in the whole suspension) and the encapsulated cyst HCl-loaded liposome were diluted to obtain 0.1 and 2.8 v/v%, respectively. The freeze dried cyst HCl-loaded liposomes were re-suspended in water and then diluted in culture medium to obtain 5.7 v/v%. These dilutions were made to obtain the same concentration of cyst HCl (60 µM) in all formulations. Kojic acid (700 µM) was prepared in water and used as positive

control. These preparations were used for the cytotoxicity tests as well as melanin and tyrosinase measurements.

2.9 Cytotoxicity analysis

B16 melanoma cell viability was determined by the (3-(4, 5-dimethylthiazol-2-yl)-2, 5-diphenyltetrazolium bromide) MTT assay. Cells were seeded in 96-well microtiter plates at a density of $6x10^3$ cells/well. After 24 h of incubation at 37°C in 5% CO_2, cells were treated with 100 µL of each formulation as described in section 2.8. After 24 and 48 h of incubation with the different formulations, the medium was removed, cells were washed twice and 100 µL of MTT solution (0.5 mg/mL) and fresh medium was added to each well. Cells were incubated for 4 h at 37°C and the produced formazan salts were then dissolved in DMSO. Absorbance was measured at 571 nm by spectroscopy on a microplate reader (Thermo Scientific, Multiskan FC).

2.10 Tyrosinase activity assay

Intracellular tyrosinase activity was determined by measuring the rate of oxidation of L-DOPA to DOPAchrome. B16 cells were seeded at a density of $10x10^4$ cells/well in 6-well plates. After 24 h, 2 mL of cyst HCl (60 µM), cystamine (60 µM), kojic acid (700 µM), blank liposomes (original suspension and re-suspended after freeze-drying), whole suspension of cyst HCl-loaded liposome, suspended cyst HCl-loaded liposome (encapsulated) and the suspended freeze-dried cyst HCl-loaded liposome were added to cells. 48 and 72h post-treatment, cells were harvested by scraping into ice-cold PBS and lysed at room temperature for 15 min with 0.5% Triton X-100 in PBS. Lysed cell supernatants (100 µL) were mixed with 100 µL of freshly prepared L-DOPA solution (0.1% in PBS). Following incubation at 37°C for 1 h, absorbance was measured at 450 nm and compared with a standard curve using mushroom tyrosinase. Tyrosinase activity was normalized to the amount of protein (determined using the Bradford assay).

2.11 Melanin measurement

B16 cells were seeded at a density of $10x10^4$ cells/well in 6-well plates. Plates were incubated for 24h at 37°C in 5% CO_2 before being treated with cyst HCl (60 µM), cystamine (60 µM), kojic acid (700 µM), blank liposomes (original suspension and re-suspended freeze-dried form), total cyst HCl-loaded liposome suspension, encapsulated cyst HCl-loaded liposome in suspension and the suspended freeze-dried cyst HCl-loaded liposome. After 24 and 48 h, cells were collected by scraping into ice-cold PBS and pelleted. Intracellular melanin was extracted by solubilizing cell pellets in 1N NaOH containing 10% DMSO for 2 h at 80°C. The melanin content of cell lysate supernatants was measured spectrophotometrically at an absorbance of 405 nm against a standard curve of synthetic melanin. Intracellular melanin content was adjusted by the amount of protein.

2.12 Reactive oxygen species content

Intracellular ROS production was detected using the oxidation-sensitive fluorescence dye 2,7-dichlorodihydrofluorescein diacetate (DCFH-DA). Cells were seeded at a density of $6x10^3$ cells/well in 96-well plates. After 24 h, they were firstly treated 2 times over a period of 72 h with 100 µL of tested substances, and secondly treated with H_2O_2 (100 µM in culture medium) for 6 h. Then DCFH-DA solution (1 µM in culture medium) was added to cells for 30 min at 37°C. Immediately after PBS washing, fluorescence was quantified using a spectrofluorophotometer (BioTek, Synergy H1) with 495 nm excitation and 527 nm emission filters. ROS were observed under an inverted fluorescence microscope (Olympus, DP50).

2.13 *Ex vivo* skin penetration study with Franz cell

Ex vivo percutaneous permeation of cyst HCl was performed on thawed skin from a female caucasian donor. Skin was defatted using a scalpel and then dermatomed with a dermatome (Zimmer Biomet Electric® Dermatome). Skin discs were realized using a circled cutter and the

thickness range was between 400 and 600 µm. Skin discs were mounted on a Franz cells system (PermeGear). Franz cells were previously filled with receptor fluid (RF) consisting of PBS-EDTA 0.1% at pH 7.4. Skin discs were equilibrated during 1 h before measurement of TEWL (Trans Epidermal Water Loss) using a tewameter TM300 (MDD 4, Courage & Khazaka). The tested formulations were cyst HCl solution, total and encapsulated cyst HCl-loaded liposomes and resuspended freeze-dried cyst HCl-loaded liposomes. 1 mL of each formulation diluted to obtain 1200µM of cyst HCl as a final concentration has been deposited on the skin. RF was sampled at different time points 0, 1, 4, 18 and 24h. At 24h, formulations were removed and skin discs were washed with RF (1 mL). Skin compartments were separated using forceps in order to obtain epidermis and dermis. Samples (Washing, Epidermis and Dermis) were weighed and then the active ingredient was extracted in methanol:water extraction solvent (50:50, v/v) after stirring during 24 h. Finally, extracts were quantified by ion pair chromatography.

2.14 Statistical analysis

The differences between the treated and the control cells were calculated using ANOVA (GraphPad Prism 9; GraphPad Software, San Diego, CA) with $p < 0.05$ defining statistical significance.

3 Results

3.1 Characterization of cyst HCl-loaded liposomes

The sizes of the blank and cyst HCl-loaded liposomes were similar with 211 ± 8 nm and 217 ± 22 nm for blank and loaded liposomes, respectively. The polydispersity index was 0.2 for the blank and cyst HCl-loaded liposomes indicating that the liposomal population was homogeneous. The zeta potential of the blank liposomes (-17.95 ± 4.0 mV) was increased after the addition of cyst HCl (-2.37 ± 0.7 mV). This result indicates the presence of an interaction between cyst HCl and the liposomal suspension. The EE% of the studied formulation was 3.74 ± 0.46 % which was lower than the EE% of cyst-loaded liposome (21 ± 5.0%) found in our previous work using the base form of cyst (Atallah, Greige-Gerges, et al., 2020). Cyst (base form) and cyst HCl differ by their aqueous solubility, pH of their aqueous solution, and their stability. The base form may interact with negatively charged phosphate of phospholipids leading to a greater encapsulation when compared with cyst HCl form.

In addition to the determination of the EEs, the remaining percentage of ethanol in the liposomal suspensions was measured as ethanol is a potential cytotoxic compound. The remaining percentage of ethanol in the liposomal suspension depended on the time of evaporation and the remaining volume of liposomal suspension. In fact, the percentage of the ethanol in the liposomal suspension increased with the increase of the final volume of liposomal suspension. The percentage of ethanol in all the studied conditions was less than 2.6% **(Table 1)**.

Table 1: The percentage of remaining ethanol in the liposomal suspension for the different evaporation times and liposomal suspension final volumes obtained.

Final volume of liposomal suspension (mL)	Time of evaporation (min)	% of ethanol in the liposomal suspension
10.5	20	0.5 %
13	10	1.9 %
15	5	2.6 %

3.2 Stability of cyst HCl-loaded liposomes

The stability of cyst HCl-loaded liposomes and free cyst HCl prepared in water was assessed after storage at 4°C. The total degradation of free cyst HCl was obtained after 16 days, whereas a remaining cyst HCl percentage of 9.5% was obtained in the cyst HCl-loaded liposomes in suspension form after 6 months of storage at 4°C. The total concentration of cyst HCl in the resuspended freeze dried liposomes was determined after 3 months of storage at 4°C showing that the concentration of cyst HCl determined at time 0 was stable after 3 months of storage **(Figure 2)**. The stability of cysteamine in its hydrochloride form was much better than in its base form. For the same concentration of the free drug (200 µg/mL), cysteamine in its base from was totally converted to cystamine after 15h of storage at 4°C (Atallah, Greige-Gerges, et al., 2020) while cyst HCl was totally converted after 16 days of storage at 4°C. The encapsulation of cyst HCl increased its stability in suspension form (total degradation after 6 months of storage) and for a longer time when the formulation was freeze-dried (no degradation after 3 months of storage). An increase in stability has been previously reported for several drugs encapsulated in liposomes and/or freeze dried liposomes, such as the encapsulation of quercetin (Azzi, Jraij, et al., 2018), nerolidol (Azzi, Auezova, et al., 2018) and anethole (Gharib et al., 2017). In addition, the base form of cysteamine (200 µg/mL) was totally oxidized after 60 h in the liposomal suspension and 4 months in the freeze-dried form (Atallah, Greige-Gerges, et al., 2020).

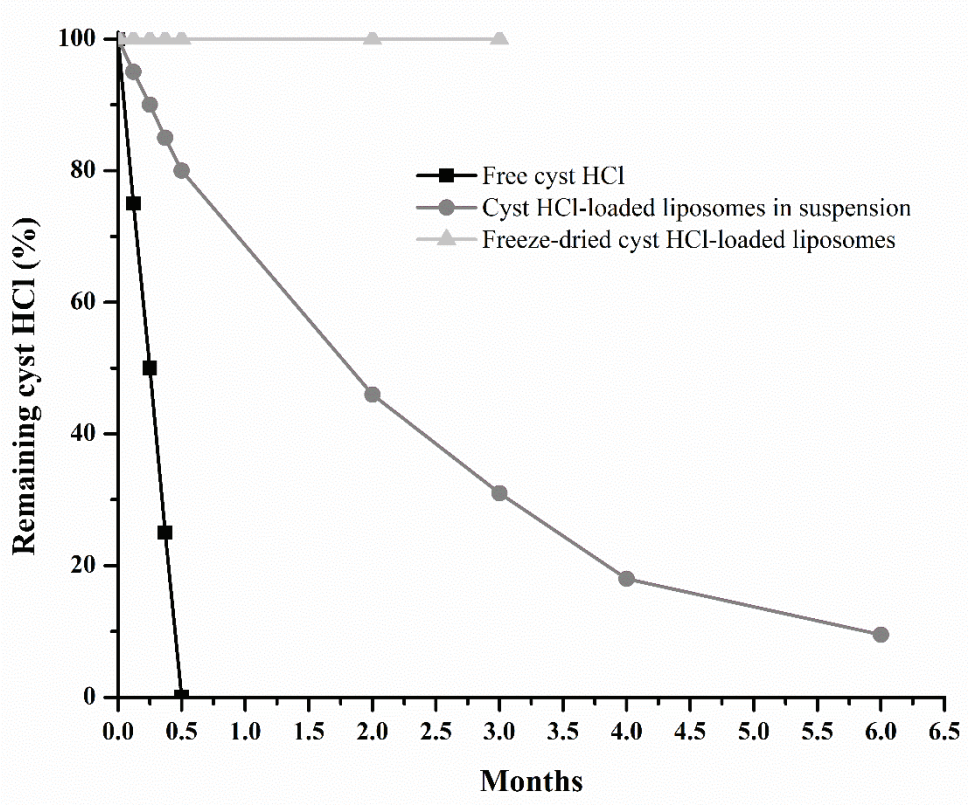

Figure 2: Stability study at 4°C of free cyst HCl, suspended cyst HCl-loaded liposome, and freeze dried form of cyst HCl-loaded liposome suspended in water the day of HPLC analysis.

3.3 Cytotoxicity of blank liposomes (original suspension and suspended freeze-dried form)

The cytotoxicity of the blank liposomes in suspension and the suspended freeze-dried form was evaluated by MTT assay on B16 murine melanoma cells after 24 and 48h of incubation. Blank liposomes in suspension form did not show any cytotoxic effect at the various volume concentrations (0.1; 1; 2; 2.8 and 5 v/v %). A slight cytotoxicity was observed for the highest v/v% which may be due to the presence of a higher quantity of residual ethanol in these liposomes. As shown in **Table 2**, 5% of H_2O/ethanol solution decreased the cell viability to 83 ± 0.05%. The cytotoxicity of the suspended freeze-dried blank liposomes showed a higher cytotoxicity than that of the liposomal suspension after 24h of incubation. For the same v/v%

of 5, the cytotoxicity of blank liposomal suspension was 90 ± 0.06% while it was 75 ± 0.11% for the suspended freeze-dried form **(Table 2)**. The cytotoxicity of the liposomes decreased after 48h. The cytotoxicity observed was probably due to the presence of the HP-β-CD (used as a cryoprotectant) in the freeze-dried vesicles (Hammoud et al., 2019).

Table 2: Cell viability of B16 melanoma cells in the presence of different percentage volume v/v% of suspended freeze-dried and liposomal suspension using MTT assay.

Samples	Concentration (%)	Cell viability after 24h (%)	Cell viability after 48h (%)
Control DMEMc	-	100 ± 0.05	100 ± 0.08
H_2O/ethanol	5	83 ± 0.05	86 ± 0.05
Blank liposomes (suspension form)	5	90 ± 0.06	95 ± 0.07
	2.8	94 ± 0.06	98 ± 0.07
	2	94 ± 0.05	99 ± 0.06
	1	96 ± 0.04	98 ± 0.05
	0.1	96 ± 0.05	98 ± 0.09
Blank liposomes (resuspended freeze-dried form)	5.7	76 ± 0.1	84 ± 0.12
	5	75 ± 0.11	86 ± 0.08
	2	92 ± 0.09	92 ± 0.12
	1	93 ± 0.12	96 ± 0.09
	0.1	94 ± 0.09	96 ± 0.11

3.4 Cytotoxicity of free cyst HCl and cystamine

The cytotoxicity of free cyst HCl and cystamine was for the first time evaluated on B16 melanoma cell lines. A cytotoxicity effect is observed if the viability of the cells are below 80%. Free cyst HCl and cystamine did not show any cytotoxicity between 50 and 100 µM (cell viability > 92%). However, cystamine showed a higher cytotoxicity than cyst HCl at 500 µM; cell viability decreased to 59 ± 0.06% and 26 ± 0.08% after 24h of 500 µM cyst HCl and cystamine treatments, respectively **(Figure 3)**. Similarly, Qiu et al. (2000) showed that cystamine (50 to 100 µM) did not present any cytotoxic effect on MM418c5, MM96L and HeLa cells after 6 days of treatment (Qiu et al., 2000). It should be noted that Cyst HCl at a concentration of 60 µM was chosen for further analysis.

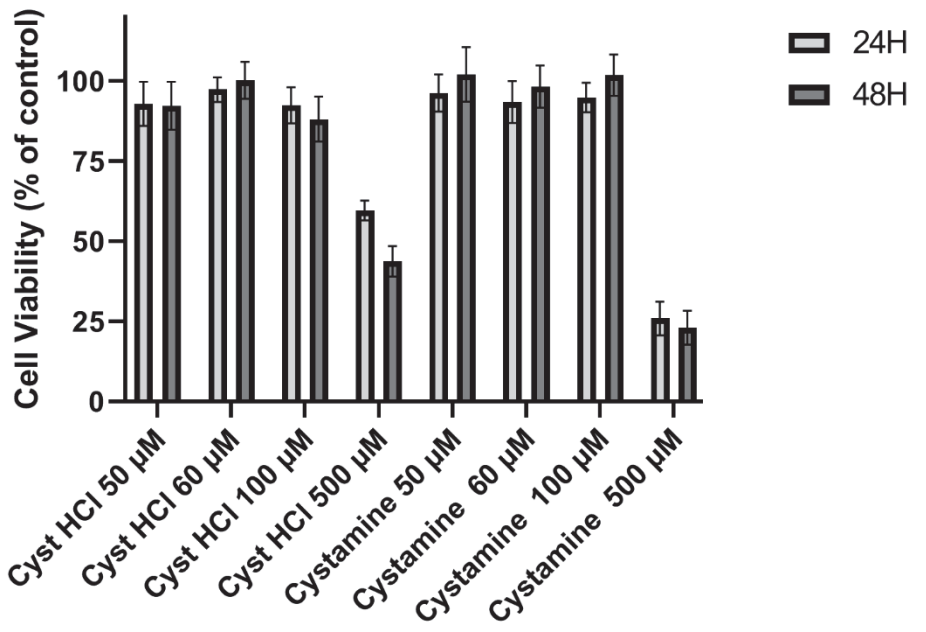

Figure 3: Cell viability of B16 melanoma cells in presence of different concentrations of cyst HCl and cystamine. Data are presented as means ± SD (n = 6).

3.5 Cytotoxicity of cyst HCl-loaded liposomes

The cytotoxicity of the total and encapsulated cyst HCl loaded liposomes was also evaluated on B16 melanoma cells. Cell viability of the total and encapsulated cyst HCl-loaded liposomes was 92 ± 0.09% and 95 ± 0.05%, respectively, after 24h of incubation. However, the suspended freeze-dried form was more cytotoxic (74 ± 0.07%) than the liposomal suspension **(Figure 4)**.

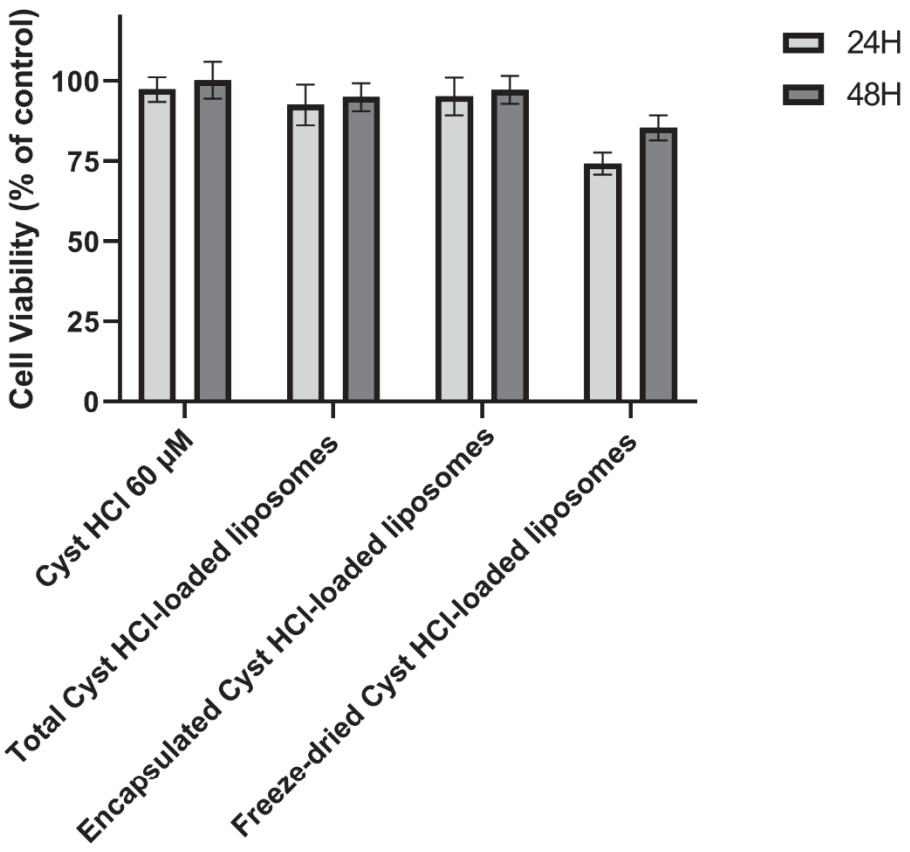

Figure 4: Cell viability of B16 melanoma cells in presence of free, total and encapsulated cyst HCl-loaded liposome in suspension and resuspended freeze-dried forms. Data are presented as means ± SD (n = 6).

3.6 Inhibition of melanin synthesis

To study the effect of cyst HCl loaded liposomes on melanogenesis, we examined the level of melanin produced in B16 cells after treating them for 72h with free cyst HCl and cystamine (culture media as control), whole liposome suspension encapsulating cyst HCl and cyst HCl-loaded liposome (original liposome suspension as control), and resuspended freeze-dried cyst HCl-loaded liposome (resuspended freeze-dried liposome as control). Kojic acid was used as a positive control.

For the same concentration of cyst HCl and cystamine (60 µM), cystamine was able to reduce the melanin content in the cells (33.0 ± 13%) more than cyst HCl (26 ± 8.6%). Kojic acid used as a reference presented an inhibition of 36 ± 9.1% of melanin. Suspended freeze-dried blank liposome did not show any inhibition of melanin. The inhibition of melanin was lower for the encapsulated (22 ± 0.9%) form compared to the free form (26 ± 8.6%). The suspended freeze-dried cyst HCl-loaded liposome (23.5 ± 6.3%) showed a better inhibition of melanin than the original suspension **(Figure 5)**.

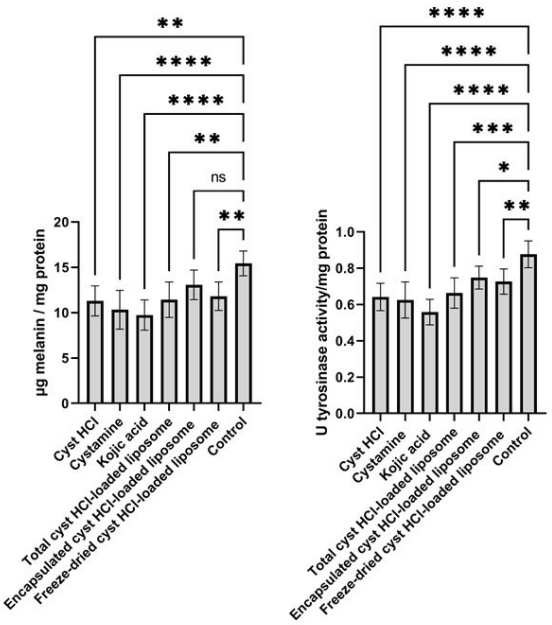

Figure 5: Melanin (A) and tyrosinase (B) contents in B16 cells treated with cyst HCl, cystamine, kojic acid, total and encapsulated cyst HCl-loaded liposome in suspension and resuspended freeze-dried forms after 72h of treatment. Data are presented as means ± SD (n = 6). Statistical analysis was performed using ANOVA test; ns: not significant, *p < 0.05, **p<0.01, ***p < 0.001, ****p < 0.0001.

3.7 Inhibition of tyrosinase activity

The tyrosinase enzyme plays a crucial role in melanogenesis. Kojic acid (used as positive control) showed a strong inhibition of the enzyme activity (36.2 ± 5.8%). Cystamine (28.2 ± 12.2%) and cyst HCl (26.8 ± 5.5%) inhibited the tyrosinase activity. Therefore, melanogenesis inhibition by cyst HCl and cystamine in B16 cells occurs via direct inhibition of tyrosinase activity and the two drugs are tyrosinase inhibitors. The effect of the cyst HCl encapsulation in liposomes on the inhibition of the tyrosinase activity was investigated. The encapsulation of cyst HCl decreased its inhibition of tyrosinase activity effect (26.8 ± 5.5% was inhibited in presence of free cyst HCl while 19.6 ± 4.4% and 18.33 ± 2.9% was inhibited for the encapsulated cyst HCl loaded liposome and resuspended freeze-dried cyst HCl-loaded, respectively) **(Figure 5)**.

To the best of our knowledge, one study investigated the depigmenting effect of cysteamine *in vitro* using pigmented melanoma MM418c5 cells and 100 µM of cysteamine inhibited 21% of melanin and 87% of tyrosinase while 50 µM of cystamine inhibited 5% of melanin and 89% of tyrosinase (Qiu et al., 2000).

Figure 6 shows the microscopic observation of the cells after 72 h of treatment with free, total and encapsulated cyst HCl-loaded liposome in suspension and resuspended freeze-dried forms. It also shows the solubilized cell pellets of the different treated cells. A whitening effect was observed for all the formulations in comparison with the control.

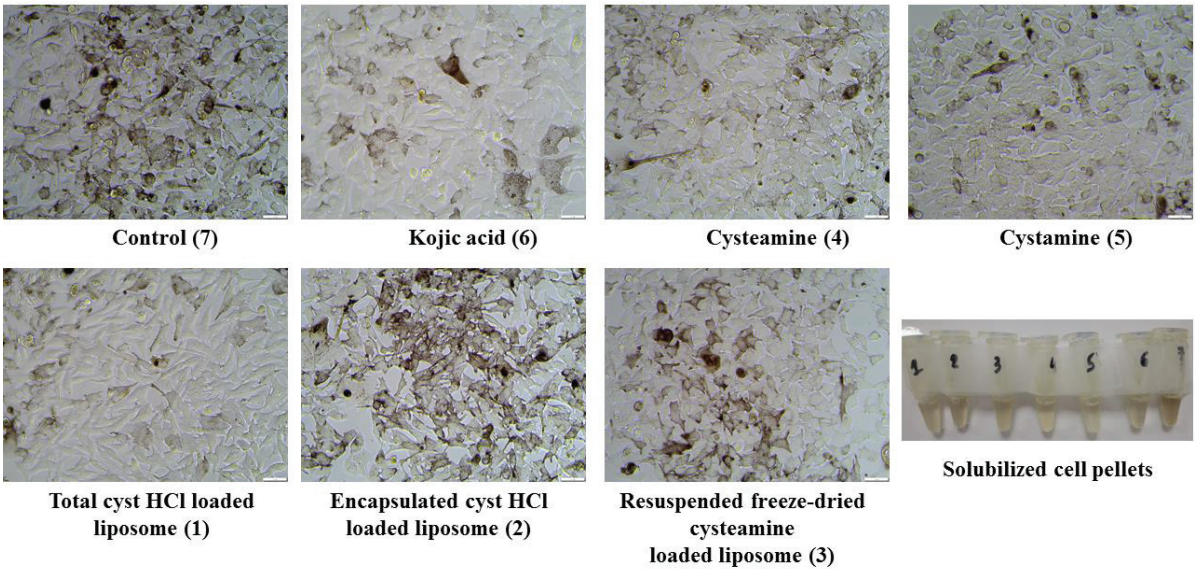

Figure 6: Microscopic observations of cells after 72 h of treatment with the different formulations and a picture of the different solubilized pellets obtained.

3.8 Reactive oxygen species content

Intracellular oxidative stress was measured by the DCFH-DA assay. The cleavage of two acetate groups of DCFH-DA by esterase can lead to the formation of DCFH that can be oxidized to a highly fluorescent compound DCF by intracellular ROS. Therefore, the fluorescence intensity of DCF can directly reflect the level of reactive oxygen species in the cell (Rhee et al., 2010). To estimate the effect of cyst HCl and its encapsulation on the intracellular production of ROS in cultured B16 cells, the cells were treated for 6h with H_2O_2 after their treatment with 60 µM of cyst HCl and cystamine; total and encapsulated cyst HCl-loaded liposome in suspension and resuspended freeze-dried forms. The inhibited percentage of ROS formation was 43.4±10.3% and 38.6±9.8% in the presence of free cyst HCl and cystamine, respectively. This percentage was not affected by the encapsulation of cyst HCl (35.4±10.1% and 33.6±11.6% for the encapsulated cyst HCl in suspension and resuspended freeze dried forms, respectively) **(Figure 7)**. After, the addition of 60 µM cysteamine or cystamine to the B16 cells, a decrease in ROS levels by a factor of 1.78 and 1.64, respectively, in comparison with the control was observed. The addition of the encapsulated cyst HCl in suspension and resupended

freeze dried forms also decreased the relative fluorescence by 1.4 and 1.5 times in comparison with the control. **Figure 8** shows the fluorescence image of B16 cells treated for 72h with free and encapsulated cyst HCl (suspension and resuspended freeze dried forms) and cystamine before the induction of the oxidant stress with H_2O_2. A decrease of the DCFH-DA fluorescence in all the formulations containing cyst HCl was observed in comparison to the control.

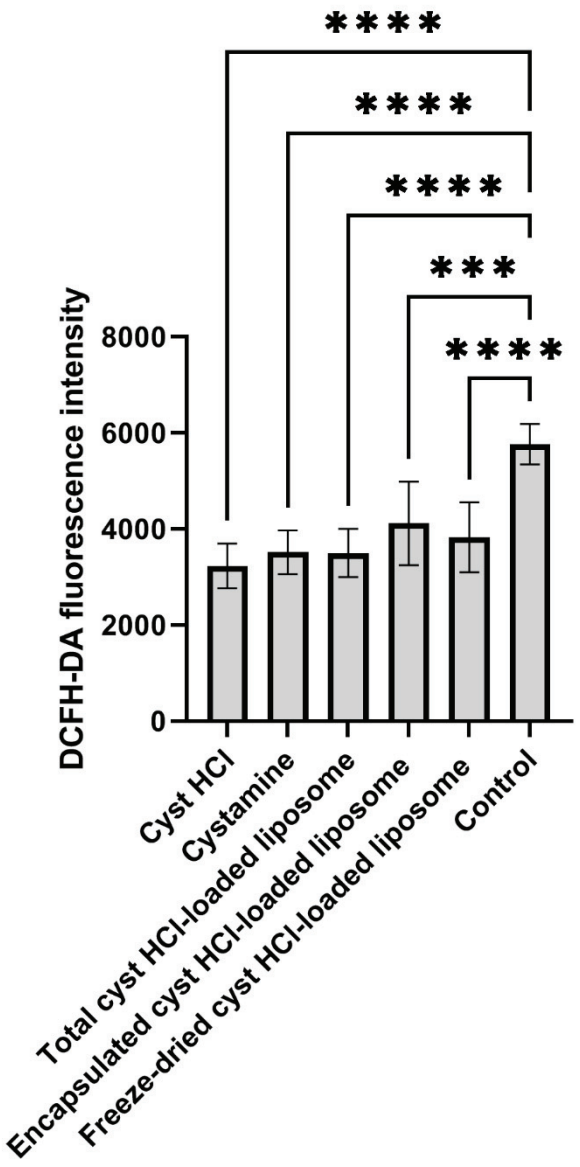

Figure 7: Intracellular ROS formation measured by relative DCFH-DA fluorescence in cultured B16 treated by H_2O_2 after their treatment with 60 µM of cyst HCl and cystamine; total and encapsulated cyst HCl-loaded liposome in suspension and resuspended freeze-dried forms.

The formation of ROS was assayed by measuring the fluorescence of DCFH-DA. Data are presented as means ± SD (n = 6). Statistical analysis was performed using ANOVA test; ***p < 0.001, ****p < 0.0001.

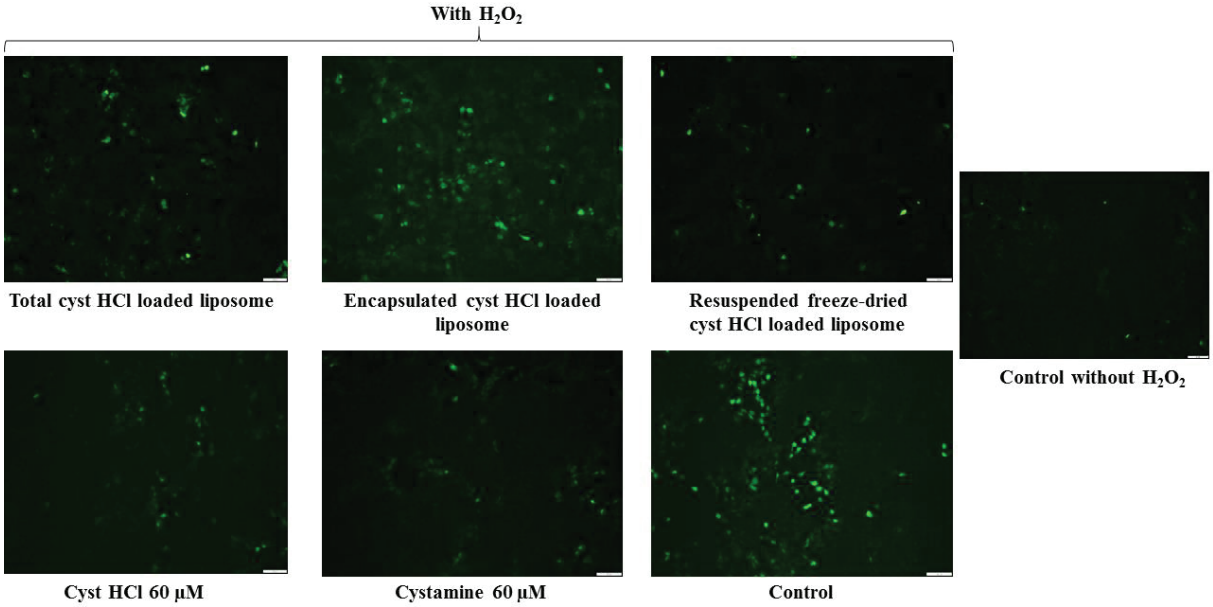

Figure 8: The fluorescence image of B16 cells treated for 72h with free and encapsulated cyst HCl and cystamine before the induction of the oxidant stress with H_2O_2.

3.9 Skin penetration study

The cumulative amounts of cyst HCl penetrating the skin and found in the receptor fluid from each of the liposomal formulation and controls over 24 h are shown in **Figure 9**. The encapsulation of cyst HCl in liposomes increased its penetration through the human skin. The quantity of cyst HCl found in the fluid receptor after 24 h of deposition was increased by 2.9-; 3.48- and 3.52-fold for the total, encapsulated and lyophilized cyst HCl loaded liposomes, respectively in comparison to the free drug in solution **(Figure 9)**. Cystamine did not penetrate the skin since it was not found in the receptor fluid nor in the epidermis layer.

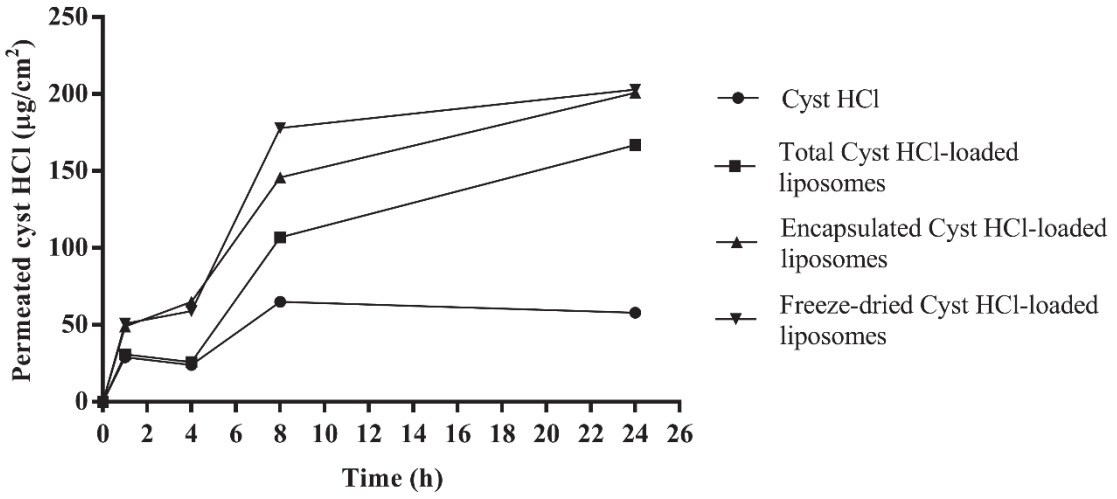

Figure 9: Skin permeation profile of free and cyst HCl loaded liposome in suspension and resuspended freeze-dried forms.

Figure 10 shows the retention of cyst HCl in the epidermis when the drug was free or encapsulated in liposomes in suspension or in resuspended freeze-dried forms. The highest quantity of retained cyst HCl in the epidermis was found for the cyst HCl-loaded liposome in the resuspended freeze-dried form (150 µg/cm^2). The presence of HP-β-CD could be the reason behind the increase of cysteamine penetration in the resuspended freeze-dried form. The cyclodextrin is known to be a penetration enhancer of the drug through the membranes (Loftsson & Sigurdardóttir, 1996; Yan et al., 2014). α-cyclodextrin demonstrated its ability to promote the trans corneal diffusion of cysteamine (Pescina et al., 2016). A slight decrease of the retention of the molecule in the epidermis was observed for cyst HCl encapsulated in liposome (120 µg/cm^2) in comparison with the free drug (140 µg/cm^2) while a higher decrease was obtained for the total cyst HCl loaded liposome (85 µg/cm^2). No trace of cystamine was found in the epidermis.

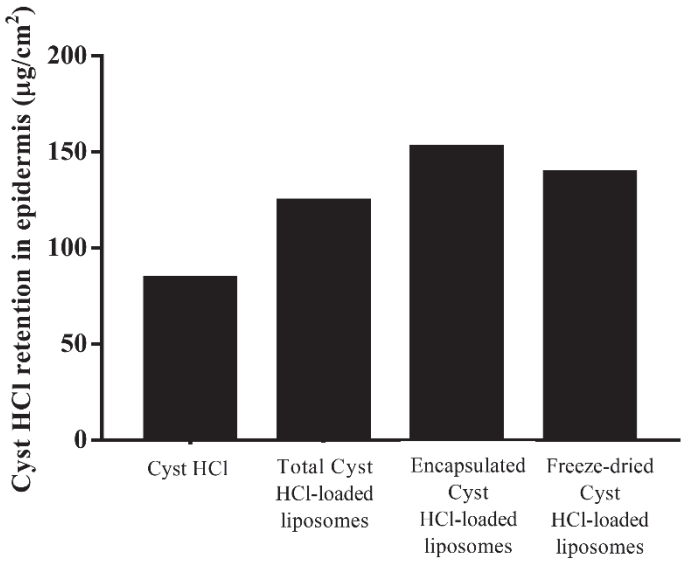

Figure 10: Cyst HCl retention in the epidermis for the free, total and encapsulated cyst HCl-loaded liposome in suspension and resuspended freeze-dried forms.

4 Conclusion

The encapsulation of cyst HCl increased the stability of the molecule especially when the formulation was freeze-dried. The formulation was not cytotoxic with the chosen concentrations. Cyst HCl and cystamine showed an inhibition of melanin and tyrosinase activity but cystamine was not able to penetrate the skin layers. The encapsulation of cyst HCl decreased its inhibition of melanin and tyrosinase activity but increased its penetration in the skin and its retention in the epidermis. The encapsulation didn't affect the antioxidant activity observed for the free cyst HCl. These findings are important for further application of cyst HCl liposomal formulations as a depigmenting agent.

5 References

Atallah, C., Charcosset, C., & Greige-Gerges, H. (2020). Challenges for cysteamine stabilization, quantification, and biological effects improvement. *Journal of Pharmaceutical Analysis*. https://doi.org/10.1016/j.jpha.2020.03.007

Atallah, C., Greige-Gerges, H., & Charcosset, C. (2020). Development of cysteamine loaded liposomes in liquid and dried forms for improvement of cysteamine stability. *International Journal of Pharmaceutics*, 119721. https://doi.org/10.1016/j.ijpharm.2020.119721

Azzi, J., Auezova, L., Danjou, P.-E., Fourmentin, S., & Greige-Gerges, H. (2018). First evaluation of drug-in-cyclodextrin-in-liposomes as an encapsulating system for nerolidol. *Food Chemistry*, *255*, 399–404. https://doi.org/10.1016/j.foodchem.2018.02.055

Azzi, J., Jraij, A., Auezova, L., Fourmentin, S., & Greige-Gerges, H. (2018). Novel findings for quercetin encapsulation and preservation with cyclodextrins, liposomes, and drug-in-cyclodextrin-in-liposomes. *Food Hydrocolloids*, *81*, 328–340. https://doi.org/10.1016/j.foodhyd.2018.03.006

Chavin, W., & Schlesinger, W. (1966). Some potent melanin depigmentary agents in the black goldfish. *Die Naturwissenschaften*, *53*(16), 413–414.

Ephrem, E., Elaissari, H., & Greige-Gerges, H. (2017). Improvement of skin whitening agents efficiency through encapsulation: Current state of knowledge. *International Journal of Pharmaceutics*, *526*(1–2), 50–68. https://doi.org/10.1016/j.ijpharm.2017.04.020

Farshi, S., Mansouri, P., & Kasraee, B. (2017). Efficacy of cysteamine cream in the treatment of epidermal melasma, evaluating by Dermacatch as a new measurement method: A

randomized double blind placebo controlled study. *Journal of Dermatological Treatment*, 1–8. https://doi.org/10.1080/09546634.2017.1351608

Frenk, E., Pathak, M. A., Szabó, G., & Fitzpatrick, T. B. (1968). Selective action of mercaptoethylamines on melanocytes in mammalian skin: Experimental depigmentation. *Archives of Dermatology*, *97*(4), 465–477.

Gharib, R., Auezova, L., Charcosset, C., & Greige-Gerges, H. (2017). Drug-in-cyclodextrin-in-liposomes as a carrier system for volatile essential oil components: Application to anethole. *Food Chemistry*, *218*, 365–371. https://doi.org/10.1016/j.foodchem.2016.09.110

Gharib, R., Greige-Gerges, H., Fourmentin, S., & Charcosset, C. (2018). Hydroxypropyl-ß-cyclodextrin as a membrane protectant during freeze-drying of hydrogenated and non-hydrogenated liposomes and molecule-in-cyclodextrin-in- liposomes: Application to trans-anethole. *Food Chemistry*, *267*, 67–74. https://doi.org/10.1016/j.foodchem.2017.10.144

Hammoud, Z., Khreich, N., Auezova, L., Fourmentin, S., Elaissari, A., & Greige-Gerges, H. (2019). Cyclodextrin-membrane interaction in drug delivery and membrane structure maintenance. *International Journal of Pharmaceutics*, *564*, 59–76. https://doi.org/10.1016/j.ijpharm.2019.03.063

Hsu, C., Mahdi, H. A., Pourahmadi, M., & Ahmadi, S. (2013). Cysteamine cream as a new skin depigmenting product. *Journal of the American Academy of Dermatology*, *68*(4). https://doi.org/10.1016/j.jaad.2012.12.781

Lee, Y.-J., Jung, S.-H., Hwang, J., Jeon, S., Han, E.-T., Park, W. S., Hong, S.-H., Kim, Y.-M., & Ha, K.-S. (2017). Cysteamine prevents vascular leakage through inhibiting

transglutaminase in diabetic retina. *Journal of Endocrinology*, *235*(1), 39–48. https://doi.org/10.1530/JOE-17-0109

Loftsson, T., & Sigurdardóttir, A. M. (1996). Cyclodextrins as Skin Penetration Enhancers. In J. Szejtli & L. Szente (Eds.), *Proceedings of the Eighth International Symposium on Cyclodextrins* (pp. 403–406). Springer Netherlands. https://doi.org/10.1007/978-94-011-5448-2_90

Mansouri, P., Farshi, S., Hashemi, Z., & Kasraee, B. (2015). Evaluation of the efficacy of cysteamine 5% cream in the treatment of epidermal melasma: A randomized double-blind placebo-controlled trial. *The British Journal of Dermatology*, *173*(1), 209–217. https://doi.org/10.1111/bjd.13424

Okamura, D. M., Bahrami, N. M., Ren, S., Pasichnyk, K., Williams, J. M., Gangoiti, J. A., Lopez-Guisa, J. M., Yamaguchi, I., Barshop, B. A., Duffield, J. S., & Eddy, A. A. (2014). Cysteamine Modulates Oxidative Stress and Blocks Myofibroblast Activity in CKD. *Journal of the American Society of Nephrology : JASN*, *25*(1), 43–54. https://doi.org/10.1681/ASN.2012090962

Pescina, S., Carra, F., Padula, C., Santi, P., & Nicoli, S. (2016). Effect of pH and penetration enhancers on cysteamine stability and trans-corneal transport. *European Journal of Pharmaceutics and Biopharmaceutics*, *107*, 171–179. https://doi.org/10.1016/j.ejpb.2016.07.009

Qiu, L., Zhang, M., Sturm, R. A., Gardiner, B., Tonks, I., Kay, G., & Parsons, P. G. (2000). Inhibition of melanin synthesis by cystamine in human melanoma cells. *The Journal of Investigative Dermatology*, *114*(1), 21–27. https://doi.org/10.1046/j.1523-1747.2000.00826.x

Rendon, M. I., & Gaviria, J. I. (2005). Review of Skin-Lightening Agents. *Dermatologic Surgery*, *31*(s1), 886–890. https://doi.org/10.1111/j.1524-4725.2005.31736

Rhee, S. G., Chang, T.-S., Jeong, W., & Kang, D. (2010). Methods for detection and measurement of hydrogen peroxide inside and outside of cells. *Molecules and Cells*, *29*(6), 539–549. https://doi.org/10.1007/s10059-010-0082-3

Ribeiro, M., Silva, A. C., Rodrigues, J., Naia, L., & Rego, A. C. (2013). Oxidizing Effects of Exogenous Stressors in Huntington's Disease Knock-in Striatal Cells—Protective Effect of Cystamine and Creatine. *Toxicological Sciences*, *136*(2), 487–499. https://doi.org/10.1093/toxsci/kft199

Shin, Y. J., Seo, J. M., Chung, T. Y., Hyon, J. Y., & Wee, W. R. (2011). Effect of Cysteamine on Oxidative Stress-induced Cell Death of Human Corneal Endothelial Cells. *Current Eye Research*, *36*(10), 910–917. https://doi.org/10.3109/02713683.2011.593726

Solano, F., Briganti, S., Picardo, M., & Ghanem, G. (2006). Hypopigmenting agents: An updated review on biological, chemical and clinical aspects. *Pigment Cell Research*, *19*(6), 550–571. https://doi.org/10.1111/j.1600-0749.2006.00334.x

Sun, L., Xu, S., Zhou, M., Wang, C., Wu, Y., & Chan, P. (2010). Effects of cysteamine on MPTP-induced dopaminergic neurodegeneration in mice. *Brain Research*, *1335*, 74–82. https://doi.org/10.1016/j.brainres.2010.03.079

Wiedmann, T. S., & Naqwi, A. (2016). Pharmaceutical salts: Theory, use in solid dosage forms and in situ preparation in an aerosol. *Asian Journal of Pharmaceutical Sciences*, *11*(6), 722–734. https://doi.org/10.1016/j.ajps.2016.07.002

Yan, Y., Xing, J., Xu, W., Zhao, G., Dong, K., Zhang, L., & Wang, K. (2014). Hydroxypropyl-β-cyclodextrin grafted polyethyleneimine used as transdermal

penetration enhancer of diclofenac sodium. *International Journal of Pharmaceutics*, *474*(1–2), 182–192. https://doi.org/10.1016/j.ijpharm.2014.08.021

Zuriarrain, A., Zuriarrain, J., Villar, M., & Berregi, I. (2015). Quantitative determination of ethanol in cider by 1H NMR spectrometry. *Food Control*, *50*, 758–762. https://doi.org/10.1016/j.foodcont.2014.10.024

Zylberberg, C., & Matosevic, S. (2016). Pharmaceutical liposomal drug delivery: A review of new delivery systems and a look at the regulatory landscape. *Drug Delivery*, *23*(9), 3319–3329. https://doi.org/10.1080/10717544.2016.1177136

Conclusion générale et perspectives

L'objectif de ce travail consiste à optimiser la formulation de la cystéamine encapsulée dans des liposomes afin d'améliorer sa stabilité pour être appliquée sur la peau en tant qu'agent dépigmentant. En premier lieu, nous avons optimisé la méthode de dosage de la cystéamine dans les suspensions liposomales ainsi que le dosage simultané de la cystéamine et de la cystamine en solution. De plus, nous avons mené une étude de stabilité de la cystéamine seule en solution, puis nous avons préparé et caractérisé les liposomes encapsulant la cystéamine sous forme liquide et lyophilisée. Nous avons, par la suite, évalué l'effet de l'encapsulation sur la stabilité de la cystéamine. Les suspensions liposomales ont été testées pour leur effet dépigmentant en dosant la cytotoxicité, la mélanine et l'activité de la tyrosinase du chlorhydrate de cystéamine, cystamine et des liposomes encapsulant le chlorhydrate de cystéamine. Enfin, une étude de la pénétration cutanée de ces différentes préparations a été réalisée.

L'étude portant sur l'optimisation de la méthode de dosage de la cystéamine par la méthode d'Ellman a révélé l'importance de l'ajout du méthanol dans le réactif d'Ellman pour la quantification de la cystéamine dans les suspensions liposomales. En revanche, pour le dosage de la cystéamine et la cystamine simultanément, il a été démontré que la méthode de chromatographie par paires d'ions est plus efficace que la chromatographie micellaire car elle permet d'obtenir une meilleure symétrie des pics et un nombre de plateau théorique plus élevé pour la cystéamine. Pour ces deux méthodes, le SDS a été ajouté dans la phase mobile afin d'augmenter la rétention des deux molécules dans la colonne. La phase mobile était composée d'acétonitrile et d'eau contenant 0,1 % d'acide phosphorique et de SDS. De plus, l'ajout d'un agent chélateur a été primordial pour la stabilité des échantillons durant l'analyse. La stabilité

de la cystéamine a été influencée par la composition du tampon utilisé pour la préparation des solutions de cystéamine, la température et l'exposition à la lumière.

Les liposomes formés de phospholipides phospholipon 90H ou de Lipoïd S100 et de cholestérol contenant la cystéamine, préparés par la méthode d'injection éthanolique, sont nanométriques et oligolamellaires. Il a été démontré que le rendement de l'encapsulation a été faible pour toutes les formulations et a diminué avec l'augmentation de la concentration de la cystéamine. Le taux d'incorporation de phospholipides a été élevé et n'a pas été influencé par la présence de la cystéamine. Cependant, le taux d'incorporation du cholestérol a diminué en présence de la cystéamine notamment dans les liposomes constitués de Lipoïd S100. L'encapsulation a augmenté la stabilité de la cystéamine à 4, 25 et 37°C. En outre, la lyophilisation des suspensions liposomales permet d'augmenter la stabilité de ces suspensions même après quatre mois de stockage.

Malgré que l'encapsulation de la cystéamine, sous sa forme basique, dans des liposomes ait augmenté sa stabilité, une forme plus stable de la cystéamine, le chlorhydrate de cystéamine a été utilisé. Pour une même concentration de 200 µg/mL, la cystéamine a été totalement oxydée après 15h de stockage à 4°C alors que pour le chlorhydrate de cystéamine l'oxydation complète a eu lieu après 16 jours. La caractérisation des liposomes encapsulant le chlorhydrate de cystéamine était identique pour la taille et le pdI. Le potentiel zêta et le taux d'encapsulation ont été trouvés différents pour les liposomes encapsulant les deux formes de cystéamine. L'encapsulation a augmenté la stabilité du chlorhydrate de cystéamine. L'oxydation totale du chlorhydrate de cystéamine est obtenue après plus de six mois de stockage des suspensions liposomales. La totalité de la quantité du chlorhydrate de cystéamine présente dans les liposomes lyophilisés a été conservée après trois mois de stockage à 4°C.

La formulation contenant le chlorhydrate de cystéamine ne doit pas être cytotoxique afin qu'elle puisse être appliquée sur la peau humaine. Le test de cytotoxicité par MTT pour des cellules mélanome B16 a montré que les liposomes blancs en suspension et resuspendus après lyophilisation ne sont pas cytotoxiques. Le chlorhydrate de cystéamine et la cystamine ne sont pas cytotoxiques pour des concentrations variant entre 50 et 100 µM. Les formulations contenant des liposomes encapsulant le chlorhydrate de cystéamine en suspension et resuspendus après lyophilisation ont été dilués afin d'arriver à une concentration de 60 µM du chlorhydrate de cystéamine. Ces dernières n'ont pas montré de cytotoxicité.

Afin d'évaluer l'impact de l'encapsulation sur l'effet dépigmentant du chlorhydrate de cystéamine, les taux de mélanine et de tyrosinase ont été quantifiés dans les cellules mélanome B16 après ajout du chlorhydrate de cystéamine, la cystamine, les liposomes encapsulant le chlorhydrate de cystéamine en suspension et resuspensdus après lyophilisation. La cystamine a inhibé la mélanine et l'activité de la tyrosinase davantage que le chlorhydrate de cystéamine. L'encapsulation a diminué l'effet dépigmentant du chlorhydrate de cystéamine.

Enfin, la pénétration cutanée est un facteur très important pour l'application d'un agent dépigmentant. Des tests *ex-vivo* de pénétration cutanée avec une cellule de Franz ont été menés. L'encapsulation du chlorhydrate de cystéamine a augmenté sa pénétration cutanée et sa rétention dans l'épiderme. La formulation qui a augmenté le plus cette pénétration est celle qui a été lyophilisée et resupendue avant application.

En perspectives, il serait intéressant d'encapsuler la cystéamine dans des liposomes déformables comme les ethosomes et les transfersomes afin de comparer les effets des différents systèmes d'encapsulation sur la stabilité, la dépigmentation et la pénétration de la cystéamine. Les ethosomes contiennent un taux d'éthanol élevé qui leur permet d'atteindre les

couches profondes de la peau et/ou la circulation systémique. Les transfersomes ressemblent aux liposomes mais sont davantage hydrophiles et élastiques, ils ont une capacité spontanée à pénétrer dans la couche cornée par des voies intracellulaires ou transcellulaires et ont des applications potentielles dans le domaine de la cosmétique et l'administration de médicaments.

En outre, une comparaison entre notre formulation et la crème commercialisée de cystéamine pour la stabilité, l'effet dépigmentant et la pénétration de la cystéamine sera aussi importante. Une étude *in vivo* doit être aussi menée afin de comparer les effets secondaires de notre formulation et celles de la crème commercialisée.